Technische Universität München
TUM School of Life Sciences

Transcriptional control of pancreatic β-cells by the transcription co-factors TBL1 and TBLR1

Alina Agnes Walth-Hummel

Vollständiger Abdruck der von der TUM School of Life Sciences der Technischen Universität München zur Erlangung einer

Doktorin der Naturwissenschaften (Dr. rer. nat.)

genehmigten Dissertation.

Vorsitz: Prof. Dr. Dr. h.c. mult Martin Hrabé de Angelis

Prüfer*innen der Dissertation:

1. Prof. Dr. Ilona Grunwald-Kadow
2. Prof. Dr. Stephan Herzig

Die Dissertation wurde am 25.01.2023 bei der Technischen Universität München eingereicht und durch TUM School of Life Sciences am 30.05.2023 angenommen.

ABSTRACT

Type 2 diabetes mellitus (T2DM) is a multifactorial disease characterized by chronic hyperglycemia due to peripheral insulin resistance, impaired insulin synthesis and release from pancreatic β-cells, and a general loss of β-cell mass, mainly caused by loss of β-cell identity. The loss of β-cell identity - also referred to as β-cell dedifferentiation - is associated with a reduced expression of β-cell identity genes, an upregulation of disallowed genes, and a reoccurrence of progenitor markers, suggestive for a dysregulation of transcriptional events.

In this context, the transcriptional co-factors transducin β-like 1 (TBL1) and transducin β-like related 1 (TBLR1), which were previously shown to mediate both expression and repression of genes, were investigated to identify their role in the regulation of transcriptional events in β-cells. Mice with a conditional and β-cell specific deletion of TBL1 (TBLβKO) or TBLR1 (TBLRβKO) appeared as metabolically healthy. Gene expression analysis revealed an upregulation of TBLR1 upon TBL1 deficiency, suggesting that the development of a clear metabolic phenotype might have been masked by this alteration in TBLR1 expression. Thus, mice lacking both transcription co-factors (TBL/RβKO) were generated. Metabolic characterization revealed that TBL/RβKO mice developed hyperglycemia starting at the age of 6 weeks. Impaired insulin gene expression, alterations in islet architecture, and reduced numbers of insulin positive cells preceded the development of hyperglycemia. A transcriptome analysis revealed a downregulation of β-cell identity genes, while disallowed genes and progenitor markers were upregulated, indicating a loss of identity in β-cells lacking TBL1 and TBLR1. Adult mice with a tamoxifen-induced knock out of TBL1 and TBLR1 (iTBL/RβKO) displayed a milder but similar phenotype compared to the TBL/RβKO mice, supporting the notion that β-cells deficient for TBL1 and TBLR1 lose their identity and dedifferentiate.

A subsequent interactome analysis identified components of the nuclear receptor corepressor/silencing mediator for retinoid and thyroid receptors (NCOR/SMRT) repressor complex - a complex of which TBL1 and TBLR1 are known to be part of -, subunits of the facilitates chromatin transcription (FACT) activator complex, and paired box 6 (PAX6), a master regulator of endocrine cells of the pancreas, to directly interact with TBL1 and TBLR1. Components of the NCOR/SMRT repressor and FACT activator complex were also interacting with PAX6. Additionally, TBL1 and TBLR1 directly regulated insulin gene expression through the binding to the same promoter region as PAX6, identifying TBL1 and TBLR1 as possible regulators of PAX6 mediated gene expression.

This study identified TBL1 and TBLR1 as novel and critical regulators of β-cell identity. Through interaction with NCOR/SMRT, FACT, and PAX6, TBL1 and TBLR1 might contribute to the maintenance of β-cell identity and its loss in pathologic conditions. Manipulation of TBL1 and TBLR1 levels, action, or binding to the respective interaction partners therefore represents a novel approach to counteract loss of β-cell identity and thereby development and progression of T2DM.

ZUSAMMENFASSUNG

Typ-2-Diabetes mellitus (T2DM) ist eine multifaktorielle Erkrankung die durch eine chronische Hyperglykämie gekennzeichnet ist. Hervorgerufen wird sie durch eine periphere Insulinresistenz, eine gestörte Insulinsynthese und -freisetzung aus den β-Zellen der Bauchspeicheldrüse sowie einem allgemeinen Verlust der β-Zellmasse. Aktuelle Studien zeigten, dass der auch als β-Zell Dedifferenzierung bezeichnete Verlust der β-Zell Identität, eine der Hauptursachen darstellt. Dieser Identitätsverlust geht mit einer verminderten Expression von β-Zell Funktionsgenen sowie einer Überexpression von in β-Zellen strikt reprimierten Genen und einer Reaktivierung von Vorläufer-Genen einher. Daher kann von einer allgemeinen Fehlregulierung der Genexpression ausgegangen werden.

Die Transkriptions-Kofaktoren *Transducin β-like 1* (TBL1) und *Transducin β-like related 1* (TBLR1) regulieren sowohl Expression als auch Repression von Genen. Daher wurde ihre Funktion in der Regulation von Transkriptionsvorgängen in β-Zellen untersucht. Mäuse mit einer konditionalen β-Zell spezifischen Deletion von TBL1 (TBLβKO) oder TBLR1 (TBLRβKO) waren metabolisch unauffällig. Genexpressionsanalysen der Inselzellen ergaben, dass bei TBL1-Deletion TBLR1 überexprimiert wird, was vermuten lässt, dass Veränderungen in der TBLR1 Genexpression die Entwicklung eines klar erkennbaren metabolischen Phänotyps verhindert haben könnte. Daher wurden Mäuse generiert, denen beide Transkriptions-Kofaktoren (TBL/RβKO) fehlten. β-Zell spezifische Deletion von TBL1 und TBLR1 führte zu Hyperglykämie ab einem Alter von 6 Wochen. Der Hyperglykämie gingen eine beeinträchtigte Insulin-Genexpression, Veränderungen in der Inselarchitektur und eine verringerte Anzahl von Insulin-positiven Zellen voraus. Das Genexpressionsprofil der Inselzellen von TBL/RβKO Mäusen wies auf einen Identitätsverlust der β-Zellen hin, da die Expression von β-Zell Funktionsgenen verringert war während in β-Zellen strikt reprimierte sowie Vorläufer-Gene verstärkt exprimiert wurden. Die Tamoxifen-induzierte Inaktivierung von TBL1 und TBLR1 in adulten Mäusen rief einen ähnlichen jedoch milderen Verlauf des Phänotyps hervor. Daher ist anzunehmen, dass β-Zellen durch den Verlust von TBL1 und TBLR1 unfähig sind ihre Identität beizubehalten und dadurch dedifferenzieren.

Eine anschließende Analyse des Interaktoms ergab, dass Komponenten des Repressionskomplexes *Nuclear receptor corepressor*/*Silencing mediator for retinoid and thyroid receptors* (NCOR/SMRT), Untereinheiten des Aktivatorkomplexes *Facilitates chromatin transcription* (FACT) und *Paired box 6* (PAX6), ein Hauptregulator der endokrinen Zellen der Bauchspeicheldrüse, direkt mit TBL1 und TBLR1 interagieren. Die Komponenten des NCOR/SMRT-Repressor- und FACT-Aktivatorkomplexes interagierten ebenfalls mit PAX6. Darüber hinaus regulierten TBL1 und TBLR1 die Insulin-Genexpression durch Bindung an dieselbe Promotorregion wie PAX6. Dies deutet darauf hin, dass TBL1 und TBLR1 als mögliche Regulatoren der PAX6-vermittelten Genexpression in Frage kommen.

In dieser Studie wurden TBL1 und TBLR1 als neuartige und zentrale Regulatoren der β-Zellidentität identifiziert. Durch die Interaktion mit NCOR/SMRT, FACT und PAX6 tragen TBL1 und TBLR1 zur Aufrechterhaltung der β-Zell-Identität und deren Verlust unter pathologischen Bedingungen bei. Die Manipulation der TBL1- und TBLR1-Expression, der Aktivität oder der Bindung an die jeweiligen Interaktionspartner stellt daher einen neuen Ansatz dar, um dem Verlust der β-Zell-Identität und damit der Entwicklung sowie dem Fortschreiten von T2DM entgegenzuwirken.

ACKNOWLEDGEMENTS

It takes a village to raise a child…or a PhD. Without the contribution, help, and support of many people, this work wouldn't have been possible.

First of all, I would like to thank my supervisor Maria Rohm. It all started more than 5 years ago with an internship, and here we are now, almost at the end of my PhD. Thank you for constant support, great mentorship, incredible optimism, and for sharing knowledge and experience. Your guidance, ideas, and commitment taught me a lot scientifically and personally. I would also like to thank Stephan Herzig for giving me the opportunity to do my PhD at the IDC. Your recommendations, ideas, and input during the lab meetings helped to shape and push this thesis forward.

Moreover, I would like to thank my thesis advisory committee members Ilona Grunwald-Kadow, Patrick E. MacDonald, Mostafa Bakhti, and Jantje Gerdes for valuable discussions and suggestions during my TAC meetings.

I highly appreciate the contributions of Ann-Christine König, Annette Feuchtinger, Inti Alberto De La Rosa Velázquez, Michael Sterr, Peter Weber, and Stephanie Hauck to this project and for the fruitful collaborations.

I'd also like to thank Kalina, Luke, Sofia, and Susanne from the Helmholtz Graduate School for Diabetes for the amazing support, the unforgettable symposium travels, and the opportunity to be part of the HRD.

I would like to thank all former and current IDC colleagues for the nice working environment, all the help and support, the ideas and input during lab meetings, and scientific/non-scientific discussions. Here I'd like to especially thank in alphabetic order Adriano, Anastasia, Anja, Celine, Daniela, Elena, Hermine, Honglei, Jeanette, Julia, Karsten, Lisa, Manuel, Mauricio, Miriam, Phivos, Quirin, Raúl, and Teresa who immensely contributed in all kind of ways to this thesis during the past 4 years. A big thank you also goes to Julia, Karsten, and Maria for proofreading the manuscript of my thesis. I also highly appreciate all the members of the TCT and MAC group for suggestions, recommendations, and interesting discussions. I'd also like to thank our former Azubis and students Jasmin, Jonas, and Judith for their excellent work.

Moreover, I'd like to thank all the members from the MacDonald Lab in particular James, Jasmine, Kunimasa, Nancy, and Patrick, for making my research stay a successful and memorable experience. Thanks also to Vincent who gave me a warm welcome and supported me during my first and last days in Edmonton.

A special thanks goes to Julia, Karsten, and Raúl for making Lab and Office more than enjoyable. I am grateful to Julia especially for transitioning together from Division F (the F in Division F stands for quality…or maybe fail?) to TCT, for our "coffees", and for all the scientific and mental support. Many thanks go to Karsten, especially for all the good laughs we had. All it took was a look across the table which said more than 1000 words. I still hope we will have an opportunity to visit a conference together…in Spain. I am also thankful to Raúl, not only for "tea and biscuits", but also for his help in the Lab, the mostly philosophical conversations when picking islets, and for being my evil twin, or am I the evil one?

Most importantly, I would like to express my deepest gratitude to my parents and my brother Andreas who were always there for me. All of this wouldn’t have been possible without your constant love and support. I owe it all to you. Lastly, I am truly thankful to Alexander who always believed in me, who cheered me up whenever things did not go well, and who helped me to manage my life during turbulent times. Thank you for everything.

INDEX

1 INTRODUCTION

1.1 Type 2 diabetes mellitus

1.1.1 Type 2 diabetes mellitus: definition, numbers, risks

The clinical features of diabetes mellitus are known to physicians for more than 3500 years and were described for the first time by ancient Egyptians 1500 BC (Ahmed 2002). Diabetes is a disorder of glucose homeostasis and is mainly divided into two main categories: type 1 diabetes mellitus (T1DM), an auto-immune disease resulting in the destruction of the insulin-producing β-cells, and T2DM, a chronic metabolic condition characterized by elevated blood glucose levels due to impaired insulin signaling in peripheral tissues, followed by insufficient insulin synthesis and release (Fu et al. 2013). To date, the global prevalence of diabetes has reached pandemic proportions with 10.5% in 2021 (Figure 1) and an estimated prevalence of 12.2% for 2045 (Sun et al. 2022).

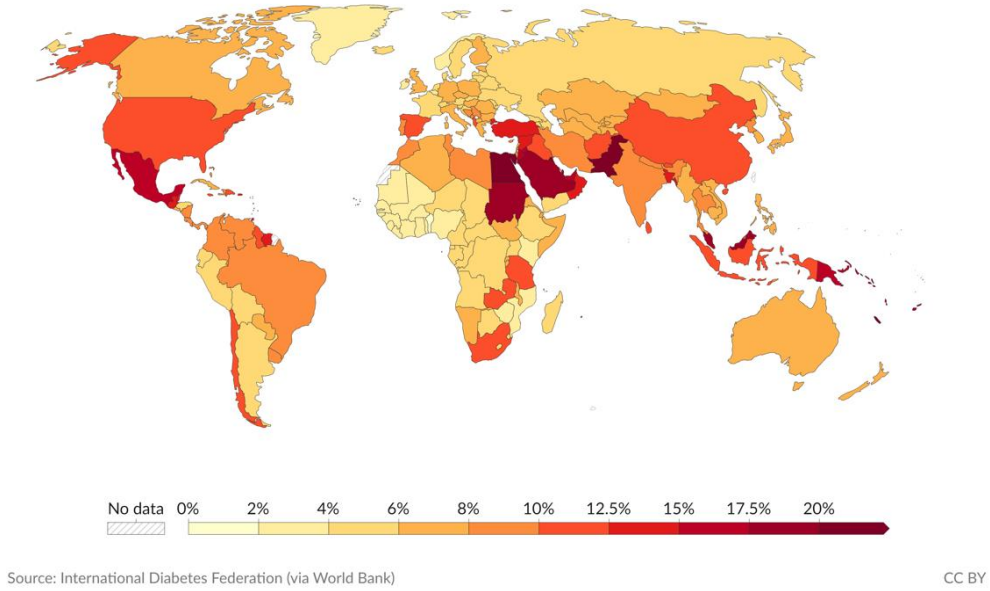

Figure 1: Diabetes prevalence in 2021. The share of people aged 20-79 years diagnosed with type1 or type 2 diabetes mellitus in 2021. From: World Development Indicators - World Bank. Data was used from: Diabetes Atlas - International Diabetes Federation.

T2DM accounts for up to 90% of the diabetes cases and is diagnosed when one of the following criteria is met in repeated measurements: 1) elevated fasting blood glucose levels (> 126 mg/dl), 2) elevated blood glucose levels 2 h after performance of an oral glucose tolerance test (> 200 mg/dl), and 3) elevated hemoglobin A1c (HbA1c) levels (> 6.5%), reflecting long-term glycemia (Sacks et al. 2011). Genetic predisposition and lifestyle factors were identified as main risk factors for T2DM development. Genome-wide association studies for instance robustly linked variants of the *TCF7L2* (Grant et al. 2006) or *KCNJ11* (Gloyn et al. 2003) gene with a higher T2DM risk. Moreover, lifestyle factors such as cigarette smoking, sedentary lifestyle, physical inactivity, and poor diet (Helmrich et al. 1991; Willi et al. 2007; Salmerón et al. 2001) were shown to contribute to T2DM development and progression. In line with this, obesity was identified as primary cause for the development of T2DM (Colditz et al. 1995).

T2DM is associated with life threatening comorbidities such as cardiovascular complications, retinopathies, and nephropathies (Long and Dagogo-Jack 2011). Accordingly, T2DM was

shown to reduce life expectancy (Heald et al. 2020; Bragg et al. 2017) and is one of the leading causes for mortality (Yang et al. 2019). A recent study identified six different T2DM subtypes based on parameters such as body mass index, HbA1c, and measures of insulin resistance and secretion. These subtypes were highly associated with the development of specific T2DM comorbidities, suggesting that for optimal treatment strategies, diabetes subtypes must be considered (Ahlqvist et al. 2020). Moreover, in the recent years, an increase in numbers of T2DM cases amongst young people was observed (Candler et al. 2018). This is of particular concern since early onset of diabetes leads to longer lifetime exposure to hyperglycemia and therefore a higher risk to develop T2DM comorbidities (Arslanian et al. 2018). Thus, with the increasing worldwide prevalence, the identification of T2DM subtypes, and the rising incidences amongst adolescent and children, studying causes and mechanisms underlying T2DM development and progression are central to develop novel treatment and prevention approaches.

1.1.2 Pathophysiology of T2DM and current therapeutic approaches

Genetic predisposition and lifestyle factors are the main risk factors for insulin resistance, a state in which insulin signaling in peripheral tissues is impaired. At first, pancreatic β-cells compensate for the increasing demand of insulin by β-cell hyperplasia (Kim et al. 2009) and elevated insulin secretion (Karam et al. 1963). Eventually, β-cells are unable to secrete adequate amounts of insulin to compensate for the insulin resistance - in part due to mitochondrial dysfunction - which results in elevated blood glucose levels and manifests as T2DM (Kulkarni et al. 1999; Haythorne et al. 2019). The resulting hyperglycemia and hypoinsulinemia affect multiple organs, which were shown to contribute to the elevated blood glucose levels, resulting in a vicious cycle. For instance, insulin signaling inhibits gluconeogenesis in the liver. Accordingly, impaired or absent insulin signaling promotes gluconeogenesis and the release of glucose from the liver, further contributing to systemic hyperglycemia (Magnusson et al. 1992). In white adipose tissue, insulin induces glucose uptake and inhibits triglyceride oxidation and free fatty acid release into the circulation (Kashiwagi et al. 1983; Chakrabarti et al. 2013). Consequently, insulin resistance promotes fatty acid oxidation resulting in elevated circulating free fatty acids (Bogardus et al. 1984), which were shown to impair glucose uptake in the muscle (Kelley et al. 1993) and β-cell function (Shimabukuro et al. 1998), thereby contributing to T2DM progression.

β-cell function progressively declines with the duration of hyperglycemia and dyslipidemia exposure. In patients in which β-cells are still capable of insulin secretion, treatment approaches include physical activity, dietary interventions, and oral medication to support glycemic control (Davies et al. 2022). Some of the frequently prescribed pharmacological agents are sodium glucose co-transporter-2 (SGLT2) inhibitors, which inhibit renal glucose reabsorption (Bailey and Day 2010) or metformin, which promotes insulin sensitization especially in liver and muscle (Scarpello and Howlett 2008). In recent years, novel combinatorial agents were developed for T2DM treatment such as dual incretin receptor agonists which improve β-cell function and insulin sensitivity in T2DM (Thomas et al. 2021). Only at advanced stages of T2DM, when insulin secretion is impaired and β-cells fail, insulin therapy, which bears a high risk for hypoglycemia is recommended (Davies et al. 2022). Modern therapy approaches include the transplantation of β-cells from cadaveric donors, which is however limited due to donor matching and availability (Shapiro et al. 2006). Major advances in the recent years in stem cell research have led to the generation of pancreatic β-cells derived from human pluripotent stem cells (hPSC). This has opened the possibility for replacement therapy in insulin-dependent diabetes. An ongoing clinical trial (NCT04786262)

is testing the safety, tolerability, and efficacy of transplanted β-cells derived from stem cells in T1DM patients. In T2DM however, underlying insulin-resistance, hyperglycemia, and dyslipidemia would lead to β-cell dysfunction and ultimately failure of transplanted β-cells (Hiramatsu and Grill 2001). Moreover, differentiation efficiency is currently not reproducible across different hPSC cell types (Merkle et al. 2022) and hPSC derived β-cells display signatures of immaturity, resulting in impaired glucose stimulated insulin secretion (Balboa et al. 2022). Thus, in depth understanding of processes during β-cell development are essential to improve or generate novel treatment approaches.

1.2 The pancreas

The pancreas is a dual gland with an exocrine and endocrine implication. The exocrine pancreas secretes digestive zymogens in response to food intake and thereby assists in digestion. It comprises of acinar cells, which produce and secrete digestive zymogens and protons and ductal cells which secrete bicarbonate and deliver the secreted zymogens towards the duodenum. The endocrine pancreas consists of cellular clusters which form hormone producing micro-organs, the so-called islets of Langerhans. These islets comprise of α-, β-, δ-, PP-, and ε-cells producing glucagon, insulin, somatostatin, pancreatic polypeptide Y, and ghrelin, respectively and are central to blood glucose homeostasis (Atkinson et al. 2020; Behrendorff et al. 2010).

1.2.1 Development of the pancreas

In mice, the first visible signs of a pancreas are observed in embryonic day (E) 9, when a ventral and dorsal bud is formed from the foregut endoderm (Pearse et al. 1973). The buds undergo expansion, branching, and subsequently fusion which results in a single definitive pancreas around E12.5 (Pictet et al. 1972). These morphological changes coincide with the formation of the three main pancreatic cell types – endocrine, acinar, and ductal. Tightly controlled spatiotemporal expression of transcription factors drive the differentiation and cell type specification of pancreatic cells as shown in Figure 2. Differentiation is initiated by the expression of the transcription factors *Pdx1* (Pancreatic and duodenal homeobox 1), *Ptf1a* (Pancreas associated transcription factor 1a), *Sox* (SRY box) *9*, and *Sox17* in endoderm epithelial cells which induces the formation of multipotent progenitor cells (Kawaguchi et al. 2002; Gu et al. 2002; Burlison et al. 2008; Seymour et al. 2007; Spence et al. 2009). Maintained expression of *Ptf1a* subsequently induces the differentiation into acinar cells (Krapp et al. 1998; Kawaguchi et al. 2002), while the expression of *Pdx1* and *Sox9* promotes the differentiation into bipotent trunk cells (Burlison et al. 2008; Seymour et al. 2007). This period, taking place between E13.5 and E14.5, is termed secondary transition and is marked by a massive rise of acinar cells, bipotent trunk cells, and a general pancreas growth (Pictet et al. 1972). Bipotent trunk cells express *Pdx1*, *Sox9*, *Nkx6.1* (NK6 homeobox 1), and *Hnf1β* (Hepatocyte nuclear factor 1 homeobox B) and are capable to further differentiate into either ductal cells, when *Hnf1β* expression is maintained (Haumaitre et al. 2005) or into endocrine progenitor cells when *Pdx1*, *Nkx6.1*, and *Sox9* expression persists (Seymour et al. 2007; Schaffer et al. 2010; Burlison et al. 2008). SOX9 induces the expression of *Ngn3* (Neurogenin 3) (Gu et al. 2002; Gradwohl et al. 2000), which is a central marker for progenitor cells of the endocrine pancreas. *Ngn3* expression is first detected at E11.5, peaks during the secondary transition, declines at E17.5, and is undetectable in the pancreas of neonates or adults (Schwitzgebel et al. 2000). Thus, *Ngn3* expression is a useful marker to determine the state of differentiation in endocrine cells.

The rise of the respective endocrine cell types was shown to take place over a spectrum of time during embryogenesis with glucagon and/or insulin-expressing cells being detected as early as E9.5-E10.5 (Herrera et al. 1991). However, lineage tracing revealed that these cells do not represent precursors of endocrine cells (Herrera 2000) and their function remains unclear. Thus, the main phase of endocrine cell differentiation is the second transition and is initiated by the expression of *Ngn3*. As differentiation proceeds, the generation of the respective endocrine cell line depends on the spatiotemporal expression of the transcription factors *Arx* (Aristaless-related homeobox), which promotes the expression of α- and PP-cells (Collombat et al. 2003; Collombat et al. 2007), and *Pax4* (Paired box 4), which induces the rise of β- or δ-cells (Sosa-Pineda 2004). Specification of ε-cells is induced through the repression of *Pax6* (Heller et al. 2005). Only after E18.5 endocrine cell clusters, namely islets are observed. Endocrine cell clustering and islet formation start with the expression of *Ngn3*. For this, endocrine precursors delaminate from the trunk epithelium, migrate through the remodelling of adhesion molecules, and eventually cluster and aggregate as islets (Cole et al. 2009; Miettinen et al. 2000). The exact mechanisms through which the endocrine cells find each other and cluster however, are not completely understood.

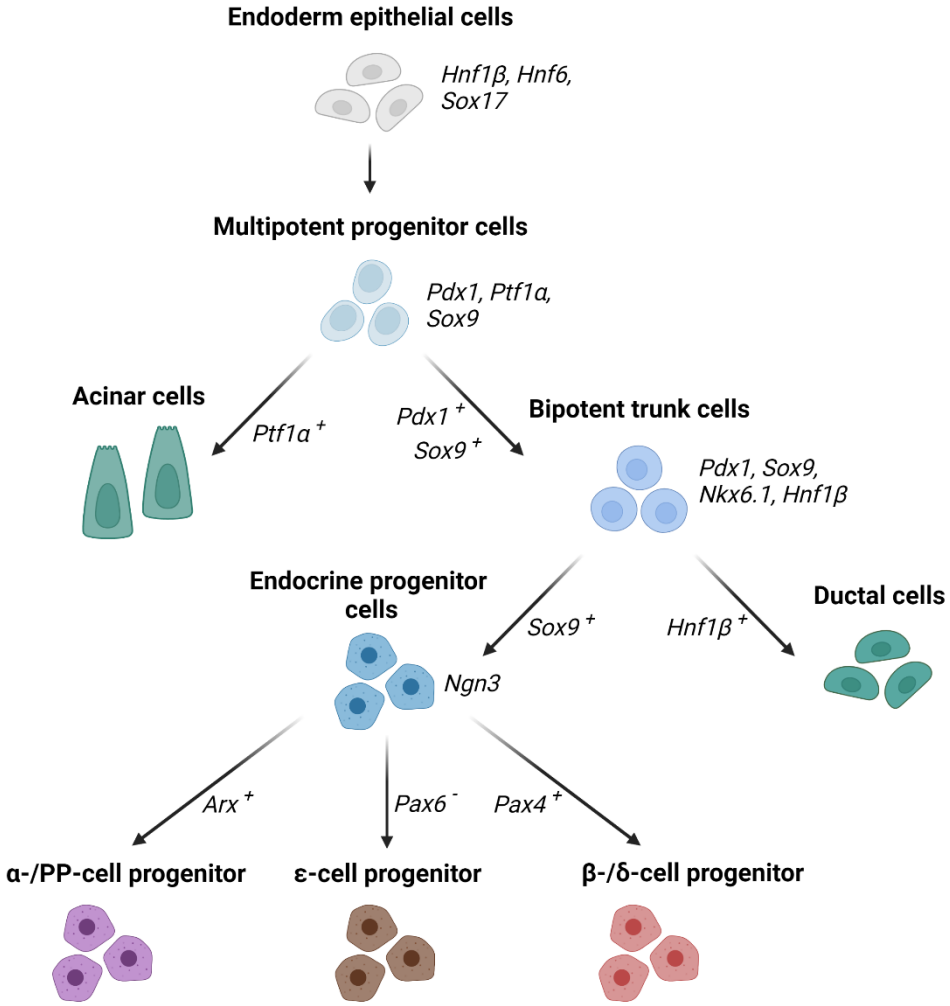

Figure 2: The differentiation of pancreatic cells. This diagram shows the process of differentiation and the respective transcription factors involved for the specification of acinar cells, ductal cells, or the endocrine α-, β-, δ-, PP-, and ε-cells from endoderm epithelial cells. Created with Biorender.com.

1.2.2 The endocrine pancreas

The endocrine pancreas comprises of 5 cell types, each synthesizing and secreting a cell type-specific hormone with autocrine, paracrine, and systemic effects. Production, release, and

action of the respective hormones is tightly controlled and regulates metabolic homeostasis and nutrient storage and utilization. Mutations during endocrinogenesis therefore often result in metabolic conditions such as diabetes.

α-cells

The glucagon producing α-cells are the second largest cell population in murine and human pancreatic islets. Up to 10-20% of the murine islet and 33-46% of the human islet consist of α-cells (Cabrera et al. 2006). In states of chronic hyperglycemia, such as T2DM, the portion of α-cells is even higher (Amo-Shiinoki et al. 2021). Secretion of glucagon from the α-cells (Gromada et al. 1997) is induced by hypoglycemia and promotes catabolic processes in peripheral tissues such as liver, muscle, kidney, and pancreas (Rix et al. 2000). In the liver for instance, glucagon signaling promotes gluconeogenesis and the release of generated glucose, thereby resulting in an increase in blood glucose levels (Bryla et al. 1977). In T2DM where α-cell mass (Amo-Shiinoki et al. 2021) but also circulating glucagon levels are increased (Müller et al. 1970), glucagon induced gluconeogenesis in the liver was shown contribute to hyperglycemia and T2DM progression. Glucagon signaling in β-cells or δ-cells induces insulin and somatostatin release, respectively (Kieffer et al. 1996; Capozzi et al. 2019). In rodents, glucagon inhibits ghrelin secretion from the ε-cells while in humans ghrelin secretion is stimulated (Qader et al. 2008).

δ-cells

The δ-cells synthesize and secrete somatostatin. In murine islets, δ-cells make up 5-10%, which is comparable to the amount observed in humans (Cabrera et al. 2006). Glucose, amino acids, and fatty acids promote somatostatin secretion which is not exclusively secreted from δ-cells but also from intestinal cells (Francis et al. 1990). Somatostatin inhibits insulin and glucagon secretion (Mandarino et al. 1981). Accordingly, somatostatin knock out mice display elevated circulating insulin and glucagon levels (Hauge-Evans et al. 2009). In T2DM, somatostatin secretion is increased (Hermansen et al. 1979) while total pancreatic somatostatin content is reduced (Henquin et al. 2017). This suggests that dysfunctional somatostatin secretion might be involved in the development or progression of T2DM (Rorsman and Huising 2018).

PP-cells

Pancreatic polypeptide Y secreting PP-cells make up to 5% of the murine islet and < 5% of the human islet (Cabrera et al. 2006). PP-cell numbers however strongly vary depending on gender and age although cell number is not affected by chronic hyperglycemia and T2DM (Stefan et al. 1982). Secretion of pancreatic polypeptide Y is induced postprandially. Accordingly, high levels of pancreatic polypeptide Y were shown to reduce food intake and appetite (Batterham et al. 2003). Its secretion promotes food digestion through the release of digestive enzymes (Adrian et al. 1976). Pancreatic polypeptide Y has no effects on insulin secretion (Bastidas et al. 1990) but represses glucagon (Aragón et al. 2015) and somatostatin release (Kim et al. 2014).

ε-cells

The ε-cells synthesize and secrete ghrelin and are the smallest cell population in the endocrine pancreas. During foetal and early postnatal life, pancreatic ε-cells represent the major source of ghrelin while in adults most of the ghrelin originates from the stomach (Wierup et al. 2002; Date et al. 2000). Accordingly ε-cell numbers are highest early in life and decrease over time (Wierup et al. 2002). Ghrelin promotes glucagon secretion while insulin, somatostatin, and

pancreatic polypeptide Y secretion are inhibited (Qader et al. 2008). Systemically, ghrelin promotes food intake and appetite (Wren et al. 2000). In T2DM patients, circulating ghrelin levels are lower in comparison to healthy subjects (Pöykkö et al. 2003).

β-cells

The insulin producing β-cells represent the largest cell population of the endocrine pancreas. In mice, β-cells make up 70-80% of the islet and are mainly located in the centre of the islet surrounded by glucagon producing α-cells. In humans, β-cells make up only ~55% and are distributed across the islet (Cabrera et al. 2006). High blood glucose levels are the main stimulus for insulin synthesis and secretion (Melloul et al. 1993; Fu et al. 2013). Insulin biosynthesis is tightly controlled on transcriptional and translational level, while proper insulin secretion is achieved in part through rate-limiting enzymes.

As most species, humans have one insulin gene (Harper et al. 1981), while rodents carry two non-allelic insulin genes, the *Ins1* (Insulin 1) and *Ins2* gene (Davies et al. 1994), of which *Ins2* corresponds to the single copy other species have. The insulin promoter region is located -300 to -100 base pairs prior to the transcription start site (German et al. 1995; Sharma and Stein 1994) and consists of regulatory elements serving as binding sites for transcription factors such as PDX1 (Qiu et al. 2002), MAF BZIP Transcription Factor A (MAFA) (Kataoka et al. 2002), and PAX6 (Sander et al. 1997). Through the recruitment of regulatory complexes and histone modifiers, transcription factors were shown to coordinate insulin transcription based on metabolic need (Mosley et al. 2004; Mosley and Ozcan 2004; McKenna et al. 2015). Like transcription, also translation of insulin is promoted by nutrients of which glucose appears to be the most important (Itoh and Okamoto 1980; Melloul et al. 1993). The insulin gene encodes for an insulin precursor, the preproinsulin which is cleaved and folded into proinsulin in the endoplasmic reticulum. Proinsulin is subsequently transported into the Golgi apparatus where it enters secretory vesicles and is further cleaved into mature insulin and the C-peptide (Fu et al. 2013) (Figure 3).

The main physiological signal for vesicle exocytosis and insulin release are increased circulating blood glucose levels at postprandial state (Fu et al. 2013). In addition, also amino acids (Herchuelz et al. 1984) and hormones such as glucagon-like polypeptide-1 (GLP1) or glucose-dependent insulinotropic polypeptide (GIP), secreted by intestinal endocrine cells were shown to induce insulin secretion (Wang et al. 1995; Fujimoto et al. 1978). Insulin secretion takes place in a biphasic manner: a triggering pathway referred to as the first phase of insulin secretion and a metabolic amplifying pathway, also known as the second phase (Henquin 2009). The first phase is induced by glucose uptake into the β-cell through the glucose transporter 2 (GLUT2) which is encoded by the *Slc2a2* (Solute carrier family 2 member 2) gene (Unger 1991). After entering the cell, glucose is phosphorylated by glucokinase (GCK), a hexokinase with a low glucose affinity to ensure glucose phosphorylation at high glucose levels only, making it a rate-limiting enzyme for glucose metabolism in the β-cell. Phosphorylated glucose is then metabolized by glycolysis into pyruvate which is subsequently oxidized in the tricarboxylic acid (TCA) cycle in mitochondria resulting in an increase in cellular adenosine triphosphate (ATP) levels (Fu et al. 2013). The increase in ATP induces a closure of ATP-sensitive potassium channels (Ashcroft et al. 1984; Cook and Hales 1984), depolarization of the membrane, and opening of voltage-dependent calcium channels (Rorsman et al. 1988). Calcium influx eventually triggers exocytosis of the insulin-containing granules (Rorsman et al. 1988) (Figure 3). This first phase results in a rapid release of insulin

shortly after the glucose stimulus. During the second phase, insulin is released at a lower but sustained rate spanning several hours (Henquin 2009).

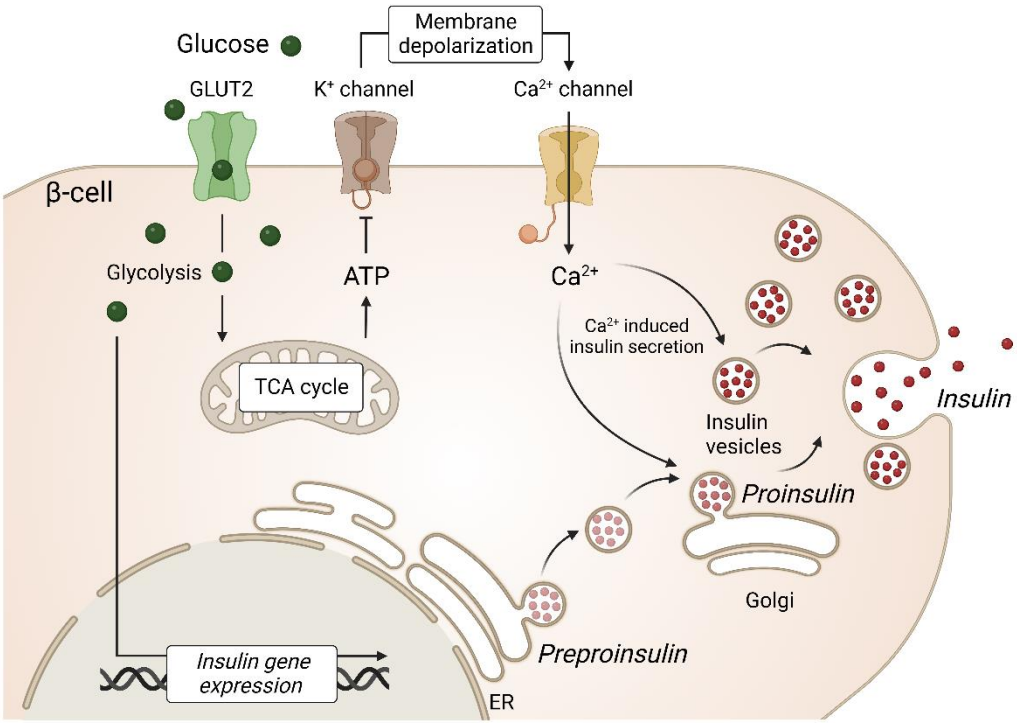

Figure 3: Glucose stimulated insulin secretion in pancreatic β-cells. The expression of the insulin gene, which encodes for the insulin precursor preproinsulin, is induced by glucose. In the endoplasmic reticulum (ER), preproinsulin is cleaved into proinsulin which is subsequently folded. The folded proinsulin is then transported from the ER into the Golgi apparatus where it is cleaved into mature insulin and C-peptide and stored in secretory vesicles. After uptake into the cell, glucose is metabolized through glycolysis into pyruvate which then enters the tricarboxylic acid (TCA) cycle in the mitochondria resulting in an increase in adenosine triphosphate (ATP) levels. ATP-sensitive potassium channels close which leads to a depolarization of the cell membrane. Voltage-dependent calcium channels open, leading to a calcium influx which triggers the exocytosis of insulin vesicles. Adopted from "Insulin Production Pathway", by Biorender.com (2023).

In peripheral tissues, insulin signaling promotes glucose uptake and utilization (Kashiwagi et al. 1983; Kelley et al. 1993), thereby lowering blood glucose levels. Moreover, insulin was shown to promote somatostatin secretion from the δ-cells and inhibit glucagon secretion from the α-cells. A recent study demonstrated that the inhibitory effects on α-cells are not directly induced by insulin but are driven by the induction of somatostatin secretion which in turn inhibits glucagon release (Vergari et al. 2019).

1.2.3 Pathophysiology of pancreatic β-cells – the progressive loss of maturity and identity

Under physiologic conditions, adult β-cells are fully differentiated and mature, which is required for optimal β-cell function. In mice, after β-cell differentiation, β-cells are still immature and lack the expression of β-cell identity genes (Blum et al. 2012; Hang et al. 2014), induce insulin secretion at lower blood glucose levels (Otonkoski et al. 1988), and are highly proliferative (Meier et al. 2008; Swenne 1983). β-cell maturation is biphasic and takes place in the first two weeks of life which is also referred to as the first wave of maturation. During this period a general increase in endocrine mass is observed suggesting that β-cells are still proliferative. With the progression of maturation, the proliferative capacity is however lost (Swenne 1983; Meier et al. 2008). The second wave of maturation coincides with the weaning period and is triggered by the transition from high fat mother's milk to high carbohydrate chow diet (Stolovich-Rain et al. 2015). During this time, β-cells acquire the expression of maturity marker such as

Syt4 (Synaptotagmin 4), which promotes glucose stimulated insulin secretion at high glucose levels (Huang et al. 2018) or *Ucn3* (Urocortin 3), of which the physiological function is currently not completely understood (Blum et al. 2012).

β-cell maturity is a fragile state and requires tightly controlled expression of β-cell enriched markers, the identity genes, and the repression of disallowed genes. β-cell identity genes are highly or exclusively expressed in β-cells (Xin et al. 2016) and are implicated in β-cell maturation, function, insulin gene expression, insulin granule formation, and exocytosis. MAFA for instance was identified as key transcription factor for insulin, but was also shown to promote glucose stimulated insulin secretion (Kataoka et al. 2002; Hang et al. 2014; Wang et al. 2007). Another example for a β-cell identity gene is *Gck* which encodes for GCK, the main hexokinase in the β-cells. In contrast to hexokinases expressed in other tissues, GCK has a low affinity to glucose. Thus, glucose phosphorylation and subsequent glucose stimulated insulin secretion is catalyzed only at high glucose levels. In contrast, β-cell disallowed genes are genes that are expressed in almost all mammalian tissues, but are selectively repressed in β-cells (Thorrez et al. 2011; Dhawan et al. 2015). *Hk1* (Hexokinase 1), which encodes for a hexokinase with a higher glucose affinity in comparison to GCK, is such a disallowed gene. Another example is *Ldha* (Lactate dehydrogenase), which is required for the conversion of the glycolysis end product pyruvate into lactate. Continuous repression of *Ldha* ensures that pyruvate is not converted into lactate but instead undergoes oxidation in the mitochondria to produce ATP (Ainscow et al. 2000). Thus, disallowed genes often express proteins or enzymes that would impair β-cell function. Disallowed genes require continuous repression, which is facilitated by β-cell enriched transcription factors such as PAX6 (Swisa et al. 2017) or NKX2.2 (Gutiérrez et al. 2017). Interestingly, PAX6, itself a β-cell identity gene, was shown to induce the expression of β-cell identity genes and simultaneously repress the expression of disallowed genes (Gosmain et al. 2012; Swisa et al. 2017). How PAX6 achieves this bidirectional gene expression is not completely understood.

The dysregulation of transcriptional events in β-cells is closely linked to the development of β-cell failure and ultimately T2DM. Development and progression of T2DM is initiated by peripheral insulin resistance which is first compensated by increased insulin secretion and hyperplasia of β-cells (Karam et al. 1963; Kim et al. 2009). Later, β-cells fail to compensate (Kulkarni et al. 1999) which is in part induced by chronic hyperglycemia and dyslipidemia also known as glucotoxicity and lipotoxicity. Since the exposure of pancreatic islets to high glucose concentrations or free fatty acids was shown to induce apoptosis (Efanova et al. 1998; Shimabukuro et al. 1998), this increase in apoptotic events was thought to cause reduced β-cell mass and insufficient circulating insulin levels observed upon chronic hyperglycemia, further contributing to T2DM progression (Butler et al. 2003). However, the apoptotic events did not fully explain the β-cell deficit observed upon T2DM (Amo-Shiinoki et al. 2021; Talchai et al. 2012; Swisa et al. 2017; Taylor et al. 2013).

In 2012, Talchai and colleagues proposed the loss of β-cell characteristics, termed β-cell dedifferentiation as novel mechanism through which β-cells fail and are lost in T2DM (Talchai et al. 2012). β-cell dedifferentiation is characterized by progressive loss of β-cell identity gene expression and subsequent increase in disallowed gene expression, resulting in a loss of functional β-cell mass (Talchai et al. 2012; Swisa et al. 2017; Gutiérrez et al. 2017). Accordingly, transcriptomic profiling revealed that expression of identity genes is reduced while the expression of disallowed genes is strongly increased in states of chronic hyperglycemia and dyslipidemia such as T2DM (Xin et al. 2016; Jonas et al. 1999; Amo-Shiinoki et al. 2021).

Apart from hyperglycemia, also oxidative stress, endoplasmic reticulum stress, and inflammation were shown to promote β-cell dedifferentiation (Lombardi et al. 2012; Nordmann et al. 2017; Talchai et al. 2012). The loss of β-cell identity is also associated with the reoccurrence of endocrine progenitor markers like *Ngn3* (Swisa et al. 2017; Schwitzgebel et al. 2000; Gradwohl et al. 2000) or *Cd81* (Cluster of differentiation 81) (Salinno et al. 2021), indicating that β-cells return to a progenitor-like state. These alterations promote a reprogramming of the β-cell, forcing the cell to exit the mature and functional state resulting in defective β-cells and abnormal glucose stimulated insulin secretion. Loss of cellular identity also coincides with the upregulation of genes characteristic for other cell types of the endocrine pancreas such as glucagon, somatostatin, or ghrelin (Taylor et al. 2013; Swisa et al. 2017). Lineage tracing experiments indeed demonstrated that β-cells which lost their identity, first returned into a progenitor-like state and eventually adopted the fate of δ-cells (Taylor et al. 2013) or ε-cells (Swisa et al. 2017). In other studies, β-cells were shown to directly convert into other terminally differentiated cell types. This reprogramming of differentiated β-cells is referred to as transdifferentiation and was observed upon PDX1 or NKX2.2 deficiency where β-cells converted into α- or δ-cells, respectively (Gutiérrez et al. 2017; Gao et al. 2014).

Of note, in opposite to dedifferentiation, transdifferentiation was only observed in knock out studies and not upon chronic hyperglycemia and T2DM thus far (Wang et al. 2014). This suggests that dedifferentiation and the return to a progenitor-like state with a subsequent adaptation of other cell fates represents a mechanism with a higher relevance for T2DM development in humans. Normalization of blood glucose levels through insulin therapy sufficiently restored β-cell identity gene expression and reduced *Ngn3* expression. Thus, loss of β-cell identity due to chronic hyperglycemia was shown to be reversible (Wang et al. 2014) (Figure 4).

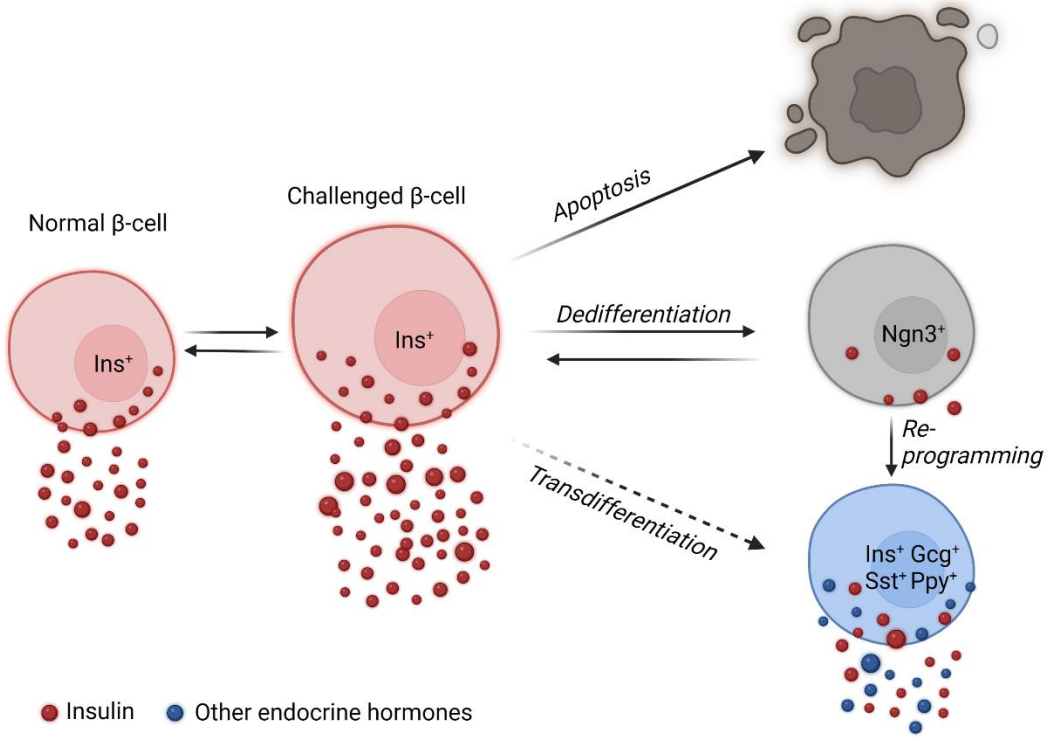

Figure 4: Chronic hyperglycemia and dyslipidemia induce β-cell dysfunction, dedifferentiation, and reprogramming. Normal β-cells are able to compensate for metabolic challenges such as insulin resistance by hyperplasia and elevated insulin secretion. Chronic hyperglycemia and dyslipidemia however result in apoptosis or a loss of β-cell identity, of which the latter represents a reversible state. Dedifferentiated β-cells enter a progenitor-like state, and are unable to properly secrete insulin and display an upregulation of progenitor marker expression

such as Neurogenin3 (Ngn3). Dedifferentiated β-cells can be also reprogrammed resulting in the expression of hormones typical for other cell types of the endocrine pancreas such as glucagon (Gcg), somatostatin (Sst), or pancreatic polypeptide Y (Ppy). The direct transdifferentiation from β-cells to other terminally differentiated cell types was observed in few murine studies but is rarely observed in humans. Created with Biorender.com. Adapted from (Dor and Glaser 2013).

In summary, in addition to undergoing apoptosis, metabolically challenged β-cells can lose their identity, which is accompanied by reduced β-cell identity gene and increased disallowed and progenitor-cell gene expression. The upregulation of disallowed and progenitor genes causes β-cells to exit their mature and differentiated state, leading to dysfunctional and insufficient glucose stimulated insulin secretion, further promoting T2DM. Reversibility of the progressive loss of β-cell identity highlights the potential for novel therapeutical approaches and the need for an in depth understanding of how β-cell identity and disallowed gene expression are regulated.

1.3 The transcription co-factors transducin β-like 1 (TBL1) and transducin β-like related 1 (TBLR1)

1.3.1 TBL1 and TBLR1 control transcriptional events as transcription co-factors

Metabolic processes are highly flexible and assure rapid adaptation to nutrient and energetic demands. This flexibility is facilitated by dynamic but also tightly controlled gene expression, mediated by transcription factors and nuclear receptors which signal dependently induce or repress transcription. Whether transcription is induced or repressed is coordinated by regulatory proteins – co-activators and co-repressors, which are recruited as complexes context specifically to the transcription factors. Although co-regulators do not directly bind to DNA, they induce histone modifications, chromatin remodelling, or DNA methylation. Modification of histone tails by acetylation, methylation, ubiquitination, or SUMOylation affect chromatin structure, DNA accessibility, and thereby whether transcription is induced or repressed (Perissi et al. 2010). Methylation of histones is associated with induction and repression of transcription depending on which amino acids are methylated and how many methyl groups are attached (Greer and Shi 2012). One example of a regulatory complex that promotes gene expression through recruitment of a demethylase to modify histone methylation, is the facilitates chromatin transcription (FACT) complex (Frost et al. 2018). An upregulation of the FACT complex, which comprises of the two subunits SPT16 homolog facilitates chromatin remodelling subunit (SUPT16H) and structure specific recognition protein 1 (SSRP1), is associated with cancer development and progression (Hudson et al. 2007; Garcia et al. 2011). Also histone acetylation is associated with the induction of gene expression (Hebbes et al. 1988). Acetylation takes place on lysine residues of the histones and neutralizes the positive charge of the tails. This decreases the interaction with the negatively charged DNA, resulting in relaxation of the chromatin and improved accessibility of the regulatory regions by transcriptional proteins (Lee et al. 1993; Hong et al. 1993). Accordingly, deacetylation results in compression of the chromatin and repression of transcription. One of the better studied co-repressors that modify chromatin structure through deacetylation is the nuclear receptor corepressor (NCOR)/silencing mediator of retinoic acid and thyroid hormone receptors (SMRT) repressor complex. This multi-protein complex comprises of NCOR, SMRT, histone deacetylase 3 (HDAC3), G protein pathway suppressor 2 (GPS2), transducin β-like 1, x-linked (TBL1X, hereafter referred to as TBL1) and transducin β-like 1, x-linked-related 1 (TBL1XR1, hereafter referred to as TBLR1) (Guenther et al. 2000; Yoon et al. 2003) and is preferentially recruited to unliganded nuclear receptors and transcription factors to induce transcriptional repression through deacetylation of histones (Ishizuka and Lazar 2003, 2005).

Depending on the signal, transcription factors interact with activator or repressor complexes, which requires coordinated recruitment and dismissal of the respective regulators. Although the transcription co-factors TBL1 and TBLR1 were identified as core components of the NCOR/SMRT repressor complex, they were found to mediate the signal dependent exchange of co-activators and co-repressors and are therefore also referred to as “nuclear exchange factors”. Regulatory complex exchange is induced through the recruitment of the ubiquitin/19S proteasome to the NCOR/SMRT repressor complex which is subsequently ubiquitinated and degraded by the proteasome, enabling co-activator binding (Perissi et al. 2004) (Figure 5).

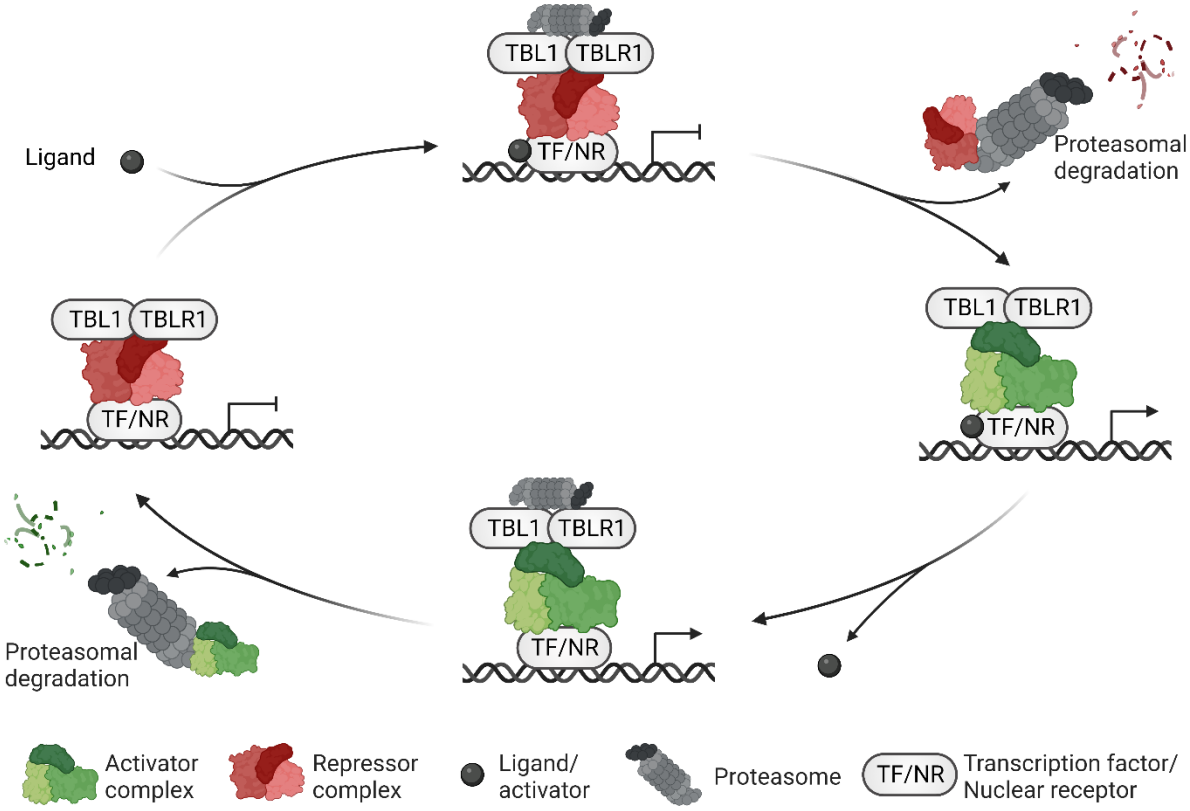

Figure 5: TBL1 and TBLR1 mediate transcriptional events through the exchange of regulatory complexes ligand or signal dependently. Unliganded transcription factors and nuclear receptors (TF/NR) predominantly bind to repressor complexes resulting in repression of transcription. Ligand binding induces recruitment of the proteasome, resulting in dismissal and proteasomal degradation of the repressor complex and binding of an activator complex all together facilitated by TBL1 and TBLR1. Binding of the activator complex promotes activation of transcription. Without ligand binding, TBL1 and TBLR1 facilitate dismissal of the activator complex resulting in its subsequent proteasomal degradation while a repressor complex is recruited. Created with Biorender.com. Adapted from (Perissi et al. 2004).

Although TBL1 and TBLR1 are highly homologous and share 90% of their protein sequence, they do not necessarily possess identical functions. For instance, TBL1 mediates the dismissal of the co-repressor C-terminal binding protein (CTBP) 1 and 2, while TBLR1 is required for NCOR/SMRT dismissal (Perissi et al. 2008). Moreover, while only TBLR1 is required for activator protein 1 (AP1) and retinoic acid receptor (RAR) mediated transcription, both TBL1 and TBLR1 induce activation of nuclear factor k-light-chain-enhancer of activated B cells (NFκB) targets or thyroid hormone signaling (Perissi et al. 2004). This highlights the diverse functions that TBL1 and TBLR1 have and indicates their importance in metabolic regulation.

1.3.2 TBL1 and TBLR1 – regulators of cell metabolism and cell fate

Full body knock out of TBL1 and TBLR1 is embryonically lethal, which underlines their importance for developmental processes and metabolism (Perissi et al. 2010). Functional

studies revealed an implication in liver and adipose tissue lipid metabolism (Kulozik et al. 2011; Rohm et al. 2013). In the liver, TBL1 and TBLR1 control peroxisome proliferator-activated receptor (PPAR) α mediated fatty acid oxidation through the recruitment and dismissal of regulatory complexes. Hence, TBL1 and TBLR1 deficiency in the liver led to impaired dismissal of the NCOR/SMRT repressor complex and therefore sustained repression of genes involved in fatty acid oxidation, resulting in lipid accumulation in the liver and ultimately steatosis. Accordingly, TBL1 expression negatively correlated with liver triglyceride content in humans and was downregulated in mouse models of hepatic steatosis (Kulozik et al. 2011). In contrast to the liver, only TBLR1 was implicated in adipose tissue lipid metabolism. Adipose tissue TBLR1 levels were increased in obese individuals and positively correlated with serum triglycerides and free fatty acids. Accordingly, adipose tissue specific TBLR1 deficiency promoted adiposity and impaired fasting induced lipolysis in mice. Work from our laboratory demonstrated that TBLR1 regulates fasting-induced lipolysis through physical interaction with PPARγ/ retinoid X receptor (RXR) α and additionally controls the transcription of key enzymes involved in lipolysis (Rohm et al. 2013).

Apart from their role in transcriptional events regulating cellular metabolism, TBL1 and TBLR1 were found to control multiple layers of oncogenesis. For instance, through phosphatidylinositol 3-kinase (PI3K)/protein kinase B (AKT) and β-catenin signaling, TBL1 and TBLR1 were found to promote proliferation and inhibit apoptosis in cancer cells (Stoy et al. 2015; Gu et al. 2020; Li et al. 2014). Accordingly, TBL1 and TBLR1 coordinate Wnt-signaling through direct interaction with β-catenin (Li et al. 2014; Li and Wang 2008), which is mediated by TBL1 and TBLR1 SUMOylation (Park et al. 2016; Choi et al. 2011). Moreover, TBL1 was shown to promote epithelial to mesenchymal transition (EMT) and thereby tumour aggressiveness and metastasis formation, in part through the activation of the Wnt/β-catenin signaling pathway (Rivero et al. 2019; Xu et al. 2022). Thus, TBL1 and TBLR1 were proposed as prognosis markers for cancer malignancies (Stoy et al. 2015; Rivero et al. 2019; Li et al. 2014). Wnt-signaling, central to development, proliferation, and specification of cell fate is also required for the maintenance of the undifferentiated state in embryonic stem cells (Sato et al. 2004). Accordingly, upregulation of Wnt-signaling in terminally differentiated cells was shown to reactivate progenitor-cell markers through which cells acquire stem cell-like properties such as self-renewal or induction of EMT (Schwitalla et al. 2013). The reactivation of a progenitor or stem cell-like program - also referred to as dedifferentiation - due to continuous Wnt-signaling was associated with carcinogenesis (Schwitalla et al. 2013; Perekatt et al. 2018). Given that TBL1 and TBLR1 are central to Wnt/β-catenin signaling and were previously associated with carcinogenesis, EMT, and tumour aggressiveness, it is tempting to speculate that TBL1 and TBLR1 might also be involved in Wnt-induced loss of cellular identity.

Dedifferentiation was previously identified as major contributor to β-cell mass reduction in T2DM. TBL1 and TBLR1 are involved in a broad range of transcriptional events and metabolic diseases, but also oncogenesis through their direct implication in Wnt-signaling, which was previously associated with loss of cellular identity. This highlights the importance of proper TBL1 and TBLR1 function and action not only in the context of cancer but also in metabolic tissues affected by dedifferentiation such as β-cells. Thus, the investigation of TBL1 and TBLR1 regulated pathways in pancreatic β-cells would contribute to a better understanding of processes involved in T2DM development such as dedifferentiation and would provide novel targets for therapeutic approaches.

1.4 Aims and objectives

T2DM is characterized by a progressive loss of β-cell identity induced by chronic hyperglycemia and dyslipidemia. Although β-cell enriched transcription factors central to β-cell identity maintenance were identified in previous studies, the exact mechanisms on how these factors facilitate the tightly coordinated transcriptional events remain elusive. The transcription co-factors TBL1 and TBLR1 are implicated in cell fate, regulation of metabolism, and transcriptional events. As TBL1 and TBLR1 interact with a variety of transcription factors and nuclear receptors, but also with regulatory complexes signal and cell type specifically, they represent ideal candidates to investigate processes involved in maintenance of β-cell identity. By generating mice with a conditional and induced β-cell specific TBL1 and/or TBLR1 knock out, the general role of TBL1 and TBLR1 in β-cells but also their possible function as regulators of β-cell identity will be investigated. Importantly, transcriptomic profiling of islets from mice deficient for β-cell specific TBL1 and/or TBLR1 will identify genes and biological processes under the control of TBL1 and TBLR. The determination of direct TBL1 and TBLR1 interaction partners using an interactome screen aims to understand the interplay between TBL1, TBLR1, and potential regulators of β-cell identity under physiological and pathological circumstances. Ultimately, this study will increase the current understanding on how β-cell identity is maintained and lay the foundation for novel treatment approaches for T2DM.

2 RESULTS

2.1 Analysis of TBL1 and TBLR1 expression in pancreatic β-cells

2.1.1 Gluco- and lipotoxicity alter TBL1 and TBLR1 expression in INS1E cells and mouse islets but not in human islets

Chronic hyperglycemia and dyslipidemia as they occur in long-term obesity are detrimental for β-cell function and physiology, ultimately resulting in β-cell stress and failure (Fu et al. 2013). The Attie Lab Diabetes Database reported a downregulation of TBL1 islet gene expression in a genetic mouse model of obesity, while TBLR1 expression was unchanged (http://diabetes.wisc.edu/). This suggests that TBL1 expression might be associated with changes in glycemia and lipidemia and consequently with β-cell function and physiology. To investigate whether the expression of TBL1 but also the expression of its homolog TBLR1 are affected by β-cell dysfunction as a result of glucose excursions, hyperglycemia was mimicked *in vitro* in cultured β-cells and *ex vivo* in primary mouse and human islets. For this INS1E cells and pancreatic islets were chronically exposed to glucose.

In INS1E cells, glucose reduced TBL1 and TBLR1 gene expression in a dose dependent manner (Figure 6A). After 96 h also TBLR1 protein levels were reduced, while TBL1 protein levels were slightly but non-significantly reduced (Figure 6B,C). Murine islets cultivated in 25 mM glucose also showed lower TBLR1 gene expression levels in comparison to islets cultivated at 5 mM glucose, which however was not observed for TBL1 (Figure 6D). In human pancreatic islets, TBL1 and TBLR1 gene expression was unchanged after cultivation for 72 h with 1 mM, 2.8 mM, 5.5 mM, 11 mM, and 16.8 mM glucose (Figure 6E).

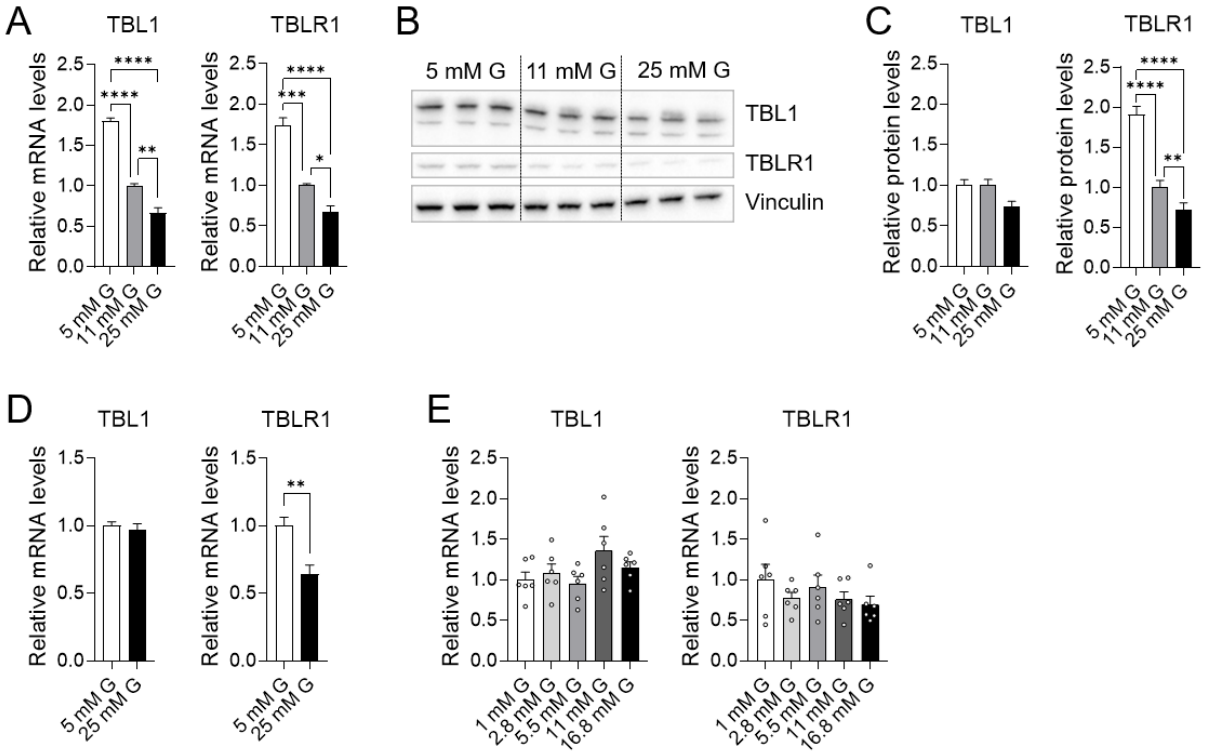

Figure 6: TBL1 and TBLR1 gene and protein expression in INS1E cells, murine islets, and human pancreatic islets after glucose exposure. (A) INS1E cells were cultivated in 5 mM, 11 mM, or 25 mM glucose for 48 h to determine TBL1 and TBLR1 gene expression (n=6) via qPCR **(B)** and for 96 h to determine protein expression with Western Blot using the indicated antibodies. **(C)** TBL1 and TBLR1 protein levels from (B) were normalized to Vinculin levels and quantified using Image J. **(D)** Murine islet TBL1 and TBLR1 gene expression was determined after 48 h of cultivation in 5 mM or 25 mM (n=4) glucose. **(E)** Human pancreatic islets were cultivated in 1 mM, 2.8 mM, 5.5 mM, 11 mM, or 16.8 mM glucose for 72 h. Subsequently, TBL1 and TBLR1 gene expression was

determined using qPCR. Data is presented as mean ± standard error of the mean (SEM). Statistical analysis was performed using an unpaired t-test (D) or a two-way analysis of variance (ANOVA) with a Tukey's multiple-comparison *post hoc* test (A,C,E). *p < 0.05, **p < 0.01, ***p < 0.001, ****p < 0.0001.

Apart from hyperglycemia, mouse models of obesity and obese individuals display dyslipidemia (Rochlani et al. 2017). The detrimental effects that chronically elevated lipid metabolites have on β-cells are referred to as lipotoxicity (Shimabukuro et al. 1998; Fu et al. 2013). To investigate whether β-cell TBL1 and TBLR1 levels are affected by a lipotoxic environment, INS1E cells and murine islets were chronically exposed to palmitate conjugated to bovine serum albumin (BSA). In INS1E cells, TBL1 and TBLR1 gene expression was significantly reduced after treatment with 300 µM palmitate for 48 h (Figure 7A). No changes in TBL1 and TBLR1 expression were observed in murine islets treated with 300 µM palmitate for 48 h (Figure 7B).

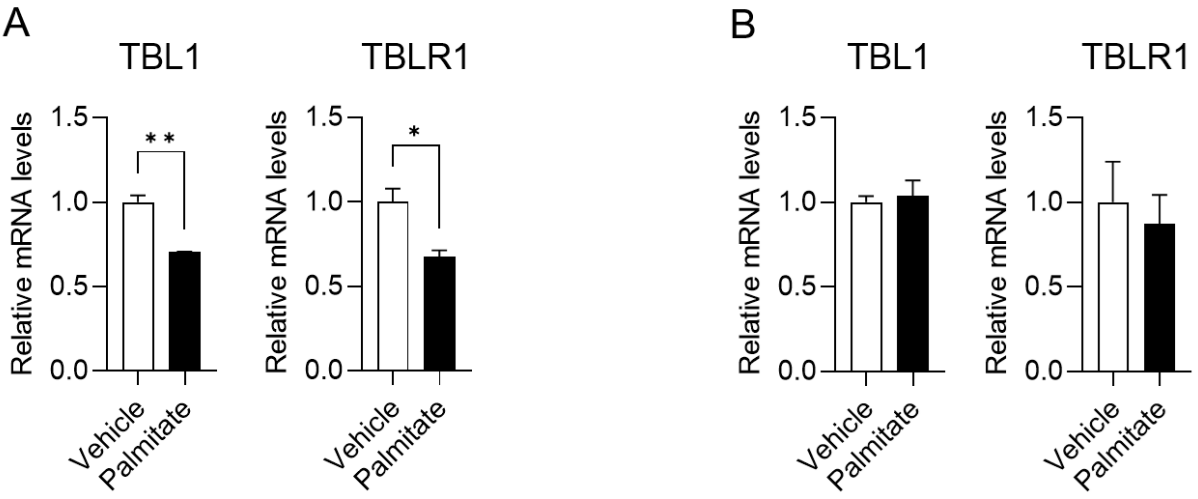

Figure 7: TBL1 and TBLR1 gene expression in INS1E cells and murine islets after palmitate treatment. (A) TBL1 and TBLR1 gene expression in INS1E cells exposed to 300 µM palmitate conjugated to BSA or vehicle for 48 h (n=4). **(B)** Murine islet TBL1 and TBLR1 gene expression after treatment with 300 µM palmitate conjugated to BSA or vehicle for 48 h (n=4). Data is presented as mean ± SEM. Statistical analysis was performed using an unpaired t-test. *p < 0.05, **p < 0.01.

2.1.2 Islet TBL1 and TBLR1 expression is altered in mouse models of aging, obesity, and diabetes

Due to the genetic and physiologic similarity to humans, mice represent a highly potent model to investigate human biology and diseases. In many cases, mice resemble human diseases and are therefore widely used to understand disease causes, to investigate the underlying mechanisms, or to develop novel treatment approaches (Rosenthal and Brown 2007). In this study, *in vitro* and *ex vivo* glucose treatment of INS1E cells and murine islets pointed towards an association between TBL1/TBLR1 expression and β-cell function. To investigate this under physiologic conditions, TBL1 and TBLR1 gene expression was determined in pancreatic islets from mouse models of β-cell stress and failure.

Aging-associated insulin resistance is a major contributor to β-cell stress and thereby promotes the development of age-related diabetes (Møller et al. 2003). Thus, TBL1 and TBLR1 expression was determined in pancreatic islets from young (2 months) and aged (18 months) mice. While TBL1 gene expression was reduced in aged mice in comparison to young mice, TBLR1 gene expression was unchanged (Figure 8A), which is in line with alterations in islet TBL1 and TBLR1 expression observed in the Attie Lab Diabetes Database. As for aging, diet-induced obesity is associated with insulin resistance. Moreover, the underlying lipotoxicity represents an additional burden for the β-cells (Fu et al. 2013). To mimic diet-induced obesity,

mice were put on a high fat diet (HFD) containing 60% calories from fat for 18 weeks. Islet TBL1 expression was not altered while TBLR1 gene expression was reduced (Figure 8B). Lastly, TBL1 and TBLR1 expression was determined in pancreatic islets from mice lacking the leptin receptor gene (*db/db*), a widely used mouse model for T2DM (Neelankal John et al. 2018). While TBL1 gene expression was reduced, TBLR1 expression was increased (Figure 8C), overall, indicating that TBL1 and TBLR1 islet expression levels are dysregulated in mouse models β-cell stress and diabetes.

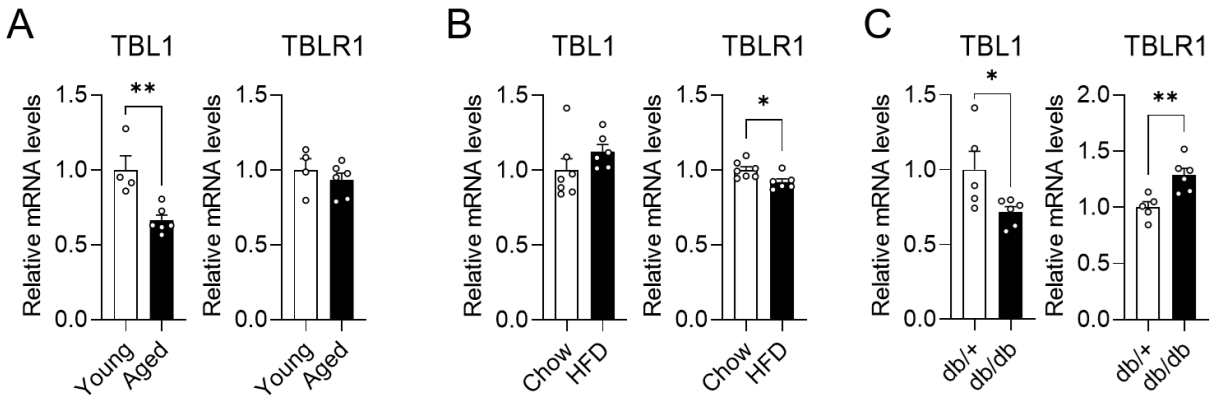

Figure 8: TBL1 and TBLR1 gene expression in mouse models of diabetes and β-cell stress. (A) TBL1 and TBLR1 gene expression in pancreatic islets from mice at the age of 2 months (Young) or 18 months (Aged). **(B)** TBL1 and TBLR1 gene expression in pancreatic islets from mice fed standard chow diet (Chow) or a high fat diet (HFD) containing 60% calories from fat for 18 weeks starting at the age of 8 weeks. **(C)** TBL1 and TBLR1 gene expression in pancreatic islets from 8 week old *db/db* mice and heterozygous control (*db/+)* mice. Data is presented as mean ± SEM. Statistical analysis was performed using an unpaired t-test. *p < 0.05, **p < 0.01.

2.1.3 TBL1 and TBLR1 expression is unchanged in human islets upon diabetes or aging

As described above, TBL1 and TBLR1 mRNA levels were found to be dysregulated in various mouse models of β-cell stress and diabetes. In particular upon aging and chronic hyperglycemia, TBL1 expression was reduced while TBLR1 gene expression was unaffected or increased. Therefore, TBL1 and TBLR1 gene expression was determined in human pancreatic islets comparing young and aged but also non-diabetic and diabetic organ donors. Table 1 summarizes donor characteristics.

Table 1: Clinical parameters of human pancreatic islet donors. All values are presented as mean ± SEM.

	Young	**Aged**
Age [years]	25.7 ± 3.6	67.6 ± 3.2
Sex	2 f / 9 m	2 f / 11 m
BMI [kg/m^2]	27.6 ± 4.5	27.5 ± 3.1
HbA1c [%]	5.3 ± 0.4	5.6 ± 0.2

	Non-diabetic (ND)	**Type 2 diabetic (T2DM)**
Age [years]	49.4 ± 7.3	57.3 ± 4.1
Sex	2 f / 5 m	2 f / 4 m
BMI [kg/m^2]	27.0 ± 2.8	26.9 ± 4.1
HbA1c [%]	4.9 ± 0.6	8.2 ± 1.3

Islet TBL1 and TBLR1 gene expression was unchanged between young (Age = 25.7 ± 3.6) and body mass index (BMI)- and hemoglobin A1c (HbA1c)-matched aged (Age = 67.6 ± 3.2) organ donors (Figure 9A). Also, no differences in islet TBL1 and TBLR1 expression between non-diabetic (ND, HbA1c = 4.9 ± 0.6) and BMI-matched type 2 diabetic donors (T2DM,

HbA1c = 8.2 ± 1.3) were observed (Figure 9B). A subsequently performed Pearson correlation analysis revealed no correlation between TBL1 or TBLR1 expression and age (Figure 9C,D). Also, TBLR1 mRNA levels and HbA1c did not correlate (Figure 9F). Interestingly, a non-significant trend towards negative correlation between TBL1 mRNA levels and HbA1c was observed (Figure 9E), further suggesting that TBL1 expression may be associated with the functionality and well-being of β-cells.

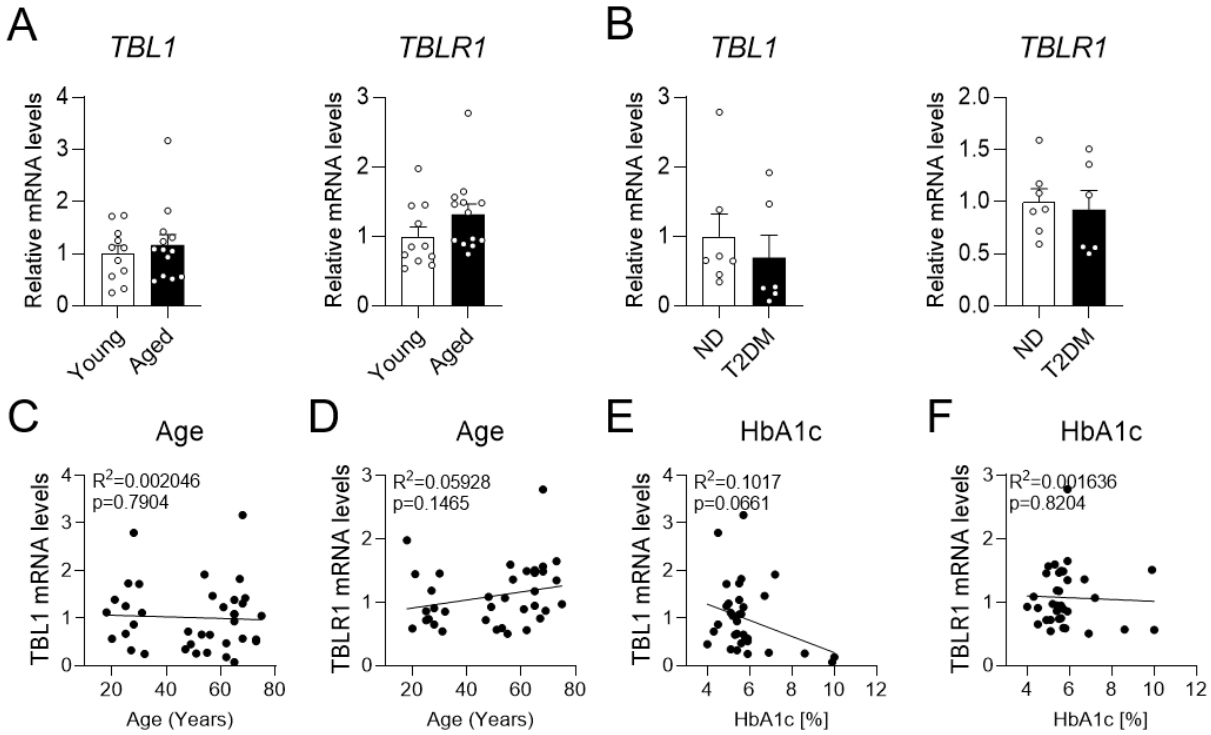

Figure 9: TBL1 and TBLR1 expression in human pancreatic islets. (A) Islet TBL1 and TBLR1 gene expression from 11 young (Age = 25.7 ± 3.6) and 13 aged (Age = 67.6 ± 3.2) organ donors. **(B)** Islet TBL1 and TBLR1 gene expression from 7 non-diabetic (ND; HbA1c = 4.9 ± 0.6) and 6 type 2 diabetic (T2DM; HbA1c = 8.2 ± 1.3) organ donors. Correlation analysis between Age and islet **(C)** TBL1 or **(D)** TBLR1 gene expression (n = 37). Correlation analysis between HbA1c and islet **(E)** TBL1 or **(F)** TBLR1 gene expression (n = 34). Pearson correlation coefficients and significance are displayed in each diagram. Data is presented as mean ± SEM (A,B). Statistical analysis was performed using an unpaired t-test (A,B) or a linear regression (C-F).

2.2 Generation of β-cell specific TBL1 and/or TBLR1 knock out mice

Cre/LoxP is a widely and frequently used site-specific recombinase system to cell type and time specifically manipulate genes. It thereby enables the identification of the tissue or developmental stage-specific function of a gene within an animal model. To achieve tissue specific manipulation of a gene, the Cre recombinase gene is inserted after a cell type-specific promoter and is thus expressed only in that particular cell type. Upon expression, the Cre recombinase protein recognizes two directly repeated loxP sites. Depending on the direction of the loxP sites the Cre induced recombination results in deletion, inversion, or translocation of the flanked regions (Kim et al. 2018).

In order to investigate the role of TBL1 and TBLR1 in pancreatic β-cells *in vivo*, conditional β-cell specific TBL1 and/or TBLR1 knock out mice were generated on a C57BL/6N background. To accomplish a β-cell specific knock out, mice carrying the Cre recombinase gene under the control of the insulin 1 gene (*Ins1*) promoter were used (Ins1Cre). Ins1Cre mice (B6(Cg)-*Ins1*$^{tm1.1(cre)Thor}$/J) were generated by Thorens et al. (Thorens et al. 2015) and purchased from *The Jackson Laboratory*. The conditional knock out was induced by backcrossing Ins1Cre mice to a C57BL/6N background and a subsequent crossing with floxed TBL1 or TBLR1 mice.

Floxed TBL1 (C57BL/6NTac-*Tbl1x*^{tm3495Arte}) and TBLR1 (C57BL/6-*Tbl1xr1*^{tm2273Arte}) mice were generated by Taconic Artemis. In the TBL1 flox and TBLR1 flox mice, loxP sites were flanking exon 5, which encodes for the F-box-like domain resulting in loss of function of the TBL1 or TBLR1 protein upon Cre recombination. Floxed TBL1 and TBLR1 litter mates genotyped negatively for the Cre recombinase were used as controls.

2.2.1 Mice heterozygous for Ins1Cre show normal glycemia and insulinemia, but reduced insulin gene expression

To exclude that any phenotype observed in the TBL1 or TBLR1 knock out mice is driven exclusively by the presence of Ins1Cre, first mice carrying the Ins1Cre but not the floxed TBL1 or TBLR1 were phenotyped. A previous study determined the efficiency and tissue specificity of the Ins1Cre mouse line (Thorens et al. 2015). Since Thorens and colleagues determined random glycemia and glycemia during an intraperitoneal glucose tolerance test (ipGTT) only (Thorens et al. 2015), mice heterozygous for Ins1Cre were characterized in this study prior to phenotypic characterization of the respective knock out mouse lines. In line with Thorens et al., body weight (Figure 10A), blood glucose levels (Figure 10B), and blood glucose clearance in an ipGTT (Figure 10C) did not differ significantly between Ins1Cre^{+} mice and Ins1Cre^{-} control mice. Moreover, no differences in fasting and refeeding blood glucose (Figure 10D) and plasma insulin (Figure 10E) were observed, suggesting an intact insulin secretion machinery.

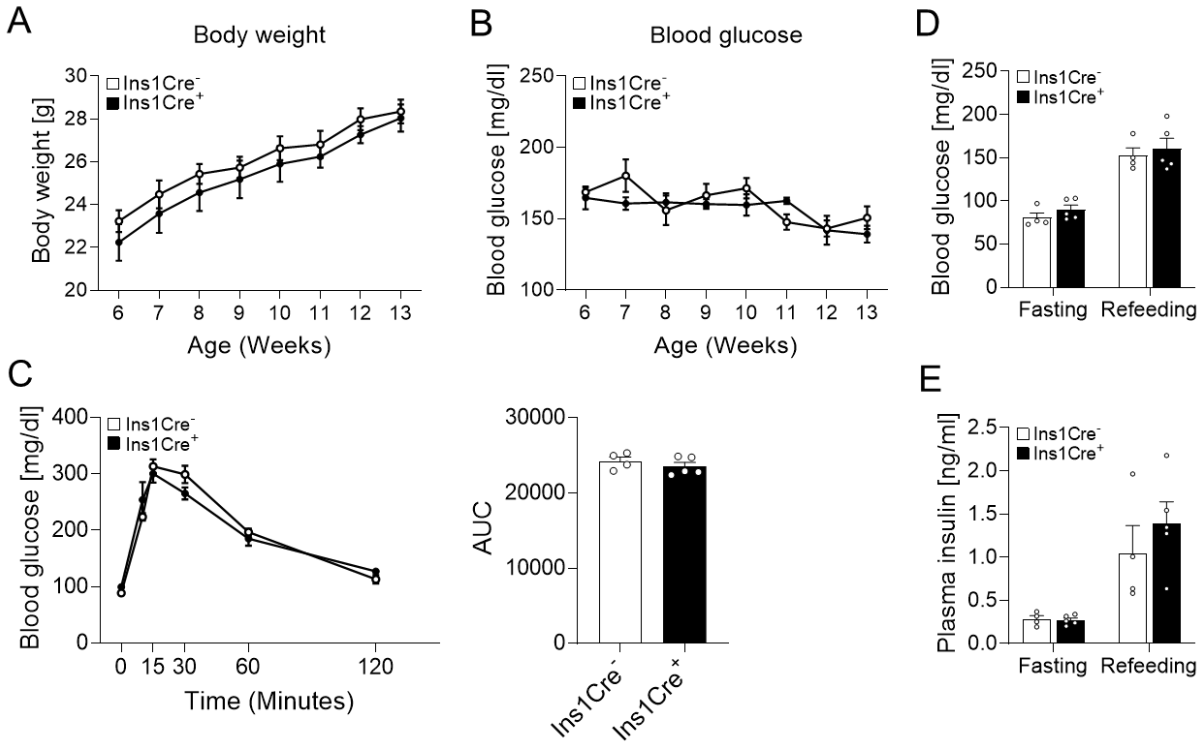

Figure 10: Mice heterozygous for Ins1Cre do not differ in glycemia and insulin secretion from control litter mates. (A) Body weight, **(B)** random blood glucose levels, **(C)** glucose clearance and area under the curve (AUC) during an ipGTT, fasting and refeeding **(D)** blood glucose and **(E)** plasma insulin levels of heterozygous Ins1Cre^{+} and Ins1Cre^{-} control litter mates. Data is presented as mean ± SEM. Statistical analysis was performed using an unpaired t-test (C for AUC), or a two-way ANOVA with repeated measures and a Šídák's multiple comparison *post hoc* test (A-C), or a two-way ANOVA with a Šídák's multiple comparison *post hoc* test (D,E).

Moreover, serum from Ins1Cre^{+} and Ins1Cre^{-} mice was analyzed using the Serum Analyzer from Beckmann Coulter to investigate whether effects on lipid or liver metabolism occur. No differences in lipid metabolism markers such as cholesterol, triglycerides, non-esterified fatty acids (NEFA), low density lipoprotein (LDL), high density lipoprotein (HDL), or ketone bodies were observed (Figure 11A-F). Also, lactate dehydrogenase (LDH) (Figure 11G) and markers

of liver function such as albumin, aspartate aminotransferase (AST), or alanine aminotransferase (ALT) (Figure 11H-J) did not differ between Ins1Cre$^+$ and Ins1Cre$^-$ mice, suggesting the Cre insertion into the *Ins1* locus does not affect liver or lipid metabolism.

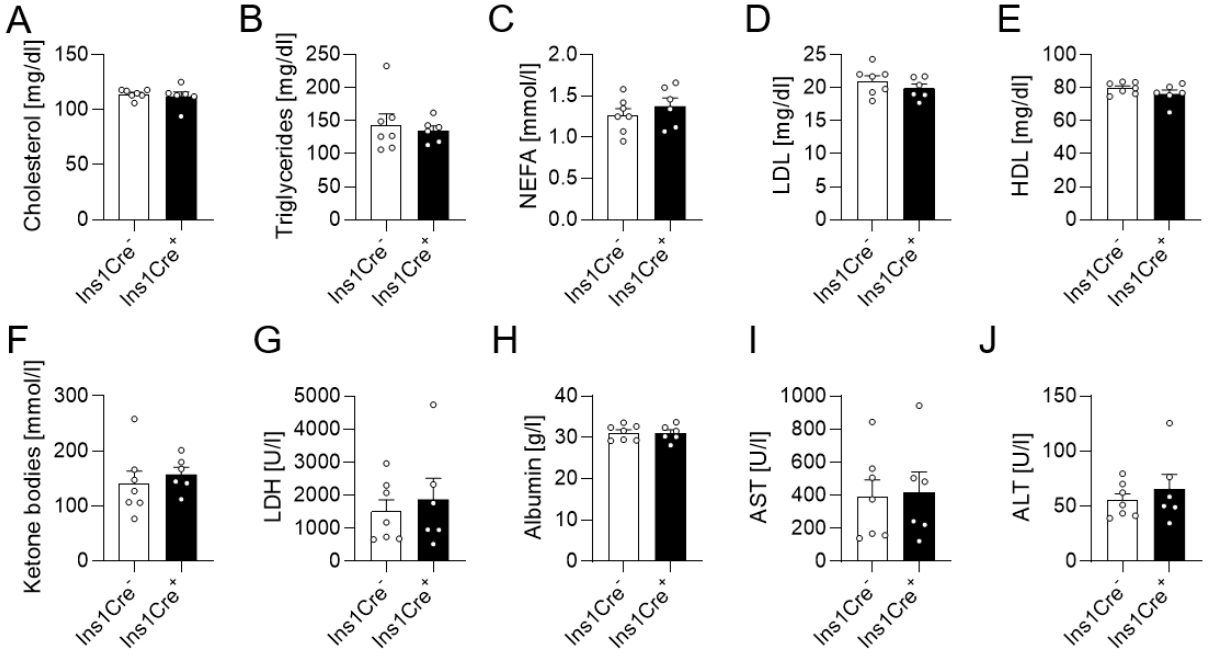

Figure 11: Serum parameters are unchanged between Ins1Cre$^+$ and Ins1Cre$^-$ control mice. Serum from mice was tested for **(A)** cholesterol, **(B)** triglycerides, **(C)** non-esterified fatty acids (NEFA), **(D)** low density lipoprotein (LDL), **(E)** high density lipoprotein (HDL), **(F)** ketone bodies, **(G)** lactate dehydrogenase (LDH), **(H)** albumin, **(I)** aspartate aminotransferase (AST), and **(J)** alanine aminotransferase (ALT). Data is presented as mean ± SEM. Statistical analysis was performed using an unpaired t-test.

Gene expression is a tightly regulated and dynamic process which ensures the rapid adaptation of the cell in response to the metabolic need. In pancreatic β-cells, dysregulation of gene expression results in loss of β-cell identity, β-cell failure, and ultimately T2DM (Neelankal John et al. 2018). The maintenance of a differentiated and mature state of the β-cell is facilitated not only by the induction of identity gene expression but also from a selective repression of disallowed genes (Swisa et al. 2017). Oxidative stress, ER stress, and inflammation, resulting from chronic hyperglycemia and dyslipidemia induce a loss of β-cell identity with a downregulation of identity genes such as *MafA*, *Slc2a2*, or *Pdx1* and an upregulation of disallowed genes which comprise of *Ldha* or *Hk1* (Bensellam et al. 2018).

To investigate whether the insertion of the Cre gene into the *Ins1* locus would alter islet gene expression, β-cell identity and disallowed gene expression was determined in islets from heterozygous Ins1Cre$^+$ mice and Ins1Cre$^-$ control litter mates. Ins1Cre$^+$ animals showed increased Cre mRNA levels, which validates the insertion and expression of the Cre recombinase gene (Figure 12A). Moreover, *Ins1* gene expression was reduced in Ins1Cre$^+$ by ~50% in comparison to control litter mates. This reduction was mainly explained by insertion of the Cre recombinase by homologous recombination into the second exon of the *Ins1* gene, resulting in a replacement of the entire *Ins1* coding sequence (Thorens et al. 2015). Surprisingly, *Nkx6.1* but also *MafA* gene expression were significantly increased (Figure 12B). The expression of the other β-cell identity genes (Figure 12B) as well as the expression of the disallowed genes (Figure 12C) remained unchanged between Ins1Cre$^+$ and Ins1Cre$^-$ mice.

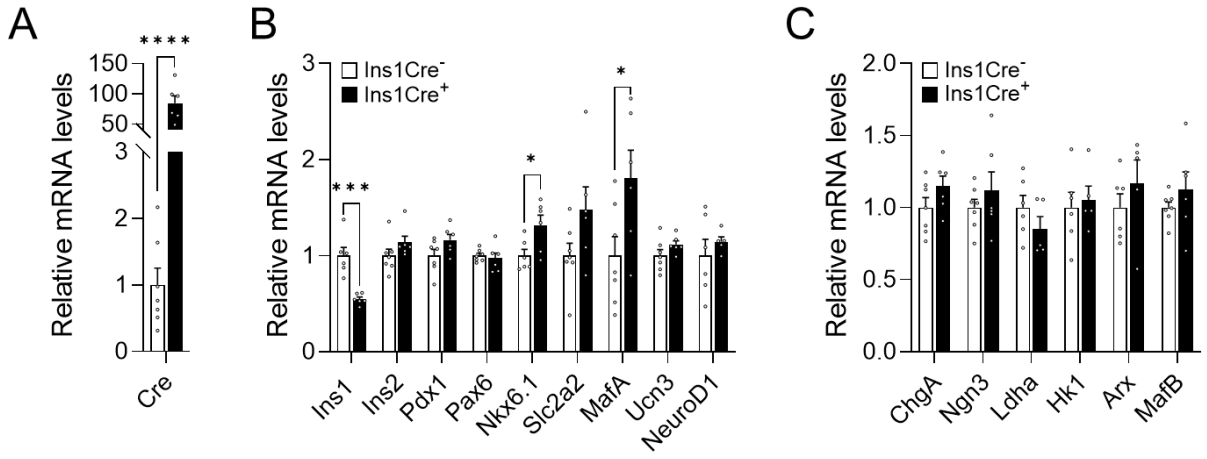

Figure 12: Mice heterozygous for Ins1Cre display altered islet *Ins1*, *Nkx6.1*, and *MafA* gene expression. (A) Pancreatic islet Cre expression, **(B)** expression of β-cell identity genes, and **(C)** expression of disallowed genes from heterozygous Ins1Cre$^+$ and Ins1Cre$^-$ control litter mates. Data is presented as mean ± SEM. Statistical analysis was performed using an unpaired t-test. *p < 0.05, ***p < 0.001, ****p < 0.0001.

Although no differences in fasting and refeeding plasma insulin levels were observed, *Ins1* gene expression was reduced by ~50% while *Nkx6.1* and *MafA* expression was increased. To investigate whether these changes in gene expression would affect hormone levels in the pancreas, total pancreatic insulin, glucagon, and somatostatin levels were determined. After dissection, pancreas weight did not differ between Ins1Cre$^+$ and control mice (Figure 13A). Also, no differences in total pancreas insulin (Figure 13B), glucagon (Figure 13C), and somatostatin (Figure 13D) content were observed. Thus, although *Ins1* gene expression was reduced in Ins1Cre$^+$ mice pancreatic insulin content but also content of other islet hormones was unchanged between Ins1Cre$^-$ and Ins1Cre$^+$ mice.

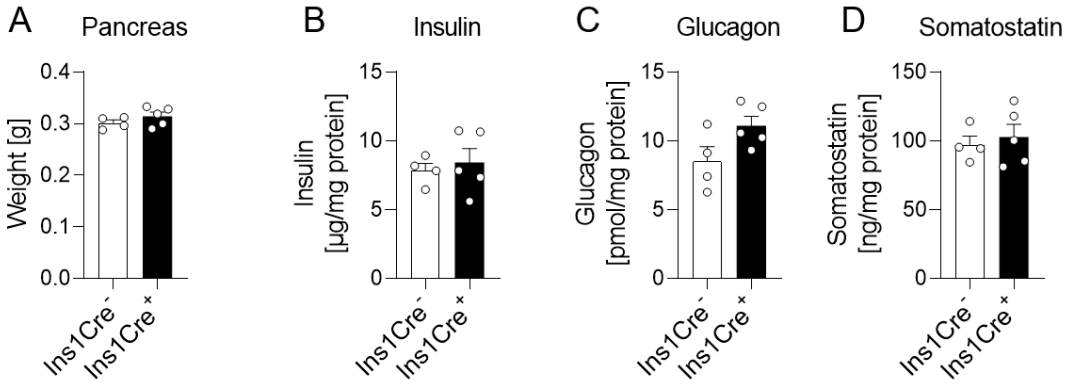

Figure 13: Ins1Cre$^+$ mice display normal islet hormone expression. (A) Pancreas weight in control Ins1Cre$^-$ and Ins1Cre$^+$ mice. After dissection, pancreas was lysed and total pancreatic **(B)** insulin, **(C)** glucagon, and **(D)** somatostatin content was determined. Subsequently, hormone levels were normalized to protein levels. Data is presented as mean ± SEM. Statistical analysis was performed using an unpaired t-test.

Although *Ins1* gene expression was reduced, no changes in glucose homeostasis and insulin secretion were observed upon Cre recombinase insertion into the *Ins1* locus. This indicates that the Ins1Cre mouse line is a suitable model to knock out TBL1 and TBLR1 β-cell specifically.

2.2.2 Validation of TBL1 and TBLR1 knock out specificity and efficiency

In line with observations from Thorens et al., insertion of the Cre recombinase into the *Ins1* locus had no effects on glucose metabolism in mice (Thorens et al. 2015). Moreover, as described above apart from the 50% downregulation of the *Ins1* gene and slight upregulation of the *Nkx6.1* and *MafA* gene no differences in islet gene expression were observed. As no

changes in pancreatic insulin content or circulating plasma insulin were observed, the Ins1Cre model was used to investigate the β-cell specific role of TBL1 and TBLR1.

Mice heterozygous for Ins1Cre and homozygous for TBL1 flox (TBLβKO) or TBLR1 flox (TBLRβKO) were born at a mendelian ratio and with normal body weight and size. Knock out specificity and efficiency were tested prior to metabolic characterization of the mice. In the TBLβKO mice, islet TBL1 mRNA levels were significantly reduced by 80% while in other tissues such as liver, epididymal white adipose tissue (eWAT), kidney, spleen, gastrocnemius (GC) muscle, brain, or small and large intestine TBL1 mRNA levels remained unchanged in comparison to controls (Figure 14A). As multicellular micro-organ, the pancreatic islet comprises of various cell types of which β-cells make up around 70-80% (Kim et al. 2009). Thus, the remaining 20% of TBL1 expression in the islets is likely attributed to other islet cell types. Accordingly, TBL1 protein levels in the islet were also strongly reduced (Figure 14B). As for the gene expression, remaining TBL1 protein levels can be explained by TBL1 expression in the other islet cell types. Comparable to the TBLβKO mice, TBLR1 gene expression was reduced by ~70% in islets of TBLRβKO mice, while the expression in the other tissues was unchanged in comparison to control litter mates (Figure 14C). In line with reduced TBLR1 mRNA levels, TBLR1 protein levels were also strongly reduced in TBLRβKO mice in comparison to controls (Figure 14D). Ultimately, this implies that TBL1 and TBLR1 were deleted with a high efficiency most likely specifically in the β-cells of TBLβKO and TBLRβKO mice, respectively.

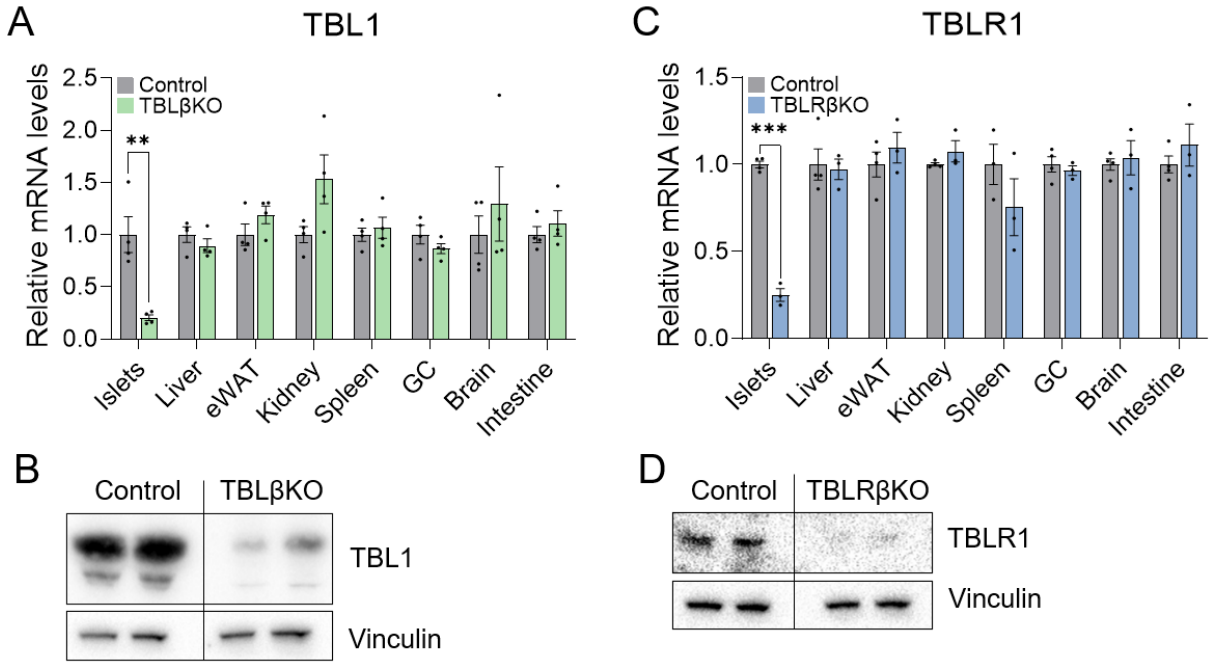

Figure 14: TBL1 and TBLR1 mRNA levels are specifically reduced in pancreatic islets of TBLβKO and TBLRβKO mice, respectively. (A) TBL1 gene expression in islets and peripheral tissues from TBLβKO mice and controls. **(B)** TBL1 and Vinculin protein expression determined in islets from TBLβKO mice and control litter mates using Western Blot. **(C)** TBLR1 gene expression in islets and peripheral tissues from TBLRβKO mice and controls. **(D)** TBLR1 and Vinculin protein expression determined in islets from TBLRβKO mice and control litter mates using Western Blot. Data is presented as mean ± SEM. Statistical analysis was performed using an unpaired t-test. **p < 0.01, ***p < 0.001.

2.3 β-cell specific TBL1 (TBLβKO) and TBLR1 (TBLRβKO) knock out mice display no metabolic phenotype

To investigate the role of TBL1 and TBLR1 in pancreatic β-cells *in vivo*, mice lacking TBL1 (TBLβKO) or TBLR1 (TBLRβKO) β-cell specifically were generated using the Cre/loxP system as previously described. After demonstrating knock out efficiency and tissue specificity and excluding effects due to the insertion of the Cre recombinase gene into the *Ins1* locus, mice were phenotypically characterized under normal and challenged conditions, including diet-induced obesity and aging.

2.3.1 Ablation of β-cell specific TBL1 or TBLR1 has no effect on β-cell physiology

TBLβKO and TBLRβKO mice, and the respective control mice were weekly monitored starting the age of 4 or 5 weeks. Weekly determined body weight or blood glucose levels determined on the day of sacrifice did not differ between controls and TBLβKO (Figure 15A) or TBLRβKO (Figure 15B) mice, respectively. In line with similar body weights, no differences in liver, eWAT, kidney, or spleen weight were observed between controls and TBLβKO (Figure 15C) or TBLRβKO (Figure 15D) mice.

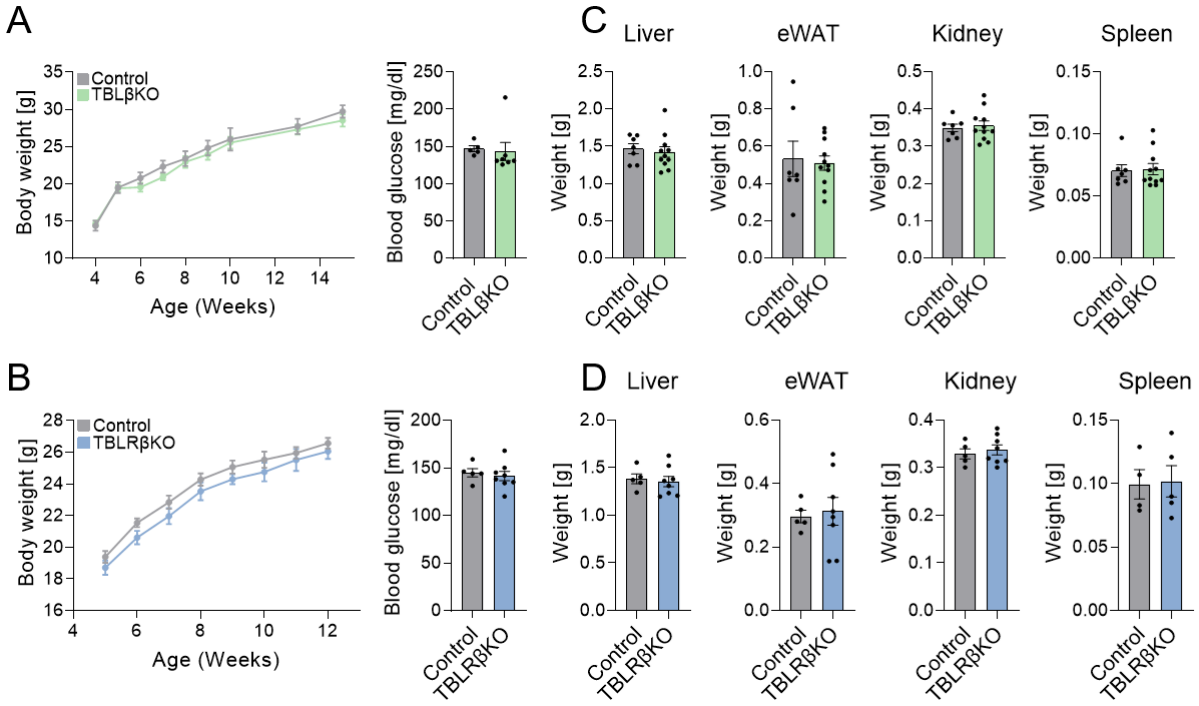

Figure 15: Body and tissue weight are unchanged upon β-cell specific TBL1 or TBLR1 knock out in comparison to controls. Weekly determined body weight and blood glucose determined on the day of sacrifice in **(A)** TBLβKO or **(B)** TBLRβKO mice and the respective controls. Liver, eWAT, kidney, and spleen weight in **(C)** TBLβKO or **(D)** TBLRβKO mice and the respective controls. Data is presented as mean ± SEM. Statistical analysis was performed using an unpaired t-test (A,B for blood glucose and C,D) or a two-way ANOVA with repeated measures and a Šídák's multiple comparison *post hoc* test (A,B for body weight).

To investigate glucose metabolism and the responsiveness to glucose of β-cells lacking TBL1 or TBLR1, blood glucose clearance during an ipGTT was investigated. No differences in blood glucose clearance during the ipGTT were observed between TBLβKO or TBLRβKO and respective control mice (Figure 16A,B). To exclude possible effects on blood glucose clearance due to impaired insulin signaling, insulin sensitivity was determined. As expected, insulin responsiveness was comparable between controls and TBLβKO (Figure 16C) or TBLRβKO (Figure 16D) mice, respectively.

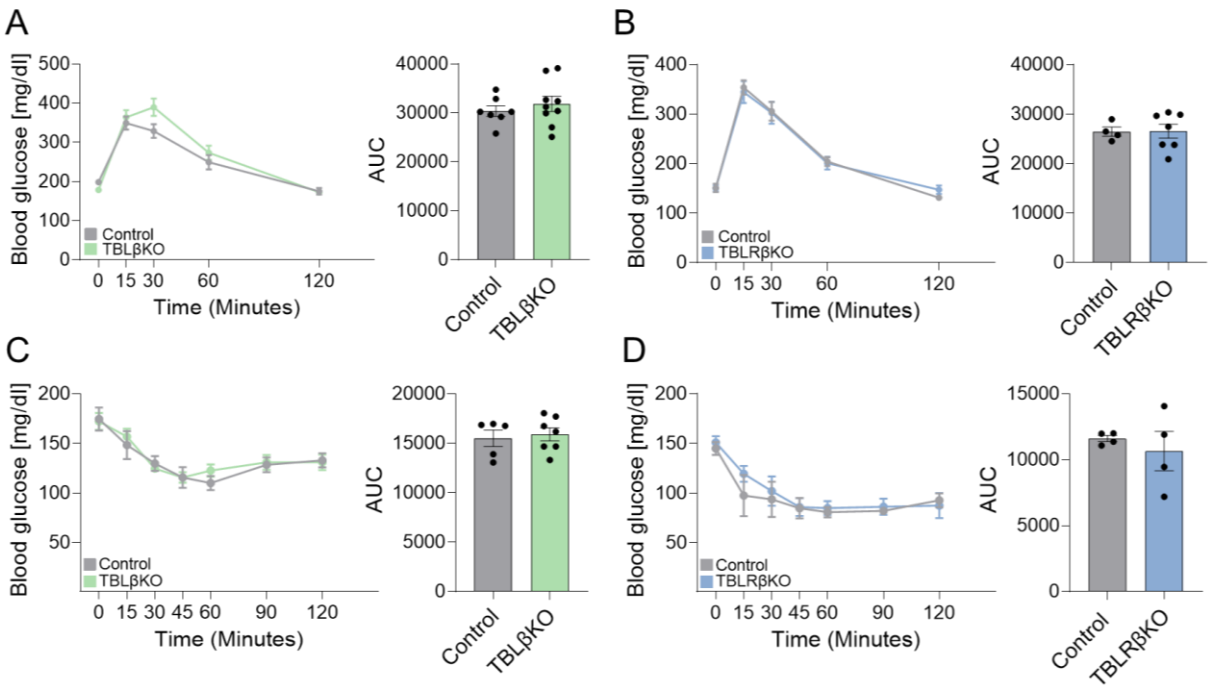

Figure 16: Blood glucose clearance is unchanged between TBLβKO or TBLRβKO mice and respective controls. ipGTT in **(A)** TBLβKO or **(B)** TBLRβKO mice and the respective controls. Mice were fasted for 6 h. After basal blood glucose determination, mice were injected with 2 g/kg D-glucose. Blood glucose levels were determined 15, 30, 60, and 120 min after injection. ipITT in **(C)** TBLβKO or **(D)** TBLRβKO mice and the respective control litter mates. Mice were fasted for 6 h. After determination of baseline blood glucose levels, mice were injected with 0.6 U/kg insulin. Blood glucose levels were determined 15, 30, 45, 60, 90, and 120 min after injection. Blood glucose levels are plotted over time course of the experiment or are displayed as AUC. Data is presented as mean ± SEM. Statistical analysis was performed using an unpaired t-test (A-D for AUC) or a two-way ANOVA with repeated measures and a Šídák's multiple comparison *post hoc* test (A-D for time course experiments).

Blood glucose clearance and insulin sensitivity were comparable between TBLβKO or TBLRβKO mice and respective controls. Next, β-cell functionality and in particular ability to secrete insulin in response to food intake was determined. Thus, fasting and refeeding blood glucose and plasma insulin levels were determined. However, no differences in fasting and refeeding glycemia and insulinemia were observed between TBLβKO (Figure 17A) or TBLRβKO (Figure 17B) mice and the respective controls. Ultimately, this implies that pancreatic β-cells lacking TBL1 or TBLR1 are functional and secrete insulin adequately in response to food intake.

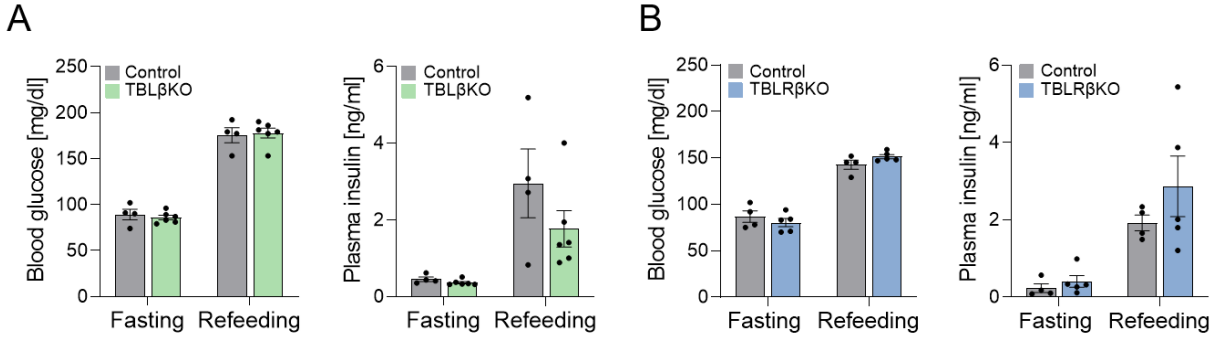

Figure 17: TBLβKO and TBLRβKO mice display normal fasting and refeeding glycemia and insulinemia. Blood glucose and plasma insulin levels after 16 h of fasting and 2 h of refeeding in controls and **(A)** TBLβKO or **(B)** TBLRβKO mice. Data is presented as mean ± SEM. Statistical analysis was performed using a two-way ANOVA with a Šídák's multiple comparison *post hoc* test.

TBL1 and TBLR1 are transcription co-factors and were previously described to regulate transcriptional events through signal dependent transcription factor binding and recruitment of

activator or repressor complexes (Perissi et al. 2008). To investigate whether TBL1 and TBLR1 were implicated in β-cell gene expression, pancreatic islets were isolated from TBLβKO and TBLRβKO mice and expression of identity genes and of genes that are commonly repressed in mature β-cells was determined. Upon TBL1 knockout, TBLR1 was significantly upregulated suggesting TBLR1 might compensate for the lack of TBL1 (Figure 18A). In contrast, TBL1 expression was unchanged upon TBLR1 knock out (Figure 18B). In islets from TBLβKO and TBLRβKO mice, *Ins1* gene expression was significantly reduced by ~50% (Figure 18C,D), an observation that was previously made when mice heterozygous for Ins1Cre were compared to control litter mates (*see Chapter 2.2.1*). This indicates that the reduction in *Ins1* expression is not induced by the lack of TBL1 or TBLR1 but results from the Cre insertion into the *Ins1* locus. Moreover, *NeuroD1* expression was significantly upregulated in TBLRβKO mice in comparison to controls (Figure 18D). Interestingly, the β-cell disallowed genes *Ngn3*, *Hk1*, and *Arx* were significantly upregulated upon TBL1 knock out (Figure 18E). No changes in the expression of β-cell disallowed genes were observed in islets from TBLRβKO mice in comparison to control litter mates (Figure 18F). Thus, although β-cell identity is maintained upon TBLR1 deficiency, changes in islet gene expression upon TBL1 knock out suggest a slight impairment of β-cell identity.

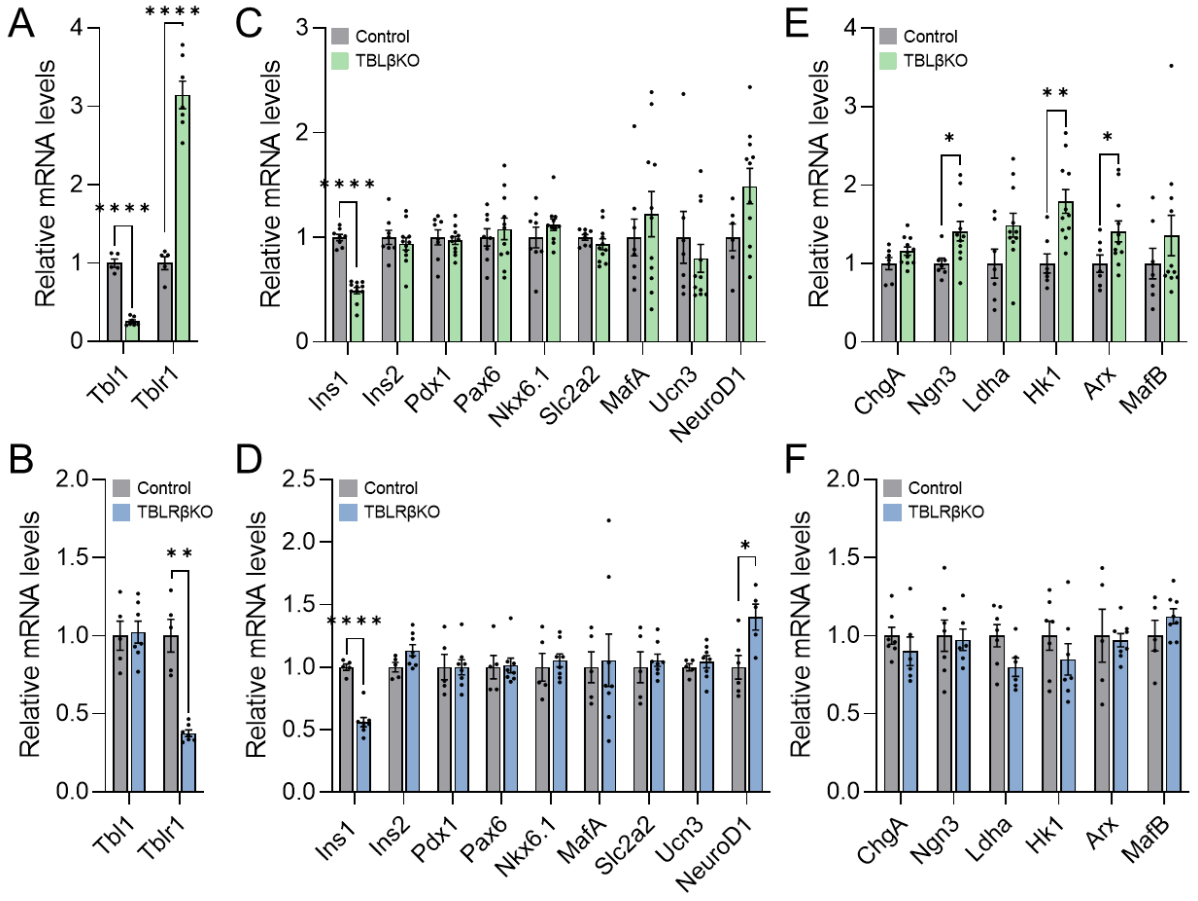

Figure 18: TBLβKO islets over express TBLR1 while TBL1 levels are unchanged in TBLRβKO islets. TBL1 and TBLR1 gene expression in **(A)** TBLβKO or **(B)** TBLRβKO mice. Expression of **(B,C)** β-cell identity genes and **(E,F)** disallowed genes in islets from controls and TBLβKO or TBLRβKO mice, respectively. Data is presented as mean ± SEM. Statistical analysis was performed using an unpaired t-test. *p < 0.05, **p < 0.01, ****p < 0.0001.

In line with previously described body and tissue weights, pancreas weight did not differ between control and TBLβKO or TBLRβKO mice (Figure 19A). Subsequently determined total pancreatic insulin content showed that no differences in insulin content were observed between controls and TBLβKO or TBLRβKO mice (Figure 19B), which is in line with

comparable circulating insulin levels at fasted and refed state shown above. Moreover, no differences in total pancreas glucagon (Figure 19C) or somatostatin (Figure 19D) content were observed between controls, TBLβKO, and TBLRβKO mice, implying that islet hormone expression is unchanged upon TBL1 or TBLR1 deficiency in pancreatic β-cells.

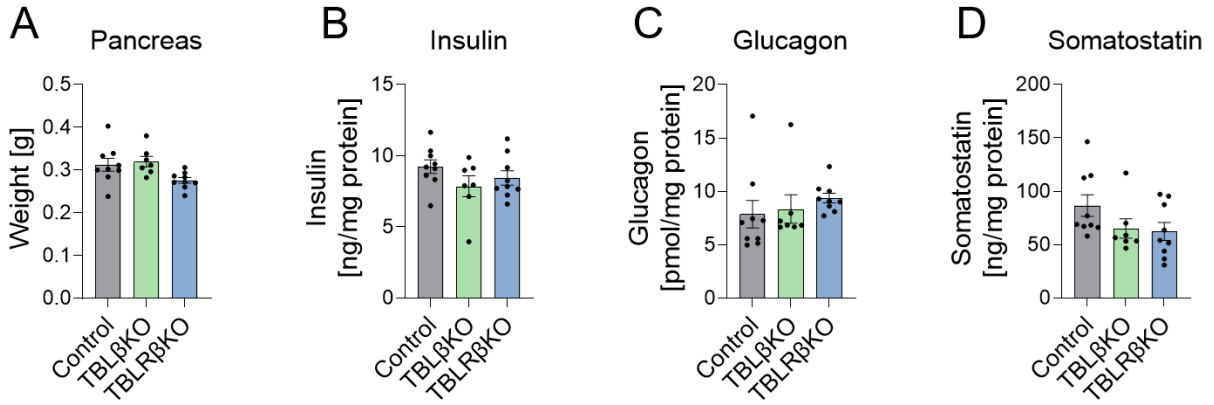

Figure 19: TBL1 or TBLR1 deficiency in β-cells does not alter insulin, glucagon, or somatostatin content in the pancreas. (A) Pancreas weight in control, TBLβKO, and TBLRβKO mice. Total pancreas **(B)** insulin, **(C)** glucagon, and **(D)** somatostatin content in control, TBLβKO, and TBLRβKO mice normalized to protein levels. Data is presented as mean ± SEM. Statistical analysis was performed using a one-way ANOVA with a Dunnett's multiple comparison *post hoc* test.

Previous studies have demonstrated that alterations in islet morphology can precede β-cell failure and hyperglycemia (Mezza et al. 2014). Therefore, islet micro-architecture was investigated upon TBL1 or TBLR1 knock out although no phenotypic alterations were observed thus far. Immunofluorescence staining for glucagon and insulin, identifying α-cells and β-cells, respectively revealed that the highly organized cell distribution commonly observed in murine islets (Cabrera et al. 2006; Kim et al. 2009) was unaffected upon TBL1 (Figure 20A) or TBLR1 (Figure 20B) knock out. Accordingly, no differences in β-cell mass or α-cell mass were observed between TBLβKO (Figure 20C) or TBLRβKO mice (Figure 20D) and the respective controls.

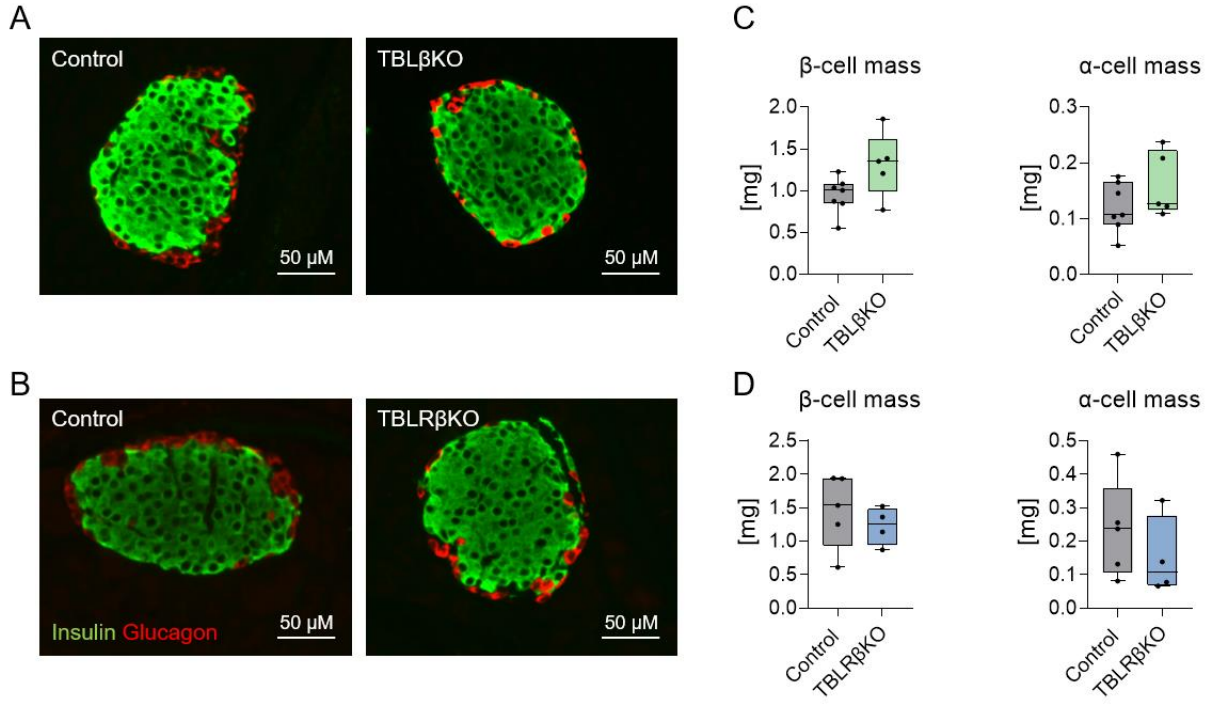

Figure 20: Islet micro-architecture is unaffected by TBL1 or TBLR1 knock out. Representative images of immunofluorescence staining of islets in the pancreas of controls and **(A)** TBLβKO or **(B)** TBLRβKO mice. β-cells

are displayed as insulin+ cells in green. α-cells are displayed as glucagon+ cells in red. Immunofluorescence staining was performed and analyzed by the core facility Pathology & Tissue Analytics at the Helmholtz Munich. **(C)** Quantification of insulin+ cell mass (β-cells) and glucagon+ cell mass (α-cells) in TBLβKO mice and control litter mates. **(D)** Quantification of insulin+ cell mass (β-cells) and glucagon+ cell mass (α-cells) in TBLRβKO mice and controls. Data is presented as median and minimum/maximum (C,D). Statistical analysis was performed using an unpaired t-test.

2.3.2 TBLβKO and TBLRβKO mice display normal glucose metabolism on high fat diet

Previous studies identified diet-induced obesity as main contributor to the development of glucose intolerance and insulin resistance. The resulting hyperglycemia and the increased insulin demand in obesity represent major stressors for the β-cells. At first, β-cells compensate for the underlying insulin resistance by increased insulin secretion and β-cell hyperplasia (Karam et al. 1963; Kim et al. 2009). Eventually, β-cells fail which leads to impaired insulin synthesis, secretion, and ultimately to the development of T2DM (Rochlani et al. 2017). Since TBLβKO and TBLRβKO mice showed no metabolic phenotype on chow diet, the effects of β-cell specific TBL1 or TBLR1 ablation were investigated at pathological conditions such diet-induced obesity.

For this, TBLβKO and TBLRβKO mice were placed on a HFD containing 60% calories from fat for 24 weeks starting at the age of 6 weeks. Weekly determined body weight and blood glucose levels were undistinguishable between control and TBLβKO (Figure 21A) or TBLRβKO mice (Figure 21B), respectively. Body composition of TBLβKO and TBLRβKO mice was determined using echo-magnetic resonance imaging (MRI) after 15 weeks of HFD. As expected from the weekly determined body weight, TBLβKO (Figure 21C) and TBLRβKO (Figure 21D) mice showed similar body composition in comparison to control mice. In line with that, no differences in eWAT weight between controls and respective knock out mice were observed. Likewise, liver, kidney, or spleen weight between TBLβKO (Figure 21E) or TBLRβKO (Figure 21F) and control litter mates were unchanged.

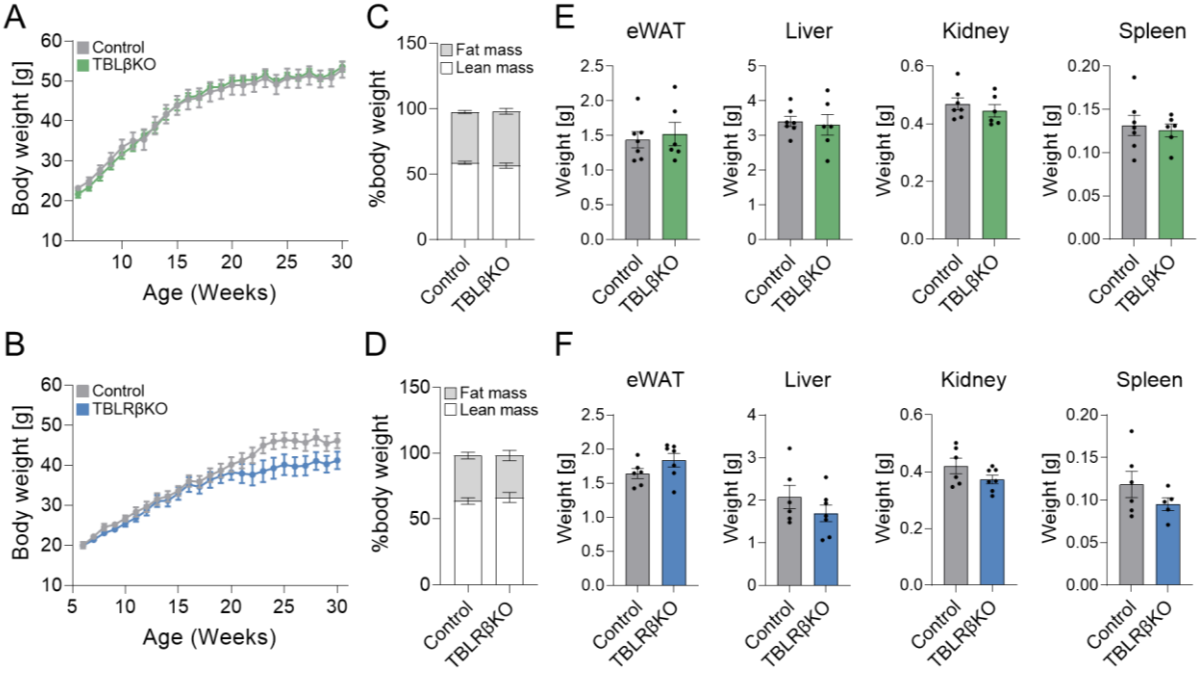

Figure 21: Body weight and composition do not differ between controls and TBLβKO or TBLRβKO mice on HFD. Weekly determined body weight in **(A)** TBLβKO or **(B)** TBLRβKO mice and respective controls. Body composition was determined using Echo-MRI after 15 weeks of HFD in controls or **(C)** TBLβKO and **(D)** TBLRβKO mice. eWAT, liver, kidney, and spleen weight after 24 weeks of HFD in **(E)** TBLβKO or **(F)** TBLRβKO mice and the respective control mice. Data is presented as mean ± SEM. Statistical analysis was performed using an unpaired t-test (C-F) or a two-way ANOVA with repeated measures and a Šídák's multiple comparison *post hoc* test (A,B).

Weekly determined blood glucose levels did not differ between TBLβKO (Figure 22A) or TBLRβKO (Figure 22B) mice and respective control litter mates. To investigate whether TBL1 or TBLR1 knock out affects glucose homeostasis, blood glucose and plasma insulin levels were determined at fasted and refed state. No differences in fasting or refeeding glycemia and insulinemia were observed in TBLβKO (Figure 22C) or TBLRβKO (Figure 22D) mice in comparison to controls, suggesting that also under challenged conditions such as diet-induced obesity blood glucose homeostasis is not affected by the β-cell specific deletion of TBL1 or TBLR1.

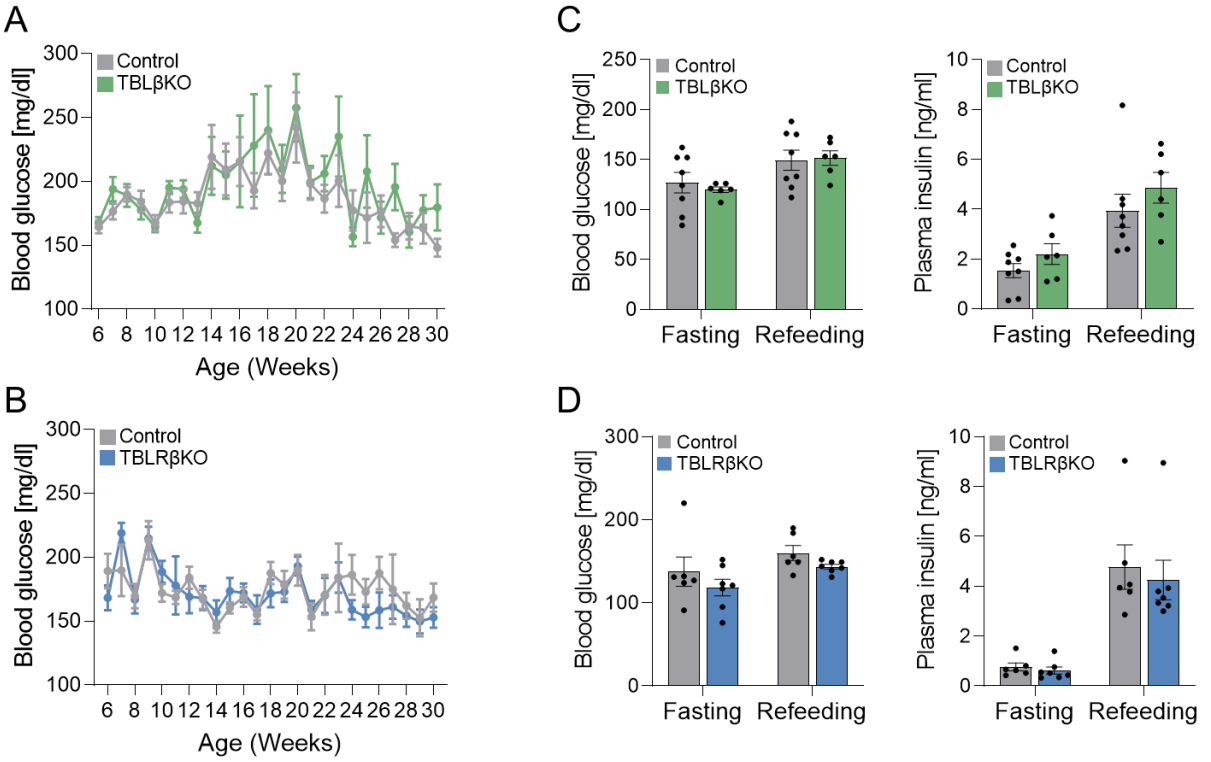

Figure 22: Mice lacking β-cell specific TBL1 or TBLR1 display normal glycemia and insulinemia on HFD. Weekly determined blood glucose levels in **(A)** TBLβKO and **(B)** TBLRβKO mice. Blood glucose and plasma insulin after 16 h fasting and 2 h refeeding in **(C)** TBLβKO and **(D)** TBLRβKO mice after 22 or 14 weeks on HFD, respectively. Data is presented as mean ± SEM. Statistical analysis was performed using a two-way ANOVA with repeated measures and a Šídák's multiple comparison *post hoc* test (A,B) or a two-way ANOVA with a Šídák's multiple comparison *post hoc* test (C,D).

Since fasting and refeeding blood glucose and plasma insulin levels did not differ between controls and knock out mice, a glucose tolerance test was performed to closely investigate blood glucose clearance and thereby the responsiveness of β-cells to glucose in the absence of TBL1 or TBLR1 upon HFD. However, blood glucose clearance was unchanged in TBLβKO (Figure 23A) and TBLRβKO (Figure 23B) mice in comparison to control litter mates, respectively suggesting insulin secretion is not affected upon TBL1 or TBLR1 knock out in diet-induced obesity. To exclude possible effects on blood glucose clearance due to differing insulin responsiveness, insulin sensitivity was determined. No differences in insulin sensitivity were observed between TBLβKO (Figure 23C) or TBLRβKO (Figure 23D) mice and controls, ultimately suggesting that β-cells are functional despite lacking TBL1 or TBLR1 on HFD.

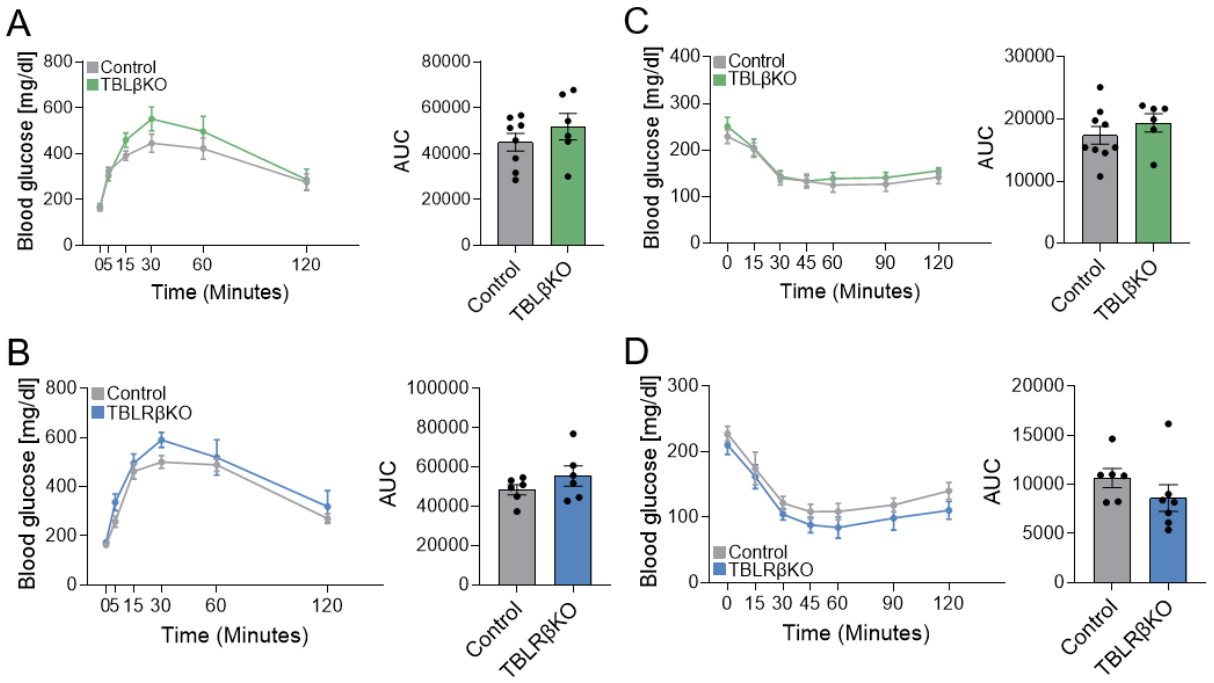

Figure 23: Glucose tolerance and insulin sensitivity are unchanged in TBLβKO and TBLRβKO mice on HFD. After 20 weeks of HFD, **(A)** TBLβKO and **(B)** TBLRβKO mice were starved for 16 h. Then, after baseline blood glucose determination mice were injected intraperitoneally with 2 g/kg D-glucose. Blood glucose levels were determined 5, 15, 30, 60, and 120 min after injection. After 12 weeks of HFD, insulin sensitivity was determined. After 6 h of fasting and baseline glucose determination, **(C)** TBLβKO and **(D)** TBLRβKO mice were injected with 1 U/kg insulin. Blood glucose levels were determined 15, 30, 45, 60, 90, and 120 min after injection. Blood glucose levels are plotted over time course of the experiment or are displayed as AUC. Data is presented as mean ± SEM. Statistical analysis was performed using an unpaired t-test (A-D for AUC) or a two-way ANOVA with repeated measures and a Šídák's multiple comparison *post hoc* test (A-D for blood glucose curve).

To investigate whether islet gene expression was affected by the ablation of TBL1 or TBLR1 on HFD, pancreatic islets were isolated and tested for TBL1/TBLR1 gene expression but also for β-cell identity and disallowed genes. Interestingly, as for the chow diet fed mice, TBLR1 gene expression was significantly upregulated upon TBL1 knock out (Figure 24A), while no changes in TBL1 expression upon TBLR1 knock out occurred (Figure 24B). Apart from the expected reduction in *Ins1* gene expression, no differences in`β-cell identity gene expression were observed in islets from TBLβKO mice in comparison to controls (Figure 24C). *Ins1* gene expression was also downregulated in TBLRβKO mice. Moreover, *Nkx6.1*, *MafA*, and *Slc2a2* expression was significantly upregulated in the TBLRβKO mice (Figure 24D). In line with observations from TBLβKO mice on chow diet, *Ngn3*, a β-cell progenitor cell marker, was upregulated in TBLβKO mice (Figure 24E). Moreover, the α-cell identity gene *MafB* (MAF BZIP Transcription Factor B) was upregulated upon TBLR1 knock out (Figure 24F), overall suggesting impairments in β-cell identity upon TBL1 and TBLR1 knock out.

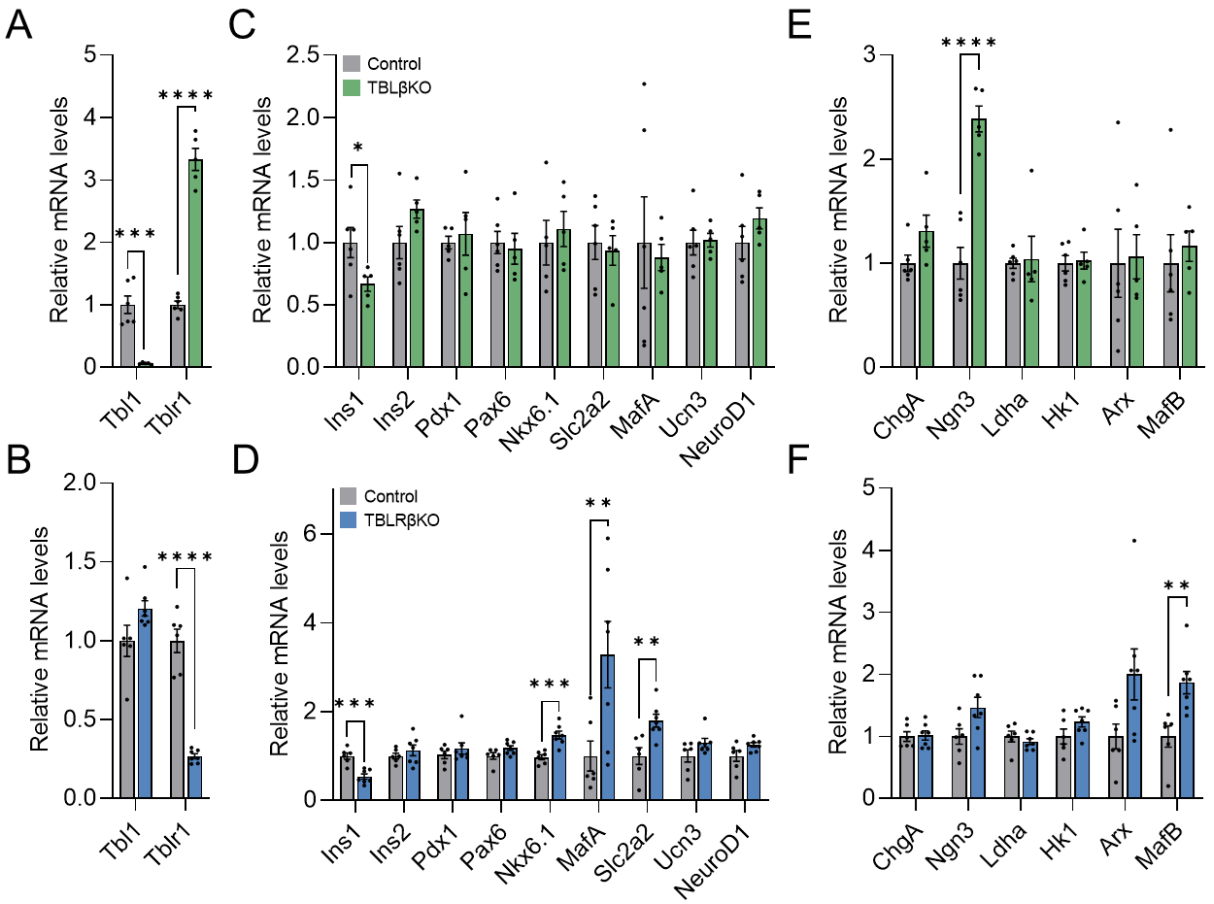

Figure 24: Islet gene expression is altered in mice lacking TBL1 or TBLR1 on HFD. After 24 weeks of HFD, islet **(A,B)** TBL1 and TBLR1, **(C,D)** β-cell identity, and **(E,F)** disallowed gene expression was determined in TBLβKO and TBLRβKO mice, respectively. Data is presented as mean ± SEM. Statistical analysis was performed using an unpaired t-test. **p < 0.01, ***p < 0.001, ****p < 0.0001

Taken together, although glucose homeostasis and insulinemia were unchanged, TBLβKO or TBLRβKO mice displayed dysregulated islet gene expression upon HFD. The increase in disallowed genes upon TBL1 or TBLR1 deficiency implies a mild impairment in β-cell identity or an initiation of dedifferentiation, suggesting a possible role of TBL1 and TBLR1 in the maintenance of β-cell identity.

2.3.3 Aged TBLβKO and TBLRβKO mice show normal islet gene expression and islet morphology

Age is a major risk factor for the development of β-cell dysfunction, mainly due to the underlying insulin resistance. In addition, processes and mechanisms that are crucial for normal β-cell function, including proliferation, dedifferentiation, regenerative capacity, are altered during aging (Møller et al. 2003). In mice, islet TBL1 expression was reduced upon aging. Thus, islet gene expression in one year old TBLβKO and TBLRβKO mice was investigated. Interestingly, as for the young TBLβKO mice, TBLR1 gene expression was significantly upregulated (Figure 25A), while TBL1 expression remained unchanged upon TBLR1 knock out (Figure 25B). No differences in β-cell identity gene expression were observed in TBLβKO (Figure 25C) and TBLRβKO (Figure 25D) mice in comparison to the control litter mates apart from a ~50% reduction in *Ins1* gene expression which is attributed to the Cre recombinase insertion into the *Ins1* locus. Genes typically disallowed in β-cells were not affected by TBL1 (Figure 25E) or TBLR1 (Figure 25F) knock out, generally suggesting that β-cell function and identity is maintained in aged mice despite TBL1 or TBLR1 ablation.

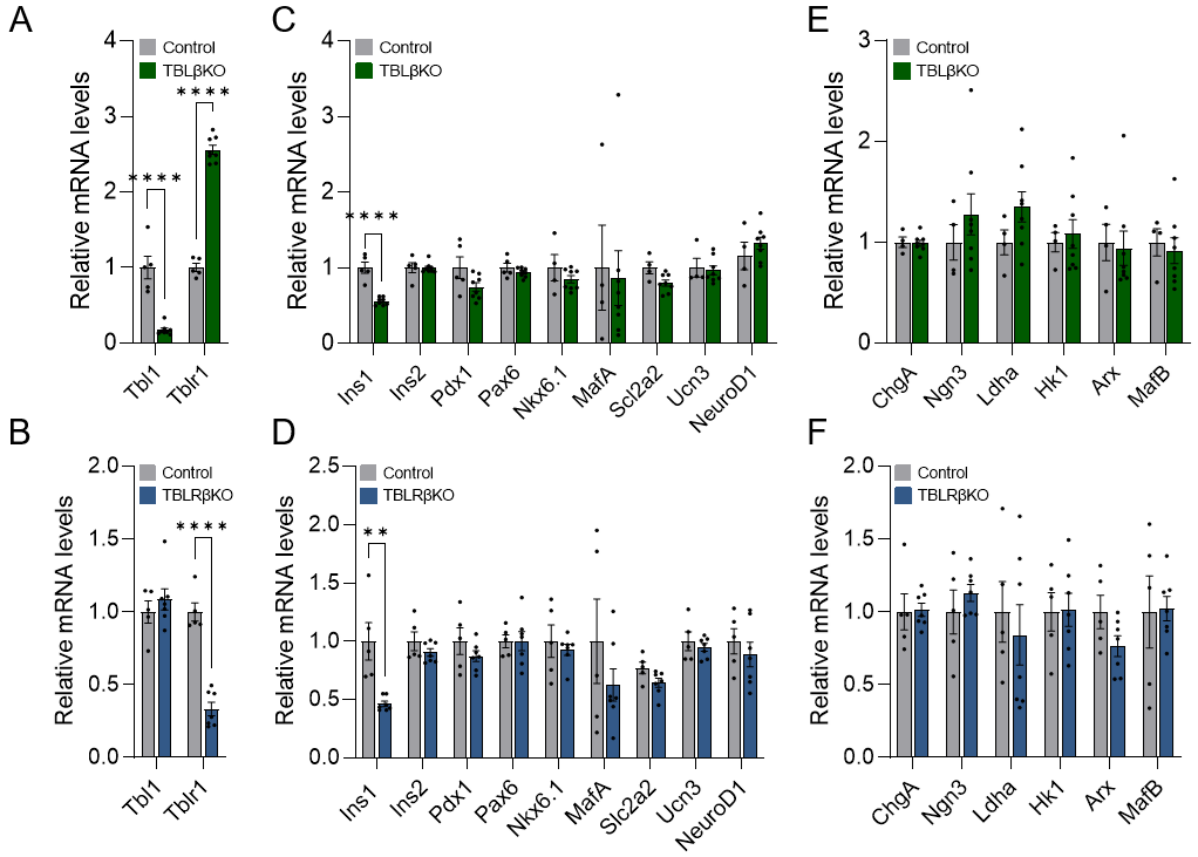

Figure 25: TBLR1 is upregulated in pancreatic islets of 1 year old TBLβKO mice. (A,B) Islet TBL1 and TBLR1, **(C,D)** β-cell identity, and **(E,F)** disallowed gene expression from 1 year old TBLβKO and TBLRβKO mice, respectively was determined by qPCR. Data is presented as mean ± SEM. Statistical analysis was performed using an unpaired t-test. **p < 0.01, ****p < 0.0001.

To investigate possible alterations in islet micro-architecture, pancreas was dissected from 1 year old controls and TBLβKO or TBLRβKO mice and histologically analyzed. Pancreas weight did not differ between controls and TBLβKO (Figure 26A) or TBLRβKO (Figure 26B) mice. In line with the unchanged gene expression profile in the islets from TBLβKO and TBLRβKO mice in comparison to the controls, no differences in islet architecture were observed upon TBL1 (Figure 26C) or TBLR1 (Figure 26D) knock out. Quantification of the immunofluorescence images showed no differences in insulin$^+$ β-cell mass or glucagon$^+$ α-cell mass in TBLβKO (Figure 26E) in comparison to control litter mates. Although no differences in insulin gene expression and islet architecture were observed in TBLRβKO mice, β-cell mass was significantly increased while α-cells mass was unchanged in TBLRβKO mice in comparison to controls (Figure 26F).

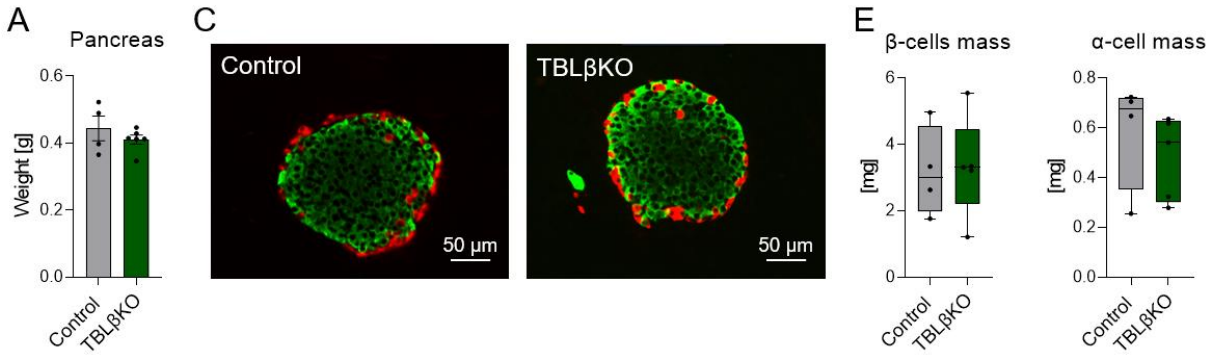

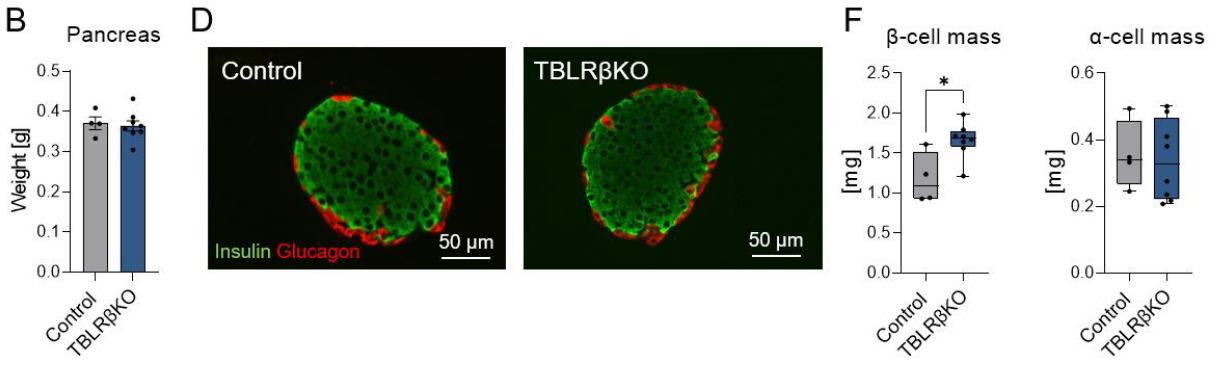

Figure 26: In aged mice, islet micro-architecture is unaffected by TBL1 or TBLR1 knock out. Pancreas weight of 1 year old **(A)** TBLβKO or **(B)** TBLRβKO mice and respective controls. Representative images of immunofluorescence staining of islets in the pancreas of controls and **(C)** TBLβKO or **(D)** TBLRβKO mice. β-cells are displayed as insulin$^+$ cells in green. α-cells are displayed as glucagon$^+$ cells in red. Immunofluorescence staining was performed and analyzed by the core facility Pathology & Tissue Analytics at the Helmholtz Munich. **(E)** Quantification of insulin$^+$ cell mass (β-cells) and glucagon$^+$ cell mass (α-cells) in TBLβKO mice and control litter mates. **(F)** Quantification of insulin$^+$ cell mass (β-cells) and glucagon$^+$ cell mass (α-cells) in TBLRβKO mice and controls. Data is presented as mean ± SEM (A,B) or as median and minimum/maximum (E,F). Statistical analysis was performed using an unpaired t-test. *p < 0.05.

2.3.4 Gene expression profiling of islets from TBLβKO and TBLRβKO mice reveals distinct functions of TBL1 and TBLR1

Characterization of mice lacking either TBL1 or TBLR1 β-cell specifically showed that the β-cells maintained their functionality under physiologic but also under challenged conditions such as in diet-induced obesity or aging. In line with this, β-cell identity genes and genes typically repressed in β-cells were also mostly unchanged by the deletion of TBL1 or TBLR1, respectively. To further investigate possible functions of TBL1 and TBLR1 in β-cells, global gene expression profiling was performed. For this, islets from four 12 week old control, TBLβKO, and TBLRβKO mice were used. Although islet and glucose metabolism were largely unchanged in mice lacking TBL1 or TBLR1 β-cell specifically, 1464 genes in the TBLβKO islets and 3053 genes in the TBLRβKO islets were differentially expressed in comparison to the controls. The volcano plot displays all expressed genes of which significantly differentially expressed genes ($p < 0.05$) are shown above the threshold (Figure 27A,B). Of the 1464 differentially expressed genes in the TBLβKO islets, 731 genes were upregulated while 733 genes were downregulated. Interestingly, as previously observed in gene expression analysis using qPCR, TBLR1 expression was significantly upregulated upon TBL1 knock out (Figure 27A). Thus, it is tempting to speculate that the development of a strong physiologic phenotype in TBLβKO mice was dampened by the over expression of TBLR1.

In the TBLRβKO islets, amongst the 3053 differentially expressed genes 1655 genes were upregulated while 1398 genes were downregulated. As previously observed in the qPCR analysis, TBL1 expression was unchanged upon TBLR1 knock out (Figure 27B). Thus, although TBLR1 may compensate for the lack TBL1, TBL1 does not compensate for the lack of TBLR1. This suggests that under physiologic conditions, TBL1 and TBLR1 might have distinct functions in the β-cells. Indeed, of the 1464 differentially expressed genes in the TBLβKO islets and the 3053 differentially expressed genes in the TBLRβKO islets, only 319 alternatively regulated genes were overlapping between TBL1 and TBLR1 knock out (Figure 27C).

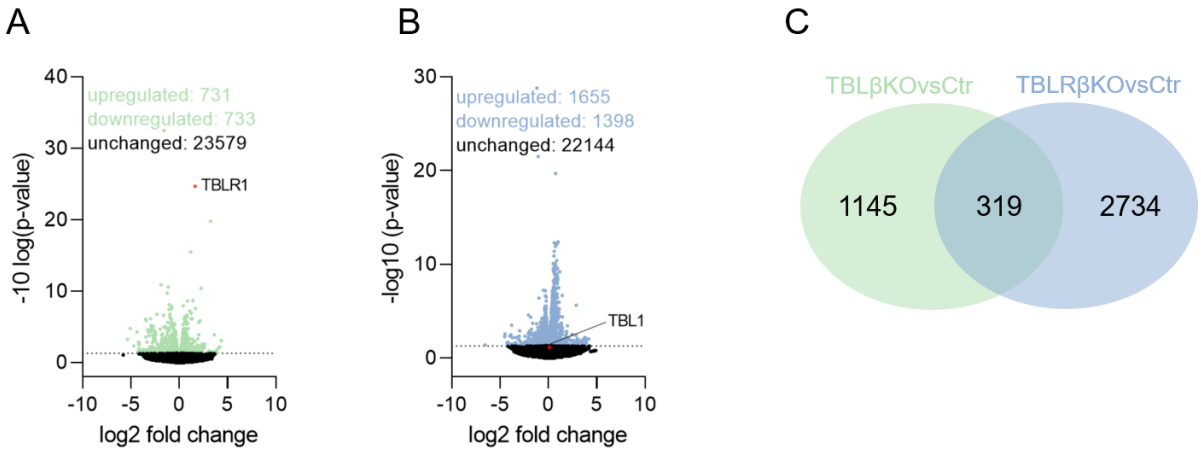

Figure 27: Gene expression profiling of TBLβKO and TBLRβKO islets reveals distinct functions between TBL1 and TBLR1 in pancreatic β-cells. Volcano plot displaying differentially expressed genes from **(A)** TBLβKO or **(B)** TBLRβKO islets vs. control islets. **(C)** Venn diagram of differentially expressed genes shared between TBLβKO and TBLRβKO islets. n=4.

A subsequently performed Kyoto Encyclopaedia of Genes and Genomes (KEGG) pathway analysis identified metabolic pathways associated with the differentially expressed genes. This analysis further underlined the difference between TBL1 and TBLR1 as only one pathway – the *MAPK signaling pathway* was upregulated (Figure 28A,B) and one pathway – the *staphylococcus aureus infection* was downregulated in both TBLβKO and TBLRβKO islets in comparison to the controls (Figure 28C,D). Interestingly, TBLR1 indeed was previously shown to regulate the *MAPK signaling pathway* in neuronal stem cells (Mastrototaro et al. 2021). No islet or diabetes related pathways were upregulated upon TBL1 knock out in β-cells (Figure 28A). However, although no metabolic differences between TBLβKO mice and controls were observed, KEGG pathway analysis revealed *pancreatic secretion* and the *type 1 diabetes mellitus* to be significantly downregulated (Figure 28C). Surprisingly, upon β-cell specific TBLR1 knock out, the *notch signaling pathway*, which is associated with the loss of β-cell maturation (Bartolome et al. 2019), was the only significantly upregulated pathway. Apart from that, differentially expressed genes were non-significantly enriched for β-cell-function associated metabolic pathways such as *type 2 diabetes mellitus*, *insulin resistance*, and the *insulin signaling pathway* (Figure 28B), suggesting an implication of TBLR1 in β-cell function. Downregulated pathways upon TBLR1 knock out included *protein export* and *protein processing in endoplasmic reticulum* (Figure 28D).

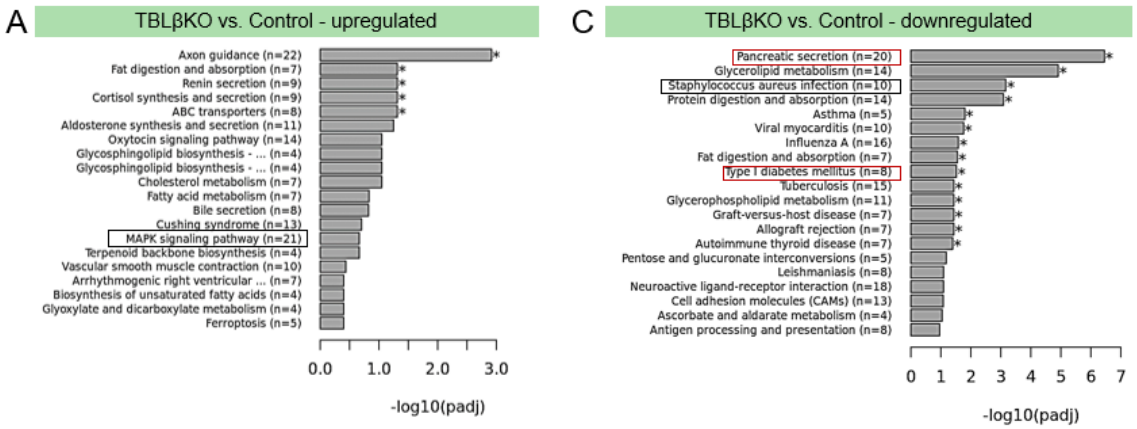

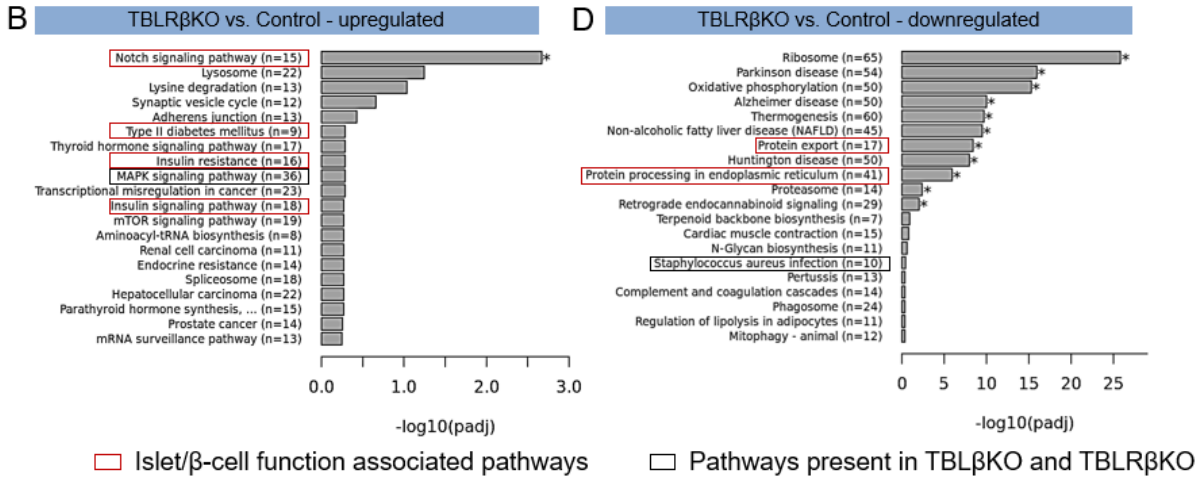

Figure 28: Kyoto Encyclopaedia of Genes and Genomes (KEGG) pathway analysis, suggests an implication of TBL1 and TBLR1 in β-cell function. Upregulated KEGG pathways associated with differentially expressed genes from **(A)** TBLβKO and **(B)** TBLRβKO islets in comparison to islets from controls. Downregulated KEGG pathways associated with differentially expressed genes from **(C)** TBLβKO and **(D)** TBLRβKO islets in comparison to islets from controls. The red box highlights islet/β-cell associated pathways. The black box highlights pathways shared by TBLβKO and TBLRβKO.

2.4 β-cell specific double knock out of TBL1 and TBLR1 (TBL/RβKO) results in β-cell dysfunction

Thus far, mice lacking either TBL1 or TBLR1 β-cell specifically did not show any alterations in β-cell function or physiology. Metabolic challenges such as diet-induced obesity or aging also did not reveal impairments in the β-cells, although the expression of disallowed genes such as *Ngn3*, *Arx*, or *MafB* was significantly upregulated in TBLβKO and TBLRβKO mice on HFD, suggesting that a transcriptional program indicative of a loss of β-cell identity is activated. Interestingly, islet TBLR1 gene expression was strongly upregulated upon TBL1 knock out, indicating a possible compensation for the lack of TBL1 by TBLR1. Indeed, previous studies demonstrated that TBL1 and TBLR1 synergistically fulfil critical functions in the liver, as ablation of both transcription co-factors resulted in a stronger phenotype than the ablation of the respective factor alone (Kulozik et al. 2011). Thus, mice lacking simultaneously TBL1 and TBLR1 β-cell specifically (TBL/RβKO) were generated and metabolically characterized.

2.4.1 TBL/RβKO mice display hyperglycemia, hypoinsulinemia, and abnormal islet gene expression

Weekly determined blood glucose levels were increasing starting at the age of 6 weeks in TBL/RβKO mice (Figure 29A). Although TBL/RβKO mice displayed significantly higher blood glucose levels during an insulin tolerance test (Figure 29B), blood glucose changes relative to baseline glucose were indistinguishable in comparison to controls (Figure 29C), indicating a comparable insulin sensitivity between TBL/RβKO and control mice. Thus, insulin resistance did not account for the hyperglycemia observed in the TBL/RβKO mice. To investigate β-cell functionality and responsiveness to changes in blood glucose levels, fasting and refeeding blood glucose and plasma insulin levels were determined in 5 week old mice, prior to the onset of hyperglycemia in the TBL/RβKO mice, and in mice at the age of 12 weeks. At the age of 5 weeks no differences in fasting and refeeding glycemia and insulinemia were observed (Figure 29D). As expected, in the adult TBL/RβKO mice fasting and refeeding blood glucose levels were significantly increased in comparison to the controls. In line with this, fasting insulin levels were non-significantly reduced (p=0.08), while refeeding plasma insulin levels were significantly lower in TBL/RβKO mice in comparison to the controls. Interestingly, while control

mice increased plasma insulin levels in response to food intake significantly, no differences in plasma insulin of the TBL/RβKO mice between fasted and refed state were observed (Figure 29E). Moreover, randomly measured plasma glucagon levels were significantly increased in TBL/RβKO mice in comparison to controls (Figure 29F). Thus, hyperglycemia observed in TBL/RβKO mice resulted from severely impaired insulin synthesis or secretion as well as from elevated circulating glucagon levels. Moreover, worsening of glycemia with age implies a progressive loss of β-cell function upon TBL1 and TBLR1 knock out.

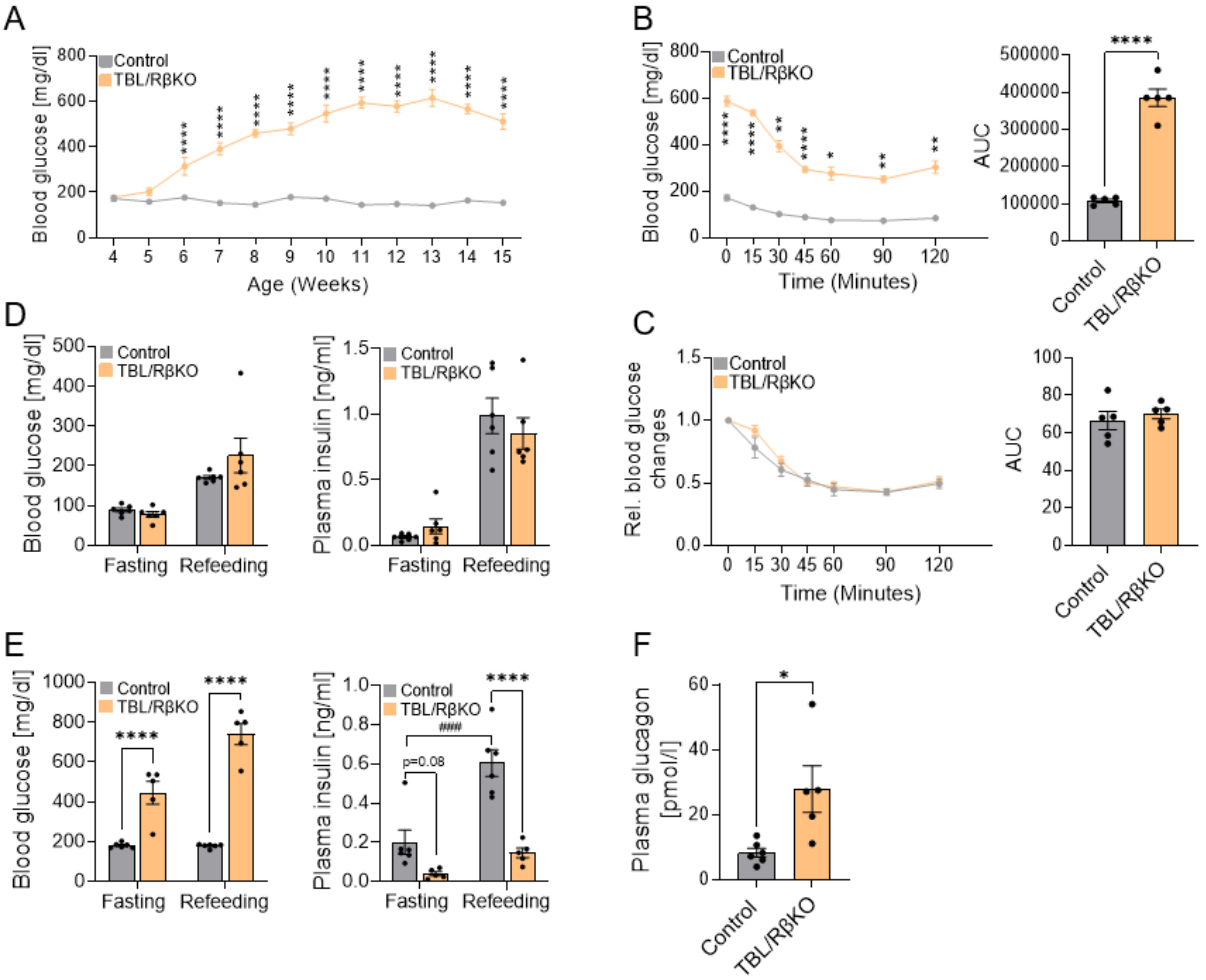

Figure 29: Hyperglycemia in TBL/RβKO mice results from impaired rise in circulating insulin in response to food intake. (A) Weekly determined random blood glucose levels in control (n=6) and TBL/RβKO (n=6) mice. **(B)** ipITT in TBL/RβKO (n=5) mice and control litter mates (n=5). After fasting for 6 h, baseline glucose levels were determined. Subsequently, mice were injected with 0.6 U/kg insulin and blood glucose levels were determined 15, 30, 45, 60, 90, and 120 min after injection. **(C)** Relative blood glucose changes from (B). For this, blood glucose was normalized to baseline blood glucose levels. Blood glucose levels are plotted over time course of the experiment or are displayed as AUC. **(D)** Blood glucose and plasma insulin levels after 16 h of fasting and 2 h of refeeding from 5 week old control and TBL/RβKO mice. **(E)** Blood glucose and plasma insulin levels after 16 h of fasting and 2 h of refeeding from 12 week old control and TBL/RβKO mice. **(F)** Plasma glucagon levels in control and TBL/RβKO mice at the age of 15 weeks. Data is presented as mean ± SEM. Statistical analysis was performed using an unpaired t-test (B,C for AUC, F), a two-way ANOVA with repeated measures and a Šídák's multiple comparison *post hoc* test (A and B,C for blood glucose), or a two-way ANOVA with a Tukey's multiple comparison *post hoc* test (D,E). *Indicates significance between control and TBL/RβKO mice, # indicates significance between fasting and refeeding.

Insulin is a central regulator of energy metabolism as it enables glucose uptake into the periphery. The absence of insulin impairs glucose uptake into the respective tissues which results in a wasting like phenotype, as observed upon type 1 diabetes mellitus (Fu et al. 2013). Indeed, although body weight between TBL/RβKO mice and control litter mates was undistinguishable until the age of 13 weeks, starting from the age of 14 weeks TBL/RβKO body

weight decreased significantly in comparison to the controls (Figure 30A). Body composition analysis at the age of 11 weeks using Echo-MRI revealed substantial loss of fat mass (Figure 30B), preceding the drop in body weight. Accordingly, eWAT weight was severely reduced. In line with mouse models of chronic hyperglycemia, kidney weight was increased (Sharma et al. 2003). No differences in liver and spleen weight were observed (Figure 30C).

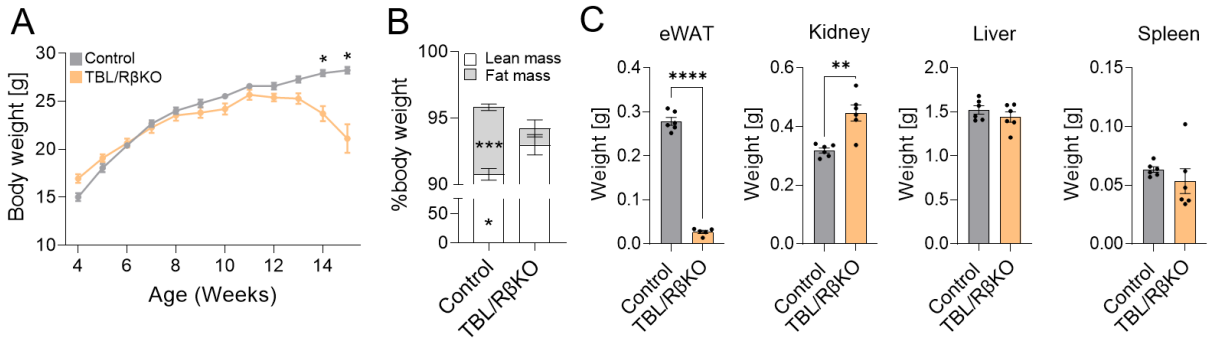

Figure 30: TBL/RβKO mice loose body weight due to fat mass wasting. (A) Weekly determined body weight of TBL/RβKO (n=6) and control (n=6) mice. **(B)** Body composition determined in TBL/RβKO (n=6) and control (n=6) mice at the age of 11 weeks using Echo-MRI. **(C)** eWAT, kidney, liver, and spleen weight determined at the age of 15 weeks. Data is presented as mean ± SEM. Statistical analysis was performed using an unpaired t-test (B,C) or a two-way ANOVA with repeated measures and a Šídák's multiple comparison *post hoc* test (A). *p < 0.05, **p < 0.01, ****p < 0.0001.

In line with the starvation-like phenotype due to lack of peripheral insulin signaling, circulating ketone body levels were increased (Figure 31A). Additionally, triglycerides were significantly increased (Figure 31B), NEFA levels were non-significantly elevated (Figure 31C), and HDL levels were significantly decreased (Figure 31D), suggesting an impairment in lipid metabolism. Interestingly, albumin levels were significantly reduced (Figure 31E) while ALT (Figure 31F) was increased, suggesting that the liver might be affected by the chronic hyperglycemia.

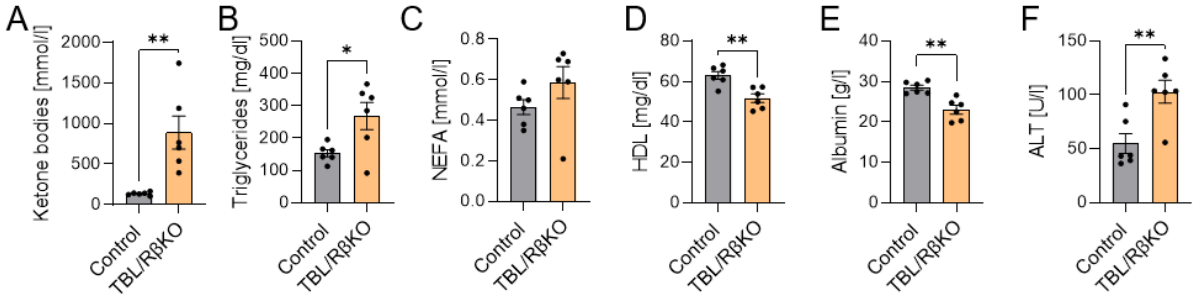

Figure 31: Serum markers related to lipolysis and liver function are altered in TBL/RβKO mice. Serum levels of **(A)** ketone bodies, **(B)** triglycerides, **(C)** NEFA, **(D)** HDL, **(E)** albumin, and **(F)** ALT from 15 week old TBL/RβKO and control mice. Data is presented as mean ± SEM. Statistical analysis was performed using an unpaired t-test. *p < 0.05, **p < 0.01.

Not only facilitates insulin the uptake of glucose, but it also regulates a large portion of metabolic pathways in peripheral tissues such as eWAT and liver. As insulin promotes anabolic pathways, the absence of insulin would trigger catabolic pathways in these tissues. Previously determined serum parameters suggested alterations in eWAT and liver metabolism. Thus, expression of genes associated with glucose and lipid metabolism were determined in eWAT and liver from TBL/RβKO and control mice. In line with reduced eWAT weight, eWAT *Lep* (Leptin) gene expression was significantly reduced in TBL/RβKO mice in comparison to controls. Moreover, according to the hypoinsulinemia in TBL/RβKO mice, expression of insulin regulated key enzymes of fatty acid synthesis such as *Scd1* (Stearoyl-coenzyme A desaturase 1) and *Fasn* (Fatty acid synthase) was reduced, although no statistical significance

was reached for *Fasn*. Additionally, the gene expression of the insulin dependent glucose transporter *Slc2a4* (Solute carrier family 2 member 4) was significantly downregulated in the eWAT of TBL/RβKO mice (Figure 32A). In accordance with eWAT gene expression, liver *Scd1* expression was also significantly reduced in TBL/RβKO animals. As expected, due to the absence of insulin fatty acid oxidation was induced as indicated by an upregulation of *Pgc1a* (Peroxisome proliferator-activated receptor-γ coactivator-1α) (Morris et al. 2012) in TBL/RβKO mice. Ultimately, *Pck1* (Phosphoenoylpyruvate carboxykinase 1), the rate-limiting enzyme of gluconeogenesis in the liver, was also significantly upregulated in TBL/RβKO mice in comparison to controls (Figure 32B). Thus, eWAT wasting in TBL/RβKO mice and alterations in serum lipid parameters result from reduced fatty acid synthesis in eWAT and liver and induced fatty acid oxidation in the liver, promoted by reduced circulating insulin levels. Moreover, hyperglycemia in the TBL/RβKO mice is additionally promoted by upregulation of the gluconeogenic pathway in the liver.

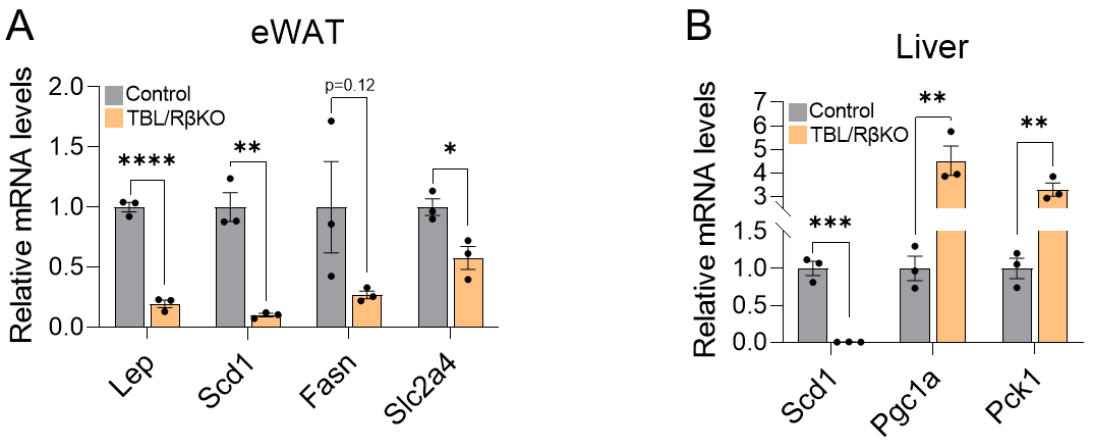

Figure 32: Catabolic pathways are induced in eWAT and liver in hypoinsulinemic TBL/RβKO mice. (A) Gene expression of *Lep*, *Scd1*, *Fasn*, and *Slc2a4* in eWAT from TBL/RβKO and control mice. **(B)** Gene expression of *Scd1*, *Pgc1a*, and *Pck1* in liver from TBL/RβKO and control mice. Data is presented as mean ± SEM. Statistical analysis was performed using an unpaired t-test. *p < 0.05, **p < 0.01, ***p < 0.001, ****p < 0.0001.

Fasting and refeeding glycemia and insulinemia revealed that mice lacking β-cell TBL1 and TBLR1 develop hyperglycemia due to insufficient increase in circulating insulin levels in response to food intake. To investigate whether the reduced circulating insulin levels result from a reduction in insulin synthesis or secretion, islet gene expression from normoglycemic 5 week old control and TBL/RβKO mice was determined. Surprisingly, although TBL1 and TBLR1 gene expression was significantly reduced in comparison to the controls, the expression was higher than expected based on observations from the respective single knock out mice (Figure 33A). Analysis of β-cell identity genes showed that *Ins1* gene expression was significantly reduced in TBL/RβKO mice which exceeded the 50% reduction due to Cre recombinase insertion. Moreover, *Ins2* gene expression was also significantly reduced in TBL/RβKO mice in comparison to control litter mates, suggesting that reduced insulin levels resulted from reduced insulin gene expression. Interestingly, expression of the β-cell identity genes *Pax6*, *Nkx6.1*, *MafA* and *Slc2a2* was downregulated in TBL/RβKO mice, suggesting a loss of β-cell identity (Figure 33B). In accordance with the reduced expression of β-cell identity genes due to β-cell specific TBL1 and TBLR1 knock out, expression of disallowed genes was upregulated. The β-cell progenitor cell marker *Ngn3* was strongly upregulated in TBL/RβKO mice in comparison to controls. Also *ChgA* (Chromogranin A), *Ldha*, and *Hk1* which are commonly repressed in β-cells showed a significant upregulation upon TBL1 and TBLR1 knock out (Figure 33C). Overall, gene expression analysis of pancreatic islets revealed that β-cells lacking TBL1 and TBLR1 lost their ability to express insulin. The downregulation of

transcription factors that control insulin gene expression such as *MafA* in part explain the impaired insulin expression. Simultaneously, β-cell specific TBL1 and TBLR1 ablation promoted the expression of disallowed genes.

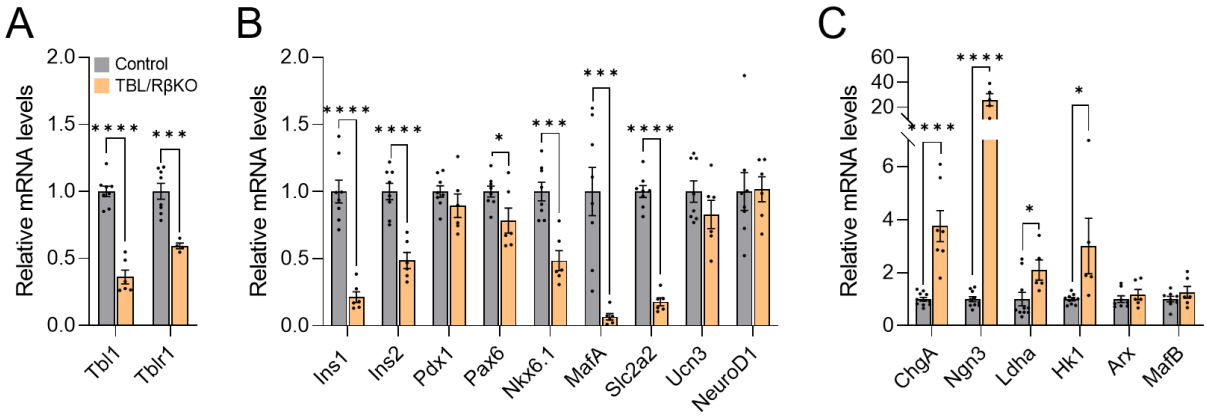

Figure 33: β-cells lacking TBL1 and TBLR1 lose their identity and induce the expression of disallowed genes. Islet **(A)** TBL1 and TBLR1, **(B)** β-cell identity, and **(C)** disallowed gene expression from 5 week old control and TBL/RβKO mice was determined by qPCR. Data is presented as mean ± SEM. Statistical analysis was performed using an unpaired t-test. *p < 0.05, ***p < 0.001, ****p < 0.0001.

In line with the analysis of islet gene expression, total pancreatic insulin content was significantly reduced in 15 week old TBL/RβKO mice (Figure 34B), although no differences in pancreas weight were observed (Figure 34A). In line with the previously observed increase in plasma glucagon levels, pancreatic glucagon content (Figure 34C) was increased in TBL/RβKO mice in comparison to the controls, while no differences in somatostatin content were observed (Figure 34D).

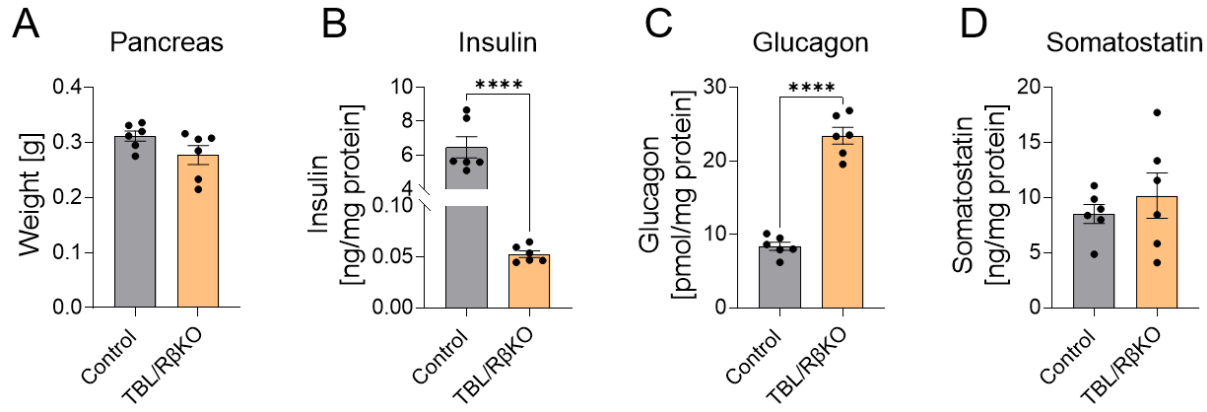

Figure 34: Total pancreas insulin content is reduced while glucagon content is increased in TBL/RβKO mice. (A) Pancreas weight in TBL/RβKO mice and controls. Total pancreas **(B)** insulin, **(C)** glucagon, and **(D)** somatostatin content normalized to protein levels in TBL/RβKO mice and control litter mates. Data is presented as mean ± SEM. Analysis was performed using an unpaired t-test. ****p < 0.0001.

Dissection of the pancreas from TBL/RβKO and control mice was performed at the age of 4 days, 5 weeks, and 20 weeks, to investigate changes in the islet morphology over time. TBL/RβKO mice had a lower body weight in comparison to control litter mates at the age of 4 days and 20 weeks, while no differences at the age of 5 weeks were observed (Figure 35A). Interestingly, 4 days old TBL/RβKO mice had lower blood glucose levels in comparison to controls and in line with previous observations, 5 week old TBL/RβKO mice displayed normoglycemia, while 20 week old TBL/RβKO mice displayed hyperglycemia (Figure 35B). Immunofluorescence staining of islets in paraffin-embedded pancreas sections showed no morphological differences between control and TBL/RβKO mice at the age of 4 days. Although TBL/RβKO mice displayed normal glycemia and insulinemia at the age of 5 weeks, islet

morphology was severely altered. In murine islets, β-cells are predominantly located in the islet core, while α-cells surround the islet in a mantle-like structure (Cabrera et al. 2006). This highly organized structure observed in the islets of 5 and 20 week old control mice was completely lost upon TBL1 and TBLR1 knock out, as glucagon^{+} cell clusters appeared in the islet core in both 5 week old and 20 week old TBL/RβKO mice (Figure 35C). Interestingly, such abnormal islet structure was previously described to occur upon chronic hyperglycemia and T2DM (Kim et al. 2009). However, in TBL1 and TBLR1 deficient mice these alterations precede the hyperglycemia, suggesting that abnormalities in islet architecture are caused by TBL1 and TBLR1 deletion. In line with previously conducted islet gene expression analysis, quantification of the immunofluorescence images revealed that β-cell mass was significantly reduced in TBL/RβKO mice in comparison to the controls independent of the age (Figure 35D). While α-cell mass was significantly reduced at the age of 4 days no differences were observed at the age of 5 weeks between controls and TBL/RβKO mice. At the age of 20 weeks, α-cell mass was significantly increased in TBL/RβKO mice in comparison to control littermates (Figure 35E). Taken together, the immunofluorescence analysis showed that apart from the hyperglycemia and hypoinsulinemia, TBL/RβKO mice display abnormalities in islet micro-architecture which is accompanied by reduced β-cell mass and increased α-cell mass.

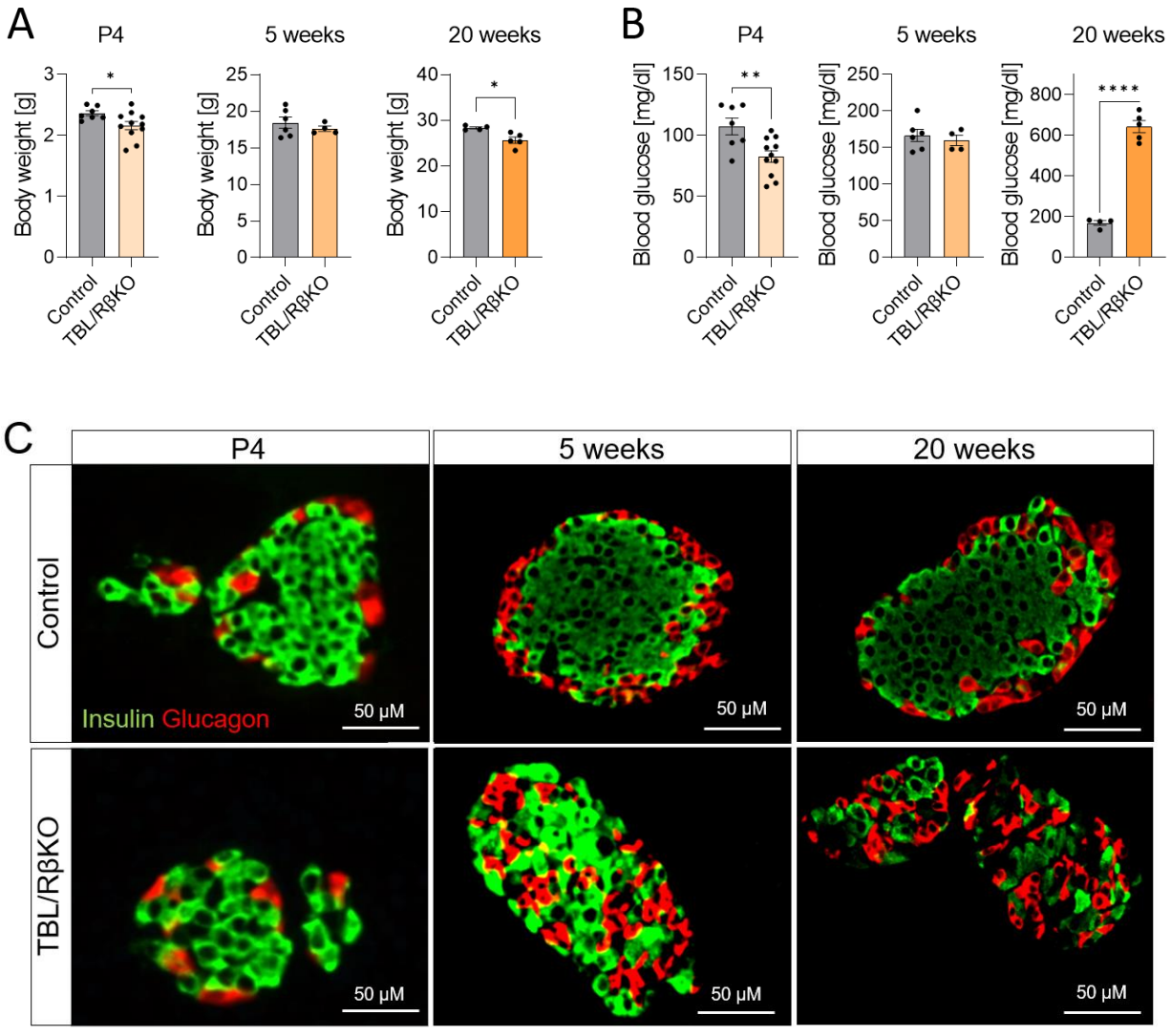

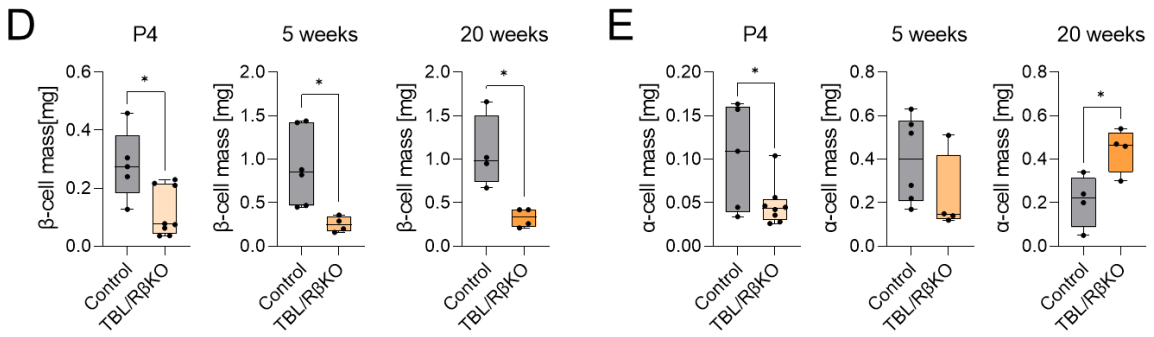

Figure 35: Islets from TBL/RβKO mice display abnormal islet morphology, reduced β-cell mass, and increased α-cell mass. (A) Body weight and **(B)** blood glucose levels from TBL/RβKO or controls at the age of 4 days (P4), 5 weeks, and 20 weeks. **(C)** Representative images of immunofluorescence staining of islets in the pancreas of control or TBL/RβKO mice at the age of 4 days, 5 weeks, and 20 weeks. β-cells are displayed as insulin$^+$ cells in green. α-cells are displayed as glucagon$^+$ cells in red. Immunofluorescence staining was performed and analyzed by the core facility Pathology & Tissue Analytics at the Helmholtz Munich. Quantification of **(D)** insulin$^+$ cell mass (β-cells) and **(E)** glucagon$^+$ cell mass (α-cells) in TBL/RβKO mice and control litter mates at the age of 4 days, 5 weeks, and 20 weeks. Data is presented as mean ± SEM (A,B) or as median and minimum/maximum (D,E). Statistical analysis was performed using an unpaired t-test. *p < 0.05, **p < 0.01, ****p < 0.0001.

2.4.2 Gene expression profiling of islets from TBL/RβKO mice reveals loss of β-cell identity and functionality

β-cell specific ablation of TBL1 and TBLR1 resulted in hyperglycemia due to impaired insulin transcription. Moreover, islets from TBL/RβKO mice showed an abnormal micro-architecture and completely lost the organized structure murine islets usually display (Cabrera et al. 2006). These observations imply a key role of TBL1 and TBLR1 in the regulation of gene expression in β-cells. Global gene expression profiling using RNA Sequencing (RNA-Seq) allows to identify genes under control of TBL1 and TBLR1 that go beyond the scope of previously performed gene expression analysis using qPCR. For this and to avoid secondary effects from chronic hyperglycemia, islets from normoglycemic TBL/RβKO and control mice at the age of 5 weeks were analyzed.

Preceding the hyperglycemia, 5680 genes were alternatively expressed upon β-cell specific TBL1 and TBLR1 knock out of which 3209 genes were upregulated and 2651 genes were downregulated (Figure 36A). Using differentially expressed genes from the RNA-Seq analysis, a Gene Set Enrichment Analysis (GSEA) was performed. In line with the previously performed gene expression analysis using qPCR, GSEA revealed that genes associated with β-cell function were enriched in islets of control mice but were downregulated in islets from TBL/RβKO mice (Figure 36B), suggestive for loss of β-cell identity upon TBL1 and TBLR1 ablation. Moreover, in contrast to islets from control mice, differentially expressed genes enriched for the epithelial-mesenchymal transition (EMT) in TBL/RβKO islets (Figure 36C). Interestingly, an upregulation of EMT signaling was previously associated with loss of β-cell identity and T2DM (Jesus et al. 2021; Avrahami et al. 2020; Roefs et al. 2017).

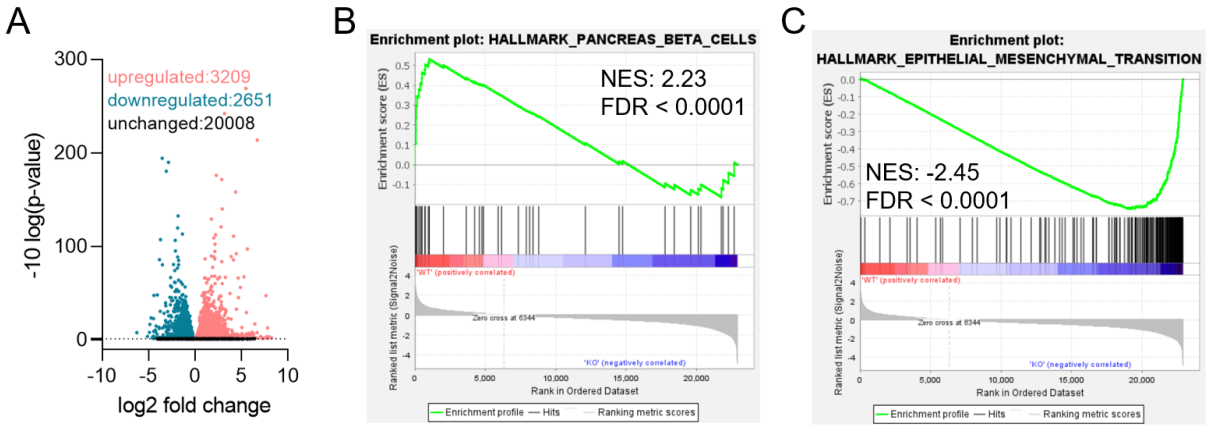

Figure 36: Gene Set Enrichment Analysis reveals loss of β-cell identity and an upregulation of the epithelial-mesenchymal transition. (A) Volcano plot displaying differentially expressed genes from TBL/RβKO islets vs. control islets. The dashed line indicates the threshold for significance (-log10(p-value) = 1.3). Gene Set Enrichment Analysis revealed a **(B)** downregulation of genes associated with β-cell function and an **(C)** upregulation of genes associated with the epithelial mesenchymal transition. NES = Normalized enrichment score; FDR = False discovery rate.

GSEA revealed that genes associated with β-cell function and identity were strongly downregulated while genes associated with the EMT were upregulated in islets from TBL/RβKO mice, suggestig a loss of β-cell identity. Indeed, while *Ins1* and *Ins2* expression were strongly downregulated, genes encoding for the other islet hormones such as glucagon were upregulated in islets from TBL/RβKO mice (Figure 37A). This is in line with previously observed increased α-cell mass, total pancreatic glucagon content, and elevated circulating insulin levels in adult TBL/RβKO mice. Additionally, TBL1 and TBLR1 deficiency resulted in a significant downregulation of not only key β-cell transcription factors such as *Pdx1*, *Nkx6.1*, or *MafA* but also of genes associated with β-cell function including *Pcsk1/2* (proprotein convertase 1/2), *Gipr* (glucose-dependent insulinotropic polypeptide receptor), or *Slc2a2* (Figure 37B). Moreover, genes typically repressed in β-cells under physiological conditions (Pullen et al. 2010; Lemaire et al. 2017), were strongly upregulated in islets from TBL/RβKO mice (Figure 37C). Lastly, also progenitor cell markers such as *Sox9* or *Ngn3* were upregulated in islets from TBL/RβKO mice (Figure 37D). Thus, β-cell specific TBL1 and TBLR1 ablation results in a reprogramming of the pancreatic islet gene expression signature.

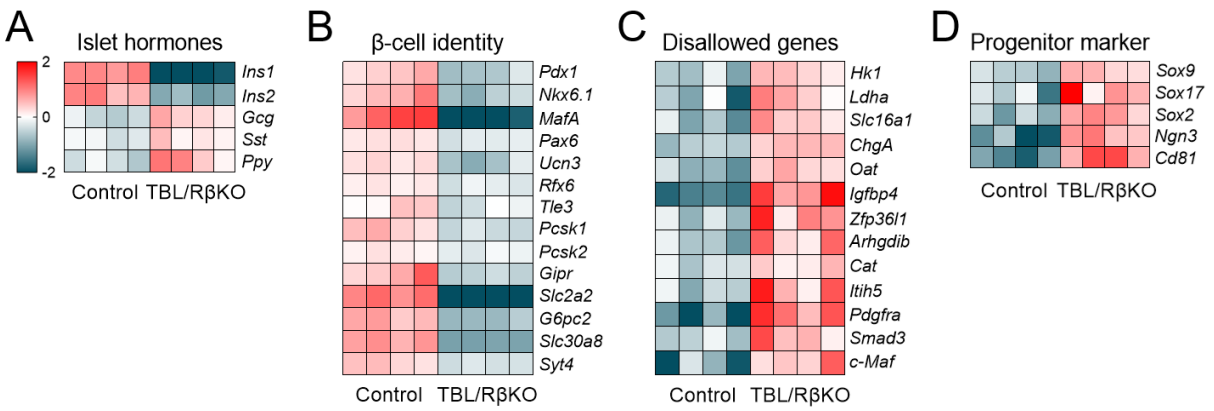

Figure 37: Gene expression profiling reveals a downregulation of β-cell identity genes and an upregulation of disallowed genes in islets from TBL/RβKO mice. Heat map displaying relative expression levels of differentially expressed genes representative for **(A)** islet hormones, **(B)** β-cell identity, **(C)** disallowed genes, and **(D)** β-cell progenitor marker genes. Each line represents one mouse. Colour represents log2 fold-change for control vs. TBL/RβKO. Threshold for significance: -log10(p-value) = 1.3 ($p < 0.05$).

Using Ingenuity Pathway Analysis (IPA) differentially expressed genes were categorized and associated with canonical pathways. Upregulated pathways are displayed in red, downregulated pathways in blue. In line with previously described alterations in β-cell gene expression and islet morphology the *insulin secretion signaling pathway* was downregulated, while *type 2 diabetes mellitus signaling* was upregulated (Figure 38A). Genes implicated in the insulin secretion signaling pathway with the strongest downregulation comprise of the *Slc2a2*, *MafA*, *Ins1*, and *Prlr* (Prolactin receptor) (Figure 38B). Expectedly, for the *type 2 diabetes mellitus signaling* also *Slc2a2* and *MafA*, but also *Ins2* and *Pdx1* showed the strongest downregulation (Figure 38C). Thus, the IPA analysis revealed that islets from TBL/RβKO mice display a gene expression signature associated with impaired insulin secretion and T2DM prior to the onset of changes in glycemia due to downregulation of β-cell identity genes.

A

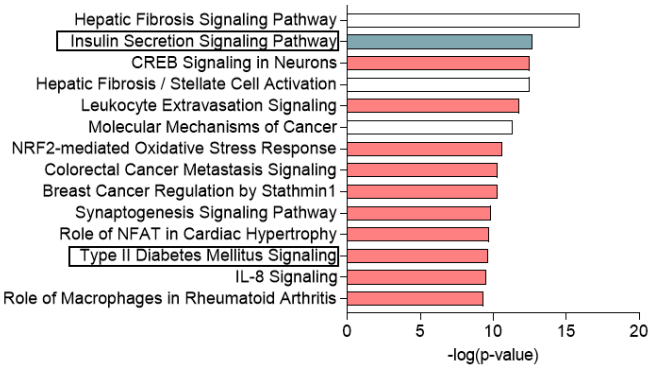

B

Insulin Secretion Signaling Pathway

Gene	Gene name	Fold change
Slc2a2	Solute carrier family 2 a	-4.043
MafA	MAF bZIP transcription factor A	-3.719
Ins1	Insulin 1	-3.086
Prlr	Prolactin receptor	-2.129

C

Type II Diabetes Mellitus Signaling

Gene	Gene name	Fold change
Slc2a2	Solute carrier family 2 a	-4.043
MafA	MAF bZIP transcription factor A	-3.719
Ins2	Insulin 2	-1.753
Pdx1	Pancreatic and duodenal homeobox 1	-1.011

Figure 38: Differentially expressed genes in islets from TBL/RβKO mice show an enrichment in pathways associated with β-cell dysfunction. (A) Enriched canonical pathways identified based on differentially expressed genes from TBL/RβKO islets vs. control islets using Ingenuity Pathway Analysis (IPA). Upregulated pathways are displayed in red, downregulated pathways are displayed in blue. Pathways displayed in white showed no clear regulation pattern. Top downregulated genes in TBL/RβKO islets from the **(B)** *insulin secretion signaling pathway* and the **(C)** *type 2 diabetes mellitus signaling* pathway identified by IPA.

An upstream regulator analysis using IPA identified transcription factors or molecules that might explain differentially expressed genes. The most significant upstream regulator predicted by IPA was TGFB1 (Transforming growth factor β 1), which was previously identified to promote EMT in β-cell dedifferentiation (Jesus et al. 2021). This further supports the notion that TBL1 and TBLR1 deficient β-cells undergo ETM and dedifferentiation, as previously suggested by GSEA. Moreover, Dexamethasone, a glucocorticoid receptor agonist was predicted to cause changes in gene expression upon TBL1 and TBLR1 knock out. Interestingly, Jones and colleagues reported TBLR1 to be implicated in glucocorticoid receptor recruitment (Jones et al. 2014). Indeed, chronic glucocorticoid receptor activation results in hyperglycemia, insulin resistance, glucose intolerance, and reduced β-cell mass which manifest as steroid-induced diabetes (Esguerra et al. 2020; Delangre et al. 2021; Walth-Hummel et al. 2022; Geer et al. 2014), which is partly in line with the phenotypic changes observed upon TBL1 and TBLR1 knock out (Figure 39).

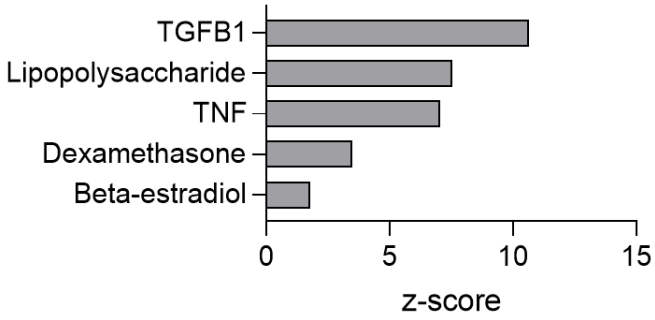

Figure 39: Upstream regulator analysis using IPA identified TGFB1 top hit. With the upstream regulator analysis, IPA identified regulators of transcription that would explain the observed gene expression changes in the data set.

According to the findings from the IPA, also the KEGG pathway analysis revealed a downregulation of pathways associated with β-cell function and physiology. Given that insulin is one of the most abundant and secreted proteins in the β-cell (Fu et al. 2013) and in line with the previously described reduction in insulin gene expression, KEGG pathway analysis revealed a downregulation in gene sets enriched in *protein processing in the endoplasmic reticulum*, *protein export*, and *insulin secretion*. Moreover, the KEGG pathways *maturity onset diabetes of the young* and *type 2 diabetes mellitus* were downregulated based on the gene set enrichment analysis (Figure 40A). Indeed, for both KEGG pathways genes related to β-cell maturity and function such as *Ins1*, *Ins2*, *Slc2a2*, or *MafA* were downregulated while genes related to loss of β-cell identity, including *Ngn3* or *Hk1* were upregulated (Figure 40B). Interestingly, in line with GSEA the most significant upregulated KEGG pathway upon TBL1 and TBLR1 knock out was the *extracellular matrix (ECM) receptor interaction* (Figure 40C). Indeed, EMT and ECM deposition were previously associated with type 2 diabetes and loss of β-cell identity (Roefs et al. 2017; Avrahami et al. 2020; Jesus et al. 2021), which is in line with the diabetes-like changes in the islet transcriptome of normoglycemic TBL/RβKO mice. Moreover, based on the KEGG pathway analysis the *PI3K-Akt signaling pathway* which is involved in cell growth, survival, and proliferation (Yu and Cui 2016) was also upregulated (Figure 40C). Interestingly, TBL1 and TBLR1 were previously identified as critical regulators of pancreatic cancer cell proliferation through the PI3K signaling pathway (Stoy et al. 2015; Gu et al. 2020). As β-cells lose their ability to proliferate during maturation (Meier et al. 2008), the dysregulation of the *PI3K-Akt signaling pathway* along with the immature-like gene expression profile suggests that TBL1 and TBLR1 deficient β-cells might show alterations in β-cell proliferation, resulting in reduced β-cell mass.

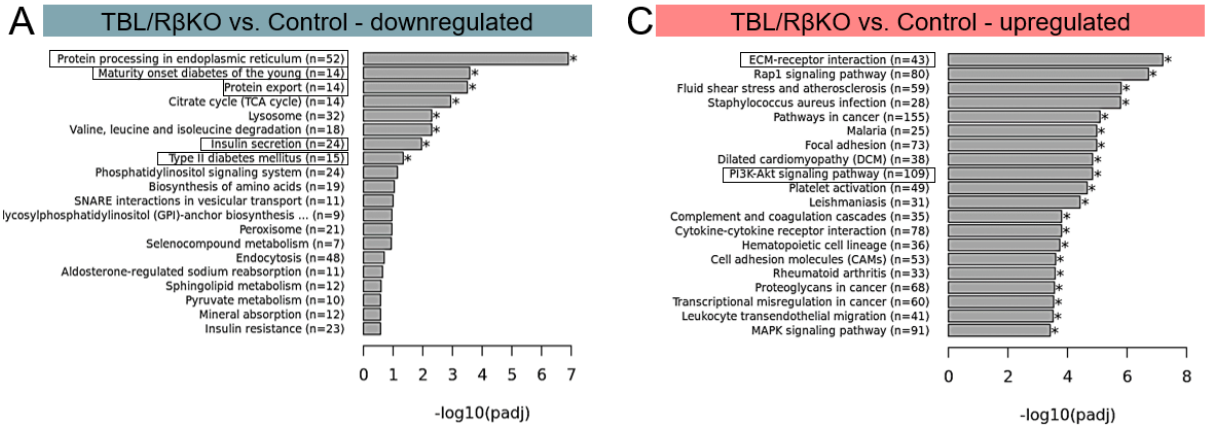

B

KEGG pathway	Gene symbol
Maturity onset diabetes of the young	*Ins1*, *Slc2a2*, *Ins2*, *Bhlha15*, *MafA*, *Ngn3*, *Hes1*, Nkx6-1, *Pax6*, *Pdx1*, *Hnf4g*, *Neurod1*, *Foxa3*, *Iapp*, *Rfx6*, *Pklr*, *Hhex*, *Hnf4a*, *Mnx1*, *Gck*
Type 2 diabetes mellitus	*Ins1*, *Slc2a2*, *Ins2*, *MafA*, *Kcnj11*, *Pdx1*, *Pik3r3*, *Irs2*, *Abcc8*, *Hk1*, *Hk2*, *Cacna1e*, *Irs3*, *Socs3*, *Pklr*, *Mapk9*, *Cacna1a*, *Pik3cd*, *Hk3*, *Cacna1g*, *Mtor*, *Socs2*, *Prkcz*, *Cacna1b*, *Gck*, *Cacna1d*, *Irs1*, *Slc2a4*

Figure 40: KEGG pathway analysis revealed a downregulation of gene sets associated with β-cell function and physiology. (A) Downregulated pathways based on enriched gene sets using KEGG pathway analysis. **(B)** Up- (red) and downregulated (blue) genes in TBL/RβKO islets from the *maturity onset diabetes of the young* and *type 2 diabetes mellitus* KEGG pathway. **(C)** Upregulated pathways based on enriched gene sets using KEGG pathway analysis.

2.4.3 TBL1 and TBLR1 are not implicated in β-cell proliferation

In humans, the proliferative capacity of pancreatic β-cells reaches its maximum during foetal life. In the first two years of life, the proliferative rate declines and only very low replication rates are observed during childhood, adolescence, and adulthood for β-cells (Meier et al. 2008), in part due to increased methylation of the promoter regions of proliferation genes (Avrahami et al. 2015). As the loss of functional β-cells is a central driver for the development of T2DM (Fu et al. 2013), promotion of proliferation and thereby the increase in the number of functional β-cells represents a widely investigated field in β-cell research. Interestingly, previous studies have identified TBL1 and TBLR1 as critical regulators of proliferation in pancreatic cancer cells (Li et al. 2014; Stoy et al. 2015; Gu et al. 2020). Moreover, an upregulation of *the PI3K-Akt signaling pathway* was observed in a global transcriptome profiling using islets from normoglycemic TBL/RβKO mice. As mice lacking TBL1 and TBLR1 display hyperglycemia and hypoinsulinemia resulting from reduced β-cell mass, proliferative capacity of β-cells lacking TBL1 and/or TBLR1 was investigated *in vivo*.

For this, TBLβKO, TBLRβKO, normoglycemic TBL/RβKO, and respective controls were *in vivo* injected with Bromodeoxyuridine (BrdU) for three consecutive days. Pancreata were subsequently collected and immunohistochemically analyzed for insulin, glucagon, and BrdU (Figure 41A). Cells that co-stained for insulin and BrdU were regarded as proliferated β-cell. Body weight, blood glucose levels, and pancreas weight did not differ between TBLβKO, TBLRβKO mice, and control litter mates (Figure 41B). In line with previously described results, no differences in pancreatic β-cell mass were observed and as expected, also no differences in proliferative rate between TBLβKO or TBLRβKO mice and controls were observed. Accordingly, β-cell mass that co-stained with BrdU relative to total β-cell mass did not differ between the respective knock outs and controls (Figure 41C). In the TBL/RβKO mice, no differences in blood glucose levels or pancreas weight were observed although body weigh was significantly reduced in comparison to the controls (Figure 41D). As previously observed, β-cell mass was significantly decreased in TBL/RβKO mice in comparison to controls. Interestingly, proliferated β-cell mass was also significantly reduced, which indicates a downregulation of proliferative capacity of β-cells lacking TBL1 and TBLR1. However, normalizing β-cells mass co-stained with BrdU to total β-cell mass, no differences between TBL/RβKO mice and controls were observed (Figure 41E). Thus, reduced β-cell mass observed upon TBL1 and TBLR1 knock out does not result from dysregulated proliferation.

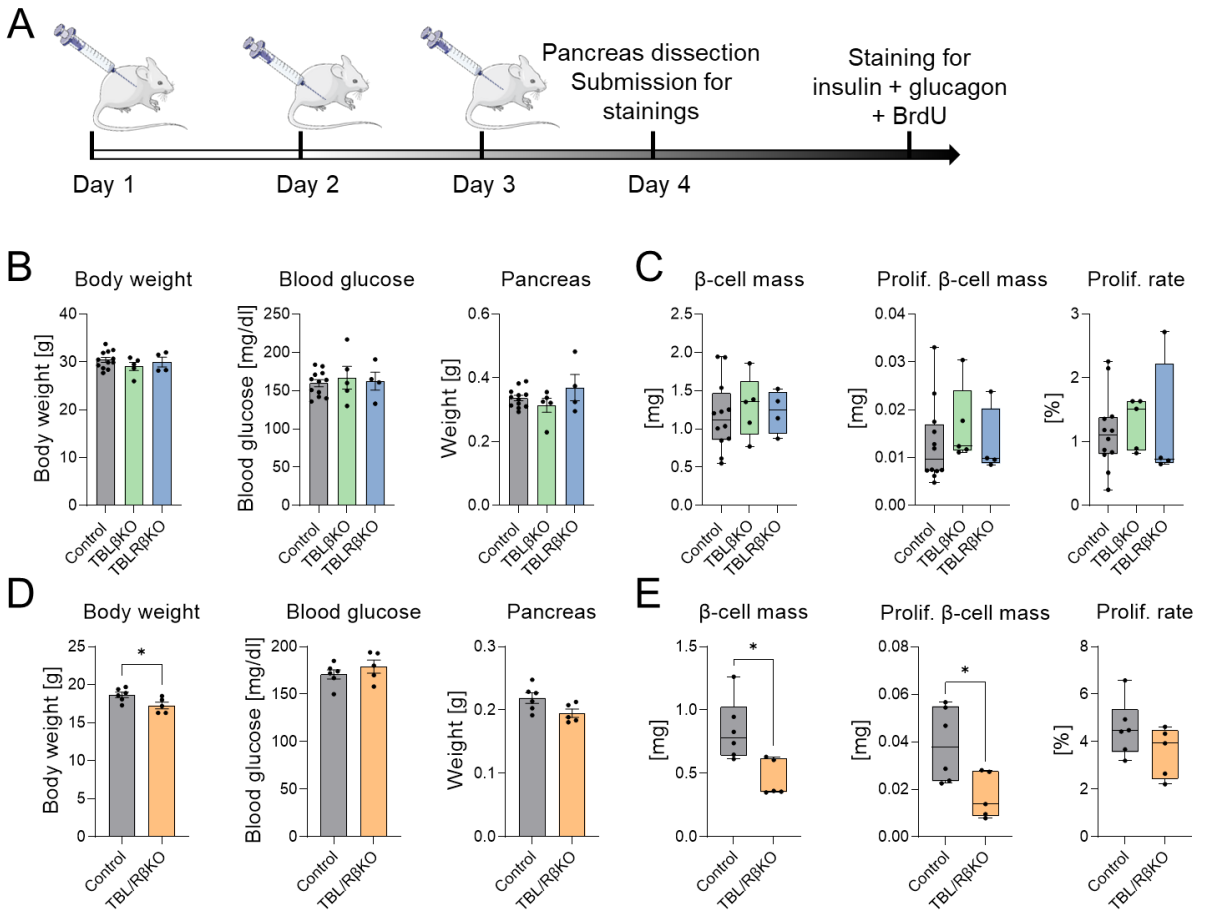

Figure 41: TBL1 and TBLR1 are not implicated in β-cell proliferation. (A) Experimental procedure of *in vivo* Bromodeoxyuridine (BrdU) injections to determine the proliferative rate of β-cells in TBLβKO, TBLRβKO, and TBL/RβKO mice. **(B)** Body weight, blood glucose, and pancreas weight of 12 week old control, TBLβKO, and TBLRβKO mice. **(C)** β-cell mass (insulin$^+$ cells), mass of proliferated β-cells (insulin$^+$BrdU$^+$ cells), and the proliferative rate of β-cells of controls, TBLβKO, and TBLRβKO mice. **(D)** Body weight, blood glucose, and pancreas weight of 5 week old control and TBL/RβKO mice. **(E)** β-cell mass (insulin$^+$ cells), mass of proliferated β-cells (insulin$^+$BrdU$^+$ cells), and the proliferative rate of β-cells of controls and TBL/RβKO mice. Immunofluorescence staining was performed and analyzed by the core facility Pathology & Tissue Analysis at the Helmholtz Munich. Data is presented as mean ± SEM (B,D) or as median and minimum/maximum (C,E). Statistical analysis was performed using an unpaired t-test (D,E) or a one-way ANOVA with a Dunnett's multiple comparison *post hoc* test (B,C). *p < 0.05.

2.4.4 TBL1 and TBLR1 are not implicated in β-cell maturation during weaning

Pancreatic β-cells lacking TBL1 and TBLR1 show signatures of immature β-cells, as genes typically expressed in β-cell progenitor cells were found to be expressed in islets from TBL/RβKO mice. Alterations in islet gene expression and morphology interestingly preceded the onset of hyperglycemia, suggesting that the occurring β-cell failure is a time dependent process and starts before the age of 5 weeks. Notably, murine β-cell maturation is a process taking place in two waves. In mice, the first wave, also called the functional maturation occurs in the early postnatal period and is characterized by the acquisition of glucose stimulated insulin secretion (Otonkoski et al. 1988; Otonkoski et al. 1991). The second wave of maturation is triggered during weaning by the transition from high fat milk to high carbohydrate chow diet (Stolovich-Rain et al. 2015). To investigate whether TBL1 and TBLR1 are required for weaning-triggered maturation, mice were either prematurely weaned at the age of 18 days (Weaned), or remained with their mothers (Suckling). At the age of 25 days, mice were sacrificed and pancreata were dissected for immunofluorescence staining (Figure 42). Thus, if TBL1 and TBLR1 play a key role in weaning-triggered maturation, alterations in islet morphology would occur only in the prematurely weaned mice and not in mice that remained with their mothers.

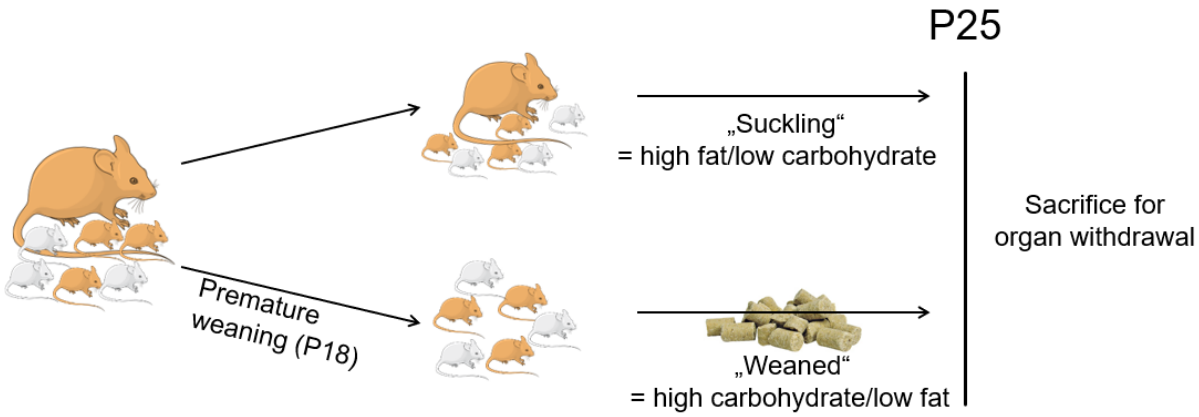

Figure 42: Experimental procedure to investigate the involvement of TBL1 and TBLR1 in β-cell maturation. Mice were either prematurely weaned at the age of 18 days (P18; Weaned) or remained with their mothers (Suckling). At the age of 25 days, mice were sacrificed. Pancreata were dissected and subsequently submitted to the core facility Pathology & Tissue Analytics at the Helmholtz Munich for immunofluorescence staining and analysis.

On the day of tissue collection, no differences in body weight, blood glucose levels (Figure 43A), or pancreas weight (Figure 43B) were observed between controls and TBL/RβKO mice from the Weaning or Suckling group. In line with previous observations, immunofluorescence staining of insulin and glucagon showed that β-cell specific deletion of TBL1 and TBLR1 lead to a loss of the highly organized islet structure. Abnormal islet micro-architecture in the TBL/RβKO mice did not differ between the Weaning and Suckling group (Figure 43C). Quantification of the immunofluorescence staining of the paraffin-embedded pancreas showed no significant differences in β-cell mass between controls and TBL/RβKO mice from the Weaning or Suckling group, although in previous observations β-cell mass was significantly reduced in TBL/RβKO mice at the age of 4 days. In line with previous observations α-cell mass was unchanged between controls and TBL/RβKO mice from the Weaning or Suckling group (Figure 43D). The α- to β-cell ratio was previously demonstrated to increase upon T2DM (Fujita et al. 2018). Preceding the hyperglycemia, the α- to β-cell ratio was significantly increased in the TBL/RβKO mice from the Suckling and Weaning group in comparison to the respective controls (Figure 43E). Thus, prolonged suckling period did not protect from the development of an abnormal islet structure, ultimately indicating that the second wave of maturation, triggered by weaning does not require TBL1 and TBLR1 function.

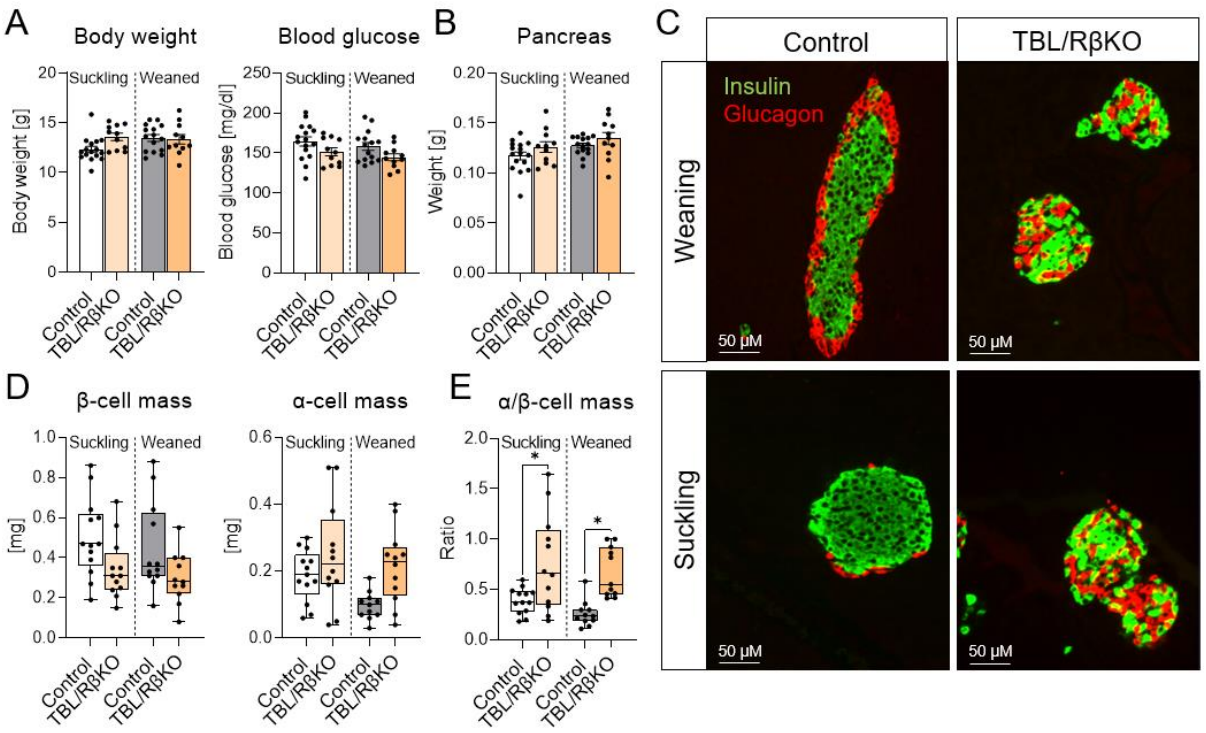

Figure 43: TBL1 and TBLR1 are not required for weaning-triggered maturation of pancreatic β-cells. Control and TBL/RβKO mice were either prematurely weaned (Weaned) at the age of 18 days or remained with their mothers (Suckling) until sacrifice at the age of 25 days. **(A)** Body weight and blood glucose levels of control and TBL/RβKO mice that were prematurely weaned or remained with their mothers. **(B)** Pancreas weight of control or TBL/RβKO mice from the respective group. **(C)** Representative immunofluorescence staining of β-cells in green (insulin$^+$) and α-cells in red (glucagon$^+$). Immunofluorescence staining was performed and analyzed by the core facility Pathology & Tissue Analytics at the Helmholtz Munich. **(D)** Quantification of insulin$^+$ cell mass (β-cells) and glucagon$^+$ cell mass (α-cells) from Weaned or Suckling TBL/RβKO mice and control litter mates. **(E)** α-cell mass relative to β-cell mass calculated from quantification of α-cell and β-cell mass from (D). Data is presented as mean ± SEM (A,B) or as median and minimum/maximum (D,E). Statistical analysis was performed using a Šídák's multiple comparison *post hoc* test. *p < 0.05.

2.4.5 Single cell sequencing of islets from TBL/RβKO animals reveals loss of β-cell identity

Bulk RNA-Seq in islets from control and TBL/RβKO mice revealed severe changes in the transcriptome and identified almost 6000 differentially expressed genes upon β-cell specific TBL1 and TBLR1 deficiency. A major limitation of RNA-Seq is that different cell types within a sample are not distinguished, which is critical in particular for pancreatic islets as multi-cellular micro-organs comprising of 5 different endocrine cell types (Cabrera et al. 2006). Thus, single cell RNA sequencing (scRNA-Seq) was performed to generate a transcriptional profile of the distinct endocrine cell types in the islets of normoglycemic TBL/RβKO mice and controls.

Pancreatic islets from 3 control and 4 TBL/RβKO mice were isolated and pooled. From each group, 150 islets were used for single cell dissociation and subsequent sequencing. In total, 6785 single cells from the controls and 5727 single cells from the TBL/RβKO mice were sequenced. Based on the expression of cell type specific marker genes, sequenced cells were identified as either endocrine cell (expressing *Ins1*, *Gcg*, *Sst*, *Ppy*, or *Ghrl*), ductal cell (expressing *Krt19*), acinar cell (expressing *Cpa1*), endothelial cell (expressing *Pecam1*), or immune cell (expressing *Cd68*), resulting in 6 major clusters. The two-dimensional projection using uniform manifold approximation and projection (UMAP) shows that the endocrine cells represent the largest cluster. The low abundance of non-endocrine cell types underlines a clean sampling of the islets (Figure 44).

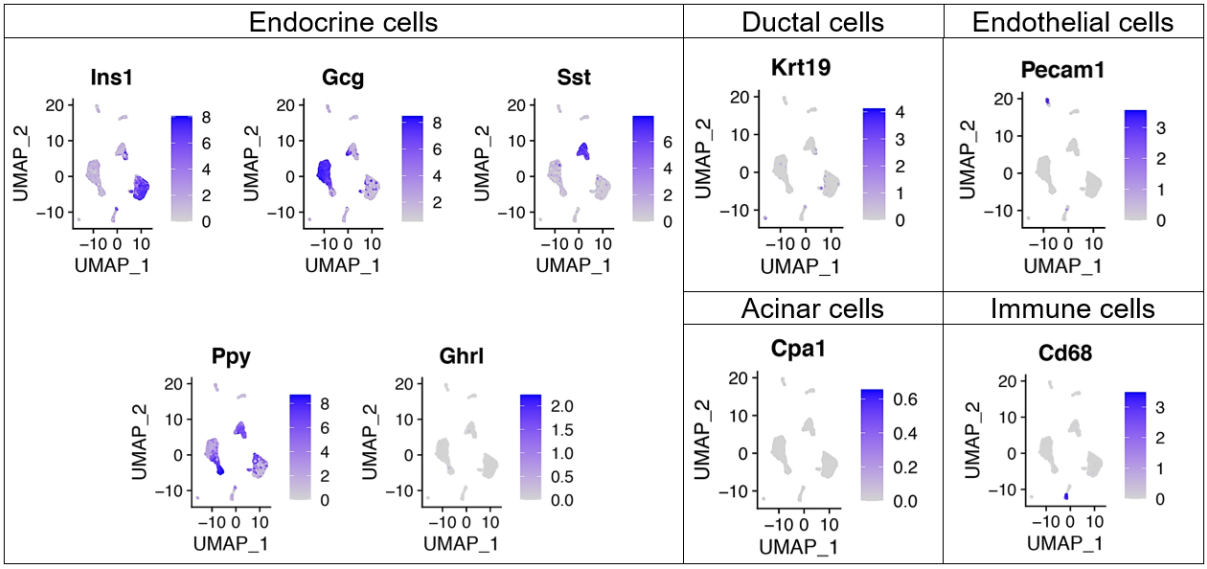

Figure 44: Two-dimensional projection of single cells reveals 6 major clusters. Uniform manifold approximation and projection (UMAP) visualization of the merged data set of the scRNA-Seq data from islet cells from controls and TBL/RβKO mice capturing all detected cell types identified by signature genes. Sample processing and library preparation was performed by the core facility Single Cell Genomics at the Helmholtz Munich. Sequencing was performed by the core facility Genomics at the Helmholtz Munich. Bioinformatic analysis was performed by Peter Weber.

Two-dimensional projection of the endocrine cell clusters using UMAP revealed that in the TBL/RβKO islets, the β-cell cluster represented as Ins1$^+$ cells was smaller than in the control, while the clusters for the other cell types appeared larger. Interestingly PP-cells identified as pancreatic polypeptide Y$^+$ (Ppy) cells were more pronounced in the β-cell cluster of the TBL/RβKO islets than in control islets. Moreover, a set of cells identified as somatostatin$^+$ (Sst) δ-cells appeared as small sub-cluster between the β-cell and δ-cell cluster in the TBL/RβKO islets (Figure 45A). Quantitative analysis of the cell type composition was in line with the UMAP observations, as in the islets of TBL/RβKO mice less β-cells but more α-, δ-, and PP-cells were identified. Interestingly, polyhormonal cells as they were previously observed in murine and human islets (Katsuta et al. 2010; Blodgett et al. 2015), occurred more often in islets from TBL/RβKO mice than in islets from the controls. In particular cells co-expressing three different hormones occurred more often in the islets from TBL/RβKO mice than in the controls, while cells co-expressing insulin and glucagon or insulin and somatostatin were observed less often in the TBL/RβKO islets (Figure 45B).

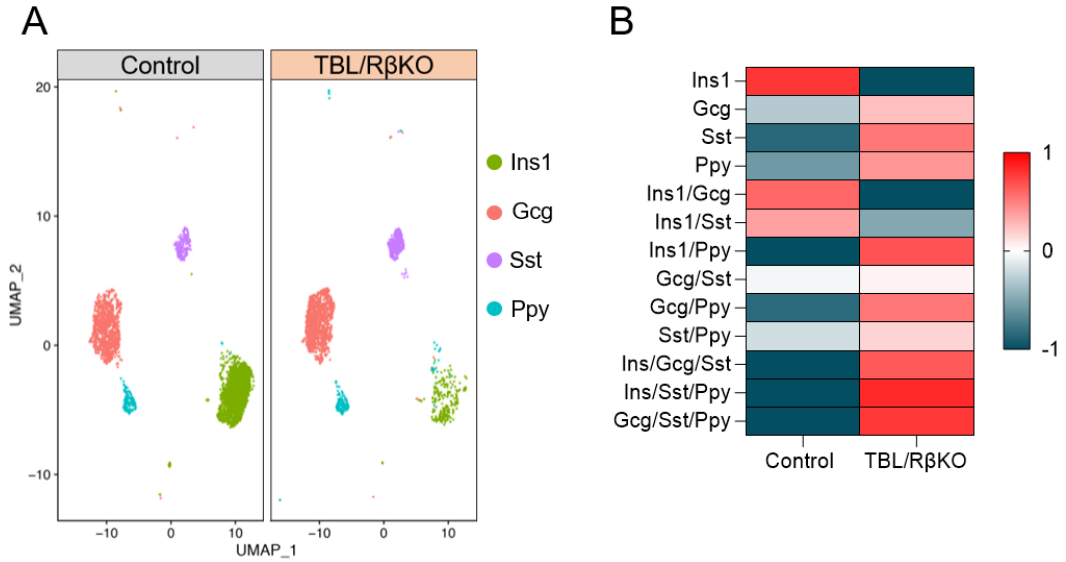

Figure 45: scRNA-Seq reveals alterations in the cell type proportions in islets of TBL/RβKO mice. (A) UMAP visualization of the endocrine cell clusters from islet cells from controls and TBL/RβKO mice with each dot representing one cell. The major clusters display the 4 main endocrine cell types in the islet. Only monohormonal cells are displayed. **(B)** Heat map showing the relative abundance of the identified cells in the islets of control and TBL/RβKO mice. Bioinformatic analysis was performed by Peter Weber.

Differentially expressed genes between controls and TBL/RβKO of cells identified as β- or α-cells were analyzed using Enrichr. As expected from previous gene expression analysis, differentially expressed genes in cells identified as β-cells were enriched in pathways associated with *Insulin Secretion, Insulin Synthesis*, or *β-cell Function* (Figure 46A). Surprisingly, cells identified as α-cells also showed an enrichment in genes associated with pathways typical for β-cells, such as *Insulin Synthesis* or *β-cell Function* (Figure 46B). This suggests that β-cells lacking TBL1 and TBLR1 might have been identified as α-cells due to the dysregulation of gene expression.

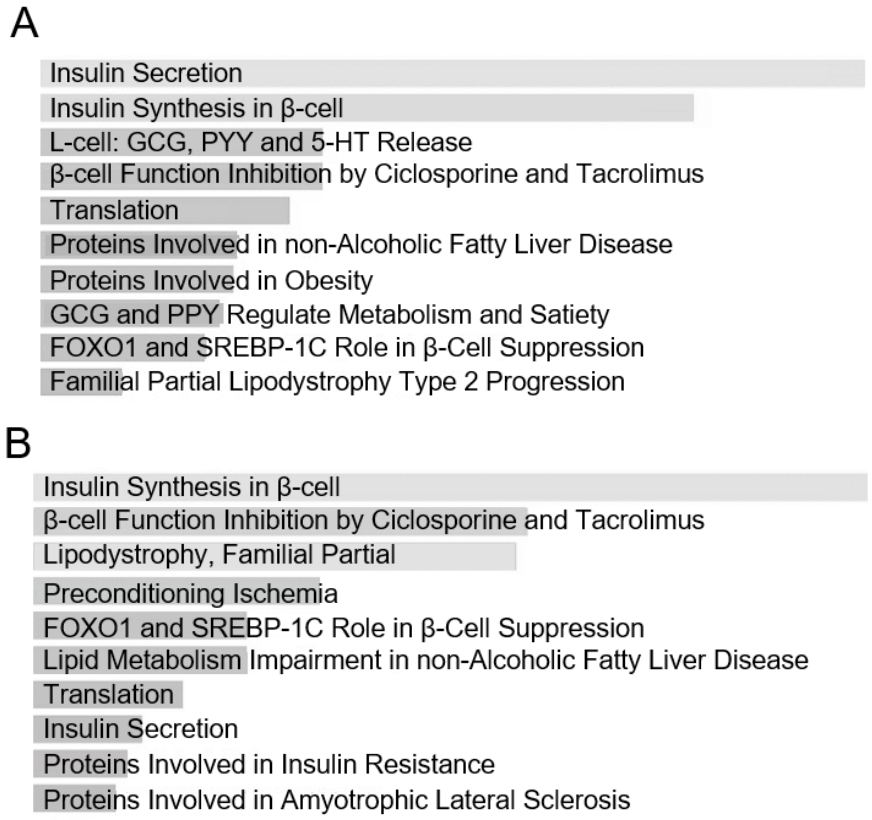

Figure 46: Differentially expressed genes in cells identified as α- and β-cells enrich for pathways associated with β-cell function. Analysis was performed using Enrichr. Displayed are the 10 most significant pathways based on differentially expressed genes in cells identified as **(A)** β-cells or **(B)** α-cells. Length of the bar is representative for the p-value of the respective pathway.

The cluster analysis and the quantification of the distinct cell types revealed that β-cell number was reduced while cell number from other endocrine cell types as well as poly-hormonal cells were increased in pancreatic islets from TBL/RβKO mice. This suggests that β-cells deficient for TBL1 and TBLR1 might transdifferentiate into other cell types. Therefore, the expression of β-cell identity genes was analyzed in β-cells but also in the other endocrine cells identified as α-, δ-, or PP-cells. In line with bulk RNA-Seq data and qPCR analysis, *MafA* expression was strongly reduced in β-cells of TBL/RβKO mice in comparison to controls. Surprisingly, *MafA* expression was also reduced in all the other endocrine cell types (Figure 47A), although TBL1 and TBLR1 knock out was restricted to the β-cells. In TBL/RβKO mice *Nkx6.1* expression was also not only reduced in β-cells but also in α- and PP-cells while in δ-cells *Nkx6.1* expression was increased (Figure 47B). Moreover, in TBL/RβKO mice the *Slc30a8* expression which

encodes for the zink transporter 8, an important marker for β-cell function was, downregulated in β-, δ-, and PP-cells while no changes in α-cells were observed (Figure 47C).

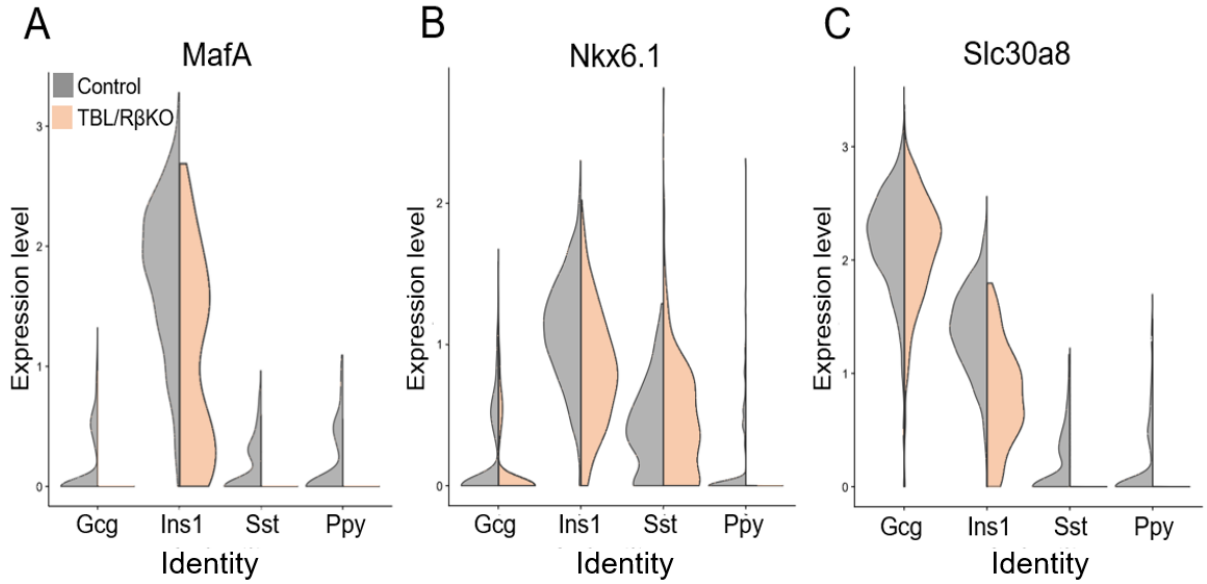

Figure 47: Expression of β-cell identity genes is changed in other endocrine cell types in TBL/RβKO mice. **(A)** *MafA*, **(B)** *Nkx6.1*, and **(C)** *Slc30a8* expression in cells identified as glucagon$^+$ (Gcg) α-cells, insulin$^+$ (Ins1) β-cells, somatostatin$^+$ (Sst) δ-cells, and pancreatic polypeptide Y$^+$ (Ppy) PP-cells in islets from TBL/RβKO mice or control litter mates. Sample processing and library preparation was performed by the core facility Single Cell Genomics at the Helmholtz Munich. Sequencing was performed by the core facility Genomics at the Helmholtz Munich. Bioinformatic analysis was performed by Peter Weber.

Of note, despite the 70-80% reduction of TBL1 and TBLR1 mRNA and protein levels in pancreatic islets from the respective knock out mice, no reduction was detected in TBL1 or TBLR1 mRNA in the scRNA-Seq. This is expected as only exon 5 is excised while the remaining mRNA is transcribed. This excludes the detection of the knock out via scRNA-Seq.

In summary, two-dimensional projection of the cells based on gene expression patterns using UMAP showed a formation of sub-clusters upon TBL/RβKO. Moreover, cells identified as non-β-cells based on the expression of cell-type specific marker, clustered together with β-cells upon TBL1 and TBLR1 knock out, suggesting that β-cells lacking TBL1 and TBLR1 start to express marker genes of other cell-types. Accordingly, although TBL1 and TBLR1 knock out was restricted to β-cells, expression of the other endocrine cells was also changed. In particular β-cell identity genes, which were dramatically downregulated in TBL1 and TBLR1 deficient β-cells were also reduced in cells identified as α-, δ-, or PP-cells. To elucidate the mechanism through which TBL1 and TBLR1 control β-cell identity and to investigate whether TBL1 and TBLR1 deficient β-cells indeed transdifferentiate into other cell types, next an *in vitro* model was established.

2.5 The role of TBL1 and TBLR1 in β-cell physiology in the β-cell lines INS1E and MIN6

Thus far, TBL1 and TBLR1 were identified as essential regulators of β-cell identity as TBL/RβKO mice displayed hyperglycemia, hypoinsulinemia, and abnormal islet micro-architecture which was accompanied by dramatic changes in the islet transcriptome. Surprisingly, TBL1 and TBLR1 were not involved in β-cell proliferation or weaning-triggered β-cell maturation. To understand the underlying mechanism through which TBL1 and TBLR1 regulate substantial processes in the β-cell such as insulin gene expression, an *in vitro* TBL1

and TBLR1 knock down model was established. TBL1 and TBLR1 knock down was induced in INS1E cells using small interference RNA (siRNA) or MIN6 cells using small hairpin RNA (shRNA). After knock down gene expression and β-cell functionality were investigated.

2.5.1 β-cell identity gene expression is upregulated upon TBLR1 and TBL1/TBLR1 double knock down in INS1E cells

INS1E cells were transfected with non-targeting siRNA or siRNA targeting TBL1 and TBLR1. After 5 days, knock down efficiency was determined. siRNA mediated knock down of TBL1 reduced efficiently TBL1 mRNA (Figure 48A) and protein (Figure 48B) levels in comparison to INS1E cells transfected with the control siRNA. Interestingly, as previously observed in the TBLβKO mice, TBLR1 mRNA (Figure 48A) and protein (Figure 48D) levels were significantly increased upon TBL1 ablation, suggesting that the upregulation of TBLR1 upon TBL1 deficiency displays a conserved mechanism in rodents. siRNA mediated knock down of TBLR1 was successful on mRNA (Figure 48C) and protein (Figure 48D) level. As previously observed in the TBLRβKO mice, TBL1 expression (Figure 48B,C) was unchanged upon TBLR1 ablation. Simultaneous knock down of TBL1 and TBLR1 reduced TBL1 mRNA levels by 80%, while TBLR1 mRNA levels were reduced by only 50% (Figure 48E). Nevertheless, TBL1 and TBLR1 protein expression was strongly reduced upon TBL1 and TBLR1 knock down in comparison to the control (Figure 48F), suggesting a successful knock down.

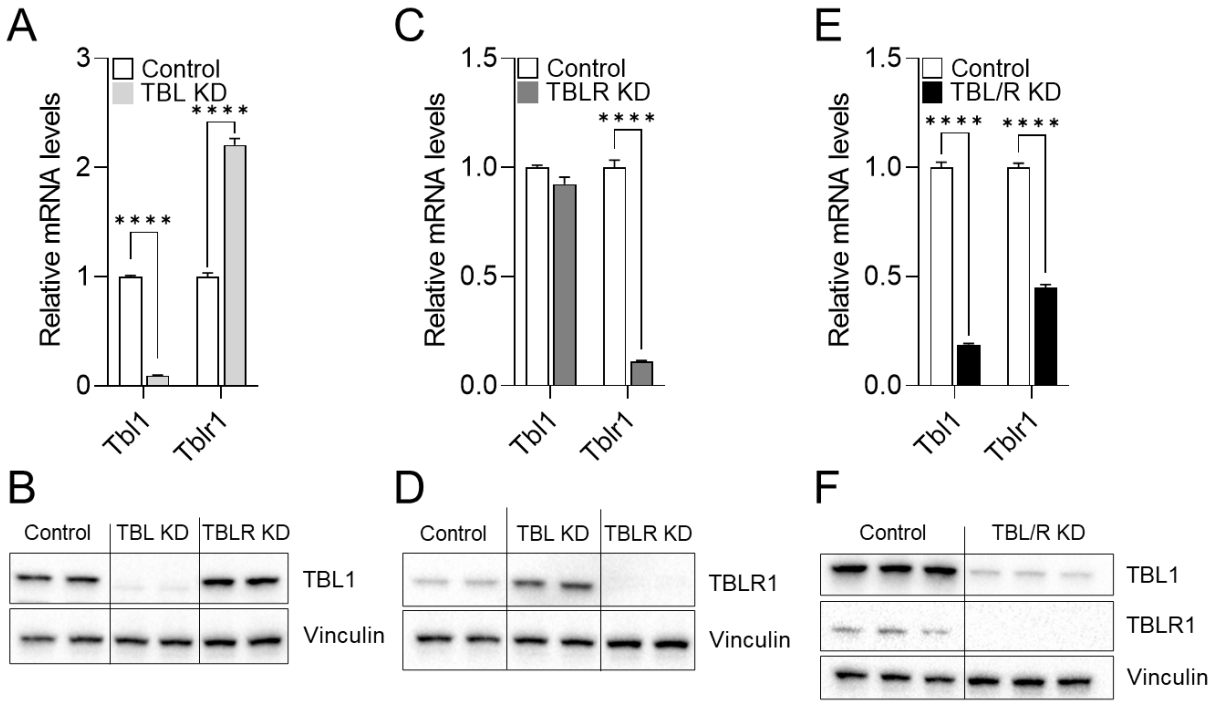

Figure 48: TBL1 and TBLR1 are successfully knocked down in INS1E cells. INS1E cells were transfected for 5 days using control siRNA (Control) or siRNA targeting TBL1 and/or TBLR1 (TBL KD, TBLR KD, or TBL/R KD). **(A)** TBL1 and TBLR1 mRNA levels in INS1E cells transfected with control siRNA (n=4) or siRNA targeting TBL1 (n=4). **(B)** TBL1 and Vinculin protein levels in INS1E cells after transfection with control siRNA or siRNA targeting TBL1 or TBLR1, respectively. **(C)** TBL1 and TBLR1 mRNA levels in INS1E cells transfected with control siRNA (n=4) or siRNA targeting TBLR1 (n=4). **(D)** Western Blot displaying Vinculin and TBLR1 protein expression in INS1E cells transfected with control siRNA or siRNA targeting TBL1 or TBLR1, respectively. TBL1 and TBLR1 **(E)** mRNA and **(F)** protein levels in INS1E cells after transfection using control siRNA (n=6) or TBL1 and TBLR1 (n=6) siRNA. Data is presented as mean ± SEM. Statistical analysis was performed using an unpaired t-test. ****p < 0.0001.

After the validation of the knock down of TBL1 and TBLR1 on mRNA and protein level, gene expression of β-cell identity genes and disallowed genes was determined. Interestingly, upon TBL1 knock down, *Ins1, Ins2*, *and Slc2a2* expression was downregulated while *Pdx1* and *Ucn3* expression was upregulated in comparison to the control (Figure 49A). Expression of genes

typically disallowed in β-cells was unchanged in INS1E cells transfected with either control siRNA or TBL1 siRNA (Figure 49B). Unexpectedly, TBLR1 knock down induced an upregulation of all determined β-cell identity genes (Figure 49C). *ChgA* expression was significantly increased, while *Ngn3* expression was unchanged (Figure 49D), suggesting an improvement of β-cell function upon TBLR1 ablation. Interestingly, as for INS1E cells upon TBLR1 knock down, simultaneous knock down of TBL1 and TBLR1 resulted in an upregulation of almost all β-cell identity genes, apart from *Ins2,* which was significantly downregulated (Figure 49E). Moreover, *ChgA* expression was upregulated (Figure 49F). Thus, in contrast to previous observations *in vivo* TBL1 and TBLR1 deficiency *in vitro* resulted in a general upregulation of β-cell identity gene expression, suggesting an improvement of β-cell function.

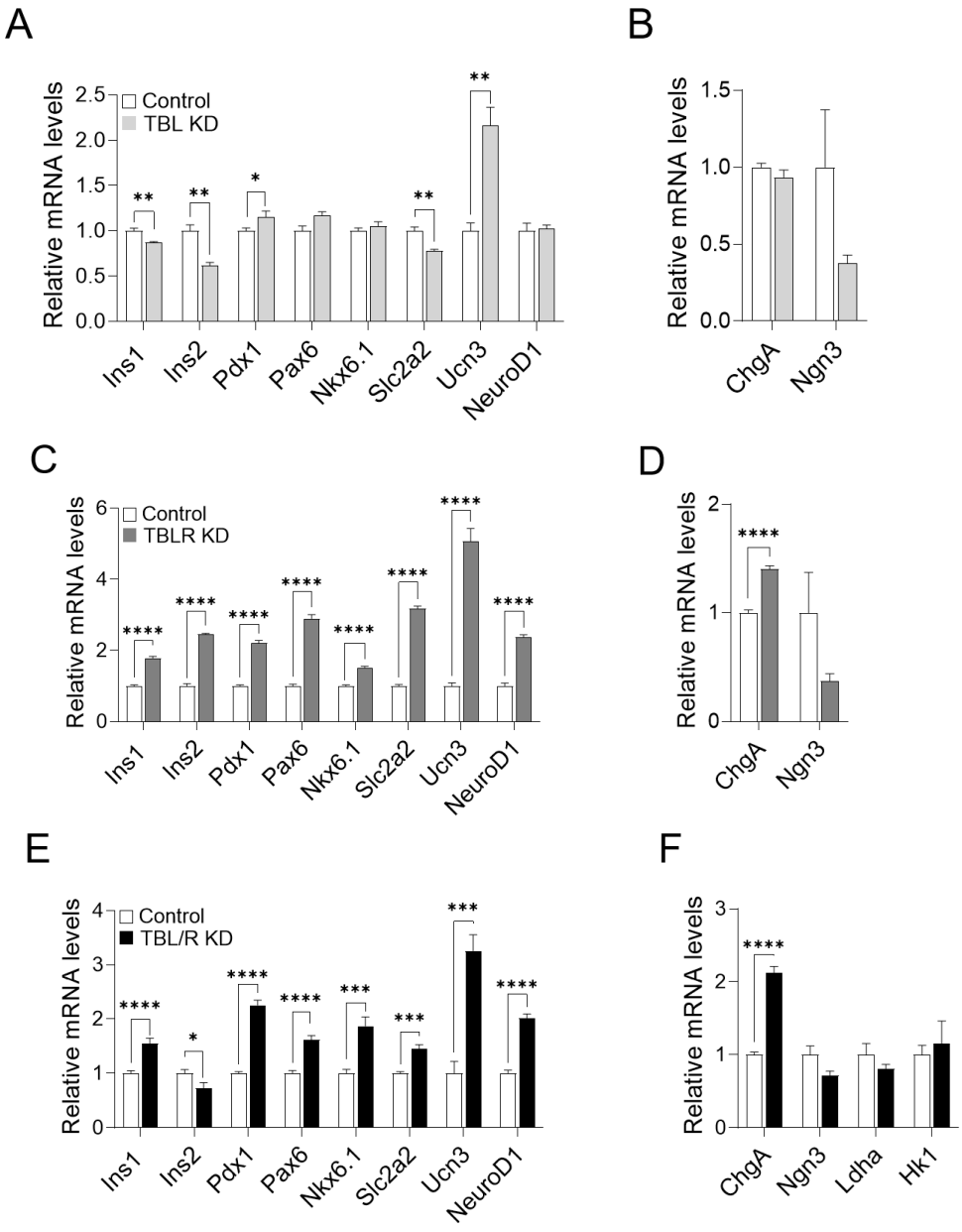

Figure 49: TBLR1 and TBL/R1 knock down promote β-cell identity gene expression. (A) β-cell identity gene expression and **(B)** expression of disallowed genes in INS1E cells transfected with control siRNA (Control) or TBL1 siRNA (TBL KD). n=4. **(C)** β-cell identity gene expression and **(D)** expression of disallowed genes in INS1E cells transfected with control siRNA (Control) or TBLR1 siRNA (TBLR KD). n=4. **(E)** β-cell identity gene expression and **(F)** expression of disallowed genes in INS1E cells transfected with control siRNA (Control) or TBL1 and TBLR1 siRNA (TBL/R KD). n=6. Data is presented as mean ± SEM. Statistical analysis was performed using an unpaired t-test. *p < 0.05, **p < 0.01, ***p < 0.001, ****p < 0.0001.

2.5.2 TBL1 and TBLR1 knockdown improves insulin secretion in INS1E cells

In contrast to previously described observations *in vivo*, TBLR1 and TBL1/TBLR1 double knock down promoted β-cell identity gene expression in INS1E cells. To investigate whether this increase in β-cell identity gene expression results in improved β-cell functionality, glucose stimulated insulin secretion and subsequently cellular insulin content upon TBL1 and/or TBLR1 knock down were determined.

TBL1 knock down and TBLR1 knock down resulted in significantly increased insulin secretion at basal condition (2 mM glucose) in comparison to the control. Insulin secretion after glucose stimulation (20 mM glucose) or maximal insulin secretion (2 mM glucose + 40 mM KCl) however, were unchanged between TBL1 knock down or TBLR1 knock down and control. Upon TBL1 knock down, insulin content was unchanged in all conditions in comparison to the control. Surprisingly, although TBLR1 knock down significantly increased insulin gene expression, insulin content was strongly reduced in comparison to the control at basal condition. No differences in insulin content at the stimulated and the maximum condition were observed upon TBLR1 knock down. Insulin secretion expressed as percentage of insulin content was unchanged upon TBL1 knock down. Upon TBLR1 knock down insulin secretion relative to insulin content was strongly increased at the basal condition, only (Figure 50).

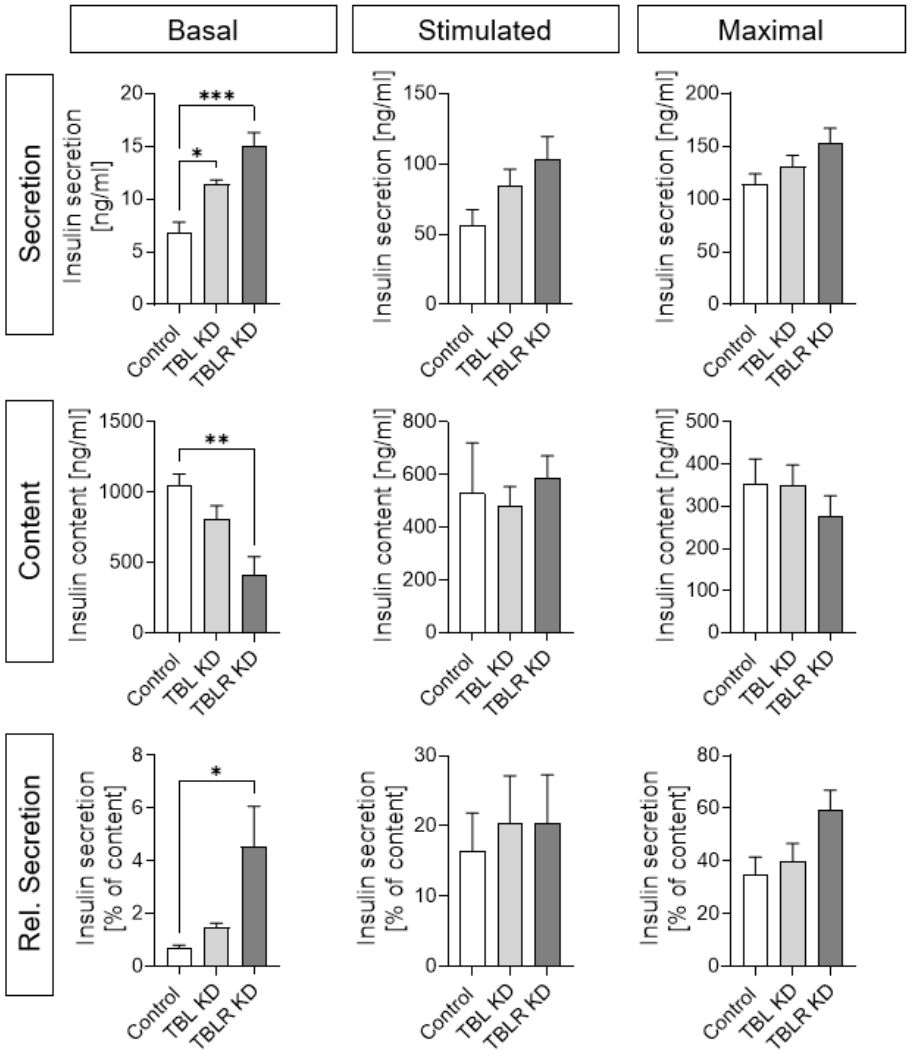

Figure 50: TBLR1 knock down promotes insulin secretion but reduces insulin content in INS1E cells. After siRNA transfection using control, TBL1, or TBLR1 siRNA, insulin secretion, content, and secretion as percentage to the content were determined in INS1E cells. For this, cells were glucose starved and then exposed to 2 mM glucose (Basal), 20 mM glucose (Stimulated), or to 2 mM glucose together with 40 mM KCl (Maximal), to stimulate

insulin secretion. Data is presented as mean ± SEM. Statistical analysis was performed using a Dunnett's multiple comparison *post hoc* test. *p < 0.05, **p < 0.01, ***p < 0.001. n=4.

Interestingly, simultaneous TBL1 and TBLR1 knock down in INS1E cells resulted in significantly increased insulin secretion at the basal (2.8 mM glucose), stimulated (16.8 mM glucose), and maximum (2.8 mM glucose + 40 mM KCl) condition. In line with the upregulation of *Ins1* gene expression and other β-cell identity genes, insulin content was strongly increased upon TBL1 and TBLR1 knock down in comparison to the control in all conditions. Insulin secretion as percentage to insulin content revealed that only basal and maximal insulin secretion were significantly increased upon TBL/R knock down in INS1E cells (Figure 51).

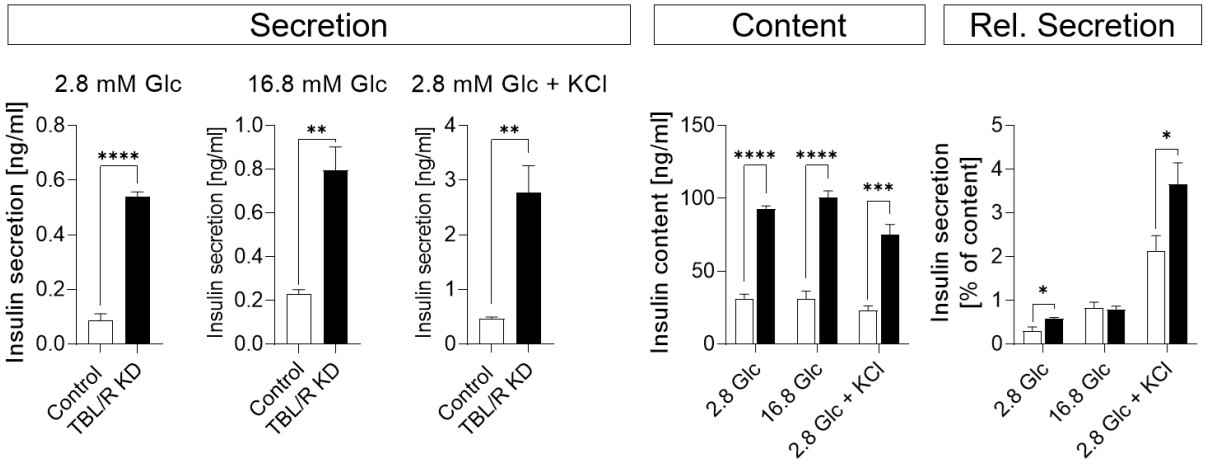

Figure 51: TBL1 and TBLR1 knock down increases insulin content in INS1E cells. After siRNA transfection using control or TBL1 and TBLR1 siRNA, insulin secretion, content, and secretion as percentage to the content (Rel. Secretion) were determined in INS1E cells. For this, cells were glucose starved and then exposed to 2.8 mM glucose (Basal), 16.8 mM glucose (Stimulated), or to 2.8 mM glucose together with 40 mM KCl (Maximal), to stimulate insulin secretion. Data is presented as mean ± SEM. Statistical analysis was performed using an unpaired t-test. *p < 0.05, **p < 0.01, ***p < 0.001, ****p < 0.0001. n=4.

In summary, knock down of TBL1 and TBLR1 in INS1E did not reproduce observations from the TBL1 and TBLR1 knock out mice. For instance, although TBLRβKO mice did not show alterations in insulin gene expression or synthesis, TBLR1 knock down *in vitro* improved β-cell functionality at basal conditions. Moreover, in contrast to *in vivo* observations, TBL1 and TBLR1 knock down in INS1E cells resulted in an upregulation of β-cell identity gene expression and insulin content. This ultimately suggests that the INS1E cells are not suitable for *in vitro* investigations on TBL1 and TBLR1 deficiency in β-cells as the phenotype observed *in vivo* was not reproduced.

2.5.3 TBL1 and/or TBLR1 knock down in MIN6 cells does not recapitulate *in vivo* observations

siRNA mediated knock down of TBL1 and/or TBLR1 in the rat insulinoma cell line INS1E did not recapitulate observations from *in vivo* studies. One explanation might be that the role of TBL1 and TBLR1 is not conserved across species and is rather mouse specific. Thus, next an *in vitro* knock down of TBL1 and/or TBLR1 was induced in MIN6 cells, an insulinoma cell line that originates from mice.

Knock down was induced using adenoviruses carrying shRNA against TBL1 and/or TBLR1. An adenovirus carrying a scrambled control sequence was used as control. 48 h after shRNA transduction, TBL1 and/or TBLR1 gene expression was significantly reduced on mRNA (Figure 52A) and protein level (Figure 52B). As previously observed *in vivo* in the TBLβKO mice and

in vitro in the INS1E cells, TBLR1 expression was significantly increased upon TBL1 deficiency (Figure 52A,B).

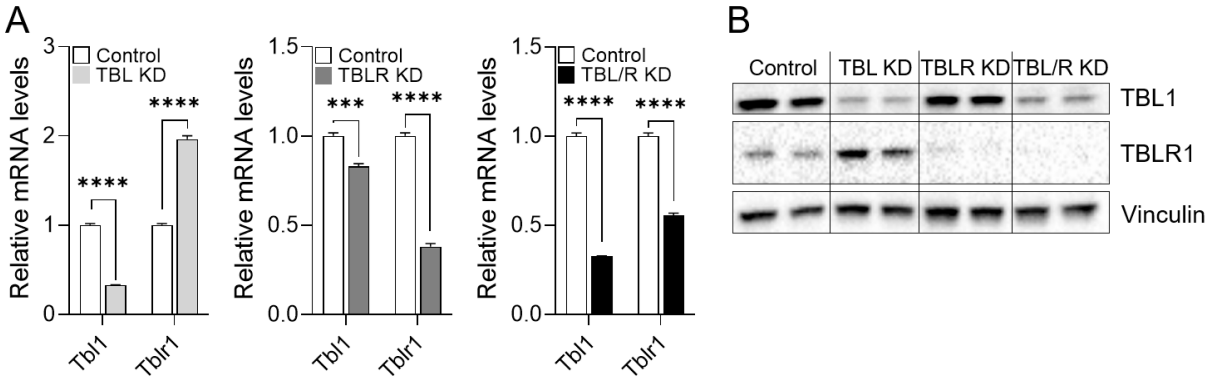

Figure 52: TBL1 knock down in MIN6 cells promotes TBLR1 expression. MIN6 cells were transduced with adenoviruses carrying shRNAs against TBL1 (TBL KD), TBLR1 (TBLR KD), both (TBL/R KD), or a scrambled control sequence (Control). Knock down efficiency was determined on **(A)** mRNA level using qPCR and **(B)** protein level using Western Blot and the indicated antibodies. Data is presented as mean ± SEM. Statistical analysis was performed using an unpaired t-test. ***p < 0.001, ****p < 0.0001. n=4.

After validation of TBL1 and/or TBLR1 knock down on mRNA and protein level, gene expression of β-cell identity genes was determined. Upon TBL1 knock down, *Ins1* gene expression was upregulated while *Nkx6.1* and *Slc2a2* was downregulated (Figure 53A). TBLR1 knock down resulted in an increase in *Ins1* and *Slc2a2* expression while *Pdx1* and *Nkx6.1* expression was decreased (Figure 53B). As for the TBLR1 knock down, TBL1 and TBLR1 knock down led to increased *Ins1* and *Slc2a2* expression. Double TBL1 and TBLR1 knock down also resulted in reduced *Pdx1* and *Pax6* expression (Figure 53C).

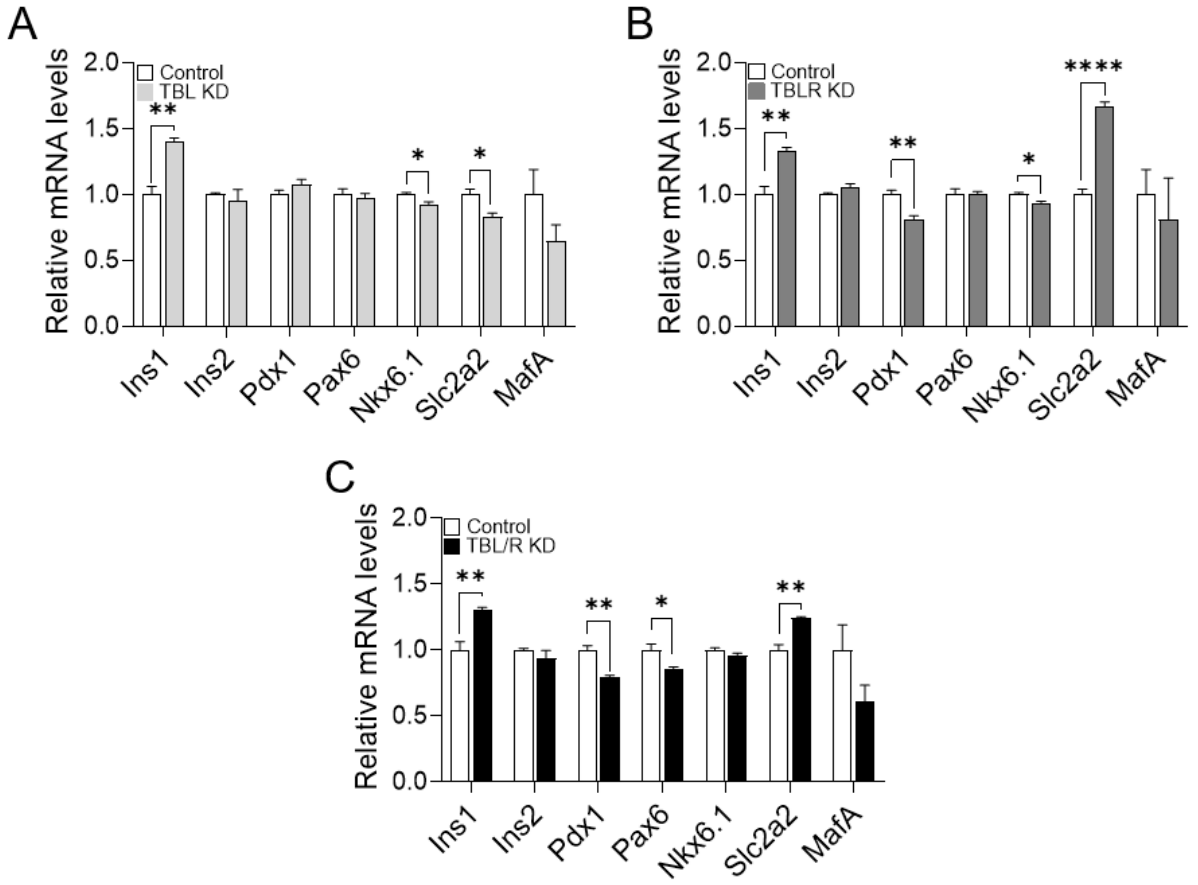

Figure 53: Knock down of TBL1 and/or TBLR1 in MIN6 cells does not recapitulate observations from *in vivo* TBL1 and TBLR1 knock out. β-cell identity gene expression in MIN6 cells upon shRNA mediated **(A)** TBL1, **(B)**

TBLR1, and **(C)** TBL1/TBLR1 knock down in MIN6 cells in comparison to MIN6 cells transduced with an adenovirus carrying a scrambled control sequence. Data is presented as mean ± SEM. Statistical analysis was performed using an unpaired t-test. *p < 0.05, **p < 0.01, ****p < 0.0001. n=4.

As for the INS1E cells, also TBL1 and TBLR1 knock down in MIN6 cells did not recapitulate the observations from the *in vivo* studies. This suggests that the phenotype observed *in vivo* cannot be reproduced *in vitro* either due to discrepancies between *in vitro* and *in vivo* models or because TBL1 and TBLR1 are involved in differentiation rather than maintenance of β-cell identity.

2.6 Induced β-cell specific TBL1 and TBLR1 (iTBL/RβKO) knock out induces a milder phenocopy of conditional TBL1 and TBLR1 ablation

Unexpectedly, *in vitro* ablation of TBL1 and TBLR1 in INS1E or MIN6 cells did not reproduce the observations from the TBL/RβKO mice, suggesting that instead of being involved in maintenance of β-cell identity, TBL1 and TBLR1 might be implicated in development or maturation. Another explanation for the discrepancy between *in vivo* and *in vitro* observations might be that β-cell dedifferentiation as result from TBL1 and TBLR1 deficiency is a time dependent process. As *in vitro* only acute ablation of TBL1 and TBLR1 is mimicked, observations can vary between cell culture and *in vivo*. To test *in vivo* whether TBL1 and TBLR1 deficiency induces dedifferentiation in adult and mature β-cells, mice with an inducible β-cell specific knock out of TBL1 and TBLR1 were generated (iTBL/RβKO). For this, previously described TBL1 and TBLR1 double-flox mice were crossed with mice carrying the tamoxifen-inducible Cre recombinase gene under the control of the rat insulin 2 (*Ins2*) promoter (Ins2-cre/ERT). Mice were generated by Dor and colleagues (Dor et al. 2004) and were kindly provided by the Ashcroft Lab. This model allows to induce the knock out at a specific age and thus to differentiate between the role of TBL1/TBLR1 during pancreas development or islet maturation from their role in adult β-cells. Tamoxifen injected floxed TBL1 and TBLR1 litter mates genotyped negatively for the Cre recombinase were used as controls.

Mice were born at a mendelian ratio and with normal body weight and size. To investigate knock out efficiency and specificity, mice were injected with tamoxifen at the age of 8 weeks. 4 weeks after tamoxifen injection, TBL1 and TBLR1 gene expression was determined in pancreatic islets, but also from tissues in the periphery. TBL1 expression was reduced in pancreatic islets by ~60%, while unchanged in liver, eWAT, kidney, spleen, intestine, and brain (Figure 54A). TBLR1 gene expression was reduced by ~55% in the islets and unchanged in liver, eWAT, kidney, spleen, intestine, and brain (Figure 54B), suggesting that the induction of TBL1 and TBLR1 knock out is restricted to islets and probably β-cell specific.

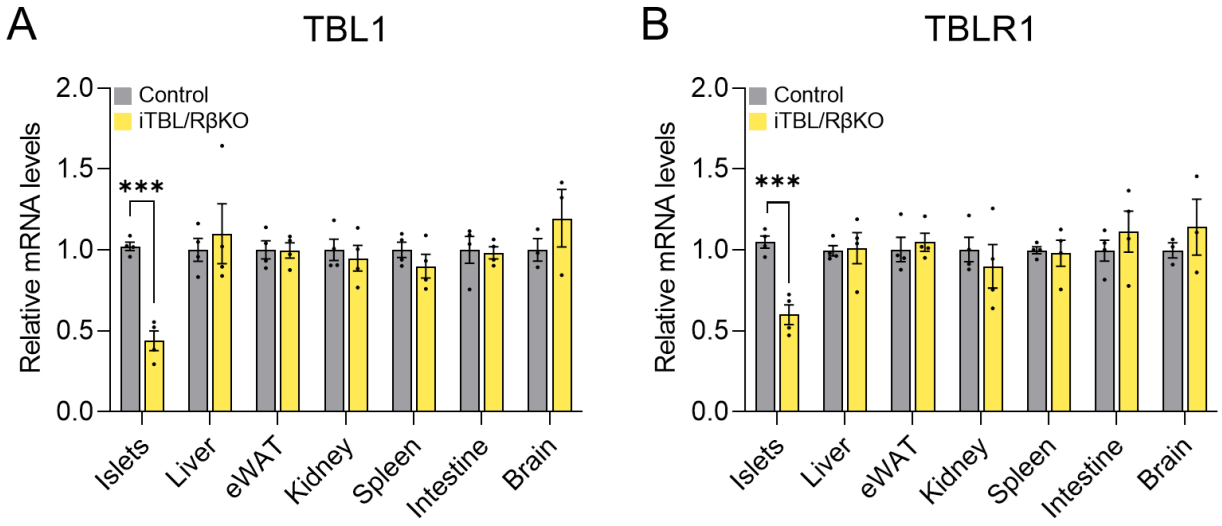

Figure 54: TBL1 and TBLR1 gene expression levels are specifically reduced in pancreatic islets. (A) TBL1 and **(B)** TBLR1 gene expression levels in islets, liver, eWAT, kidney, spleen, large and small intestine, and brain. Data is presented as mean ± SEM. Statistical analysis was performed using an unpaired t-test. ***p < 0.001.

2.6.1 iTBL/RβKO mice display no overt metabolic phenotype but dedifferentiation-like islet gene expression signature

At the age of 8 weeks, when the mice were injected with tamoxifen no differences in body weight or blood glucose levels were observed between controls and iTBL/RβKO (Figure 55A,B). Although no differences in body weight occurred, iTBL/RβKO unexpectedly developed hypoglycemia starting one week after knock out induction, which is similar to the observed hypoglycemia in TBL/RβKO mice at the age of 4 days.

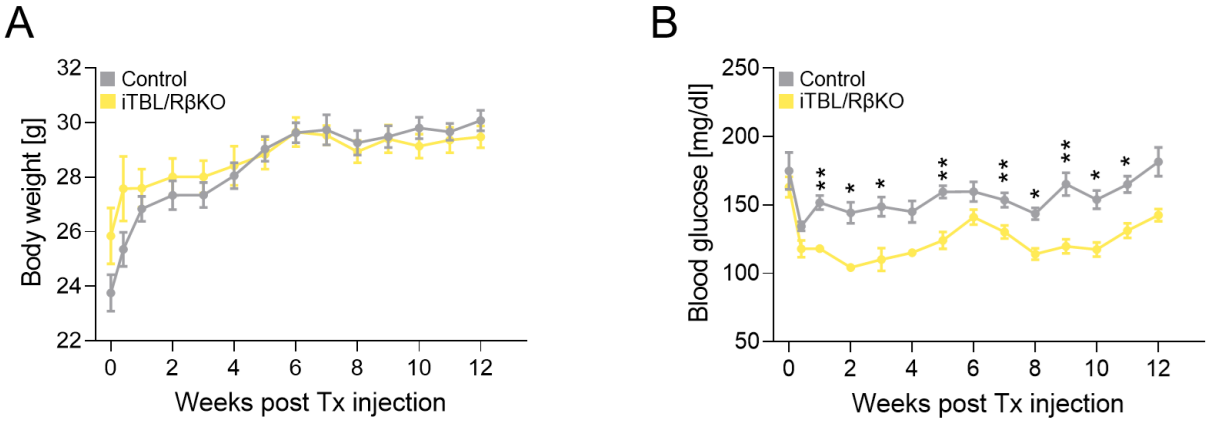

Figure 55: Mice with an induced β-cell specific TBL1 and TBLR1 knock out develop hypoglycemia. Weekly determined **(A)** body weight and **(B)** blood glucose levels in control (n=8) and iTBL/RβKO (n=8) mice after knock out induction with tamoxifen (Tx) at the age of 8 weeks. Data is presented as mean ± SEM. Statistical analysis was performed using a two-way ANOVA with repeated measures and a Šídák's multiple comparison *post hoc* test. *p < 0.05, **p < 0.01.

To investigate whether underlying hypoglycemia results from increased insulinemia, blood glucose and plasma insulin levels were determined at fasted and refed state. Although iTBL/RβKO mice had significantly lower blood glucose levels at fasted and refed state in comparison to control litter mates, no differences in insulinemia were observed (Figure 56A). Therefore, next glucose clearance during an oral glucose challenge was determined. In line with glycemia determined at fasted state, baseline blood glucose levels in the oral glucose tolerance test (oGTT) were significantly lower in the iTBL/RβKO mice. Accordingly, blood glucose levels from the iTBL/RβKO mice were continuously lower during the oGTT (Figure

56B), suggesting increased insulin secretion upon induced TBL1 and TBLR1 knock out. However, insulin levels determined during the oGTT did not differ between controls and iTBL/RβKO (Figure 56C), suggesting that iTBL/RβKO mice might have an improved insulin sensitivity. Surprisingly, fasting plasma glucagon levels were significantly increased in iTBL/RβKO mice in comparison to controls (Figure 56D).

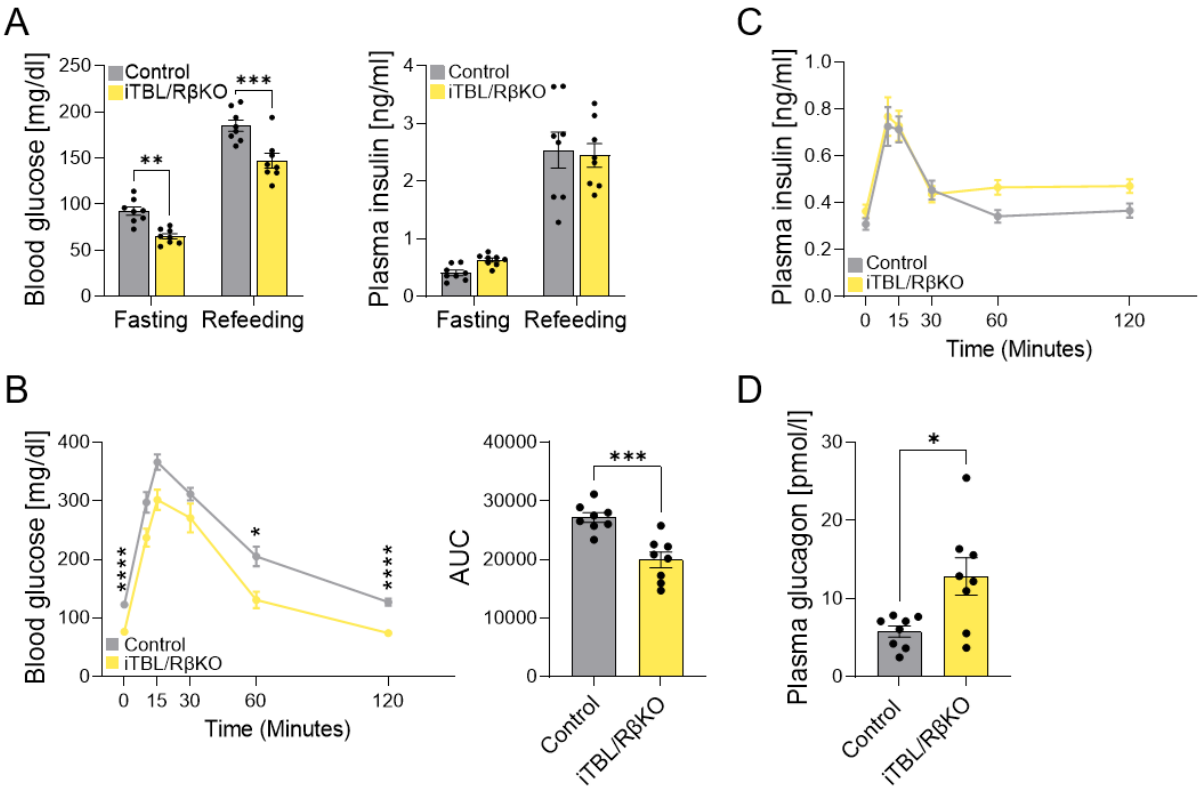

Figure 56: Plasma insulin levels do not differ between controls and hypoglycemic iTBL/RβKO mice. (A) Blood glucose and plasma insulin levels after 16 h of fasting and 2 h of refeeding from control and iTBL/RβKO mice. **(B)** Oral glucose tolerance test (oGTT) in iTBL/RβKO (n=8) mice and control litter mates (n=8). After fasting for 16 h, baseline glucose levels were determined. Subsequently, mice were administered orally with 2 g/kg D-glucose via oral gavage. Blood glucose levels were determined and blood for subsequent plasma insulin determination was collected 10, 15, 30, 60, and 120 min after administration. Blood glucose levels are plotted over time course of the experiment or are displayed as AUC. **(C)** Plasma insulin levels from iTBL/RβKO (n=8) and control mice (n=8) determined from blood collected during the oGTT from (B). Plasma insulin levels are plotted over time course of the experiment. **(D)** Plasma glucagon levels determined in control and iTBL/RβKO mice after 16h of fasting. Data is presented as mean ± SEM. Statistical analysis was performed using a two-way ANOVA with a Šídák's multiple comparison *post hoc* test (A), or an unpaired t-test (B for AUC, D), or a two-way ANOVA with repeated measures and a Šídák's multiple comparison *post hoc* test (B,C). *p < 0.05, **p < 0.01, ***p < 0.001, ****p < 0.0001.

Since no differences in plasma insulin levels were observed between control and iTBL/RβKO mice, insulin sensitivity using an ipITT was determined. As previously observed, iTBL/RβKO mice had significantly lower baseline blood glucose levels in comparison to control littermates. Although iTBL/RβKO mice displayed continuously lower blood glucose levels in comparison to controls, only the last timepoint reached statistical significance (Figure 57A). AUC was significantly lower for iTBL/RβKO mice (Figure 57B), suggesting an improved insulin sensitivity upon induced TBL1 and TBLR1 knock out. However, blood glucose changes relative to baseline blood glucose levels, revealed no differences in insulin sensitivity between iTBL/RβKO and control mice (Figure 57C). Thus, it is currently unclear why iTBL/RβKO mice develop hypoglycemia as neither plasma insulin levels nor insulin sensitivity were altered.

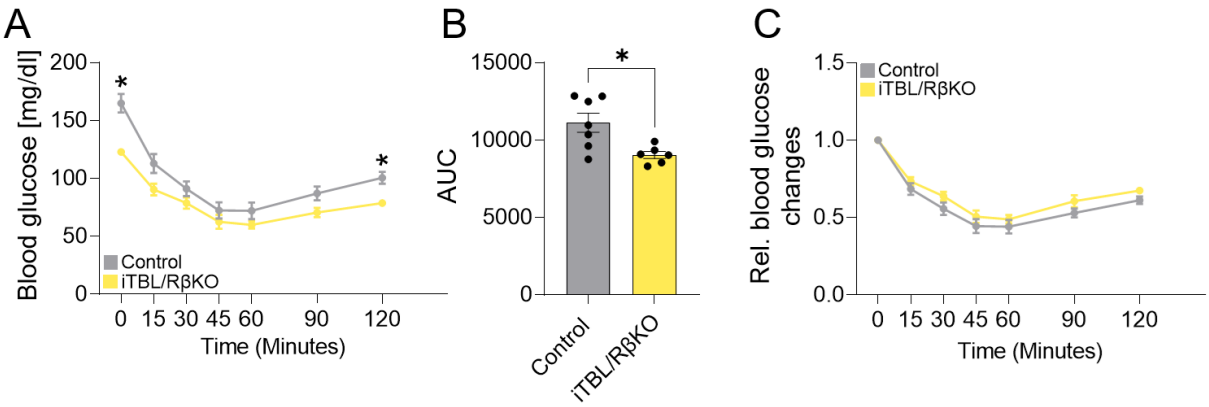

Figure 57: No alterations in insulin sensitivity upon induced β-cell specific TBL1 and TBLR1 knock out. (A) ipITT in iTBL/RβKO (n=7) mice and control litter mates (n=6). After fasting for 6 h, baseline glucose levels were determined. Subsequently, mice were injected with 0.8 U/kg insulin and blood glucose levels were determined 15, 30, 45, 60, 90, and 120 min after injection. Blood glucose levels are plotted over time course of the experiment or are displayed as **(B)** AUC. **(C)** Relative blood glucose changes from (A). For this, blood glucose was normalized to baseline blood glucose levels. Changes in blood glucose levels are plotted over time course of the experiment. Data is presented as mean ± SEM. Statistical analysis was performed using an unpaired t-test (B) or a two-way ANOVA with repeated measures and a Šídák's multiple comparison *post hoc* test (A,C). *p < 0.05.

12 weeks after induction of the TBL1 and TBLR1 knock out, tissue weight was determined and pancreatic islets were isolated for gene expression analysis. In line with undistinguishable body weights, no differences in liver, eWAT, kidney, and spleen weight between controls and iTBL/RβKO mice were observed (Figure 58A). Determination of knock out efficiency in the islets revealed a reduction of TBL1 gene expression by ~60% and of TBLR1 gene expression by ~40% (Figure 58B). Thus, it is tempting to speculate that incomplete knock out of TBL1 and TBLR1 in β-cells dampened the development of the expected phenotype. Interestingly, although no changes in plasma insulin levels were observed, most of the β-cell identity genes were significantly downregulated, including both insulin genes (Figure 58C), suggesting an underlying loss of β-cell identity. In line with this, β-cell progenitor cell markers and dedifferentiation markers were strongly upregulated in islets of iTBL/RβKO mice (Figure 58D).

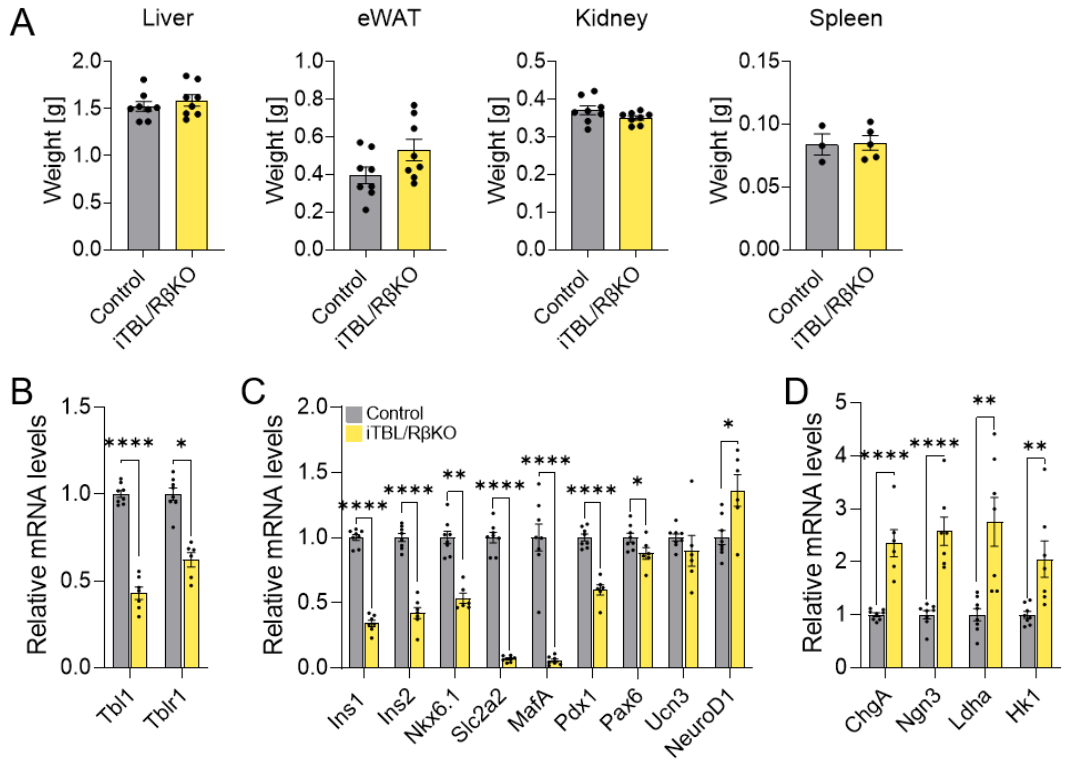

Figure 58: Islets from iTBL/RβKO mice display loss of β-cell identity-like gene expression signature. (A) Liver, eWAT, kidney, and spleen weight from control and iTBL/RβKO mice 12 weeks after knock out induction. Islet **(B)** TBL1 and TBLR1, **(C)** β-cell identity, and **(D)** disallowed gene expression from control and iTBL/RβKO mice was determined by qPCR. Data is presented as mean ± SEM. Statistical analysis was performed using an unpaired t-test. *p < 0.05, **p < 0.01, ****p < 0.0001.

2.6.2 iTBL/RβKO mice on high fat diet develop mild hyperglycemia and hypoinsulinemia

Induction of β-cell specific TBL1 and TBLR1 knock out in adult mice resulted in lowered glycemia, although no differences in circulating plasma insulin or in insulin sensitivity were observed. Surprisingly, islet gene expression analysis revealed a downregulation of β-cell identity genes and an upregulation of disallowed genes, suggesting an underlying loss of β-cell identity, as previously observed in the conditional TBL/RβKO mice. As knock out efficiency was lower than expected, it is tempting to speculate that β-cells with a remaining TBL1 and TBLR1 expression were compensating for the dedifferentiation and impaired function in β-cells with a successful knock out. Thus, mice with an induced TBL1 and TBLR1 knock out were challenged with a HFD. TBL1 and TBLR1 knock out was induced at the age of 8 weeks. HFD started immediately after tamoxifen injection.

At the time of knock out induction and the start of HFD feeding, no differences in body weight between control and iTBL/RβKO mice were observed. Also, during the course of HFD feeding both groups gained weight comparably (Figure 59A). Weekly determined random blood glucose levels showed that iTBL/RβKO mice had lower blood glucose levels in comparison to control litter mates in the first 5 weeks, although no statistical significance was reached. Interestingly, 16 weeks after knock out induction and HFD, iTBL/RβKO mice developed hyperglycemia, which increased over time (Figure 59B), suggesting a progressive loss of β-cell function.

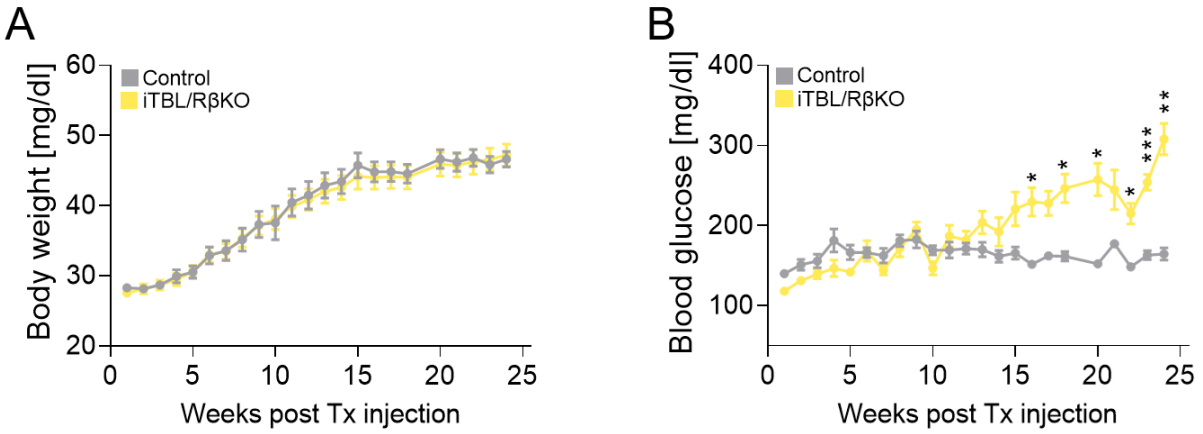

Figure 59: iTBL/RβKO mice develop hyperglycemia after 15 weeks of HFD. Weekly determined **(A)** body weight and **(B)** blood glucose levels in iTBL/RβKO mice (n=9) and control litter mates (n=9) on HFD. Knock out was induced at the age of 8 weeks with tamoxifen (Tx). HFD was started immediately after knock out induction. Data is presented as mean ± SEM. Statistical analysis was performed using a Šídák's multiple comparison *post hoc* test. *p < 0.05, **p < 0.01, ***p < 0.001.

4 weeks after knock out induction, fasting and refeeding glycemia and insulinemia were determined to investigate the functionality of TBL1 and TBLR1 deficient β-cells. In line with weekly determined blood glucose levels, iTBL/RβKO mice had lower blood glucose levels at fasted and refed state in comparison to controls. Although no differences in fasting plasma insulin levels were observed, refeeding plasma insulin levels were elevated in iTBL/RβKO mice (Figure 60A), suggesting improved β-cell functionality upon TBL1 and TBLR1 knock out. However, 24 weeks after knock out induction, iTBL/RβKO mice had significantly higher fasting

blood glucose levels in comparison to controls, which is in accordance with the progression of hyperglycemia in the knock out mice. No differences in refeeding glycemia or fasting and refeeding insulinemia were observed (Figure 60B). In this experiment, refeeding was performed using HFD containing 60% calories from fat. Thus, low carbohydrate content in the HFD might dampen effects on glycemia. Therefore, an oGTT was performed in order to specifically investigate glucose tolerance upon induced TBL1 and TBLR1 knock out. As previously observed, iTBL/RβKO mice showed elevated fasting glycemia in comparison to controls. Accordingly, after glucose administration iTBL/RβKO mice had continuously higher blood glucose levels in comparison to the controls (Figure 60C). Determination of blood glucose changes relative to baseline blood glucose revealed that no differences between control and iTBL/RβKO mice were observed in the first 15 minutes. However, after 30 minutes iTBL/RβKO mice showed elevated blood glucose levels normalized to baseline blood glucose (Figure 60D), indicating that iTBL/RβKO mice are unable to effectively clear glucose from the blood. In line with impaired glucose clearance in iTBL/RβKO mice, plasma insulin levels determined during the oGTT showed that the rise in circulating insulin after glucose administration was completely absent in iTBL/RβKO mice (Figure 60E). Thus, when challenged with a HFD, adult and mature β-cells with an induced TBL1 and TBLR1 deficiency fail to adequately secrete insulin in response to elevations in blood glucose levels, resulting in hyperglycemia.

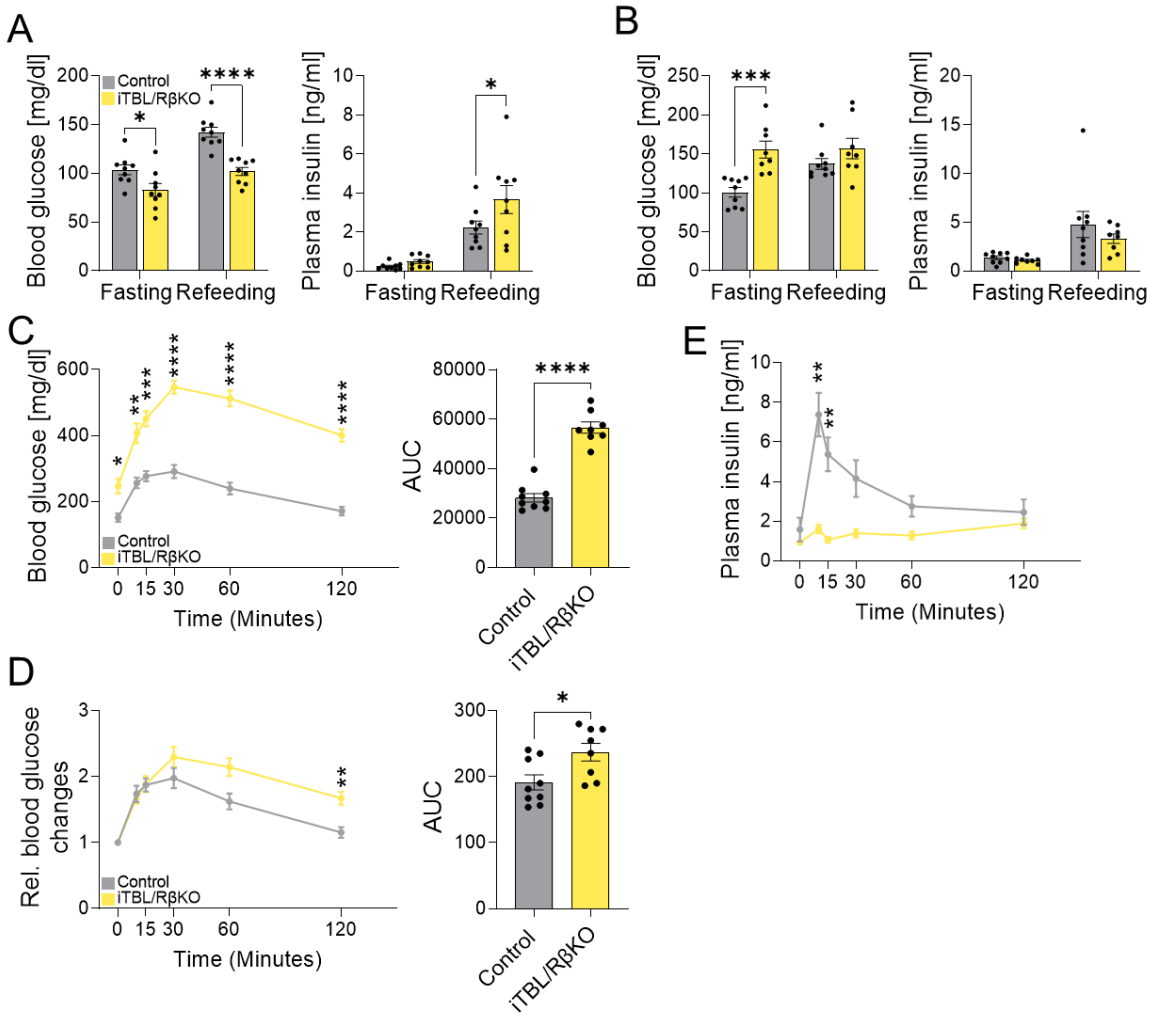

Figure 60: iTBL/RβKO mice on HFD fail to secrete insulin in response to rises in blood glucose levels. Blood glucose and plasma insulin after 16 h of fasting and 2 h of refeeding in iTBL/RβKO mice and controls **(A)** 4 weeks after knock out induction and HFD or **(B)** 24 weeks after knock out induction and HFD. **(C)** oGTT in iTBL/RβKO mice (n=8) and control litter mates (n=9). Mice were starved for 16 h. After baseline blood glucose determination

mice were administered with 3 g/kg D-glucose via oral gavage. Blood glucose levels were determined 10, 15, 30, 60, and 120 min after administration. Blood glucose levels are plotted over time course of the experiment or are displayed as AUC. **(D)** Blood glucose changes relative to baseline blood glucose levels from (C). Blood glucose changes are plotted over time course of the experiment or are displayed as AUC. **(E)** Plasma insulin levels from iTBL/RβKO (n=8) and control mice (n=9) determined from blood collected during the oGTT from (C). Plasma insulin levels are plotted over time course of the experiment. Data is presented as mean ± SEM. Statistical analysis was performed using a two-way ANOVA with a Šídák's multiple comparison *post hoc* test (A,B), or an unpaired t-test (C,D for AUC), or a two-way ANOVA with repeated measures and a Šídák's multiple comparison *post hoc* test (C-E). *p < 0.05, **p < 0.01, ***p < 0.001, ****p < 0.0001.

2.6.3 Loss of β-cell identity in iTBL/RβKO mice progresses over time

Thus far, it was demonstrated that although β-cells dedifferentiate upon induced TBL1 and TBLR1 knock out, β-cells with maintained TBL1 and TBLR1 expression are sufficient to compensate. Under challenged conditions such as diet-induced obesity, this compensation fails resulting in hyperglycemia and hypoinsulinemia in iTBL/RβKO mice. To next investigate whether β-cell failure and dedifferentiation indeed progress over time total pancreatic hormone content was determined 4 weeks and 11 weeks after knock out induction. Although no differences in pancreas weight between the respective groups were observed (Figure 61A), total pancreatic insulin content was strongly reduced in iTBL/RβKO mice in comparison to the controls 4 weeks and 11 weeks after knock out induction. In the controls, insulin content did not differ between the 4 weeks and 11 weeks group. In the iTBL/RβKO mice however, mice from the 11 weeks group had significantly lower insulin content in comparison to mice from the 4 weeks group (Figure 61B). Thus, the reduction of insulin content with knock out duration implies a progressive loss of β-cell function upon induced TBL1 and TBLR1 knock out. Total pancreas glucagon (Figure 61C) or somatostatin (Figure 61D) content were unchanged in iTBL/RβKO mice in comparison to controls regardless knock out duration.

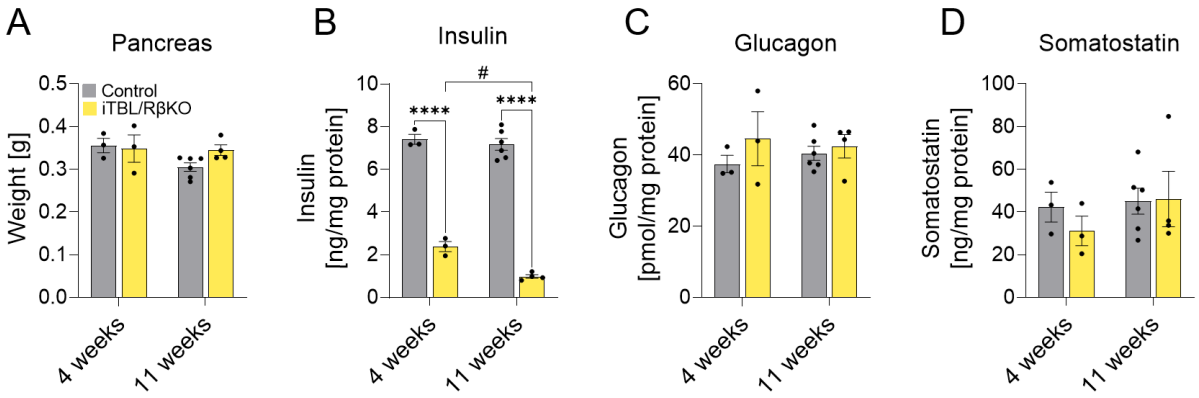

Figure 61: Reduction of pancreatic insulin content progresses over time in iTBL/RβKO mice. (A) Pancreas weight, total pancreas **(B)** insulin, **(C)** glucagon, **(D)** and somatostatin content normalized to protein content in controls and iTBL/RβKO mice 4 weeks or 11 weeks after knock out induction. Data is presented as mean ± SEM. Statistical analysis was performed using a two-way ANOVA with a Tukey's multiple comparison *post hoc* test. *Indicates significance between control and iTBL/RβKO, #indicates significance between 4 weeks and 11 weeks.

To investigate whether changes in islet micro-architecture, comparable to conditional TBL/RβKO occur and whether these changes worsen over time and with HFD feeding, pancreas was dissected from iTBL/RβKO mice on chow diet and HFD. Indeed, loss of the organized islet structure occurred upon induced TBL1 and TBLR1 knock out (Figure 62A) and these morphological changes worsened with HFD feeding (Figure 62B). Quantification of immunofluorescence images revealed that no differences in β-cell mass were observed in contrast to what was expected after total pancreas insulin content determination. One explanation might be that immunofluorescence images only detect β-cells without actual quantification of the insulin content. Insulin synthesis as previously determined via qPCR was downregulated, which is in line with the determined reduction in total pancreas insulin content.

Therefore, although β-cell mass determined by immunofluorescence staining was unchanged, the capacity to synthesize insulin and thus the insulin content is reduced. Interestingly, α-cell mass was increased in iTBL/RβKO mice on chow diet. Accordingly, the α- to β-cell ratio was increased upon TBL1 and TBLR1 knock out (Figure 62C). In iTBL/RβKO mice on HFD, β-cell mass was reduced by 2-fold in comparison to the controls although no significance was reached. No differences in α-cell mass were observed. Accordingly, α- to β-cell mass ratio was significantly increased (Figure 62D), which was previously associated with T2DM in humans (Fujita et al. 2018).

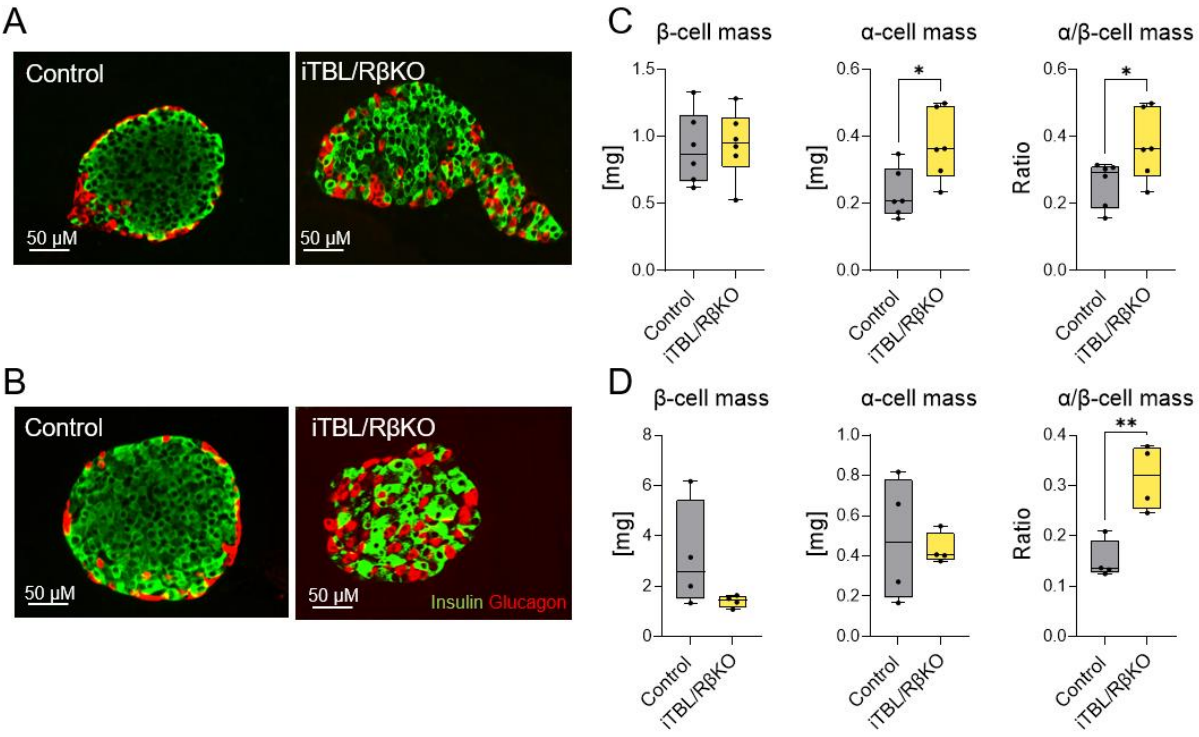

Figure 62: Induced TBL1 and TBLR1 knock out in β-cells induces disorganization of islet micro-architecture. Pancreas from chow diet mice was dissected 11 weeks after knock out induction. Pancreas from HFD mice was dissected 24 weeks after knock out induction and HFD. Representative images of immunofluorescence staining of islets in the pancreas of control or iTBL/RβKO mice on **(A)** chow diet or **(B)** HFD. β-cells are displayed as insulin$^+$ cells in green. α-cells are displayed as glucagon$^+$ cells in red. Immunofluorescence staining was performed and analyzed by the core facility Pathology & Tissue Analytics at the Helmholtz Munich. Quantification of insulin$^+$ cell mass (β-cells), glucagon$^+$ cell mass (α-cells), and α-cell mass relative to β-cell mass in iTBL/RβKO mice and control litter mates on **(C)** chow diet **(D)** HFD. Data is presented as median and minimum/maximum. Statistical analysis was performed using an unpaired t-test. *$p < 0.05$, **$p < 0.01$.

2.7 PAX6 as novel TBL1 and TBLR1 interaction partner

Thus far, observations from conditional and inducible TBL1 and TBLR1 knock out mouse models demonstrated that TBL1 and TBLR1 play a critical role in β-cell function and maintenance of β-cell identity. It is however unclear how TBL1 and TBLR1 manage to control gene expression in the β-cells. Previous studies have shown that TBL1 and TBLR1 are implicated in transcriptional regulation by interaction with transcription factors or nuclear receptors (Li and Wang 2008; Jones et al. 2014; Kulozik et al. 2011; Perissi et al. 2004). Therefore, in order to understand the mechanism and identify transcription factors or nuclear receptors through which TBL1 and TBLR1 control β-cell gene expression, an interactome screen was performed.

2.7.1 An interactome analysis identifies direct TBL1 and TBLR1 interaction partners

For the interaction partner screen, endogenous TBL1 and TBLR1 was enriched from MIN6 cells via immunoprecipitation. Subsequently, interaction partners were identified through mass spectrometry and displayed as ratio between the enrichment in the endogenous TBL1 or TBLR1 pulldown and enrichment in the control pulldown using a Flag antibody. Interestingly, although TBL1 and TBLR1 are primarily localized in the nucleus and in few cell lines also in the cytoplasm (Zhang et al. 2006; Daniels et al. 2014), the majority of identified interaction partners was localized in the cytoplasm or other cell compartments. Of the 816 identified TBL1 binding partners only 304 were localized in the nucleus. 440 interaction partners were localized in the cytoplasm, and 75 in the mitochondria. Moreover, 117 proteins were found in other cell compartments such as the Golgi apparatus or the cell membrane, while no clear localization was found for 101 proteins that bound to TBL1 (Figure 63A). Of note, some of the interaction partners were not restricted to one localization. Out of the 853 TBLR1 interaction partners, 302 proteins were identified with a nuclear localization. 455 interaction partners were localized in the cytoplasm and 77 in the mitochondria. While 137 interaction partners were localized in other cellular compartments, 108 interaction partners had no clear localization (Figure 63B). Moreover, from the 816 TBL1 interaction partners and 853 TBLR1 interaction partners, 784 proteins were interacting with both TBL1 and TBLR1 (Figure 63C).

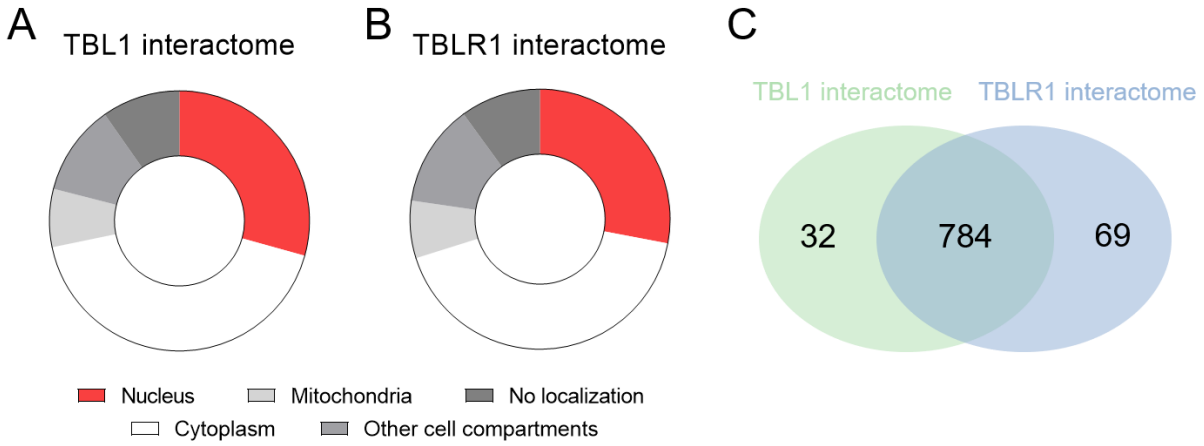

Figure 63: Non-nuclear proteins represent the majority of identified TBL1 and TBLR1 interaction partners. Cellular localisation of **(A)** TBL1 and **(B)** TBLR1 interaction partners identified in the interactome screen. **(C)** Venn diagram of shared interaction partners between TBL1 and TBLR1 in MIN6 cells. Interaction partners used for this quantification had a peptide count > 1. Mass spectrometry and annotation were performed by the core facility Research Unit Proteomics at the Helmholtz Munich.

Whether TBL1 and TBLR1 are indeed located in other cellular compartments or are able to shuttle to other cell compartments or whether interactions with non-nuclear proteins result from combining all cellular proteins during cell lysis, remains to be investigated and goes beyond the scope of this thesis. Thus, only interaction partners with a nuclear localization were included in the following analysis.

Previous studies showed that TBL1 regulates transcriptional events through recruitment of regulatory complexes or histone modifiers. Table 2 displays the top 20 nuclear interaction partners of TBL1. Endogenous TBL1 bound to all components of the NCOR/SMRT repressor complex (NCOR1, NCOR2, HDAC3, GPS2, TBLR1) as demonstrated in previous studies (Yoon et al. 2003), underlining the successful execution of the interactome screen. Additionally, histone modifiers such as histone acetyl or methyl transferases (HDAC3, KDM1A) but also histone compartments (H3C2) were identified in the screen as TBL1 interaction partners, suggesting that TBL1 might control β-cell gene expression through recruitment of

histone modifiers to histones. Moreover, TBL1 bound to proteins related to ubiquitination (USP28, UBE2N), which is in line with its known function as recruiter for the ubiquitin/19S proteasome complex (Perissi et al. 2004). Interestingly, the screen for interaction partners found PAX6, which is known for its essential role in β-cells (Gosmain et al. 2012; Swisa et al. 2017) to directly bind to TBL1.

Table 2: Top 20 nuclear interaction partners of TBL1 in MIN6 cells. After enrichment of TBL1 with an endogenous immunoprecipitation, direct interaction partners were identified using mass spectrometry. The ratio TBL1/Ctr shows the enrichment of the respective protein in the TBL1 pulldown relative to the enrichment in the control (Ctr) pulldown using Flag antibody. Mass spectrometry and annotation were performed by the core facility Research Unit Proteomics at the Helmholtz Munich. Statistical analysis was performed using an unpaired t-test. n=4.

Gene name	Protein description	Ratio TBL1/Ctr	p-value	
Eftud2	116 kDa U5 small nuclear ribonucleoprotein component	27,2	6,6E-06	****
Hdac3	Histone deacetylase 3	26,0	0,0002	***
Ncor2	Nuclear receptor corepressor 2	21,3	0,00038	***
Gps2	G protein pathway suppressor 2	17,9	0,00018	***
Ncor1	Nuclear receptor corepressor 1	17,1	0,00101	**
Usp28	Ubiquitin carboxyl-terminal hydrolase 28	15,9	9,4E-05	****
Uprt	Uracil phosphoribosyltransferase homolog	14,3	0,00047	***
Pax6	Paired box protein Pax-6	12,4	0,00547	**
Qki	Protein quaking	6,8	8,4E-06	****
Kdm1a	Lysine-specific histone demethylase 1A	6,1	0,00147	**
Rcor3	REST corepressor 3	5,2	0,00381	**
Ube2n	Ubiquitin-conjugating enzyme E2	4,6	0,01266	*
Tbl1xr1	F-box-like/WD repeat-containing protein TBL1XR1	4,6	0,00293	**
Mvp	Major vault protein	3,9	0,02067	*
Vapa	Vesicle-associated membrane protein-associated protein A	3,9	0,00159	**
Prpf8	Pre-mRNA-processing-splicing factor 8	3,4	0,04118	*
H3c2	Histone H3.2	3,3	0,00239	**
Pabpc1	Polyadenylate-binding protein 1	2,8	0,00113	**
Tbl1x	F-box-like/WD repeat-containing protein TBL1X	2,8	0,07123	
Dld	Dihydrolipoyl dehydrogenase	2,8	0,00855	**

Similar to TBL1, TBLR1 bound to all the components of the NCOR/SMRT repressor complex (NCOR1, NCOR2, HDAC3, GPS2). Interestingly, amongst the top 20 nuclear interaction partners of TBLR1, SUPT16H - core component of the facilitates chromatin transcription (FACT) activator complex (Orphanides et al. 1998) was identified suggesting that TBLR1 might not only facilitate repressor complex recruitment but also recruitment of activator complexes. Moreover, in line with previously described functions of TBLR1, histone modifiers (HDAC3, RBBP4, KDM1A) but also proteins involved in protein degradation (PSMB5) bound to endogenous TBLR1 (Perissi et al. 2008). In contrast to TBL1, TBLR1 bound to various transcription factors (MEOX2, CUX1) of which however PAX6, with its function as master regulator of β-cell identity was the most intriguing (Table 3).

Table 3: Top 20 nuclear interaction partners of TBLR1 in MIN6 cells. After enrichment of TBLR1 with an endogenous immunoprecipitation, direct interaction partners were identified using mass spectrometry. The ratio TBLR1/Ctr shows the enrichment of the respective protein in the TBLR1 pulldown relative to the enrichment in the control (Ctr) pulldown using Flag antibody. Mass spectrometry and annotation were performed by the core facility Research Unit Proteomics at the Helmholtz Munich. Statistical analysis was performed using a t-test. n=4.

Gene name	Protein description	Ratio TBLR1/Ctr	p-value	
Eif4e	Eukaryotic translation initiation factor 4E	28,1	6,6E-06	****
Tbl1xr1	F-box-like/WD repeat-containing protein TBL1XR1	11,4	3,7E-05	****
Pax6	Paired box protein Pax-6	9,7	0,00876	**
Hdac3	Histone deacetylase 3	9,6	0,00035	***
Meox2	Homeobox protein MOX-2	6,8	0,00451	**
Ncor2	Nuclear receptor corepressor 2	5,2	0,00022	***
Ncor1	Nuclear receptor corepressor 1	5,1	0,0016	**
Dld	Dihydrolipoyl dehydrogenase	4,8	0,00222	**
Gps2	G protein pathway suppressor	4,7	0,00376	**
Psmb5	Proteasome subunit beta type-5	3,3	0,01049	*
Cux1	Homeobox protein cut-like 1	3,2	0,00373	**
Uaca	Uveal autoantigen with coiled-coil domains and ankyrin repeats	3,1	0,00044	***
Rmi1	RecQ-mediated genome instability protein 1	2,9	0,01035	*
Rbbp4	Histone-binding protein RBBP4	2,9	0,00724	**
Smc2	Structural maintenance of chromosomes protein 2	2,8	0,11904	
Ndufa13	NADH dehydrogenase	2,7	0,17337	
Tfe3	Transcription factor E3	2,5	0,03615	*
Kdm1a	Lysine-specific histone demethylase 1A	2,4	0,02477	*
Supt16h	FACT complex subunit SPT16	2,4	0,12075	
Prpf8	Pre-mRNA-processing-splicing factor 8	2,3	0,08926	

Based on all identified interaction partners, a gene ontology (GO) analysis revealed that genes encoding for TBL1 interaction partners significantly enriched for mitochondria metabolism GO terms. Moreover, one of the top GO terms was the *transcription repressor complex* (Figure 64A). In line with previous studies, associated genes contained all the components of the NCOR/SMRT repressor complex but also CTBP1 and CTBP2 which were also previously identified as TBL1 interaction partners (Perissi et al. 2008) (Figure 64B). Expectedly, also for the TBLR1 interaction partner gene sets enriched for *transcription repressor complex* (Figure 64C) due to the interaction with all the components of the NCOR/SMRT complex (Figure 64D). Interestingly, only an interaction between CTBP1/CTBP2 and TBL1 was observed but not with TBLR1 (Figure 64B,D), which was previously demonstrated by Perissi et al. (Perissi et al. 2008), further underlining the successful execution of this interactome screen and the specificity of identified interaction partners. Moreover, gene sets enriched for the GO term *endocrine pancreas development* (Figure 64C), due to the interaction of TBLR1 with PAX6 (Figure 64D) further supporting the notion that TBLR1 is an essential regulator of β-cells.

A

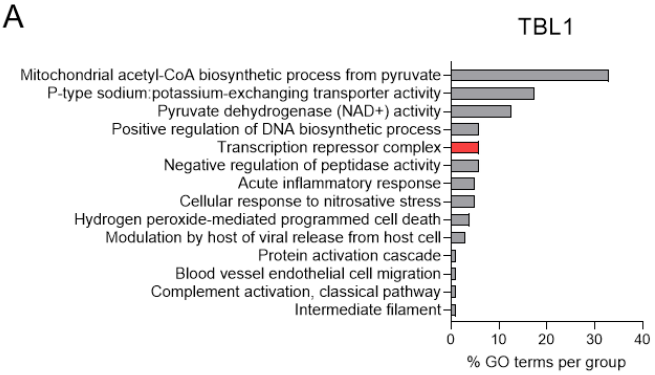

B

GO term	Associated genes
Transcription repressor complex	Ctbp1, Ctbp2, Gps2, Hdac3, Hdgf, Ncor1, Ncor2, Tbl1xr1

C

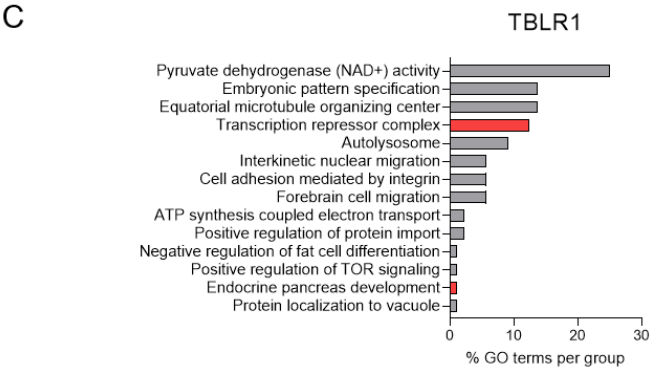

D

GO term	Associated genes
Transcription repressor complex	Gps2, Hdac3, Hdgf, Ncor1, Ncor2, Tbl1x, Ywhab
Endocrine pancreas development	Onecut2, Pax6, Pdhx

Figure 64: Gene ontology (GO) analysis using interaction partners identified in the interactome screen reveals that TBL1 and TBLR1 are implicated in transcriptional repression and endocrine pancreas development. (A) GO analysis of TBL1 interaction partners identified in the interactome screen. **(B)** TBL1 interaction partners that enriched in the respective GO term highlighted in red from (A). **(C)** GO analysis of TBLR1 interaction partners identified in the interactome screen. **(D)** TBLR1 interaction partners that enriched in the respective GO term highlighted in red from (C).

2.7.2 TBL1 and TBLR1 but also components of the regulatory complexes NCOR/SMRT and FACT interact with PAX6

Intriguingly, in the above-described interaction partner screen, PAX6, a key transcription factor in β-cells (Gosmain et al. 2012; Swisa et al. 2017) was identified as novel and direct TBL1 and TBLR1 interaction partner. To validate this interaction, endogenous TBL1 and TBLR1 was immunoprecipitated in murine MIN6 (Figure 65A) and rat INS1E (Figure 65B) cells. Indeed, in both β-cell lines immunoprecipitated TBL1 and TBLR1, but not the control pulldown using a Flag antibody enriched PAX6 detected via Western Blot. Thus, the interaction between TBL1/TBLR1 and PAX6 was validated but most importantly reproduced using two different β-cell lines from different species, suggesting that the TBL1/TBLR1 and PAX6 interaction is conserved across species. Interestingly, it was previously shown that PAX6 maintains β-cell identity by inducing the expression of β-cell identity genes while simultaneously repressing the expression of disallowed genes (Swisa et al. 2017). How exactly PAX6 mediates this bidirectional gene expression is not completely understood. As transcription co-factors, TBL1 and TBLR1 were demonstrated to facilitate transcriptional events by recruitment of regulatory complexes to transcription factors (Li and Wang 2008; Perissi et al. 2004). One of the better studied regulatory complexes TBL1 and TBLR1 interact with is the NCOR/SMRT complex which predominantly represses gene expression (Guenther et al. 2001; Perissi et al. 2004). Components of the NCOR/SMRT complex bound to TBL1 and TBLR1 in the interactome screen as expected. In addition, SUPT16H which is a core component of the FACT complex and previously described to induce gene expression (Belotserkovskaya et al. 2003; Frost et al. 2018) was also identified as novel TBL1 and TBLR1 interaction partner. Therefore, it is tempting to speculate that TBL1 and TBLR1 might recruit the NCOR/SMRT and the FACT

complex to the transcription factor PAX6 to mediate both repression and activation of PAX6 mediated transcription in a context-specific manner. Indeed, endogenous HDAC3 and SUPT16H immunoprecipitation enriched PAX6 in INS1E cells (Figure 65C) and murine islets (Figure 65D) in comparison to the immunoglobulin G (IgG) control pulldown. Thus, TBL1 and TBLR1 might be indeed implicated in PAX6 mediated gene expression by recruitment of the regulatory complexes NCOR/SMRT and FACT.

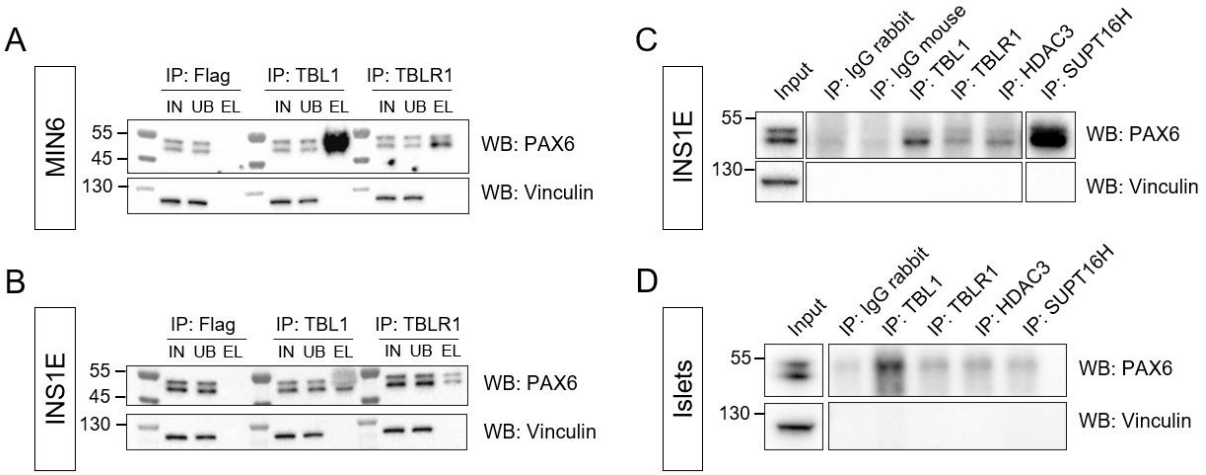

Figure 65: TBL1 and TBLR1 but also components of the regulatory complexes NCOR/SMRT and FACT bind to PAX6. Endogenous TBL1 and TBLR1 was immunoprecipitated (IP) using TBL1 or TBLR1 antibody from **(A)** MIN6 cells or **(B)** INS1E cells. Total cell lysates before IP (IN), lysate after IP (UN) and immunoprecipitated TBL1 and TBLR1 (EL) were immunoblotted (WB) using the indicated antibodies. Control IP was performed using a Flag antibody. Endogenous TBL1, TBLR1, HDAC3, and SUPT16H were immunoprecipitated (IP) from **(C)** INS1E cells or **(D)** murine islets. Total cell lysates (Input) and IPs were immunoblotted (WB) using the indicated antibodies. Control pulldown was performed using an immunoglobulin G (IgG) antibody.

To investigate whether TBL1 and TBLR1 are required for the recruitment or binding of the NCOR/SMRT or FACT complex to PAX6, endogenous HDAC3 and SUPT16H were immunoprecipitated after siRNA mediated knock down of TBL1 and TBLR1 in INS1E cells. Transfection of INS1E cells with siRNA targeting TBL1 and TBLR1 resulted in a strong downregulation of TBL1 and TBLR1 protein levels in comparison to cells transfected with a non-targeting siRNA control (Figure 66A). In comparison to the IgG control pulldown, immunoprecipitation of HDAC3 and SUPT16H resulted in an enrichment of PAX6 protein in the INS1E lysates. Interestingly, immunoprecipitation of HDAC3 enriched more PAX6 protein upon TBL1 and TBLR1 knock down, suggesting a stronger or more frequent interaction between HDAC3 and PAX6 in the absence of TBL1 and TBLR1. Intriguingly, less PAX6 was detected in the SUPT16H pulldown upon TBL1 and TBLR1 KD, suggesting a reduced interaction between SUPT16H and PAX6 upon TBL1 and TBLR1 deficiency (Figure 66B). Thus, TBL1 and TBLR1 indeed mediate the binding between components of the NCOR/SMRT or FACT complex to PAX6, indicating that TBL1 and TBLR1 are implicated in PAX6 mediated gene expression through selective recruitment of regulatory complexes.

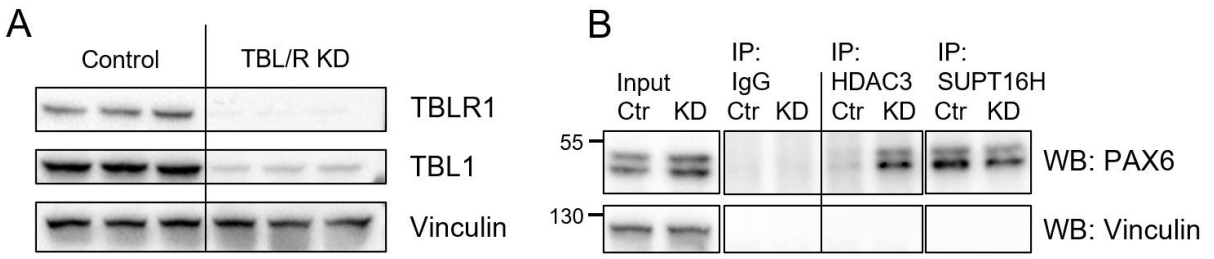

Figure 66: HDAC3 and SUPT16H interaction with PAX6 is TBL1 and TBLR1 dependent. (A) Western Blot displaying TBL1, TBLR1, and Vinculin levels in protein lysates of INS1E cells transfected either with control siRNA

(Control) or siRNA targeting TBL1 and TBLR1 (TBL/R KD). **(B)** Endogenous HDAC3 and SUPT16H immunoprecipitation (IP) in INS1E cells transfected with control siRNA (Ctr) or siRNA targeting TBL1 and TBLR1 (KD). Total cell lysates (Input) and immunoprecipitated HDAC3 or SUPT16H were immunoblotted (WB) using PAX6 and Vinculin antibody. Control pulldown was performed using an IgG antibody.

2.7.3 TBL1 and TBLR1 control promoter regions of PAX6 target genes

The identification of PAX6 as direct TBL1 and TBLR1 interaction partner and the differential binding of regulatory complexes to PAX6 upon TBL1 and TBLR1 deficiency, suggest that TBL1 and TBLR1 are implicated in PAX6 mediated gene expression in pancreatic β-cells. To determine whether TBL1 and TBLR1 bind to the same promoter regions as PAX6 and are therefore involved in PAX6 mediated gene expression, a quantitative chromatin immunoprecipitation (ChIP-qPCR) and a luciferase reporter assay were performed. For this, the PAX6 target genes *Ins1* and *Ins2* were selected as their expression was strongly downregulated in islets from TBL/RβKO mice in comparison to islets from controls determined by bulk RNA-Seq (Figure 67A). In comparison to the IgG control, PAX6 immunoprecipitation enriched the assayed *Ins1* locus in MIN6 cells. Interestingly, also TBL1 and TBLR1 enriched the *Ins1* locus in comparison to the IgG control suggesting that TBL1 and TBLR1 indeed bind to the same promoter region as PAX6 (Figure 67B). Furthermore, knock down of TBL1 but also double knock down of TBL1 and TBLR1 in INS1E cells resulted in a reduction in the activity of a luciferase reporter bearing the murine *Ins2* promoter sequence, suggesting that TBL1 is required for *Ins2* gene expression in mice. Surprisingly TBLR1 knock down increased the luciferase activity (Figure 67C). Similar to that, activity of a luciferase reporter under control of the human insulin (*INS*) promoter was also reduced upon TBL1 and TBL1/TBLR1 knock down, while no changes were observed upon TBLR1 knock down (Figure 67D). Thus, TBL1 and TBLR1 are implicated in the regulation of the two murine PAX6 target genes *Ins1* and *Ins2* and the human PAX6 target gene *INS*.

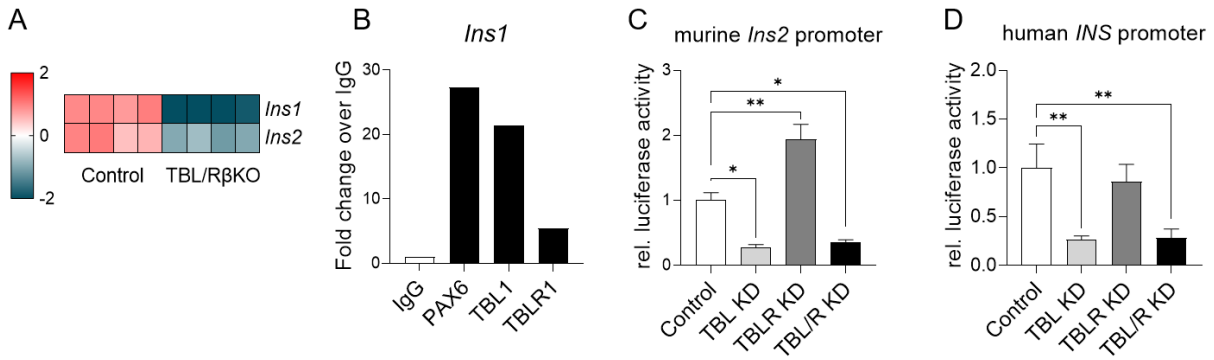

Figure 67: TBL1 and TBLR1 bind to the murine *Ins1* and *Ins2* and the human *INS* promoters. (A) Heat map displaying relative gene expression of PAX6 target genes *Ins1* and *Ins2* in islets from TBL/RβKO mice vs. controls determined by bulk RNA sequencing. Each line represents one mouse. Colour represents log2 fold-change. Threshold for significance: -log10(p-value) = 1.3 ($p < 0.05$). **(B)** ChIP-qPCR assay was performed in MIN6 cells using indicated antibodies of which IgG was used as control. Results show fold increase in the qPCR signal of the assayed *Ins1* promoter locus over IgG. Relative luciferase levels of a reporter construct containing the **(C)** murine *Ins2* promoter and **(D)** human insulin (*INS*) promoter in INS1E cells upon siRNA mediated TBL1 (TBL KD), TBLR1 (TBLR KD), or TBL1 and TBLR1 (TBL/R KD) knock down. As control, INS1E cells were transfected with non-targeting siRNA. Data is presented as mean ± SEM. Statistical analysis was performed using a Dunnett's multiple comparison *post hoc* test (C,D). *$p < 0.05$, **$p < 0.01$. n=4.

Whether TBL1 and TBLR1 bind to the *Ins1*, *Ins2,* and *INS* promoter regions through PAX6 and whether TBL1 and TBLR1 are recruited to other PAX6 promoter targets remains to be investigated.

3 DISCUSSION

3.1 TBLR1 compensates for the lack of TBL1 in pancreatic β-cells

TBL1 and TBLR1 are transcription co-factors regulating oncogenesis, lipid metabolism, and transcriptional evens in numerous tissues and cell types. Their importance for metabolic functions in the body is underlined by the embryonic lethality upon full body TBL1 and TBLR1 knock out (Perissi et al. 2010). Although TBL1 and TBLR1 are highly homologous, with a 90% similarity in their protein sequence, they do not always possess identical functions. Moreover, previous studies have demonstrated that the function of TBL1 and TBLR1 is highly tissue and interaction partner specific. For instance, adipose tissue specific TBLR1 knock out impaired fasting-induced lipolysis by direct PPARγ/RXRα interaction (Rohm et al. 2013). In contrast, Perissi and colleagues demonstrated that both, TBL1 and TBLR1 were required for PPARγ signaling in a cancer cell line (Perissi et al. 2004). This highlights that the binding of TBL1 and TBLR1 to an interaction partner varies depending on the tissue type. Interestingly, not only in the adipose tissue but also in the liver TBL1 and TBLR1 were implicated in lipid metabolism. In hepatocytes, TBL1 and TBLR1 were found to physically interact with PPARα and thereby control PPARα-mediated fatty acid oxidation (Kulozik et al. 2011). Thus, although TBL1 and TBLR1 regulate lipid metabolism in adipose tissue and the liver, the underlying mechanisms, the involved interaction partner, and the role of TBL1 and TBLR1 were proven to be tissue specific.

This study aimed to identify the β-cell specific function of TBL1 and TBLR1 in β-cells. Here, mice with a β-cell specific knock out of either TBL1 or TBLR1 did not display any major impairments in glucose metabolism or β-cell function. Also, during aging or diet-induced obesity, states at which β-cells are metabolically challenged, the knock out mice appeared phenotypically undistinguishable from the control mice. Interestingly, TBLR1 expression was strongly upregulated *in vitro* upon siRNA mediated TBL1 knock down. Also *in vivo* in pancreatic islets from TBLβKO mice, TBLR1 expression was upregulated, while TBL1 expression was unchanged upon TBLR1 depletion. Since the upregulation of TBLR1 upon TBL1 knock down was observed *in vitro* using INS1E and MIN6 cells deriving from rats and mice, respectively and *in vivo* using islets from TBLβKO mice, this supports the notion that the upregulation of TBLR1 upon TBL1 deficiency represents a highly conserved process. One possible explanation for this is that TBLR1 compensates for the loss of TBL1, but not the other way around. This implies that TBL1 and TBLR1 might control key mechanisms crucial for β-cell function and physiology. Indeed, deletion of both transcription co-factors together had detrimental effects on β-cell physiology and function. This points towards an identical or similar function of TBL1 and TBLR1 as suggested in previous studies (Yoon et al. 2003; Kulozik et al. 2011) also in pancreatic β-cells. Indeed, the interactome screen revealed that most of the identified interaction partners were interacting with both, TBL1 and TBLR1, supporting the notion that TBL1 and TBLR1 fulfil similar roles, at least in β-cells. However, gene expression profiling using islets from TBLβKO and TBLRβKO mice suggested that TBL1 and TBLR1 have distinct functions, since only 319 genes were shared between the 1464 differentially expressed genes upon TBL1 knock out and the 3053 differentially expressed genes upon TBLR1 knock out. Moreover, using KEGG pathway analysis only two pathways, the *MAPK signaling pathway* and the *staphylococcus aureus infection pathway* were commonly dysregulated between islets from TBLβKO and TBLRβKO mice. Thus, in the presence of TBL1, TBL1 and TBLR1 might have distinct functions in β-cells. Upon TBL1 deficiency however, TBLR1 might compensate and take over regulatory functions facilitated by TBL1, which is supported by the large amount

of interaction partners shared between TBL1 and TBLR1. This would explain why single knock out of TBL1 or TBLR1 did not affect β-cell function and physiology while simultaneous knock out had detrimental effects. Another explanation for the upregulation of TBLR1 expression upon TBL1 deficiency might be that TBL1 represses TBLR1 expression. It needs to be addressed in future studies however, whether TBL1 is able to bind to TBLR1 promoter regions, which was not investigated in this study or any previous studies.

3.2 TBL1 and TBLR1 are essential for the maintenance of β-cell identity

In vivo TBL1 and TBLR1 ablation in β-cells resulted in dramatic changes in β-cell physiology and islet morphology. Alterations in the islet gene expression profile and the impaired insulin synthesis suggest that β-cells lacking TBL1 and TBLR1 fail to function properly and lose their differentiated and mature state.

β-cell maturity is characterized by reduced proliferative capacity (Swenne 1983; Meier et al. 2008), insulin secretion at a higher glucose threshold (Otonkoski et al. 1988), and expression of maturity markers such as *Ucn3* (Blum et al. 2012). β-cells mature during the post-natal period between birth and weaning (Blum et al. 2012; Stolovich-Rain et al. 2015). Triiodothyronine (T3) was previously identified as possible driver of β-cell maturation as treatment of isolated immature rat islets and foetal human islets with T3 promoted *MafA* gene expression and improved glucose stimulated insulin secretion. Additionally, murine T3 receptor expression is elevated during the second and third week of life suggesting an implication of T3 signaling in β-cell maturation (Aguayo-Mazzucato et al. 2013; Aguayo-Mazzucato et al. 2015). Interestingly, Perissi and colleagues demonstrated that TBL1 and TBLR1 are required for T3 receptor mediated gene expression (Perissi et al. 2004). Thus, ablation of TBL1 and TBLR1 in the critical period of functional maturation would trap the β-cells in an immature state. Although the interactome screen did not show an interaction between the T3 receptor and TBL1 or TBLR1 in pancreatic β-cells, islets from TBL/RβKO mice displayed characteristics of immature β-cells. For instance, *Hk1*, *Ldha*, *Cd81*, and *Slc16a1* which are highly expressed in immature β-cells but become repressed during postnatal maturation (Thorrez et al. 2011; Dhawan et al. 2015; Salinno et al. 2021), were strongly upregulated while maturity markers such as *Ucn3* and *Syt4* (Blum et al. 2012; Huang et al. 2018) were downregulated in islets from conditional TBL1 and TBLR1 knock out mice as revealed by transcriptomic profiling. Moreover, maturation of β-cells is in part induced by the transition from high fat mothers' milk to high carbohydrate chow diet (Stolovich-Rain et al. 2015). Although TBL/RβKO mice developed hyperglycemia starting at the age of 6 weeks, changes in the transcriptome preceded the onset of hyperglycemia. In addition, islet micro-architecture was undistinguishable between controls and TBL/RβKO mice at P4 but at the age of 5 weeks abnormal changes in the cell type distribution were observed, suggesting that the onset of the phenotype would start during this period coinciding with the period of weaning-triggered maturation. Thus, to investigate whether TBL1 and TBLR1 are implicated in weaning-triggered maturation, control and TBL/RβKO mice were either prematurely weaned or underwent prolonged suckling. However, islet morphology was unchanged in TBL/RβKO mice irrespective of the weaning group, suggesting that TBL1 and TBLR1 are not required for the weaning induced maturation of β-cells. Moreover, proliferative capacity of β-cells which reduces progressively during and after maturation (Swenne 1983; Meier et al. 2008) was unchanged in TBL/RβKO mice in comparison to controls. In addition, expression of disallowed genes such as *ChgA*, *Ngn3*, *Ldha*, and *Hk1* was also upregulated when TBL1 and TBLR1 knock out was induced in mature and differentiated

β-cells. Ultimately this suggests that, instead of being trapped in an immature state it seems that β-cells lacking TBL1 and TBLR1 lose their mature state and identity over time.

In most cases the progressive pathogenesis of T2DM is induced by insulin resistance. At first, pancreatic β-cells successfully compensate through hyperplasia and increased insulin secretion for the gradually increasing insulin demand to maintain normoglycemia. Eventually, β-cells fail to maintain blood glucose levels in a physiologic range leading to overt diabetes (Fu et al. 2013). Ultimately, β-cell failure and T2DM result in reduced β-cell number, β-cell dysfunction, and dedifferentiation. For a long time, depletion of β-cell number during prolonged hyperglycemia was attributed to increased apoptotic events (Butler et al. 2003). Although β-cell mass was strongly reduced upon β-cell specific TBL1 and TBLR1 knock out, apoptosis did not seem to account for the reduction in β-cell number in this study, as bulk RNA-Seq and scRNA-Seq revealed that apoptosis-related genes were unchanged between control and TBL/RβKO mice, and TUNEL staining did not show any differences in the amount of apoptotic β-cells between genotypes (data not shown). Accordingly, using the IPA and KEGG pathway analysis tools, differentially expressed genes did not enrich for apoptosis related pathways. Thus, apoptosis does not explain the strong reduction in β-cell mass observed in TBL/RβKO mice. Talchai and colleagues observed that β-cell specific *Foxo1* (Forkhead box O 1) knock out in mice reduced β-cell mass upon physiological stress such as aging or multiple pregnancies, while the number of apoptotic events was not increased. Instead, dedifferentiation was identified as contributor to β-cell failure (Talchai et al. 2012) and was later also described as major pathologic mechanism in T2DM (Amo-Shiinoki et al. 2021; Cinti et al. 2016). β-cell dedifferentiation is the loss of β-cell identity and is characterized by a downregulation of β-cell enriched genes, an upregulation of β-cell disallowed genes, and a reoccurrence of progenitor cell associated genes (Talchai et al. 2012; Swisa et al. 2017). However, not only FOXO1 deficiency is sufficient to drive β-cell dedifferentiation but also ablation of the β-cell enriched transcription factors NKX6.1, PDX1, or PAX6 result in β-cell dedifferentiation (Taylor et al. 2013; Gao et al. 2014; Swisa et al. 2017). Islets from TBL/RβKO mice showed a strong downregulation of β-cell enriched genes while disallowed genes were upregulated. Moreover, conditional and induced TBL1 and TBLR1 knock out in β-cells resulted in an upregulation of genes characteristic for almost all developmental stages of the β-cell such as *Ngn3*, a marker for endocrine progenitor cells (Jensen et al. 2000; Schwitzgebel et al. 2000) or *Sox9* (SRY box transcription factor 9), a markers of pre-endocrine cells (Seymour et al. 2007). Even marker for the early stages of pancreatic endocrine cell development such as *Sox2* or *Sox17*, mainly expressed in pluripotent stem cells or definitive endoderm cells respectively (Nair and Hebrok 2015), were upregulated in islets from TBL/RβKO mice. This implies that in the absence of TBL1 and TBLR1 β-cells cannot maintain their mature and differentiated state and are forced towards a pre-β-cell differentiation state. Interestingly, apart from the upregulation of β-cell precursor and disallowed genes, islets from TBL/RβKO mice showed an upregulation of genes characteristic to other cell types of the endocrine pancreas such as *Gcg*, *Sst*, and *Ppy*. Accordingly, plasma glucagon levels, total pancreas glucagon content, and α-cell mass were strongly increased in TBL/RβKO mice. Indeed, the rise of other endocrine cell populations was shown to be increased upon dedifferentiation (Amo-Shiinoki et al. 2021; Talchai et al. 2012; Swisa et al. 2017). Lineage tracing demonstrated that β-cells dedifferentiate into progenitor like cells and subsequently convert into other cells types such as α-cells or ε-cells (Talchai et al. 2012; Swisa et al. 2017), suggesting a similar mechanism may occur in TBL/RβKO islets.

Another mechanism in T2DM in which β-cells are lost in favour to other endocrine cell types is transdifferentiation, a process in which β-cells convert into other terminally differentiated cells without returning to a progenitor like state. For instance, PDX1 or NKX2.2 deficient β-cells were shown to transdifferentiate into cells co-expressing insulin and glucagon or insulin and somatostatin, respectively (Yang et al. 2011; Gao et al. 2014; Gutiérrez et al. 2017). As *Pdx1* and *Nkx2.2* expression is reduced in states of chronic hyperglycemia (Yang et al. 2012; Sussel et al. 1998), this would suggest that transdifferentiation contributes to the β-cell depletion observed in T2DM. However, unlike dedifferentiation, transdifferentiation was only observed in knock out studies and not upon chronic hyperglycemia and T2DM (Wang et al. 2014), suggesting that dedifferentiation is the more physiologic process of hyperglycemia induced loss of β-cell mass. Here, scRNA-Seq revealed that upon TBL1 and TBLR1 knock out more cells were co-expressing two or even three endocrine hormones in comparison to the control. This was however not validated using immunofluorescence staining for insulin and glucagon for instance and the increased appearance of cells with dual signal in the scRNA-Seq may stem from an increased detection of cell duplets in the knock out mice, as suggested by a more stringent data analysis (Peter Weber, personal communication). Thus, in the specific case of TBL1 and TBLR1 deficiency this suggests that β-cells do not transdifferentiate but rather dedifferentiate as they first enter a precursor cell state and only then convert into other cell types.

Induction of the EMT, ECM deposition in the islets, and islet fibrosis were previously associated with β-cell dedifferentiation (Jesus et al. 2021). Indeed, markers of EMT are upregulated in α- and β-cells upon T2DM (Avrahami et al. 2020; Roefs et al. 2017). These fibrotic changes of the islet during β-cell dedifferentiation were in part driven by transforming growth factor β (TGFβ) signaling (Jesus et al. 2021). Accordingly, pharmacological inhibition of the TGFβ receptor restored β-cell identity gene expression and reduced collagen deposition in islets of human and murine models of dedifferentiation (Jesus et al. 2021; Blum et al. 2014). Induction of the EMT was also identified as central mechanism through which endocrine precursor cells cluster and form islets during pancreas development (Cole et al. 2009), indicating that with the reactivation of EMT, pancreatic islets move backwards in their differentiation state. In line with the dedifferentiation-like phenotype in TBL/RβKO mice, *ECM-receptor interaction* was the most significantly upregulated pathway identified by KEGG pathway analysis. In addition, GSEA revealed an overrepresentation of differentially expressed genes that are associated with EMT upon TBL1 and TBLR1 knock out. Moreover, using IPA to predict upstream regulators that would explain alternatively expressed genes in islets from TBL/RβKO mice, TGFβ was identified as most significant hit. Of note, TBL1 was shown to play a central role in the EMT in breast cancer cells (Rivero et al. 2019). This further supports the notion that β-cells deficient for TBL1 and TBLR1 lose their identity and undergo dedifferentiation.

Taken together, β-cell specific ablation of TBL1 and TBLR1 results in a dedifferentiation of β-cells. Islets from TBL/RβKO mice display various hallmarks of dedifferentiation such as impaired β-cell identity gene expression, reactivation of β-cell progenitor marker, the rise of non-β-cell islet cells, as well as induction of the EMT. This establishes TBL1 and TBLR1 as central regulators of β-cell identity.

3.3 TBL1 and TBLR1 deficiency induced dedifferentiation of β-cells is not reproduced *in vitro*

In vitro knock down of TBL1 and TBLR1 in INS1E and MIN6 cells did not recapitulate the observations from the *in vivo* studies. For instance, while glycemia or insulinemia were unchanged in TBLRβKO mice, siRNA mediated TBLR1 knock down in INS1E cells increased insulin secretion at low glucose conditions. Insulin secretion at high glucose levels or KCl-induced insulin secretion were unchanged. Elevated insulin secretion in particular at low glucose levels is characteristic for immature β-cells. As described above, only after functional maturation β-cells achieve the ability to secrete insulin at higher glucose thresholds (Blum et al. 2012). Another hallmark of β-cell immaturity is the low expression of *Ucn3* (Blum et al. 2012). However, *Ucn3* expression but also expression of other β-cell identity genes was strongly upregulated upon TBLR1 knock down, suggesting that maturity is still maintained in INS1E cells lacking TBLR1. Also, simultaneous knock down of TBL1 and TBLR1 in INS1E cells promoted β-cell identity gene expression and insulin secretion although β-cells from TBL/RβKO mice were dysfunctional and underwent dedifferentiation. This discrepancy between *in vivo* and *in vitro* observations suggests that insulinoma cell lines might not be able to undergo dedifferentiation and are thereby not a suitable model. However, exposure of the murine insulinoma cell line MIN6 to a FOXO1-inhibitor induced dedifferentiation as indicated by reduced β-cell identity gene expression and increased progenitor and α-cell marker expression (Casteels et al. 2021). Moreover, glucosamine and high glucose exposure induced endoplasmic reticulum stress in INS1E cells led to dedifferentiation and thereby to reduced β-cell identity gene expression and dampened glucose stimulated insulin secretion (Lombardi et al. 2012). Thus, although dedifferentiation can be mimicked *in vitro* in INS1E and MIN6 cells, TBL1 and TBLR1 knock down was not sufficient to trigger this process *in vitro*. The absence of dedifferentiation in INS1E and MIN6 cells upon TBL1 and TBLR1 knock down might be explained by remaining TBL1 and TBLR1 expression upon siRNA/shRNA mediated knock down or by analysis of phenotypic changes too shortly after knock down induction. Moreover, since *in vitro* cell lines represent an isolated and simplified model, essential factors for the development of the phenotype might be missing such as cell-cell interactions between β-cells and other cell types of the endocrine pancreas or circulating factors such as ligands for nuclear receptors.

After siRNA transfection of INS1E cells, TBL1 mRNA levels were reduced by ~90% while TBLR1 mRNA levels were reduced by only 60%. Thus, the remaining TBLR1 expression might have blunted or inhibited the progression of the dedifferentiation. In line with this, tamoxifen-induced TBL1 and TBLR1 knock out in mice also resulted in an incomplete depletion and phenotypic alterations were not as severe as previously observed in the conditional TBL/RβKO mice. In contrast, induced knock out of *Pax6*, *Nkx2.2*, or *Pdx1* in previous studies was more efficient, resulting in a rapid development of β-cell dedifferentiation within one or two weeks (Gao et al. 2014; Swisa et al. 2017; Gutiérrez et al. 2017). This suggests that incomplete ablation of TBL1 and TBLR1 might cause the absent development of the phenotype *in vitro* but also *in vivo* in the inducible TBL/RβKO mice on chow diet.

Another reason for the inconsistent observations between *in vivo* and *in vitro* models might be the duration of phenotype development. TBL/RβKO mice developed severe hyperglycemia starting at the age of 6 weeks. Conversely, in iTBL/RβKO mice, blood glucose levels dropped significantly after knock out induction while islet gene expression and islet micro-architecture displayed characteristics of dedifferentiation. Discrepancies in phenotype severity between

conditional and induced knock out were also described in other models of β-cell dedifferentiation (Gutiérrez et al. 2017). Only 18 weeks after knock out induction and HFD feeding, iTBL/RβKO mice started to show impaired β-cell function. This suggests that the development of the dedifferentiation due to TBL1 and TBLR1 deficiency is a time dependent process and that β-cell function is progressively lost. This would indicate that the knock down in INS1E and MIN6 cells, which displays only acute changes requires more time in order to show a similar phenotype as observed in the knock out mice.

Moreover, terminally differentiated β-cells lose their ability to proliferate after maturation (Swenne 1983; Meier et al. 2008). In contrast, INS1E and MIN6 cells are cells that originate from insulinomas and retain their proliferative ability (Asfari et al. 1992; Ishihara et al. 1993). This substantial difference between primary β-cells and β-cell lines affects not only pathways associated with proliferation but also with apoptosis and cell cycle (Skelin et al. 2010). Thus, the function and action of TBL1 and TBLR1 in β-cells might also be affected by these alterations. Additionally, INS1E cells require β-mercaptoethanol in their culture medium for continuous proliferation (Asfari et al. 1992), which is toxic, denatures proteins (Skelin et al. 2010), and thereby might induce β-cell stress and affect TBL1 and TBLR1 expression or function. MIN6 cells are cultured in 25 mM glucose medium (Ishihara et al. 1993), which would metabolically stress primary β-cells and induce apoptosis due to glucotoxicity (Efanova et al. 1998). Moreover, high glucose levels reduced TBL1 and TBLR1 mRNA and protein levels in INS1E cells and murine islets, suggesting that the high glucose concentration in the media of MIN6 cells might also affect TBL1 and TBLR1 expression. Thus, metabolic differences between primary β-cells and the insulinoma β-cell lines and conditions for cultivation might explain the absence of phenotypic changes *in vitro* that were observed *in vivo*.

Nevertheless, although INS1E cells or MIN6 cells lacking TBL1 and TBLR1 did not display the same phenotype as observed in the TBL/RβKO mice, some features such as the upregulation of TBLR1 upon TBL1 deficiency were reproduced. Moreover, the interactome analysis using MIN6 cells identified all components of the NCOR/SMRT repressor complex as direct TBL1 and TBLR1 interaction partners. As TBL1 and TBLR1 are known components of this NCOR/SMRT repressor complex (Guenther et al. 2001; Yoon et al. 2003), this implies that main regulatory mechanisms or at least protein-protein interactions are conserved in the insulinoma cells used in this study.

3.4 Bidirectional PAX6 gene expression in β-cells might be facilitated by TBL1 and TBLR1

Inflammation (Nordmann et al. 2017), oxidative stress (Talchai et al. 2012), and endoplasmic reticulum stress (Lombardi et al. 2012) were identified as main driver of β-cell dedifferentiation ultimately leading to reduced β-cell identity gene expression and induction of disallowed and progenitor cell genes. To maintain a differentiated state, a constant repression of disallowed genes is required which is in part facilitated by β-cell enriched transcription factors. For instance, during metabolic stress FOXO1 is required to promote β-cell identity gene expression through repression of endocrine progenitor genes (Talchai et al. 2012). The transcription factor NKX2.2 was shown to directly bind to promoter regions of β-cell identity genes and disallowed genes thereby functioning as activator and repressor (Gutiérrez et al. 2017). PDX1 was demonstrated to maintain β-cell identity (Gao et al. 2014) and to modulate insulin gene expression through the recruitment of regulatory complexes and histone modifiers such as p300 (Mosley et al. 2004), HDAC1/2 (Mosley and Ozcan 2004), or the switch/sucrose non-

fermentable (SWI/SNF) complex (McKenna et al. 2015), depending on glucose availability in the β-cell. PAX6 was shown to maintain β-cell identity through induction of β-cell identity genes and repression of disallowed genes (Swisa et al. 2017). Accordingly, β-cell specific *Pax6* knock out resulted in hyperglycemia, hypoinsulinemia, downregulation of β-cell identity genes, upregulation of disallowed genes, and abnormal islet micro-architecture (Gosmain et al. 2012; Swisa et al. 2017; Mitchell et al. 2017) – a phenocopy of β-cell TBL1 and TBLR1 ablation. As TBL1 and TBLR1 directly bind to PAX6, this indicates that TBL1 and TBLR1 might be involved in PAX6 mediated gene regulation. One of the most prominent PAX6 targets genes is the insulin gene (Sander et al. 1997). Indeed, TBL1 and TBLR1 were found to directly or indirectly bind to the same *Ins1* promoter region as PAX6 in MIN6 cells. Moreover, promoter activity of the murine *Ins2* gene and the human *INS* gene was reduced by TBL1 and double TBL1 and TBLR1 knock down in INS1E cells. It is however unclear whether TBL1 and TBLR1 directly bind to the PAX6 target gene promoter regions or whether they instead bind to PAX6 itself and thereby control PAX6-mediated gene expression. Indeed, previous studies demonstrated that TBL1 and TBLR1 are able to directly bind to DNA (Li and Wang 2008) but also to bind to nuclear receptors (Perissi et al. 2004) or histones (Guenther et al. 2000; Yoon et al. 2003) in order to regulate transcriptional events.

In hepatocytes, TBL1 and TBLR1 were shown to physically interact with PPARα, a key regulator of fatty acid oxidation in the liver (Kulozik et al. 2011). TBL1 and TBLR1 deficiency resulted in hepatic steatosis in part through an increased NCOR1 and HDAC3 recruitment to the promoters of PPARα target genes. Accordingly, less of the PPARα co-activators bound to these promoter regions leading to an overall repression of the PPARα-mediated fatty acid oxidation (Kulozik et al. 2011). This supports the notion that TBL1 and TBLR1 recruit regulatory complexes signal dependently and thereby function as exchange factors for these complexes (Perissi et al. 2004; Ogawa et al. 2004). Here, not only TBL1 and TBLR1 were found to bind to PAX6 but also HDAC3, part of the NCOR/SMRT repressor complex, and SUPT16H, a subunit of the FACT activator complex. Indeed, PAX6 has previously been shown to interact with regulatory complexes and histone modifiers to facilitate transcriptional events. For instance, the BAF chromatin remodelling complex interacts with PAX6 during neurogenesis (Ninkovic et al. 2013) while HDAC1, which belongs to the same HDAC-family as HDAC3, has been shown to bind to PAX6 to regulate retinal development (Kim et al. 2017). This suggests that PAX6 mediated gene expression in part requires regulatory complexes including histone deacetylases – prototypic TBL1 and TBLR1 interaction partners. Thus far, β-cell specific PAX6 interaction partners were not identified. Since PAX6 was shown to induce the expression of β-cell identity genes while simultaneously repressing the expression of disallowed genes (Swisa et al. 2017), it is likely that regulatory complexes such as the NCOR/SMRT repressor complex and the FACT activator complex are recruited to PAX6 to control this bidirectional gene expression. In this context, TBL1 and TBLR1 might function as exchange factors. It was previously demonstrated that in order to exchange regulatory complexes, TBL1 and TBLR1 recruit the ubiquitin/19S proteasome complex to induce the ubiquitination and subsequent proteasomal degradation of the respective regulatory complexes (Perissi et al. 2004). In this study, the interactome screen revealed that TBL1 and TBLR1 interact with ubiquitination and proteasomal degradation associated proteins such as USP28, UBE2N, or PSMB5, indicating that also in the pancreatic β-cells TBL1 and TBLR1 might facilitate ubiquitination and degradation of regulatory complexes. Interestingly, binding intensity of the respective regulatory complex component to PAX6 was TBL1 and TBLR1 dependent. In the absence of TBL1 and TBLR1, more HDAC3 and less SUPT16H bound to PAX6 suggesting that in the absence to TBL1 and TBLR1 the NCOR/SMRT repressor complex is not dismissed resulting

in sustained repression of gene expression. This fits with the general downregulation of β-cell identity gene expression observed in islets from TBL/RβKO mice, but not with the upregulation of disallowed genes and progenitor cell markers. In future studies, it therefore needs to be investigated whether TBL1 and TBLR1 indeed recruit the ubiquitin/19S proteasome complex in order to induce the proposed regulatory complex switch. Moreover, the promoter regions to which TBL1 and TBLR1 but also the respective complex components bind need to be identified to understand the underlying mechanism.

Of note, the only known TBL1 and TBLR1 interaction partners identified in the interactome analysis, apart from the NCOR/SMRT complex, were β-catenin (Li and Wang 2008) and CTBP1 (Perissi et al. 2008). However, the enrichment over the control pulldown was either not significant or the enrichment fold-change was below the threshold (fold change < 2.1). Thus, the roles of TBL1/TBLR1 in the context of β-catenin and CTBP1 in β-cells were not investigated in this study.

Here, the NCOR/SMRT repressor complex component HDAC3 and the FACT activator complex subunit SUPT16H were directly interacting not only with TBL1 and TBLR1, but also with PAX6, the master regulator of pancreatic endocrine cells. Apart from HDAC3, none of the NCOR/SMRT or FACT complex components were addressed in the context of pancreatic β-cell function and physiology. Induced β-cell specific HDAC3 knock out improved glucose tolerance and insulin secretion (Remsberg et al. 2017). This is in line with previous studies where pharmacological HDAC3 inhibition improved β-cell function (Lundh et al. 2015; Lundh et al. 2012). One of the major roles of HDAC3 is the deacetylation of histone tails resulting in condensed chromatin and thereby repression of gene expression. In turn, ablation or inhibition of HDAC3 would result in hyperacetylated histone tails, open chromatin, and thus induction of gene expression (Yoon et al. 2005). Upregulation of insulin secretion and synthesis due to HDAC3 inhibition or deletion suggests that HDAC3 binds and modulates promoter regions of β-cell identity genes. This supports observations from this present study as upon TBL1 and TBLR1 deficiency more HDAC3 bound to PAX6, probably resulting in an overall downregulation of β-cell identity genes. In contrast, conditional HDAC3 knock out enhanced susceptibility to streptozotocin induced β-cell death and induced glucose intolerance in part through downregulation of insulin gene expression (Chen et al. 2016). The conflicting observations between induced and conditional HDAC3 deficiency might be explained by a possible role of HDAC3 in β-cell development or differentiation. Moreover, this also indicates that HDAC3 might have a TBL1/TBLR1 independent function.

Although the role of the FACT complex was not investigated in β-cells thus far, interactome screens from previous studies showed that the FACT subunits SUPT16H and SSRP1 were interacting with pluripotency marker homeobox protein NANOG and SOX2 (Nitzsche et al. 2011; Samudyata et al. 2019), indicating a role in β-cell development and differentiation. During embryogenesis, spatiotemporal repression and activation of genes is facilitated by histone modifications such as methylation in order to drive β-cell development (van Arensbergen et al. 2010). Also in adult β-cells, methylation is central for the maintenance of a mature and differentiated state as β-cell disallowed genes such as *Hk1*, *Ldha*, or *Slc16a1* are repressed by methylation of the respective promoter region (van Arensbergen et al. 2010; Thorrez et al. 2011). Interestingly, the TBL1 and TBLR1 interaction partner KDM1A – a histone demethylase, was previously identified as SUPT16H and SSRP1 interaction partner (Latos et al. 2015). Accordingly, the FACT complex was shown to regulate transcriptional events through demethylation (Frost et al. 2018). Thus, a dysregulation of FACT complex recruitment

to promoter regions, possibly due to TBL1 and TBLR1 deficiency, would induce the demethylation of promoter regions of β-cell disallowed genes resulting in their expression. Indeed, alterations in the epigenome and in histone modifications were associated with β-cell dedifferentiation and T2DM (Lu et al. 2018). It however needs to be addressed whether the FACT complex is capable of binding to promoter regions of β-cell disallowed genes and whether TBL1 and TBLR1 are indeed required for selective FACT complex recruitment or dismissal.

3.5 TBL1 and TBLR1 as targets for T2DM prevention

Impaired β-cell function is a major contributor to diabetes. Attempts to cure insulin-dependent diabetes comprise of pancreas transplantation (Nath et al. 2005), pancreatic islet transplantation (Shapiro et al. 2006), or transplantation of β-cells or pancreatic islets derived from human stem cells (Shapiro et al. 2021). One of the main limitations in the β-cell transplantation field is the organ donor availability, emphasizing the need for in depth understanding of mechanisms involved in β-cell differentiation from stem cells. In the past decade, great progress was achieved in the field of β-cell differentiation from human pluripotent stem cells (hPSC). However, differentiation efficiency is not reproducible across hPSC lines (Merkle et al. 2022) and glucose stimulated insulin secretion is impaired due to immature mitochondrial glucose coupling (Balboa et al. 2022). Interestingly, TBL1 and TBLR1 are differentially expressed between grafted stem cell-islets or stage 6 stem cell-islets and primary human cadaveric islets (Augsornworawat et al. 2020). Given that TBL1 and TBLR1 were identified here as central regulators of β-cell identity, this suggests that modulation of TBL1 and TBLR1 expression during β-cell differentiation from hPSC might have beneficial effects on the differentiation process and maturation.

The loss β-cell identity due to dedifferentiation is recognized as main mechanism through which β-cells are lost in T2DM (Amo-Shiinoki et al. 2021; Cinti et al. 2016). Maintaining the differentiated state or reversing β-cell dedifferentiation would therefore represent a novel approach to prevent the development or progression of T2DM. Indeed, reversal of β-cell dedifferentiation was previously achieved using TGFβ inhibitors (Blum et al. 2014) or through inhibition of NFκB signaling (Chen et al. 2018). Moreover, infusion of umbilical cord-derived mesenchymal stem cells was sufficient to normalize blood glucose levels in T2DM patients (Hu et al. 2016), mainly due to reversal of β-cell dedifferentiation as observed in *db/db* mice (Li et al. 2021). This suggests that the dedifferentiation of β-cells due to hyperglycemia and dyslipidemia is a reversible process. As islet TBL1 and TBLR1 levels were reduced in aged and diabetic mice, β-cell specific upregulation of TBL1 or TBLR1 expression, or the improvement of TBL1 and TBLR1 action would represent a promising approach to counteract β-cell dedifferentiation.

Targeting TBL1, TBLR1, or their interaction partners such as components of the FACT or NCOR/SMRT complex systemically was shown to be difficult due to the variety of processes regulated by these factors. For instance, full body knock out of TBL1, TBLR1, or components of the NCOR/SMRT repressor complex such as NCOR1 and HDAC3 are embryonically lethal (Perissi et al. 2010; Montgomery et al. 2008; Jepsen et al. 2000), suggesting that they control central mechanisms in the whole body. Moreover, alterations in the function and expression of TBL1 and TBLR1 (Li and Wang 2008; Rivero et al. 2019; Xu et al. 2022), but also of the components of the FACT complex (Hudson et al. 2007; Garcia et al. 2011) were associated with cancer progression and aggressiveness, making it dangerous to alter their expression or

activity systemically. It is therefore important to target TBL1 and TBLR1 tissue specifically but also to target specifically the interaction between TBL1, TBLR1 and their interaction partners. Curaxin (CBL0137) for instance directly targets the FACT complex and thereby inhibits FACT-mediated proliferation of cancer cells and promotes their apoptosis (Maluchenko et al. 2016; Gasparian et al. 2011). Thus far it remains to be investigated whether Curaxin would also affect the interaction between FACT and TBL1 or TBLR1, or how Curaxin would affect pancreatic β-cell identity. Interestingly, Tegavivint (BC2059) was identified to specifically disrupt the interaction between TBL1 and β-catenin in cancer cells (Fiskus et al. 2015). Although both, β-catenin and the NCOR/SMRT complex were shown to bind to the N-terminal domain of TBL1 (Oberoi et al. 2011; Li and Wang 2008), Tegavivint specifically disrupted the TBL1/β-catenin interaction (Soldi et al. 2021). How Tegavivint achieves this specificity is not completely understood. However, this indicates that pharmacological manipulation of TBL1 and TBLR1 activity is possible through disruption of interaction partner binding. Of note, PAX6 which was identified as direct TBL1 and TBLR1 interaction partner in this study is a central regulator for β-cell differentiation but also for the development of endocrine cells of the pancreas, retinal cells, and the central nervous system (St-Onge et al. 1997; Nishina et al. 1999; Walther and Gruss 1991). It therefore needs to be assessed which functions of PAX6 are under the regulation of TBL1 and TBLR1. Thus, understanding the interplay between TBL1, TBLR1 and the respective interaction partners in pancreatic β-cells is central to decipher mechanisms underlying dedifferentiation and to develop novel approaches to prevent T2DM.

3.6 Summary and outlook

In this study, TBL1 and TBLR1 were identified as central regulators of β-cell identity in mice. Through their interaction with PAX6 but also components of the NCOR/SMRT and the FACT complexes, TBL1 and TBLR1 seem to recruit regulatory complexes to promoter regions of β-cell identity genes and disallowed genes to modulate β-cell gene expression and maintain β-cell identity. Accordingly, disruption of TBL1 and TBLR1 function was shown to have detrimental systemic consequences as β-cells underwent dedifferentiation. Moreover, it is likely that after entering a progenitor cell-like state, β-cells differentiated into other cell types of the endocrine pancreas. The exact mechanisms however need further investigations.

As TBL1 and TBLR1 were shown to physically interact with PAX6, one central aspect would be to identify further TBL1 and TBLR1 target genes in β-cells apart from the insulin genes and to find out whether those coincide with PAX6 targets. To this end, a successful quantitative ChIP protocol was established and optimized for MIN6 cells. The next step would be to perform ChIP sequencing to identify promoter regions targeted by TBL1, TBLR1, and PAX6 in an unbiased-manner. Based on observations from this study and on the known roles of TBL1 and TBLR1 in other cell types, it was hypothesized that TBL1 and TBLR1 would recruit regulatory complexes to PAX6 in order to facilitate bidirectional PAX6-mediated gene expression. Indeed, components of the NCOR/SMRT repressor complex and the FACT activator complex were found to not only bind to TBL1 and TBLR1 but also to PAX6. Thus, binding sites of these regulatory complexes using ChIP sequencing but also the underlying mechanism of the hypothesized regulatory complex recruitment or dismissal would be essential to further understand how TBL1 and TBLR1 maintain β-cell identity. Additionally, the determination of the acetylome and the methylome of the chromatin using ChIP sequencing would be of great interest to investigate whether gene expression regulated by TBL1 and TBLR1 is indeed mediated by acetylation and methylation facilitated by the NCOR/SMRT and FACT complex.

Lastly, it would also be of great interest to identify stimuli which control this proposed regulatory complex switch facilitated by TBL1 and TBLR1.

It was observed that TBL1 and TBLR1 expression was downregulated upon aging and diabetes in mice. Underlying causes might be chronic hyperglycemia and dyslipidemia. Thus far, attempts to observe changes in TBL1 or TBLR1 expression in islets upon aging or T2DM in humans remained inconclusive, probably due to human variability and incomplete donor information. Therefore, to investigate whether the findings from this present study are translatable to humans, using islets from donors bearing more information on current treatment or blood lipids would be central. Moreover, increasing sample size would also be beneficial to identify possible changes on TBL1 and TBLR1 expression. Of note, although the insulinoma β-cell lines INS1E and MIN6 did not display phenotypic alterations upon TBL1 and TBLR1 deficiency, they were proven to be suitable for mechanistic investigations. Thus, to investigate whether protein-protein interactions and complex recruitment are also conserved in humans, the human β-cell line EndoC-βH1, which was previously used as β-cell dedifferentiation and drug testing model (Tsonkova et al. 2018; Diedisheim et al. 2018), will be established.

The loss of β-cell identity is generally acknowledged as main contributor to β-cell failure and loss of β-cell mass observed in T2DM. In this study, a link between TBL1/TBLR1 and β-cell identity was established (Figure 68), which highlights TBL1 and TBLR1 as promising novel therapeutical target for β-cell identity and β-cell mass maintenance. Importantly, a recently identified compound was able to specifically disrupt the binding between TBL1 and its interaction partner β-catenin. In the light of TBL1/TBLR1 and their implication in maintenance of β-cell identity, manipulation of protein-protein interactions between TBL1, TBLR1 and specifically negative regulators of β-cell identity such as HDAC3 would therefore represent a promising approach to maintain β-cell identity and thereby prevent or even reverse T2DM.

Ultimately, this present work showed the importance of TBL1 and TBLR1 action in pancreatic β-cells. Further efforts to elucidate the underlying mechanisms on how TBL1 and TBLR1 control β-cell identity are essential to understand the processes upon β-cell dedifferentiation but also to develop novel treatment or prevention approaches in T2DM.

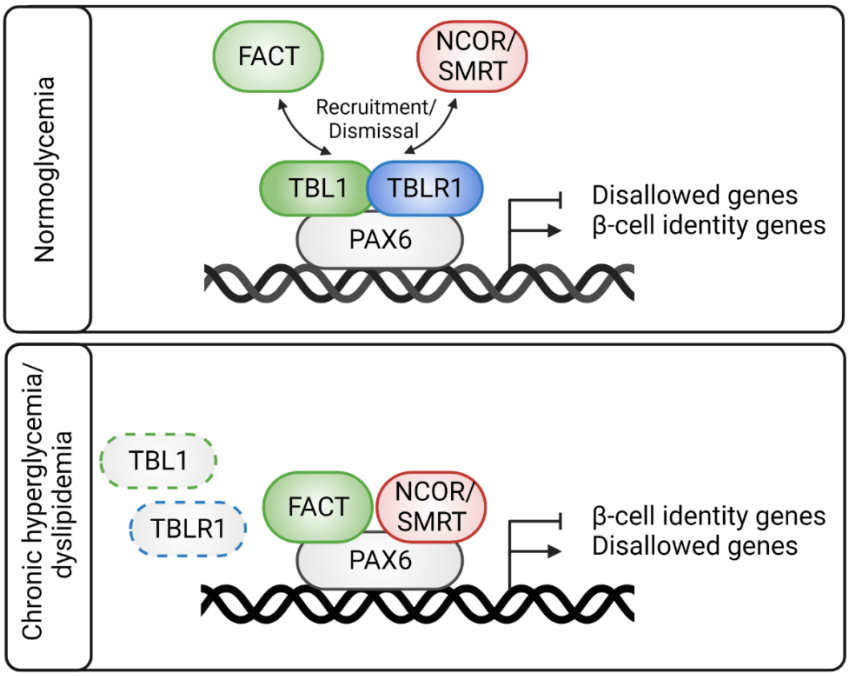

Figure 68: Proposed mechanism through which TBL1 and TBLR1 control β-cell identity in pancreatic β-cells. (Normoglycemia) TBL1 and TBLR1 dynamically, promoter specifically, and signal dependently facilitate recruitment or dismissal of the FACT activator and the NCOR/SMRT repressor complex. Thus, PAX6-mediated expression of β-cell identity genes is induced while disallowed genes are repressed. **(Chronic hyperglycemia/dyslipidemia)** Chronic hyperglycemia and dyslipidemia result in reduced TBL1 and TBLR1 levels. Controlled recruitment of the FACT or NCOR/SMRT complex is not possible anymore resulting in dysregulation of gene expression and loss of β-cell identity. Created with Biorender.com.

4 METHODS

4.1 Animal experiments

Mouse studies were performed using C57BL/6J or C57BL/6N mice. Animals were housed at standard conditions with a 12 h dark-light cycle at 22°C and *ad libitum* access to regular rodent chow diet and water if not stated otherwise. Animal handling and experimentation was performed in accordance with the institutional animal welfare officer and approved by local authorities (Government of Upper Bavaria; ROB-55.2-2532.Vet_02-16-117, ROB-55.2-2532.Vet_02-21-133 and ROB-55.2-2532.Vet_02-18-93).

Tamoxifen treatment
Tamoxifen was prepared in corn oil at 20 mg/ml. A single dose of 200 µg/kg body weight tamoxifen was administered subcutaneously to the mice at the age of 8 weeks.

Body composition
Body composition was determined using echo magnetic resonance imaging (EchoMRI, Echo Medical Systems, Houston).

Bromodeoxyuridine (BrdU) treatment
BrdU is a synthetic nucleoside that incorporates into the DNA of proliferating cells. To investigate the proliferative rate of β-cells *in vivo*, mice were injected intraperitoneally with 100 mg/kg body weight BrdU in 1xPBS. Mice were injected on 3 consecutive days and sacrificed on day 4.

Fasting and refeeding
To determine fasting and refeeding blood glucose and circulating insulin and glucagon levels, mice were fasted for 16 h and refed for 2 h. For fasting, mice were transferred to fresh cages without food but with *ad libitum* access to fresh water. Blood glucose determination and withdrawal was performed by nicking the tail with a razor blade. Blood glucose levels were measured using a glucometer. For the determination of circulating insulin and glucagon levels, blood was collected in Microvette® CB 300 K2E tubes.

Blood plasma
Blood collected in Microvette® CB 300 K2E tubes was incubated at room temperature (RT) for 5 min. After centrifugation at 2000 g, 4°C for 10 min, plasma was collected in fresh tubes, snap frozen in liquid nitrogen, and stored at -80°C.

Intraperitoneal glucose tolerance test (ipGTT)
An ipGTT was performed to determine the clearance of intraperitoneally injected glucose from the blood. Functional insulin secretion from the β-cells and insulin signaling in peripheral tissues results in quick normalization of blood glucose levels. For this, mice were fasted for 6-16 h. After determination of body weight and basal blood glucose levels, mice were i. p. injected with 2 g/kg D-glucose in 0.9% sodium chloride (NaCl). Blood glucose levels were determined 15, 30, 60, and 120 min after injection by nicking the tail with a razor blade.

Oral glucose tolerance test (oGTT)
To determine glucose clearance and insulin secretion in a more physiologic approach, an oGTT was performed. In addition to blood glucose determination, blood was collected at all stated time points to determine circulating insulin levels. Mice were fasted for 16 h. After

determination of body weight and basal blood glucose levels, mice were orally administered with 2-3 g/kg D-glucose in 0.9% NaCl via oral gavage. Blood glucose level determination and withdrawal was performed 10, 15, 30, 60, and 120 min after glucose administration.

Intraperitoneal insulin tolerance test (ipITT)
To exclude possible effects of insulin sensitivity on blood glucose clearance, an ipITT was performed. For this, mice were fasted for 6 h prior to the experiment. After determination of body weight and baseline blood glucose levels, mice were injected i. p. with 0.6-1 U/kg insulin in 0.9% NaCl. Blood glucose levels were determined 15, 30, 45, 60, 90, and 120 min after injection.

Mouse preparation
After cervical dislocation mice were decapitated. Blood glucose levels were determined using a glucometer and the remaining blood was collected in Serum Gel Z/1.1 microtubes. Organs including liver, kidney, spleen, fat pads, and gastrocnemius muscle were collected, weighed, and snap-frozen in liquid nitrogen. Brain and intestines were snap frozen without weighing. Until further usage, organs were stored at -80°C. Pancreas, collected for histological analysis was weighed, placed into histological cassettes, and immediately submerged in 4% formalin. Subsequent immunofluorescence staining and analysis was performed by the core facility Pathology & Tissue Analytics at the Helmholtz Munich.

Blood serum
Serum was obtained by incubation of the collected blood at RT for 5 min and subsequent centrifugation at 10000 g, 4°C for 10 min. Serum was then transferred to a fresh tube, snap frozen in liquid nitrogen, and stored at -80°C until further processing. Albumin, ALT, AST, cholesterol, HDL, ketone body, LDH, LDL, NEFA, and triglyceride serum levels were determined using the Beckman Coulter AU480 Chemistry Analyzer.

Total pancreas hormone content
For determination of total pancreas hormone content, pancreata were dissected and immediately placed in 5 ml ice-cold 0.2 M HCl in 70% ethanol. Pancreata were then homogenized and incubated for 2 days at -20°C by adding 5 ml of 0.2 M acid ethanol daily. Tissue residues were then pelleted by centrifugation for 10 min at 4000 g, 4°C. Supernatant was stored at -80°C until determination of hormone concentration using ELISAs. Total pancreas hormone content was normalized to protein levels.

Pancreatic islet isolation
Mice were sacrificed by cervical dislocation. Then, the hepato-pancreatic duct was closed at the Ampulla of Vater using a thread which was clamped and pulled gently in order to expose and stretch the pancreatic duct. 3 ml of ice-cold Collagenase P solution, prepared by dissolving 6 U Collagenase P in 3 ml HBSS containing 1% BSA, were injected into the pancreatic duct. Inflated pancreas was then dissected and placed in a 15 ml tube containing Collagenase P on ice. Pancreatic tissue was digested at 37°C for 14 min. The reaction was stopped by adding 8 ml ice-cold HBSS containing 1% BSA. Islets were washed 3 times with 8 ml HBSS containing 1% BSA and were then hand-picked 4 times prior to cultivation in murine islet medium.

4.2 Cell biology

All cell cultural procedures were performed under sterile conditions. Cells were cultured at 37°C, 5% CO_2 and 95% air atmosphere. Prior to use, all media and additives were warmed to

37°C. Chapter *5.1 Cell culture medium* summarizes a list of media used for cell cultural experiments.

Thawing cells
Eukaryotic cells in freezing medium were stored in liquid nitrogen. After thawing the cells in a water bath at 37°C, cells were seeded in 15 cm tissue culture dishes containing 20 ml culture medium. 24 h after seeding, media was changed to remove the remaining DMSO**.**

Cultivation of INS1E and MIN6 β-cell lines
Eukaryotic cell lines were cultivated on 15 cm dishes containing 20 ml culture medium. Passaging of the cells was performed twice per week. For this, medium was aspirated and the cells were washed once with 1xPBS. Then, cells were trypsinized for 3-5 min at 37°C. Trypsinization was stopped by addition of 8 ml culture medium. After collecting cells in a fresh 15 ml tube, cells were pelleted by centrifugation for 2 min at 1000 g, RT. Supernatant was aspirated and the cell pellet was subsequently resuspended in 6 ml culture medium. Cell number was determined using the CellCountess and $3x10^6$ INS1E or $6x10^6$ MIN6 cells were plated onto a fresh 15 cm tissue culture dish containing 20 ml fresh culture medium.

Cryopreservation of cell lines
Long-term preservation of cell lines was achieved by storage in liquid nitrogen. For this, cells were washed once with 1xPBS, and trypsinized for 3-5 min at 37°C. After centrifugation for 2 min at 1000 g, RT, $3x10^6$ INS1E cells and $6x10^6$ MIN6 cells were resuspended in 1 ml freezing medium. The cells were frozen at -80°C with a cooling rate of -1°C/min by placing the cell aliquots into a Mr. Frosty™ Freezing Container. Cells were then transferred to liquid nitrogen tanks for long-term storage.

Small interfering RNA (siRNA) transfection
INS1E cells were seeded on 24-well plates with a density of $1x10^5$ cells. After attachment, cells were transfected with 6-25 nM siRNA using 1.5 µl Lipofectamine RNAiMAX Transfection Reagent. For this, siRNA and RNAiMAX Transfection Reagent were diluted separately in 50 µl OptiMEM – Reduced Serum Medium, respectively. Subsequently, dilutions were mixed and incubated at RT for 15 min. 100 µl of the transfection mix were then added dropwise per well to the cells. Cells were harvested 5 days after transfection.

Short hairpin RNA (shRNA) transduction
MIN6 cells were seeded on 24-well plates with a density of $2x10^5$ cells. On the next day, medium was changed to media containing 1 µl crude lysate of the adenovirus carrying the respective shRNA per well. Cells were harvested 48 h after transduction.

Plasmid DNA transfection
INS1E cells were seeded on 24-well plates with a density of $2x10^5$ cells. On the next day, cells were transfected for 48 h with 0.5-2 µg plasmid DNA using 2 µl Lipofectamine 2000 Transfection Reagent. Transfection mix was prepared as described for the siRNA transfection.

Luciferase Assay
The construct containing the luciferase reporter gene under the human insulin gene (pGL410_INS421) and the murine insulin 2 gene (pGL410_Ins2500) were a gift from Kevin Ferreri and were purchased from Addgene (human insulin gene: RRID:Addgene_49057; murine insulin 2 gene: RRID:Addgene_49058) (Kuroda et al. 2009).

$2.5x10^4$ INS1E cells were seeded into 96-well culture plates. 48 h after siRNA transfection, INS1E cells were transfected with vectors for the Luciferase assay as described for plasmid DNA transfection for 48 h.

The Luciferase assay was performed using the Promega Dual-Luciferase Reporter Assay System. For this, cells were lysed using 25 µl of the 1xPassive Lysis Buffer for 15 min on a plate shaker at 800 rpm, RT. Then, 20 µl cell lysate were transferred to a white 96-well assay plate. LARII and Stop&Glo solutions were prepared as described in the manufacturer's manual.

The Varioscan LUX Multimode Microplate Reader was primed using the respective solutions. The assay program comprised of addition of 100 µl LARII reagent, followed by shaking at 240 rpm for 5 s, and a Firefly Luciferase activity measurement for 8 s. Then, 100 µl Stop&Glo solution was added followed by shaking at 240 rpm for 5 s and Renilla Luciferase activity measurement for 8 s. For analysis, Firefly Luciferase activity values were normalized to Renilla Luciferase activity.

Insulin secretion assay

INS1E cells were grown on 24-well plates to a 90% confluency. Tanaka-Robertson Krebs Ringer Buffer (KRB) was supplemented with 0.1% BSA and prewarmed to 37°C. Cells were washed twice with the KRB then glucose-starved with 500 µl KRB at 37°C for 1 h. The buffer was aspired and insulin secretion was stimulated at 37°C for 1 h using 500 µl of glucose or glucose in combination with potassium chloride (KCl) to stimulate the maximal insulin secretion. 200 µl of the supernatant were collected and centrifuged at 1000 g, 4°C, for 5 min. Then 100 µl were transferred to fresh tubes and the samples were stored at -80°C. The remaining supernatant on the cells was aspired and the cells were lysed in 200 µl acid ethanol (1.5% HCl in 70% ethanol). Lysis was supported by freezing at -80°C for 1 h. Cells were collected in fresh tubes by scraping and pipetting up and down. To pellet the cell debris, samples were centrifuged at 5000 g, 4°C for 5 min. 100 µl were transferred to fresh tubes and the samples were stored at -80°C until further usage.

4.3 Molecular biology

RNA isolation

A) From INS1E and MIN6 cells

Cells were harvested in 500 µl Trizol and transferred to fresh RNase free tubes. Then, 150 µl chloroform was added to the lysates. The mixtures were shaken vigorously for 2 min and incubated for 2 min at RT prior to centrifugation for 20 min at 12000 g, 4°C. The upper aqueous phase containing the RNA was transferred to fresh RNase free tubes. For RNA precipitation, 250 µl isopropanol was added. The mixture was inverted, incubated at RT for 10 min, and centrifuged for 20 min at 12000 g, 4°C. The supernatant was discarded and the pellet was washed three times using 1 ml ice cold 75% ethanol and centrifugation at 7500 g, 4°C for 5 min. After the last wash, the supernatant was aspired and the pellet was vacuum-dried for 10 min. The pellet was then air dried for 30 min at RT and dissolved in 20 µl RNase free water followed by incubation for 10 min at 55°C. Samples were stored at -80°C.

B) From pancreatic islets

Isolated pancreatic islets were transferred to fresh RNase free tubes and subsequently lysed in 500 µl Trizol. Lysis was supported by thorough vortexing for 10 sec and freezing at -80°C

for a least 1 h. After the samples thawed, 150 µl chloroform was added. The mixtures were shaken vigorously for 30 sec and incubated on ice for 5 min. Samples were then centrifuged for 20 min at 12000 g. RNA was further isolated and purified using the RNeasy Plus Kit from Qiagen following the manufacturer's instructions.

C) From tissue

Tissue samples were transferred to pre-cooled fresh 2 ml RNase free tubes containing a stainless steel bead. Then 1 ml Trizol was added and the samples were lysed using the TissueLyzer for 2 min at 30 Hz. Lysates were then transferred to fresh RNAse free tubes before adding 200 µl chloroform. Further isolation and purification steps were performed as described for RNA isolation from INS1E and MIN6 cells.

Determination of RNA concentration

RNA concentration was determined at 260 nm using the NanoDrop 2000 spectrophotometer. Quality and purity of the RNA was assessed based on the ratio of the absorbance at 260 nm and 230 nm. Samples with a 260/230 ratio of 2.0-2.2 were regarded as "pure".

Complementary DNA (cDNA) synthesis

For the generation of cDNA, 100-1000 ng RNA were used. cDNA synthesis was carried out using the High-Capacity cDNA Reverse Transcription Kit from Applied Biosystems following the manufacturer's instructions. Briefly, respective amount of RNA was brought to a final volume of 14.2 µl using RNase free water. Then, 5.8 µl of the prepared master mix containing 2 µl RT Buffer, 2 µl Random Primers, 0.8 µl dNTPs, and 1 µl Reverse Transcriptase was added per sample. Water was used as negative control and samples containing no reverse transcriptase were used as control for genomic DNA contamination. cDNA samples were diluted to a final concentration of 5 ng/µl with RNase free water and stored at -20°C until further usage.

Real-time quantitative polymerase chain reaction (qPCR)

The real-time qPCR was performed in MicroAmp® 384-well reaction plates. For gene expression analysis, reaction mix was added per well comprising of 5-15 ng of cDNA obtained from reverse transcription, 3.5 µl Takyon™ Low Rox Probe MasterMix dTTP blue, 0.2 µl TaqMan probe, and RNase free water depending on the cDNA volume, resulting in a final volume of 7 µl. Samples were assayed in technical duplicates. After loading, the plate was sealed with a MicroAmp® Optical Adhesive Film. The plate was spun and the quantitative PCR was performed using the Applied Biosystems QuantStudio™ 6 or 7 Flex Real-Time PCR System. RNA data was quantified according to the ΔCt method and normalized to levels of a housekeeper.

RNA sequencing

To investigate the RNA expression across the transcriptome RNA sequencing was performed. For this, pancreatic islets were isolated, lysed in 500 µl Trizol, and stored at -80°C until further usage. RNA isolation was performed as described above. Sample processing and sequencing procedures were performed by Novogene (UK) Company Limited. First, RNA was quantified and underwent a quality control: RNA degradation and contamination was monitored on a 1% agarose gel. RNA purity was assessed using a NanoPhotometer® spectrophotometer. RNA integrity and quantitation was determined using the RNA Nano 6000 Assay Kit of the Bioanalyzer system from Agilent. Then the RNA library was prepared. For this, 1 µg RNA per sample was used. The sequencing library was generated using NEBNext® Ultra™ RNA

Library Prep Kit for Illumina® following the manufacturer's recommendations. Briefly, mRNA was purified with poly-T oligo-attached magnetic beads and subsequently fragmented. Then, cDNA was synthesized using random hexamer primers. Afterwards, second strand cDNA synthesis was performed using DNA Polymerase I and RNase H followed by end repair, poly-A-tailing, adaptor addition, size selection, and PCR enrichment. Sequencing was performed using the NovaSeq6000 (Illumina). Shared functions among differentially expressed genes were identified using Gene Ontology (GO) for biological processes and Kyoto Encyclopedia of Genes and Genomes (KEGG) for pathways. Additionally, data was analyzed using the Ingenuity Pathway Analysis software (IPA) from Qiagen or Gene Set Enrichment Analysis (GSEA).

Single cell RNA sequencing (scRNA-Seq)

With the scRNA-Seq transcriptomic sequencing of single cells is achieved, which allows to distinguish between the different cell populations within a pancreatic islet. For this, pancreatic islets were isolated and cultured overnight in islet culture medium. Cell dissociation and library preparation was performed by the core facility Single Cell Genomics at the Helmholtz Munich. After dissociation of the islets into single cells, viability was determined. Library preparation was performed using the Chromium Next GEM Single Cell 3' Reagent Kit from 10x Genomics. First, a Gel Bead-in-emulsion (GEM) was generated comprising of a single cell and a 10x Barcoded gel bead. The 10x gel beads contain barcoded primers which allow to generate uniquely barcoded cDNA to associate reads back to the individual GEM. After GEM generation, the gel bead is dissolved, resulting in release of the barcoded primers and lysis of the co-partitioned cell. Full length cDNA is subsequently synthesized inside the GEM which contains the cell lysate, a Master Mix containing reverse transcriptase reagents, and the released primers. Barcoded cDNA is then amplified via PCR and enzymatically fragmented. Sequencing was performed by the core facility Genomics at the Helmholtz Munich using the NovaSeq 6000 (Illumina). Bioinformatic analysis was performed by Peter Weber. Data analysis was performed using IPA and Enrichr.

Genotyping

Genotyping of mouse lines by PCR was performed using DNA isolated from ear clips. DNA was isolated by boiling tissue samples in 50 µl 50 mM NaOH at 95°C, 550 rpm for 20 min. Lysates were then neutralized with 400 µl 12.5 mM Tris-HCl and stored at -20°C until further usage. Specific primers for DNA amplification were diluted 1:40 in RNase free water. DNA was amplified by PCR using 1.5 µl DNA, 10 µl DreamTaq PCR Master Mix (2x), 6.5 µl RNase free water, and 2 µl primer mix. Primer sequences and the respective amplification programs are listed in *5.7 Oligonucleotides*. Genotyping of the floxed locus was performed by separation of the DNA fragments on a 2% agarose gel in TAE buffer containing 1:10000 SYBR Safe. For this, amplified DNA samples were mixed with 6x purple loading dye and separated for 30 min at 80 V. DNA bands was visualized using the Bio-Rad Gel Doc XR Imaging System.

Genotyping of the Cre locus was performed using the QIAxcel Advanced System (Qiagen) according to the manufacturer's recommendations.

Transformation of E. coli

25 µl of an E. coli cell suspension was thawed on ice and mixed with 10 ng plasmid DNA. After an incubation on ice for 20 min, the cells were heat shocked at 42°C for 30 sec. Cells were then immediately placed on ice for 2 min followed by addition of 200 µl SOC medium and an

incubation at 37°C, 300 rpm for 2 h. Subsequently, cells were plated onto a LB agar plate containing the specific antibiotic for selection.

Bacterial liquid cultures
LB medium was supplemented with the appropriate antibiotic. Then 6 ml of the LB medium were inoculated with a single colony and incubated under vigorous shaking at 37°C for 6 h. The complete volume was then transferred to 250 ml LB medium and incubated at 37°C overnight under vigorous shaking.

Isolation of plasmid DNA from E. coli
Plasmid DNA was isolated using the Qiagen Plasmid Maxi Kit according to the manufacturer's instructions. Plasmid concentration was determined using the NanoDrop 2000 spectrophotometer. Isolated plasmid DNA was aliquoted and stored at -20°C.

4.4 Biochemistry

Protein isolation
A) From INS1E and MIN6 cells
INS1E and MIN6 cells were grown on 12-well plates. Cells were washed once with 1xPBS, harvested in 200 µl radioimmunoprecipitation assay (RIPA) buffer containing a protease inhibitor, and transferred to 1.5 ml tubes. Samples were then vortexed thoroughly and incubated for 15 min on ice. Cell debris was pelleted for 10 min at 13000 g, 4°C and 150 µl supernatant was then transferred to fresh 1.5 ml tubes. Samples were diluted in 6x SDS sample buffer prior to boiling for 10 min at 95°C. Samples were stored at -20°C.

B) From pancreatic islets
Isolated pancreatic islets were transferred to 1.5 ml tubes. 75 islets were lysed in 25 µl RIPA buffer containing a protease and phosphatase inhibitor by sonication in an ice-cold water bath for 5 min. Cell debris was pelleted for 10 min at 13000 g, 4°C and the supernatant was transferred to fresh 1.5 ml tubes. Samples were diluted in 6x SDS sample buffer prior to boiling for 10 min at 95°C. Samples were stored at -20°C.

Determination of protein concentration
A) Determination of protein concentration in cell lysates
The protein concentration in cell lysates was determined using the Pierce™ BCA Protein Assay Kit according to the manufacturer's instructions. In brief, 20 µl of the albumin standards (0-2000 µg/µl) along with 20 µl of the protein lysate dilutions were pipetted on a 96-well assay plate in triplicates. The reaction mix was prepared by diluting BCA Reagent B 1:50 in BCA Reagent A. Then, 200 µl of the reaction mix was added to the samples. After 30 min incubation at 37°C, absorption was measured at 562 nm using the Varioscan LUX Microplate Reader.

B) Determination of protein concentration in pancreas lysates
Protein concentration in total pancreas lysates was determined using the Bradford assay. The Bradford assay reagent was prepared by dissolving 10 mg Coomassie Brilliant Blue G-250 dye in 5 ml 95% ethanol absolute. Subsequently, 10 ml of 85% phosphoric acid was added. The solution was diluted using 85 ml pure and sterile water and subsequently sterile filtered. Protein concentration was determined by loading 10 µl of the albumin standards (0-2000 µg/µl) along with 10 µl of the sample dilutions onto a 96-well assay plate in triplicates. Then 200 µl of the Bradford reagent was added. The plate was mixed for 10 seconds using a microplate shaker, then incubated for 10 min at RT. Absorption was measured at 595 nm.

SDS polyacrylamide gel electrophoresis (SDS-PAGE) and immunoblotting

20-40 µg protein were loaded onto Novex™ Tris-Glycine Mini Gels and separated at 90 V for 90 min. Proteins were then blotted onto nitrocellulose membranes using the Trans Blot Turbo® system using the following settings: 12 V, 2.5 A, for 16 min. The membrane was then blocked in 5% skimmed milk or 5% BSA in TBS-T at RT on a vertical plate shaker for 1 h. Subsequently, the membrane was incubated in the primary antibody diluted in milk or BSA at 4°C on a vertical plate shaker overnight. On the next day, the primary antibody was discarded and the membrane was washed with TBS-T. Then, the membrane was incubated with the secondary antibody conjugated with horse radish peroxidase (HRP) diluted in milk or BSA for 1 h at RT. After washing the membrane in TBS-T, bands were detected using the enhanced chemiluminescence system (ECL) Western Blotting Detection Reagent. Signal generation, enhancement, and detection was performed using the ChemiDoc Imaging System from Bio-Rad.

Endogenous immunoprecipitation (IP)

Cells were washed once with ice-cold 1xPBS and subsequently lysed in IP-buffer containing a protease and phosphatase inhibitor. After thorough vortexing and incubation on ice for 15 min, cell debris was pelleted by centrifugation at 13000 g, 4°C for 10 min. In the meantime, 40 µl Protein G Magnetic Beads per IP were washed three times with PBS-T (PBS+0.1% Tween 20) and resuspended in RNase free water. The protein lysates were then precleared for 30 min at 4°C using Protein G Magnetic Beads. The precleared protein lysate was then distributed into fresh tubes and incubated with 4 µl of the respective antibody on a rotating wheel at 4°C, overnight. The next day, 40 µl of the washed Protein G Magnetic Beads were added per IP and incubated for 2h at 4°C on a rotating wheel. Beads were then washed four times with IP-buffer and twice with IP-buffer without NP-40. Proteins were eluted by adding 25 µl 2x SDS sample buffer prior to boiling at 95°C for 10 min.

Chromatin-IP (ChIP) qPCR

A) Fixation

MIN6 cells were grown to 80% confluence on 15 cm dishes. The cells were washed once with 1xPBS and subsequently fixed with 1% methanol-free formaldehyde in 1xPBS for 10 min at RT on a vertical plate shaker. Then, 1.5 ml 1 M glycine was added to quench the formaldehyde for 5 min at RT on a vertical plate shaker.

B) Cell lysis and chromatin shearing

The fixation solution was aspired, the cells were rinsed once with 1xPBS, and collected in 1 ml 1xPBS using a cell scraper. Cell suspension was then transferred into a 2 ml tube and the cells were pelleted by centrifugation at 12000 rpm, 4°C for 1 min. After removal of the supernatant, cells were lysed in 1 ml Fast IP Buffer containing a protease inhibitor, by pipetting up and down. After running the samples through a 24G syringe the samples were incubated on ice for 10 min. The lysates were centrifuged at 12000 rpm, 4°C for 1 min and the procedure was repeated. After the second lysis, the supernatant was removed and 1 ml Shearing Buffer containing a protease inhibitor was added to the nuclei pellet by pipetting up and down. The nuclei suspensions were then transferred to 1.5 ml TPX Biotuptor Plus microtubes. Shearing was performed in a BioRuptor (Diagenode) using 22 cycles, 30 s on/30 s off, high mode.

C) Reverse-crosslinking

50 µl of the sheared chromatin were taken aside for reverse-crosslinking overnight to assess fragment size, while the remaining chromatin was left at 4°C on ice overnight. For the reverse-

crosslinking, 2 µl of 5 M NaCl were added to the 50 µl chromatin. The mix was incubated at 65°C, 300 rpm overnight. The next day, 2 µl RNAse A (10 µg/µl) was added and the mixture was incubated at 37°C for 30 min. Then, the Proteinase K solution was added comprising of 2 µl Proteinase K (10 µg/µl), 8 µl 1 M Tris (pH 7.5), and 4 µl 0.5 M EDTA (pH 8). After incubation at 56°C for 1 h, the DNA was purified using the MinElute PCR Purification Kit from Qiagen according to the manufacturer's recommendations. DNA was eluted in 12 µl Elution Buffer provided from the kit. 10 µl of the purified DNA were the loaded on a 1.7% agarose gel in TAE buffer containing 1:10000 SYBR Safe to visualize the fragmentation. Shearing cycles were added as needed.

D) Immunoprecipitation and preparation of the beads

The sheared chromatin was cleared by centrifugation at 12000 rpm, 4°C for 10 min. 60 µl of the cleared chromatin were set aside and frozen at -20°C (= Input DNA). 100 µl of the chromatin were distributed to 1.5 ml DNA LoBind tubes containing 900 µl Dilution Buffer. For each IP, 3 µg antibody were added prior to placing the tubes on a rotating wheel at 4°C overnight.

20 µl Protein A/G Sepharose beads were used per pulldown. For this, the beads were washed twice with 1 ml 1xPBS and once with 1 ml 0.5% BSA in 1xPBS by centrifugation at 1000 rpm, 4°C for 1 min. Then, the beads were blocked using 1 ml 0.5% BSA in 1xPBS overnight at 4°C on a rotating wheel.

The next day, the IPs were cleared by centrifugation at 12000 rpm, 4°C for 10 min, while the beads were washed once with 1 ml Dilution Buffer. Then, 20 µl of beads were distributed to fresh DNA LoBind tubes and 900 µl of the precleared IPs were added. IPs and beads were incubated for 2 h at 4°C on a rotating wheel.

E) Washes and elution

The beads were spun down by centrifugation at 1000 rpm and 4°C for 1min. The supernatant was aspirated and the beads were washed five times with 1 ml Fast IP Buffer. The beads were then washed once with 1xTris-EDTA buffer. Supernatant was removed and the beads were eluted in 50 µl Bead Elution Buffer by vortexing and subsequent incubation on a thermocycler at RT, 1000 rpm for 15 min. After centrifugation at RT, 3000 rpm for 1 min, the supernatant was collected. Then the elution step was repeated and the supernatants were combined yielding in 100 µl eluate.

F) Reverse cross-linking and DNA purification

The input was thawed and 40 µl 1xTris-EDTA buffer were added. 4 µl 5 M NaCl were added to the input and the eluates which were then incubated at 65°C and 300 rpm, overnight. The next day, 1 µl RNAse A (10µg/µl) was added and the samples were incubated at 37°C for 30 min. Then, 7 µl Proteinase K solution consisting of 1 µl Proteinase K (10 µg/µl), 4 µl 1 M Tris-HCl (pH 7.5), and 2 µl 0.5 M EDTA (pH 8) were added. The mixture was incubated at 45°C for 2 h. The DNA was purified using the MinElute PCR Purification Kit from Qiagen according to the manufacturer's recommendations. DNA was eluted in 25 µl Elution Buffer provided from the kit.

G) qPCR

Purified input and ChIP'ed DNA were diluted 1:8 in RNase free water. qPCR was performed in MicroAmp® 384-well reaction plates. Per reaction, 5 µl sample, 4.8 µl Takyon™ Low ROX

SYBR® MasterMix dTTP Blue, and 0.2 µl primer mix were used. Primers are listed in *5.7 Oligonucleotides*. Samples were assays in technical triplicates. After loading, the plate was sealed with a MicroAmp® Optical Adhesive Film. The plate was spun and the quantitative PCR was performed using the Applied Biosystems QuantStudio™ 6 or 7 Flex Real-Time PCR System. Data was normalized to the IgG pulldown and a negative locus.

Insulin enzyme-linked immunosorbent assays (ELISA)

A) Mouse plasma

To determine circulating insulin levels in the plasma, the Ultra Sensitive Mouse Insulin ELISA Kit from Crystal Chem was used according to the manufacturer's instructions. 5 µl of the standards as duplicates and 5 µl undiluted plasma were assayed.

B) Insulin secretion assay and total pancreas insulin content

Insulin levels were determined using the Mouse Insulin ELISA kit from ALPCO according to the manufacturer's instructions. For this, 10 µl of the standards as duplicates and 10 µl of the sample were pipetted per well. Dilutions were prepared in Robertson-Tanaka KRB supplemented with 0.1% BSA.

Glucagon ELISA

Circulating plasma glucagon levels and total pancreas glucagon levels were determined using the Glucagon ELISA Kit from Mercodia according to the manufacturer's instructions. 10 µl of the standards in duplicates and 10 µl sample were added per well. Plasma samples were used undiluted while total pancreas lysates were diluted using the assay diluent provided in the kit.

Somatostatin ELISA

Total pancreas somatostatin content was determined using the Elabscience Somatostatin ELISA kit. Samples were diluted 1:7 with the diluent provided in the kit. 50 µl of the standards as duplicates and 50 µl of the diluted sample were assayed according to the manufacturer's instructions.

4.5 Human studies

Human pancreatic islets were obtained from The Alberta Diabetes Institute IsletCore, Edmonton, Canada (https://www.isletcore.ca), either as fresh islets immediately after isolation or as cryopreserved samples. Cryopreserved islets were thawed as described in Lyon et al. (Lyon et al. 2018). In short, islets were thawed in a water bath at 37°C followed by centrifugation at 1000 rpm, 4°C for 1 min. Supernatant was aspired and DMSO was removed with a sucrose gradient. Finally, islets were centrifuged, supernatant was aspired, and islets were resuspended in human islet culture medium.

4.6 Statistical analysis

Results are presented as mean ± standard error of the mean (SEM). All statistical analyses were performed using GraphPad Prism 9.4. Two conditions were compared using the unpaired t-test. Multiple comparisons were performed using two-way analysis of variances (ANOVA) with a Šídák, Tukey, or a Dunnett multiple comparisons test, respectively. Multiple measurements were compared using a two-way ANOVA with repeated measures and a Šídák's multiple comparison *post hoc* test. Correlation was determined using Pearson correlation coefficient. $p < 0.05$ was considered as statistically significant. *$p < 0.05$, **$p < 0.01$, ***$p < 0.001$, ****$p < 0.0001$.

5 MATERIAL

5.1 Cell culture medium

Medium	Component	Concentration
Freezing medium	RPMI + GlutaMAX	
	Foetal bovine serum (FBS)	30%
	Penicillin/streptomycin	1%
	Sodium pyruvate	1 mM
	HEPES (4-(2-hydroxyethyl)-1-piperazineethanesulfonic acid)	10 mM
	β-mercaptoethanol	50 µM
	DMSO (Dimethyl sulfoxide)	10%
Human islet culture medium	RPMI + GlutaMAX	
	Fetal bovine serum	10%
	Penicillin/streptomycin	1%
INS1E medium	RPMI + GlutaMAX	
	FBS	10%
	Penicillin/streptomycin	1%
	Sodium pyruvate	1 mM
	HEPES (4-(2-hydroxyethyl)-1-piperazineethanesulfonic acid)	10 mM
	β-mercaptoethanol	50 µM
MIN6 medium	DMEM + 4.5 g/l D-Glucose + L-Glutamine	
	FBS	20%
	Penicillin/streptomycin	1%
	Sodium pyruvate	1 mM
	β-mercaptoethanol	50 µM
Murine islet culture medium	RPMI + GlutaMAX	
	FBS	10%
	Penicillin/streptomycin	1%

5.2 Buffers

All buffers were prepared in MilliQ water. Dilution, Fast IP, Robertson Tanaka Krebs Ringer, and Shearing Buffer were sterile filtered after preparation. Dilution, Fast IP, and RIPA Buffer were stored at 4°C. IP-Buffer and the Bead Elution Buffer were always prepared freshly.

Buffer	Components	Concentration
Dilution Buffer	SDS (Sodium dodecyl sulfate)	0.01%
	Triton X 100	2.2%
	EDTA (Ethylenediaminetetraacetic acid) (pH 8)	1.2 mM
	Tris-HCl (pH 8)	16.7 mM
	NaCl	167 mM
Bead Elution Buffer	$NaHCO_3$	100 mM
	SDS	1%
Fast IP Buffer	NaCl	167.5 mM
	EDTA (Ethylenediaminetetraacetic acid) (pH 7.5)	5 mM
	Tris-HCl (pH 7.5)	50 mM
	NP-40	0.5%
	Triton X 100	1%

IP-Buffer	Tris HCl (pH 6.8)	50 mM
	NP-40	1%
	NaCl	150 mM
	EDTA (Ethylenediaminetetraacetic acid) (pH 8)	1 mM
	Na_3VO_4	2 mM
	NaF	1 mM
	DTT (Dithiothreitol)	1 mM
RIPA Buffer	Tris HCl	50 mM
	NaCl	150 mM
	Triton X 100	1%
	SDS (Sodium dodecyl sulfate)	0.1%
	Sodiumdeoxycholate	0.5%
Robertson Tanaka Krebs Ringer Buffer (KRB)	NaCl	118.5 mM
	$NaHCO_3$	25 mM
	HEPES(4-(2-hydroxyethyl)-1-piperazineethanesulfonic acid)	10 mM
	KCl	4.74 mM
	$CaCl_2$	2.54 mM
	KH_2PO_4	1.19 mM
	$MgSO_4$	1.19 mM
SDS running buffer (10x)	Tris	0.25 M
	Glycine	1.92 M
	SDS	1%
Shearing Buffer	SDS	
	EDTA (pH 8)	
	Tris HCl (pH 8)	
TAE (50x) (pH 8.5)	EDTA	50 mM
	Tris	2 M
	Acetic acid	1 M
TBS (10x) (pH 7.6)	NaCl	1.5 M
	Tris Base	0.25 M
TBS-T	TBS buffer (1X)	
	Tween-20	0.1%

5.3 Antibodies

Primary Antibody	Final dilution	Isotype	Distributor, #
Flag	1:1000	rabbit	Cell signaling, #2368
PAX6	1:1000	rabbit	Cell signaling, #60433
TBL1	1:1000	rabbit	Abcam, #ab24548
TBLR1	1:1000	mouse	Santa Cruz, sc-517365
Vinculin	1:10000	rabbit	Abcam, #ab129002

Secondary Antibody	Final dilution	Isotype	Distributor, #
Anti-mouse IgG-HRP	1:5000	goat	Bio Rad, #1721011
Anti-rabbit IgG-HRP	1:5000	goat	Bio Rad, #1706515
Peroxidase-conjugated IgG Fraction Monoclonal Mouse Anti-Rabbit IgG, Light Chain	1:10000	mouse	Rockland, #211-032-171

Antibody for IP	Isotype	Distributor, #
Flag	rabbit	Cell signaling, #2368
Histone H3 (acetyl K27)	rabbit	Abcam, #4729
HDAC3	rabbit	Abcam, #ab32369
Normal rabbit IgG	rabbit	Cell signaling, #2729
PAX6	rabbit	Merck, #AB2237
Rabbit mAb IgG Isotype control	rabbit	Cell signaling, #5415
SUPT16H	rabbit	Proteintech, #20551-1-AP
TBL1	rabbit	Abcam, #ab24548
TBLR1	rabbit	Novus Biologicals, #NB600-270

5.4 TaqMan probes

Probes were purchased from Applied Biosystems.

Taqman Probe	Assay ID	TaqMan probe	Assay ID
Arx	Mm00545903_m1	*Pck1*	Mm01247058_m1
β-Actin	Rn00667869_m1	*Pdk4*	Mm01166879_m1
ChgA	Mm00514341_m1	*Pdx1*	Mm00435565_m1
Cre recombinase	Mm00635245_cn	*Pgc1a*	Mm01208835_m1
Fasn	Mm00662319_m1	*TBP*	Hs00427620_m1
Hk1	Mm00439344_m1	*Tbp*	Mm01277042_m1
Ins1	Mm01259683_g1	*TBL1*	Hs00959540_m1
Ins2	Mm00731595_gH	*Tbl1*	Mm1222202_m1
Ldha	Mm01612132_g1	*Tbl1*	Rn01222199_m1
Lep	Mm00434759_m1	*TBLR1*	Hs00226564_m1
MafA	Mm00845206_s1	*Tblr1*	Mm01283877_m1
MafB	Mm00627481_s1	*Tblr1*	Rn01283875_m1
NeuroD1	Mm01946604_s1	*Ucn3*	Mm00453206_s1
Ngn3	Mm00437606_s1	*Scd1*	Mm00772290_m1
Nkx6.1	Mm00454961_m1	*Slc2a2*	Mm00446229_m1
Pax6	Mm00443081_m1	*Slc2a4*	Mm00446229_m1

5.5 siRNA

siRNAs were purchased from Dharmacon™. Upon arrival, siRNAs were resuspended to a concentration of 20-100 µM in RNAse free water and incubated for 30 min on a rotator at RT. Afterwards, siRNA was aliquoted and stored at -20°C.

siRNA	Catalog ID
Non-targeting Control Pool	D-001810-10-05
Tbl1	J-096212-09-0005
Tblr1	J-088126-11-0010

5.6 shRNA

Adenoviruses carrying shRNA against TBL1, TBLR1, or a scrambled control sequence were kindly provided by Dr. Maria Rohm (Rohm et al. 2013). Crude lysates were prepared by

infecting HEK-293A cells with the respective adenovirus. Cells were subsequently harvested in 1xPBS. Lysate was generated by three cycles of freezing and thawing.

shRNA	5' → 3'
Scrambled control sequence	GATCTGATCGACACTGTAATG
Tbl1	GCGAGGATATGGAACCTTAAT
Tblr1	GGATGTCACGTCTCTAGATT

5.7 Oligonucleotides

All oligonucleotides were purchased from Sigma-Aldrich. For genotyping, primers were diluted 1:40 in RNase free water. Amplification for Cre was performed using the following protocol: 5 min at 95°C, 35 cycles of 30 s at 95°C, 30 s at 60°C, and 1 min at 72°C, followed by 10 min at 72°C. For TBL1 and TBLR1 amplification, samples were heated for 1 min at 94°C, 30 cycles of 1 min at 94°C, 1 min at 55°C, and 2 min at 68°C, followed by 10 min at 72°C.

Oligonucleotide	5' → 3'
Cre_fw	ATGTTTAGCTGGCCCAAATGT
Cre_rv	ACGAGTGATGAGGTTCGCA
Tbl1_fw	GAACCTGATGGACATGTTCAGG
Tbl1_rv	AGTGCGTTCGAACGCTAGAGCCTGT
Tblr1_fw	TTACGTCCATCGTGGACAGC
Tblr1_rv	TGGGCTGGGTGTTAGCCTTA

ChIP primers were diluted 1:10 in RNase free water.

Oligonucleotide	Species	5' → 3'
Foxl2_fw	mouse	GCTGGCAGAATAGCATCCG
Foxl2_rv	mouse	TGATGAAGCACTCGTTGAGGC
Ins1_fw	mouse	CTGGGGAATGATGTGGAAAAT
Ins1_rv	mouse	GACCAGATGGCCTGATGAAC

5.8 Kits

Kit System	Distributor
Dual-Luciferase Reporter Assay System	Promega, Wisconsin
Glucagon ELISA, 10 µl	Mercodia, Uppsala
High-Capacity cDNA Reverse Transcription Kit	Applied Biosystems, Darmstadt
Maxi Prep Kit	Qiagen, Hilden
MinElute PCR Purification Kit	Qiagen, Hilden
Mouse Insulin ELISA	ALPCO, Salem, USA
Pierce™ BCA Protein Assay Kit	Thermo Scientific, Rockfort, USA
RNeasy Plus Mini Kit	Qiagen, Hilden
Somatostatin ELISA	Elabscience, Texas
Ultra Sensitive Mouse Insulin ELISA Kit	Crystal Chem, Zaandam

5.9 Software

Software	Distributor
BioRender	BioRender, Toronto
Citavi	QSR International, Doncaster, Australia
Gene set enrichment analysis (GSEA)	UC San Diego and Broad Institute, USA
GraphPad Prism	GraphPad Software Inc., La Jolla, USA
ImageJ	University of Wisconcin, USA
Image Lab Software	Bio-Rad, Munich
Ingenuity Pathway Analysis	Qiagen, Hilden
Microsoft Office	Microsoft, Unterschleißheim
QuantStudio Real-Time PCR Software	Applied Biosystems, Darmstadt

5.10 Chemicals and reagents

All unlisted chemicals and reagents were purchased from Roth, Karlsruhe

Chemical	Distributor
Agarose	Sigma, Munich
Ampicillin sodium salt	Sigma, Munich
Bovine Serum Albumin	Sigma, Munich
β-mercaptoethanol	Sigma, Munich
Bromodeoxyuridine	Sigma, Munich
Chloroform	VWR Prolabo, Darmstadt
Collagenase P	Sigma, Munich
cOmplete™ protease inhibitor cocktail	Roche, Mannheim
Coomassie brilliant blue 250-G dye	Thermo Scientific, Ulm
Corn oil	Sigma, Munich
D-Glucose	Sigma, Munich
Dimethyl sulfoxide	Sigma, Munich
DTT	Sigma, Munich
Dulbecco's Modified Eagle Medium (DMEM)	Thermo Fisher, Waltham
Dublecco's Phosphate Buffered Saline (DPBS)	Thermo Fisher, Waltham
Ethanol absolute	VWR Prolabo, Darmstadt
Fetal bovine serum	Invitrogen, Karlsruhe
Formaldehyde, methanol-free (16%)	Thermo Scientific, Ulm
Glycine	Sigma, Munich
Hanks' Balanced Salt Solution (HBSS)	Sigma, Munich
HEPES (1M)	Life Technologies, Darmstadt
Human insulin	Sigma-Aldrich, St. Louis
Hyperfilm ECL Western Blotting Detection Reagent	Amersham, Freiburg
Isopropanol	Sigma, Munich
Laemmli SDS sample buffer, reducing (6x)	Thermo Fisher, Waltham
LB broth	Sigma, Munich
L-Glutamine	Thermo Fisher, Waltham
Lipofectamine RNAiMAX Transfection Reagent	Invitrogen, Karlsruhe
NP-40	Sigma, Munich
OptiMEM – Reduced Serum Medium	Life Technologies, Darmstadt
PageRuler™ Prestained Protein Ladder	Thermo Scientific, Ulm
Penicillin/Streptomycin	Invitrogen, Karlsruhe

PhosphoSTOP *EASY*pack	Roche, Mannheim
Ponceau S	Sigma, Munich
Potassium bicarbonate	Sigma, Munich
Proteinase K	Sigma, Munich
Protein A/G Sepharose beads	Rockland, Philadelphia, USA
Purple loading dye (6x)	New England Biolabs, Frankfurt a.M.
RNse A	AppliChem, Darmstadt
RNase free water	Invitrogen, Karlsruhe
Roswell Park Memorial Institute (RPMI) medium + GlutaMAX	Invitrogen, Karlsruhe
SDS	Sigma, Munich
Skim milk powder	Sigma, Munich
SOC Medium	Invitrogen, Karlsruhe
Sodium chloride (0.9%) for injections	VWR International, Randor
Sodium hydroxide	Sigma, Munich
Sodium pyruvate (100 mM)	Invitrogen, Karlsruhe
SureBeads™ Protein G Magnetic Beads	Bio-Rad, Munich
SYBR Safe	APExBIO, Housten
Takyon™ Low ROX Probe MasterMix dTTP Blue	Eurogentec, Seraing, Belgium
Takyon™ Low ROX SYBR® MasterMix dTTP Blue	Eurogentec, Seraing, Belgium
Tamoxifen	Sigma, Munich
Transblot Turbo Buffer (5x)	Bio-Rad, Munich
Tris Base	Sigma, Munich
Tris-EDTA (100x)	Sigma, Munich
Tris HCl	Sigma, Munich
Trizol™ Reagent	Invitrogen, Karlsruhe
Trypan blue solution, 0.4%	Life Technologies, Darmstadt
Trypsin 0.05% EDTA	Invitrogen, Karlsruhe
Tween-20	Sigma, Munich

5.11 Consumables

Consumable	**Distributor**
96-well assay plate	Sigma, Munich
96-well assay plate - white	Thermo Fisher, Waltham
Cell culture plate (6-, 12-, 24-, 96-well)	Falcon, Gräeling-Lochham
Cell culture plate (10, 15 cm)	Falcon, Gräeling-Lochham
Cell scraper	Sarstedt, Nümbrecht
CombiTips Advanced (0.1, 0.5, 2.5, 5, 10 ml)	Eppendorf, Hamburg
Conical Centrifugal Tubes (15, 50 ml)	Falcon, Gräeling-Lochham
Countess® Cell counting chamber slide	Life Technologies, Darmstadt
Entsorgungsbeutel, klar	Carl Roth, Karlsruhe
Embedding cassette	Carl Roth, Karlsruhe
Falcon conical centrifugal tubes (15, 30 ml)	Falkon, Gräfelfing-Lochham
Gel Loading Tips, round	Invitrogen, Karlsruhe
Gloves (Safe Skin Purple Nitrile)	Kimberly Clark, BE
Glucometer Test strips Accu Check Inform II	Roche, Basel
Insulin syringes BD Microfine, 0.3/0.5 ml, 8 mm	BD, Franklin Lakes
MicroAmp® Optical 384-well Reaction Plate	Applied Biosystems, Darmstadt

MicroAmp® Optical Adhesive Film	Applied Biosystems, Darmstadt
Microvette® CB 300 K2E tubes	Sarstedt, Nümbrecht
Nitrocellulose Membrane	Amersham, Freiburg
Novex™ Tris-Glycine Mini Gel	Invitrogen, Karlsruhe
Parafilm	Pechinery Inc., Wisconsin
Pasteurpipettes, PE, sterile	Th. Greiner, Hamburg
PCR SingleCap 8-er Softstrips, farblos (0.1, 0.2 ml)	Biozym, Oldendorf
Petri dish (6, 10 cm)	Greiner Bio-One, Kremsmünster
Pipet tips (12.5 µl)	INTEGRA Biosciences AG, Bibertal
Safe-Lock Tubes (0.5, 1.5, 2.0, 5.0 ml)	Eppendorf, Hamburg
Serum Gel Z/1.1 microtubes	Sarstedt, Nümbrecht
Stainless Steel Beads, 5 mm	Qiagen, Hilden
Sterican® Standardkanülen (23, 24, 30G)	B. Braun, Melsungen
Serological pipettes (5, 10, 25, 50 ml)	Grainer Bio-One, Kremsmünster
Sterile filter (0.22 µM)	Satorius, Göttingen
Surebeads Protein G Magnetic Beads	Bio-Rad, Munich
TipOne Filter Tips (10, 20, 100, 200, 1000 µl)	StarLab, Hamburg
TPX Bioruptor Microtubes (1.5 ml)	Diagenode, Liege, Belgium
U-100 Insulin syringe	BD Micro-Fine, Allschwil, Switzerland
Wypall X60	Kimberly-Clark, Texas

5.12 Instruments

Instrument	Distributor
Analytical scales	Sartorius, Göttingen
Bacterial shaker	Axon Labortechnik, Kaiserslautern
Beckman Coulter	Brea, CA, USA
Bioruptor Sonication device	Diagenode, Liege, Belgium
ChemiDoc Imaging System	Bio Rad, Munich
Countess Automated Cell Counter	Life Technologies, Darmstadt
EchoMRI Body Composition Analyzer	Zinsser Analytic GmbH, Eschborn
Electrophoresis chamber	Invitrogen, Karlsruhe
Electrophoresis power supply	Invitrogen, Karlsruhe
Eppendorf Concentrator Plus (Vacuum dryer)	Eppendorf, Hamburg
Freezer, -20°C	Liebherr, Biberach
Freezer, -80°C	Thermo Fisher, Waltham
Fridge, 4°C	Liebherr, Biberach
GelDoc XR+ Imaging System	Bio Rad, Munich
Glucometer Accu-Check Performa	Roche, Basel
Heat Block (Thermostat Plus), ThermoMixer	Eppendorf, Hamburg
Horizontal shaker, WS10	Edmund Bühler GmbH, Bodelshausen
Incubator CO_2	Thermo Fisher, Waltham
Intelli Mixer RM-2M	LTF Labortechnik, Wasserburg
Microplate Shaker	VWR International, Radnor
Microscope	Zeiss, Göttingen
Mr. Frosty, Freezing Container	Thermo Fisher, Waltham
Multichannel pipette	Eppendorf, Hamburg
Multichannel Stepper Voyager	INTEGRA Biosciences AG, Bibertal

Multipipette E3	Eppendorf, Hamburg
NanoDrop 2000 spectrophotometer	Thermo Scientific, Dreieich
pH-meter	VWR International, Radnor
Pipettes (2.5, 10, 20, 100, 200, 1000 µl)	Eppendorf, Hamburg
QIAxcel Advances system	Qiagen, Hilden
QuantStudio 6/7 Flex-Real-Time PCR System	Applied Biosystems, Darmstadt
Table Centrifuge	Thermo Fisher, Waltham
Table Centrifuge 5702 R	Eppendorf, Hamburg
Thermocycler PCR	Applied Biosystems, Darmstadt
TissueLyser II	Qiagen, Hilden
Trans-Blot cell	Bio-Rad, Munich
Trans-Blot Turbo Blotting System	Bio Rad, Munich
Vacuum pump	Neolab, Heidelberg
Varioskan LUX multimode microplate reader	Thermo Fisher, Waltham
Vortex Genie-2	Scientific Industries Inc., New York, USA
Water bath	Neolab, Heidelberg

6 APPENDIX

6.1 Abbreviations

AKT	Protein kinase B
ALT	Alanine transaminase
ANOVA	Analysis of variances
AP1	Adaptor protein 1
Arx	Aristaless-related homeobox
AST	Aspartate aminotransferase
ATP	Adenosine triphosphate
AUC	Area under the curve
BrdU	Bromodeoxyuridine
BMI	Body mass index
BSA	Bovine serum albumin
ChgA	Chromogranin A
ChIP	Chromatin immunoprecipitation
CTBP1/2	C-terminal binding protein
E	Embryonic day
ECM	Extra cellular matrix
EDTA	Ethylenediaminetetraacetic acid
EMT	Epithelial mesenchymal transition
ELISA	Enzyme-linked immunosorbent assay
eWAT	Epididymal white adipose tissue
FACT	Facilitates chromatin transcription
Fasn	Fatty acid synthase
FoxO1	Forkhead box O1
GC	Glucocorticoid
Gcg	Glucagon
Gck	Glucokinase
GC muscle	Gastrocnemius muscle
GEM	Gel Bead-in-emulsion
Gipr	Glucose-dependent insulinotropic polypeptide receptor
GO	Gene ontology
GPS2	G protein pathway suppressor 2
GR	Glucocorticoid receptor
GSEA	Gene set enrichment analysis
HbA1c	Hemoglobin A1c
HDAC1/2/3	Histone deacetylase 1/2/3
HDL	High density lipoprotein
HFD	High fat diet
Hk1	Hexokinase 1
IgG	Immunoglobulin G
Ins1	Insulin 1
Ins2	Insulin 2
IP	Immunoprecipitation
ipGTT	Intraperitoneal glucose tolerance test
ipITT	Intraperitoneal insulin tolerance test
iTBL/RβKO	Induced β-cell specific TBL1 and TBLR1 knock out
IPA	Ingenuity pathway analysis
KEGG	Kyoto Encyclopedia of Genes and Genomes
KRB	Krebs Ringer Buffer
Ldha	Lactate dehydrogenase A
LDH	Lactate dehydrogenase

LDL	Low density lipoprotein
MafA	MAF BZIB transcription factor A
MafB	MAF BZIB transcription factor B
MRI	Magnetic resonance imaging
NCOR	Nuclear receptor co-repressor 1
NEFA	Non-esterified fatty acids
NFκB	nuclear factor k-light-chain-enhancer of activated B cells
NeuroD1	Neuronal differentiation 1
Ngn3	Neurogenin 3
Nkx2.2	NK2 homeobox 2
Nkx6.1	NK6 homeobox 1
oGTT	Oral glucose tolerance test
Pax4/6	Paired box gene 4
Pck1	Phosphoenolpyruvate carboxykinase 1
Pcsk1/2	Prohormone convertase 1/2
Pdx1	Pancreatic and duodenal homeobox 1
Pgc1α	Peroxisome proliferator-activated receptor gamma coactivator 1α
PI3K	Phosphoinositide 3-kinase
PPARα/γ	Peroxisome proliferator-activated receptor α/γ
Ppy	Pancreatic polypeptide Y
Prlr	Prolactin receptor
qPCR	Quantitative polymerase chain reaction
RAR	Retinoic acid receptor
RIPA	Radio immunoprecipitation assay
RNA-Seq	RNA sequencing
RXR	Retinoid X receptor
Scd1	Stearoyl-CoA desaturase 1
scRNA-Seq	Single cell RNA sequencing
SEM	Standard error of the mean
shRNA	Short hairpin RNA
siRNA	Small interfering RNA
Slc2a2	Solute carrier family 2 member 2
Slc2a4	Solute carrier family 2 member 4
Slc16a1	Solute carrier family 16 member 1
Slc30a8	Solute carrier family 30 member 8
SMRT	Silencing mediator of retinoid and thyroid hormone receptors
Sox2/9/17	SRY box 2/9/17
Sst	Somatostatin
SUPT16H	SPT16 homolog
SWI/SNF	Switch/sucrose non-fermentable
T2DM	Type 2 Diabetes mellitus
TBL1	Transducin beta like 1 x-linked
TBLβKO	β-cell specific TBL1 knock out
TBLR1	Transducin beta like 1 x-linked related 1
TBLRβKO	β-cell specific TBLR1 knock out
TBL/RβKO	β-cell specific TBL1 and TBLR1 knock out
TCA	Tricarboxylic acid
TGFβ	Transforming growth factor β
Ucn3	Urocortin 3
UMAP	Uniform manifold approximation and projection

6.2 Figures and tables

Figures

Tables

6.3 References

Adrian, T. E.; Bloom, S. R.; Bryant, M. G.; Polak, J. M.; Heitz, P. H.; Barnes, A. J. (1976): Distribution and release of human pancreatic polypeptide. In *Gut* 17 (12), pp. 940–944. DOI: 10.1136/gut.17.12.940.

Aguayo-Mazzucato, Cristina; DiIenno, Amanda; Hollister-Lock, Jennifer; Cahill, Christopher; Sharma, Arun; Weir, Gordon et al. (2015): MAFA and T3 Drive Maturation of Both Fetal Human Islets and Insulin-Producing Cells Differentiated From hESC. In *The Journal of Clinical Endocrinology and Metabolism* 100 (10), pp. 3651–3659. DOI: 10.1210/jc.2015-2632.

Aguayo-Mazzucato, Cristina; Zavacki, Ann Marie; Marinelarena, Alejandra; Hollister-Lock, Jennifer; El Khattabi, Ilham; Marsili, Alessandro et al. (2013): Thyroid hormone promotes postnatal rat pancreatic β-cell development and glucose-responsive insulin secretion through MAFA. In *Diabetes* 62 (5), pp. 1569–1580. DOI: 10.2337/db12-0849.

Ahlqvist, Emma; Prasad, Rashmi B.; Groop, Leif (2020): Subtypes of Type 2 Diabetes Determined From Clinical Parameters. In *Diabetes* 69 (10), pp. 2086–2093. DOI: 10.2337/dbi20-0001.

Ahmed, Awad M. (2002): History of diabetes mellitus. In *Saudi medical journal* 23 (4), pp. 373–378.

Ainscow, E. K.; Zhao, C.; Rutter, G. A. (2000): Acute overexpression of lactate dehydrogenase-A perturbs beta-cell mitochondrial metabolism and insulin secretion. In *Diabetes* 49 (7), pp. 1149–1155. DOI: 10.2337/diabetes.49.7.1149.

Amo-Shiinoki, Kikuko; Tanabe, Katsuya; Hoshii, Yoshinobu; Matsui, Hiroto; Harano, Risa; Fukuda, Tatsuya et al. (2021): Islet cell dedifferentiation is a pathologic mechanism of long-standing progression of type 2 diabetes. In *JCI insight* 6 (1). DOI: 10.1172/jci.insight.143791.

Aragón, F.; Karaca, M.; Novials, A.; Maldonado, R.; Maechler, P.; Rubí, B. (2015): Pancreatic polypeptide regulates glucagon release through PPYR1 receptors expressed in mouse and human alpha-cells. In *Biochimica et biophysica acta* 1850 (2), pp. 343–351. DOI: 10.1016/j.bbagen.2014.11.005.

Arslanian, Silva; Bacha, Fida; Grey, Margaret; Marcus, Marsha D.; White, Neil H.; Zeitler, Philip (2018): Evaluation and Management of Youth-Onset Type 2 Diabetes: A Position Statement by the American Diabetes Association. In *Diabetes care* 41 (12), pp. 2648–2668. DOI: 10.2337/dci18-0052.

Asfari, M.; Janjic, D.; Meda, P.; Li, G.; Halban, P. A.; Wollheim, C. B. (1992): Establishment of 2-mercaptoethanol-dependent differentiated insulin-secreting cell lines. In *Endocrinology* 130 (1), pp. 167–178. DOI: 10.1210/endo.130.1.1370150.

Ashcroft, F. M.; Harrison, D. E.; Ashcroft, S. J. (1984): Glucose induces closure of single potassium channels in isolated rat pancreatic beta-cells. In *Nature* 312 (5993), pp. 446–448. DOI: 10.1038/312446a0.

Atkinson, Mark A.; Campbell-Thompson, Martha; Kusmartseva, Irina; Kaestner, Klaus H. (2020): Organisation of the human pancreas in health and in diabetes. In *Diabetologia* 63 (10), pp. 1966–1973. DOI: 10.1007/s00125-020-05203-7.

Augsornworawat, Punn; Maxwell, Kristina G.; Velazco-Cruz, Leonardo; Millman, Jeffrey R. (2020): Single-Cell Transcriptome Profiling Reveals β Cell Maturation in Stem Cell-Derived Islets after Transplantation. In *Cell reports* 32 (8), p. 108067. DOI: 10.1016/j.celrep.2020.108067.

Avrahami, Dana; Li, Changhong; Zhang, Jia; Schug, Jonathan; Avrahami, Ran; Rao, Shilpa et al. (2015): Aging-Dependent Demethylation of Regulatory Elements Correlates with Chromatin State and Improved β Cell Function. In *Cell metabolism* 22 (4), pp. 619–632. DOI: 10.1016/j.cmet.2015.07.025.

Avrahami, Dana; Wang, Yue J.; Schug, Jonathan; Feleke, Eseye; Gao, Long; Liu, Chengyang et al. (2020): Single-cell transcriptomics of human islet ontogeny defines the molecular basis of β-cell dedifferentiation in T2D. In *Molecular Metabolism* 42, p. 101057. DOI: 10.1016/j.molmet.2020.101057.

Bailey, Clifford J.; Day, Caroline (2010): SGLT2 inhibitors: glucuretic treatment for type 2 diabetes. In *Diabetes & Vascular Disease* 10 (4), pp. 193–199. DOI: 10.1177/1474651410377832.

Balboa, Diego; Barsby, Tom; Lithovius, Väinö; Saarimäki-Vire, Jonna; Omar-Hmeadi, Muhmmad; Dyachok, Oleg et al. (2022): Functional, metabolic and transcriptional maturation of human pancreatic islets derived from stem cells. In *Nature biotechnology* 40 (7), pp. 1042–1055. DOI: 10.1038/s41587-022-01219-z.

Bartolome, Alberto; Zhu, Changyu; Sussel, Lori; Pajvani, Utpal B. (2019): Notch signaling dynamically regulates adult β cell proliferation and maturity. In *The Journal of clinical investigation* 129 (1), pp. 268–280. DOI: 10.1172/JCI98098.

Bastidas, J. A.; Couse, N. F.; Yeo, C. J.; Schmieg, R. E.; Andersen, D. K.; Gingerich, R. L.; Zinner, M. J. (1990): The effect of pancreatic polypeptide infusion on glucose tolerance and insulin response in longitudinally studied pancreatitis-induced diabetes. In *Surgery* 107 (6), pp. 661–668.

Batterham, R. L.; Le Roux, C. W.; Cohen, M. A.; Park, A. J.; Ellis, S. M.; Patterson, M. et al. (2003): Pancreatic polypeptide reduces appetite and food intake in humans. In *The Journal of Clinical Endocrinology and Metabolism* 88 (8), pp. 3989–3992. DOI: 10.1210/jc.2003-030630.

Behrendorff, Natasha; Floetenmeyer, Matthias; Schwiening, Christof; Thorn, Peter (2010): Protons released during pancreatic acinar cell secretion acidify the lumen and contribute to pancreatitis in mice. In *Gastroenterology* 139 (5), 1711-20, 1720.e1-5. DOI: 10.1053/j.gastro.2010.07.051.

Belotserkovskaya, Rimma; Oh, Sangtaek; Bondarenko, Vladimir A.; Orphanides, George; Studitsky, Vasily M.; Reinberg, Danny (2003): FACT facilitates transcription-dependent nucleosome alteration. In *Science* 301 (5636), pp. 1090–1093. DOI: 10.1126/science.1085703.

Bensellam, Mohammed; Jonas, Jean-Christophe; Laybutt, D. Ross (2018): Mechanisms of β-cell dedifferentiation in diabetes: recent findings and future research directions. In *The Journal of endocrinology* 236 (2), R109-R143. DOI: 10.1530/JOE-17-0516.

Blodgett, David M.; Nowosielska, Anetta; Afik, Shaked; Pechhold, Susanne; Cura, Anthony J.; Kennedy, Norman J. et al. (2015): Novel Observations From Next-Generation RNA Sequencing of Highly Purified Human Adult and Fetal Islet Cell Subsets. In *Diabetes* 64 (9), pp. 3172–3181. DOI: 10.2337/db15-0039.

Blum, Barak; Hrvatin, Siniša; Schuetz, Christian; Bonal, Claire; Rezania, Alireza; Melton, Douglas A. (2012): Functional beta-cell maturation is marked by an increased glucose threshold and by expression of urocortin 3. In *Nature biotechnology* 30 (3), pp. 261–264. DOI: 10.1038/nbt.2141.

Blum, Barak; Roose, Adam N.; Barrandon, Ornella; Maehr, René; Arvanites, Anthony C.; Davidow, Lance S. et al. (2014): Reversal of β cell de-differentiation by a small molecule inhibitor of the TGFβ pathway. In *eLife* 3, e02809. DOI: 10.7554/eLife.02809.

Bogardus, C.; Lillioja, S.; Howard, B. V.; Reaven, G.; Mott, D. (1984): Relationships between insulin secretion, insulin action, and fasting plasma glucose concentration in nondiabetic and noninsulin-dependent diabetic subjects. In *Journal of Clinical Investigation* 74 (4), pp. 1238–1246. DOI: 10.1172/JCI111533.

Bragg, Fiona; Holmes, Michael V.; Iona, Andri; Guo, Yu; Du, Huaidong; Chen, Yiping et al. (2017): Association Between Diabetes and Cause-Specific Mortality in Rural and Urban Areas of China. In *JAMA* 317 (3), pp. 280–289. DOI: 10.1001/jama.2016.19720.

Bryla, J.; Harris, E. J.; Plumb, J. A. (1977): The stimulatory effect of glucagon and dibutyryl cyclic AMP on ureogenesis and gluconeogenesis in relation to the mitochondrial ATP content. In *FEBS letters* 80 (2), pp. 443–448. DOI: 10.1016/0014-5793(77)80494-8.

Burlison, Jared S.; Long, Qiaoming; Fujitani, Yoshio; Wright, Christopher V. E.; Magnuson, Mark A. (2008): Pdx-1 and Ptf1a concurrently determine fate specification of pancreatic multipotent progenitor cells. In *Developmental biology* 316 (1), pp. 74–86. DOI: 10.1016/j.ydbio.2008.01.011.

Butler, Alexandra E.; Janson, Juliette; Bonner-Weir, Susan; Ritzel, Robert; Rizza, Robert A.; Butler, Peter C. (2003): Beta-cell deficit and increased beta-cell apoptosis in humans with type 2 diabetes. In *Diabetes* 52 (1), pp. 102–110. DOI: 10.2337/diabetes.52.1.102.

Cabrera, Over; Berman, Dora M.; Kenyon, Norma S.; Ricordi, Camillo; Berggren, Per-Olof; Caicedo, Alejandro (2006): The unique cytoarchitecture of human pancreatic islets has implications for islet cell function. In *Proceedings of the National Academy of Sciences of the United States of America* 103 (7), pp. 2334–2339. DOI: 10.1073/pnas.0510790103.

Candler, T. P.; Mahmoud, O.; Lynn, R. M.; Majbar, A. A.; Barrett, T. G.; Shield, J. P. H. (2018): Continuing rise of Type 2 diabetes incidence in children and young people in the UK. In *Diabetic medicine : a journal of the British Diabetic Association* 35 (6), pp. 737–744. DOI: 10.1111/dme.13609.

Capozzi, Megan E.; Wait, Jacob B.; Koech, Jepchumba; Gordon, Andrew N.; Coch, Reilly W.; Svendsen, Berit et al. (2019): Glucagon lowers glycemia when β-cells are active. In *JCI insight* 5 (16). DOI: 10.1172/jci.insight.129954.

Casteels, Tamara; Zhang, Yufeng; Frogne, Thomas; Sturtzel, Caterina; Lardeau, Charles-Hugues; Sen, Ilke et al. (2021): An inhibitor-mediated beta-cell dedifferentiation model reveals distinct roles for FoxO1 in glucagon repression and insulin maturation. In *Molecular Metabolism* 54, p. 101329. DOI: 10.1016/j.molmet.2021.101329.

Chakrabarti, Partha; Kim, Ju Youn; Singh, Maneet; Shin, Yu-Kyong; Kim, Jessica; Kumbrink, Joerg et al. (2013): Insulin inhibits lipolysis in adipocytes via the evolutionarily conserved mTORC1-Egr1-ATGL-mediated pathway. In *Molecular and Cellular Biology* 33 (18), pp. 3659–3666. DOI: 10.1128/MCB.01584-12.

Chen, Hong; Zhou, Wenjun; Ruan, Yuting; Yang, Lei; Xu, Ningning; Chen, Rongping et al. (2018): Reversal of angiotensin ll-induced β-cell dedifferentiation via inhibition of NF-κb signaling. In *Molecular medicine (Cambridge, Mass.)* 24 (1), p. 43. DOI: 10.1186/s10020-018-0044-3.

Chen, Wen-Bin; Gao, Ling; Wang, Jie; Wang, Yan-Gang; Dong, Zheng; Zhao, Jiajun et al. (2016): Conditional ablation of HDAC3 in islet beta cells results in glucose intolerance and enhanced susceptibility to STZ-induced diabetes. In *Oncotarget* 7 (36), pp. 57485–57497. DOI: 10.18632/oncotarget.11295.

Choi, Hyo-Kyoung; Choi, Kyung-Chul; Yoo, Jung-Yoon; Song, Meiying; Ko, Suk Jin; Kim, Chul Hoon et al. (2011): Reversible SUMOylation of TBL1-TBLR1 regulates β-catenin-mediated Wnt signaling. In *Molecular cell* 43 (2), pp. 203–216. DOI: 10.1016/j.molcel.2011.05.027.

Cinti, Francesca; Bouchi, Ryotaro; Kim-Muller, Ja Young; Ohmura, Yoshiaki; Sandoval, P. R.; Masini, Matilde et al. (2016): Evidence of β-Cell Dedifferentiation in Human Type 2 Diabetes. In *The Journal of Clinical Endocrinology and Metabolism* 101 (3), pp. 1044–1054. DOI: 10.1210/jc.2015-2860.

Colditz, G. A.; Willett, W. C.; Rotnitzky, A.; Manson, J. E. (1995): Weight gain as a risk factor for clinical diabetes mellitus in women. In *Annals of internal medicine* 122 (7), pp. 481–486. DOI: 10.7326/0003-4819-122-7-199504010-00001.

Cole, Lori; Anderson, Miranda; Antin, Parker B.; Limesand, Sean W. (2009): One process for pancreatic beta-cell coalescence into islets involves an epithelial-mesenchymal transition. In *The Journal of endocrinology* 203 (1), pp. 19–31. DOI: 10.1677/JOE-09-0072.

Collombat, Patrick; Hecksher-Sørensen, Jacob; Krull, Jens; Berger, Joachim; Riedel, Dietmar; Herrera, Pedro L. et al. (2007): Embryonic endocrine pancreas and mature beta cells acquire alpha and PP cell phenotypes upon Arx misexpression. In *The Journal of clinical investigation* 117 (4), pp. 961–970. DOI: 10.1172/JCI29115.

Collombat, Patrick; Mansouri, Ahmed; Hecksher-Sorensen, Jacob; Serup, Palle; Krull, Jens; Gradwohl, Gerard; Gruss, Peter (2003): Opposing actions of Arx and Pax4 in endocrine pancreas development. In *Genes & development* 17 (20), pp. 2591–2603. DOI: 10.1101/gad.269003.

Cook, D. L.; Hales, C. N. (1984): Intracellular ATP directly blocks K+ channels in pancreatic B-cells. In *Nature* 311 (5983), pp. 271–273. DOI: 10.1038/311271a0.

Daniels, Garrett; Li, Yirong; Gellert, Lan Lin; Zhou, Albert; Melamed, Jonathan; Wu, Xinyu et al. (2014): TBLR1 as an androgen receptor (AR) coactivator selectively activates AR target genes to inhibit prostate cancer growth. In *Endocrine-Related Cancer* 21 (1), pp. 127–142. DOI: 10.1530/erc-13-0293.

Date, Y.; Kojima, M.; Hosoda, H.; Sawaguchi, A.; Mondal, M. S.; Suganuma, T. et al. (2000): Ghrelin, a novel growth hormone-releasing acylated peptide, is synthesized in a distinct endocrine cell type in the gastrointestinal tracts of rats and humans. In *Endocrinology* 141 (11), pp. 4255–4261. DOI: 10.1210/endo.141.11.7757.

Davies, Melanie J.; Aroda, Vanita R.; Collins, Billy S.; Gabbay, Robert A.; Green, Jennifer; Maruthur, Nisa M. et al. (2022): Management of Hyperglycemia in Type 2 Diabetes, 2022. A Consensus Report by the American Diabetes Association (ADA) and the European Association for the Study of Diabetes (EASD). In *Diabetes care* 45 (11), pp. 2753–2786. DOI: 10.2337/dci22-0034.

Davies, P. O.; Poirier, C.; Deltour, L.; Montagutelli, X. (1994): Genetic reassignment of the insulin-1 (Ins1) gene to distal mouse chromosome 19. In *Genomics* 21 (3), pp. 665–667. DOI: 10.1006/geno.1994.1334.

Delangre, Etienne; Liu, Junjun; Tolu, Stefania; Maouche, Kamel; Armanet, Mathieu; Cattan, Pierre et al. (2021): Underlying mechanisms of glucocorticoid-induced β-cell death and dysfunction: a new role for glycogen synthase kinase 3. In *Cell death & disease* 12 (12), p. 1136. DOI: 10.1038/s41419-021-04419-8.

Dhawan, Sangeeta; Tschen, Shuen-Ing; Zeng, Chun; Guo, Tingxia; Hebrok, Matthias; Matveyenko, Aleksey; Bhushan, Anil (2015): DNA methylation directs functional maturation of pancreatic β cells. In *The Journal of clinical investigation* 125 (7), pp. 2851–2860. DOI: 10.1172/JCI79956.

Diedisheim, Marc; Oshima, Masaya; Albagli, Olivier; Huldt, Charlotte Wennberg; Ahlstedt, Ingela; Clausen, Maryam et al. (2018): Modeling human pancreatic beta cell dedifferentiation. In *Molecular Metabolism* 10, pp. 74–86. DOI: 10.1016/j.molmet.2018.02.002.

Dor, Yuval; Brown, Juliana; Martinez, Olga I.; Melton, Douglas A. (2004): Adult pancreatic beta-cells are formed by self-duplication rather than stem-cell differentiation. In *Nature* 429 (6987), pp. 41–46. DOI: 10.1038/nature02520.

Dor, Yuval; Glaser, Benjamin (2013): β-cell dedifferentiation and type 2 diabetes. In *The New England journal of medicine* 368 (6), pp. 572–573. DOI: 10.1056/NEJMcibr1214034.

Efanova, I. B.; Zaitsev, S. V.; Zhivotovsky, B.; Köhler, M.; Efendić, S.; Orrenius, S.; Berggren, P. O. (1998): Glucose and tolbutamide induce apoptosis in pancreatic beta-cells. A process dependent on intracellular Ca2+ concentration. In *The Journal of biological chemistry* 273 (50), pp. 33501–33507. DOI: 10.1074/jbc.273.50.33501.

Esguerra, Jonathan L. S.; Ofori, Jones K.; Nagao, Mototsugu; Shuto, Yuki; Karagiannopoulos, Alexandros; Fadista, Joao et al. (2020): Glucocorticoid induces human beta cell dysfunction by involving riborepressor GAS5 LincRNA. In *Molecular Metabolism* 32, pp. 160–167. DOI: 10.1016/j.molmet.2019.12.012.

Fiskus, W.; Sharma, S.; Saha, S.; Shah, B.; Devaraj, S. G. T.; Sun, B. et al. (2015): Pre-clinical efficacy of combined therapy with novel β-catenin antagonist BC2059 and histone deacetylase inhibitor against AML cells. In *Leukemia* 29 (6), pp. 1267–1278. DOI: 10.1038/leu.2014.340.

Francis, B. H.; Baskin, D. G.; Saunders, D. R.; Ensinck, J. W. (1990): Distribution of somatostatin-14 and somatostatin-28 gastrointestinal-pancreatic cells of rats and humans. In *Gastroenterology* 99 (5), pp. 1283–1291. DOI: 10.1016/0016-5085(90)91151-u.

Frost, Jennifer M.; Kim, M. Yvonne; Park, Guen Tae; Hsieh, Ping-Hung; Nakamura, Miyuki; Lin, Samuel J. H. et al. (2018): FACT complex is required for DNA demethylation at heterochromatin during reproduction in Arabidopsis. In *Proceedings of the National Academy of Sciences of the United States of America* 115 (20), E4720-E4729. DOI: 10.1073/pnas.1713333115.

Fu, Zhuo; Gilbert, Elizabeth R.; Liu, Dongmin (2013): Regulation of insulin synthesis and secretion and pancreatic Beta-cell dysfunction in diabetes. In *Current diabetes reviews* 9 (1), pp. 25–53.

Fujimoto, W. Y.; Ensinck, J. W.; Merchant, F. W.; Williams, R. H.; Smith, P. H.; Johnson, D. G. (1978): Stimulation by gastric inhibitory polypeptide of insulin and glucagon secretion by rat islet cultures. In *Proceedings of the Society for Experimental Biology and Medicine. Society for Experimental Biology and Medicine (New York, N.Y.)* 157 (1), pp. 89–93. DOI: 10.3181/00379727-157-39997.

Fujita, Yukari; Kozawa, Junji; Iwahashi, Hiromi; Yoneda, Sho; Uno, Sae; Eguchi, Hidetoshi et al. (2018): Human pancreatic α- to β-cell area ratio increases after type 2 diabetes onset. In *Journal of diabetes investigation* 9 (6), pp. 1270–1282. DOI: 10.1111/jdi.12841.

Gao, Tao; McKenna, Brian; Li, Changhong; Reichert, Maximilian; Nguyen, James; Singh, Tarjinder et al. (2014): Pdx1 maintains β cell identity and function by repressing an α cell program. In *Cell metabolism* 19 (2), pp. 259–271. DOI: 10.1016/j.cmet.2013.12.002.

Garcia, Henry; Fleyshman, Daria; Kolesnikova, Katerina; Safina, Alfiya; Commane, Mairead; Paszkiewicz, Geraldine et al. (2011): Expression of FACT in mammalian tissues suggests its role in maintaining of undifferentiated state of cells. In *Oncotarget* 2 (10), pp. 783–796. DOI: 10.18632/oncotarget.340.

Gasparian, Alexander V.; Burkhart, Catherine A.; Purmal, Andrei A.; Brodsky, Leonid; Pal, Mahadeb; Saranadasa, Madhi et al. (2011): Curaxins: anticancer compounds that simultaneously suppress NF-κB and activate p53 by targeting FACT. In *Science translational medicine* 3 (95), 95ra74. DOI: 10.1126/scitranslmed.3002530.

Geer, Eliza B.; Islam, Julie; Buettner, Christoph (2014): Mechanisms of glucocorticoid-induced insulin resistance: focus on adipose tissue function and lipid metabolism. In *Endocrinology and metabolism clinics of North America* 43 (1), pp. 75–102. DOI: 10.1016/j.ecl.2013.10.005.

German, M.; Ashcroft, S.; Docherty, K.; Edlund, H.; Edlund, T.; Goodison, S. et al. (1995): The insulin gene promoter. A simplified nomenclature. In *Diabetes* 44 (8), pp. 1002–1004. DOI: 10.2337/diab.44.8.1002.

Gloyn, Anna L.; Weedon, Michael N.; Owen, Katharine R.; Turner, Martina J.; Knight, Bridget A.; Hitman, Graham et al. (2003): Large-scale association studies of variants in genes encoding the pancreatic beta-cell KATP channel subunits Kir6.2 (KCNJ11) and SUR1 (ABCC8) confirm that the KCNJ11 E23K variant is associated with type 2 diabetes. In *Diabetes* 52 (2), pp. 568–572. DOI: 10.2337/diabetes.52.2.568.

Gosmain, Yvan; Katz, Liora S.; Masson, Mounia Heddad; Cheyssac, Claire; Poisson, Caroline; Philippe, Jacques (2012): Pax6 is crucial for β-cell function, insulin biosynthesis, and glucose-induced insulin secretion. In *Molecular Endocrinology* 26 (4), pp. 696–709. DOI: 10.1210/me.2011-1256.

Gradwohl, G.; Dierich, A.; LeMeur, M.; Guillemot, F. (2000): neurogenin3 is required for the development of the four endocrine cell lineages of the pancreas. In *Proceedings of the National Academy of Sciences of the United States of America* 97 (4), pp. 1607–1611. DOI: 10.1073/pnas.97.4.1607.

Grant, Struan F. A.; Thorleifsson, Gudmar; Reynisdottir, Inga; Benediktsson, Rafn; Manolescu, Andrei; Sainz, Jesus et al. (2006): Variant of transcription factor 7-like 2 (TCF7L2) gene confers risk of type 2 diabetes. In *Nature genetics* 38 (3), pp. 320–323. DOI: 10.1038/ng1732.

Greer, Eric L.; Shi, Yang (2012): Histone methylation: a dynamic mark in health, disease and inheritance. In *Nature reviews. Genetics* 13 (5), pp. 343–357. DOI: 10.1038/nrg3173.

Gromada, J.; Bokvist, K.; Ding, W. G.; Barg, S.; Buschard, K.; Renström, E.; Rorsman, P. (1997): Adrenaline stimulates glucagon secretion in pancreatic A-cells by increasing the Ca2+ current and the number of granules close to the L-type Ca2+ channels. In *J Gen Physiol* 110 (3), pp. 217–228. DOI: 10.1085/jgp.110.3.217.

Gu, Guoqiang; Dubauskaite, Jolanta; Melton, Douglas A. (2002): Direct evidence for the pancreatic lineage: NGN3+ cells are islet progenitors and are distinct from duct progenitors. In *Development (Cambridge, England)* 129 (10), pp. 2447–2457. DOI: 10.1242/dev.129.10.2447.

Gu, Jian-Feng; Fu, Wei; Qian, Hai-Xin; Gu, Wen-Xiu; Zong, Yang; Chen, Qian; Lu, Long (2020): TBL1XR1 induces cell proliferation and inhibit cell apoptosis by the PI3K/AKT pathway in pancreatic ductal adenocarcinoma. In *WJG* 26 (25), pp. 3586–3602. DOI: 10.3748/wjg.v26.i25.3586.

Guenther, M. G.; Barak, O.; Lazar, M. A. (2001): The SMRT and N-CoR corepressors are activating cofactors for histone deacetylase 3. In *Molecular and Cellular Biology* 21 (18), pp. 6091–6101. DOI: 10.1128/MCB.21.18.6091-6101.2001.

Guenther, M. G.; Lane, W. S.; Fischle, W.; Verdin, E.; Lazar, M. A.; Shiekhattar, R. (2000): A core SMRT corepressor complex containing HDAC3 and TBL1, a WD40-repeat protein linked to deafness. In *Genes & development* 14 (9), pp. 1048–1057.

Gutiérrez, Giselle Domínguez; Bender, Aaron S.; Cirulli, Vincenzo; Mastracci, Teresa L.; Kelly, Stephen M.; Tsirigos, Aristotelis et al. (2017): Pancreatic β cell identity requires continual repression of non-β cell programs. In *The Journal of clinical investigation* 127 (1), pp. 244–259. DOI: 10.1172/JCI88017.

Hang, Yan; Yamamoto, Tsunehiko; Benninger, Richard K. P.; Brissova, Marcela; Guo, Min; Bush, Will et al. (2014): The MafA transcription factor becomes essential to islet β-cells soon after birth. In *Diabetes* 63 (6), pp. 1994–2005. DOI: 10.2337/db13-1001.

Harper, M. E.; Ullrich, A.; Saunders, G. F. (1981): Localization of the human insulin gene to the distal end of the short arm of chromosome 11. In *Proceedings of the National Academy of Sciences of the United States of America* 78 (7), pp. 4458–4460. DOI: 10.1073/pnas.78.7.4458.

Hauge-Evans, Astrid C.; King, Aileen J.; Carmignac, Danielle; Richardson, Carolyn C.; Robinson, Iain C. A. F.; Low, Malcolm J. et al. (2009): Somatostatin secreted by islet delta-cells fulfills multiple roles as a paracrine regulator of islet function. In *Diabetes* 58 (2), pp. 403–411. DOI: 10.2337/db08-0792.

Haumaitre, C.; Barbacci, E.; Jenny, M.; Ott, M. O.; Gradwohl, G.; Cereghini, S. (2005): Lack of TCF2/vHNF1 in mice leads to pancreas agenesis. In *Proceedings of the National Academy of Sciences of the United States of America* 102 (5), pp. 1490–1495. DOI: 10.1073/pnas.0405776102.

Haythorne, Elizabeth; Rohm, Maria; van de Bunt, Martijn; Brereton, Melissa F.; Tarasov, Andrei I.; Blacker, Thomas S. et al. (2019): Diabetes causes marked inhibition of mitochondrial metabolism in pancreatic β-cells. In *Nature communications* 10 (1), p. 2474. DOI: 10.1038/s41467-019-10189-x.

Heald, Adrian H.; Stedman, Mike; Davies, Mark; Livingston, Mark; Alshames, Ramadan; Lunt, Mark et al. (2020): Estimating life years lost to diabetes: outcomes from analysis of National Diabetes Audit and Office of National Statistics data. In *Cardiovascular endocrinology & metabolism* 9 (4), pp. 183–185. DOI: 10.1097/XCE.0000000000000210.

Hebbes, T. R.; Thorne, A. W.; Crane-Robinson, C. (1988): A direct link between core histone acetylation and transcriptionally active chromatin. In *The EMBO journal* 7 (5), pp. 1395–1402. DOI: 10.1002/j.1460-2075.1988.tb02956.x.

Heller, R. Scott; Jenny, Marjorie; Collombat, Patrick; Mansouri, Ahmed; Tomasetto, Catherine; Madsen, Ole D. et al. (2005): Genetic determinants of pancreatic epsilon-cell development. In *Developmental biology* 286 (1), pp. 217–224. DOI: 10.1016/j.ydbio.2005.06.041.

Helmrich, S. P.; Ragland, D. R.; Leung, R. W.; Paffenbarger, R. S. (1991): Physical activity and reduced occurrence of non-insulin-dependent diabetes mellitus. In *The New England journal of medicine* 325 (3), pp. 147–152. DOI: 10.1056/NEJM199107183250302.

Henquin, J. C. (2009): Regulation of insulin secretion: a matter of phase control and amplitude modulation. In *Diabetologia* 52 (5), pp. 739–751. DOI: 10.1007/s00125-009-1314-y.

Henquin, Jean-Claude; Ibrahim, Majeed M.; Rahier, Jacques (2017): Insulin, glucagon and somatostatin stores in the pancreas of subjects with type-2 diabetes and their lean and obese non-diabetic controls. In *Scientific reports* 7 (1), p. 11015. DOI: 10.1038/s41598-017-10296-z.

Herchuelz, A.; Lebrun, P.; Boschero, A. C.; Malaisse, W. J. (1984): Mechanism of arginine-stimulated Ca2+ influx into pancreatic B cell. In *The American journal of physiology* 246 (1 Pt 1), E38-43. DOI: 10.1152/ajpendo.1984.246.1.E38.

Hermansen, K.; Orskov, H.; Christensen, S. E. (1979): Streptozotocin diabetes: a glucoreceptor dysfunction affecting D cells as well as B and A cells. In *Diabetologia* 17 (6), pp. 385–389. DOI: 10.1007/BF01236274.

Herrera, P. L. (2000): Adult insulin- and glucagon-producing cells differentiate from two independent cell lineages. In *Development (Cambridge, England)* 127 (11), pp. 2317–2322. DOI: 10.1242/dev.127.11.2317.

Herrera, P. L.; Huarte, J.; Sanvito, F.; Meda, P.; Orci, L.; Vassalli, J. D. (1991): Embryogenesis of the murine endocrine pancreas; early expression of pancreatic polypeptide gene. In *Development (Cambridge, England)* 113 (4), pp. 1257–1265. DOI: 10.1242/dev.113.4.1257.

Hiramatsu, S.; Grill, V. (2001): Influence of a high-fat diet during chronic hyperglycemia on beta-cell function in pancreatic islet transplants to streptozotocin-diabetic rats. In *European journal of endocrinology* 144 (5), pp. 521–527. DOI: 10.1530/eje.0.1440521.

Hong, L.; Schroth, G. P.; Matthews, H. R.; Yau, P.; Bradbury, E. M. (1993): Studies of the DNA binding properties of histone H4 amino terminus. Thermal denaturation studies reveal that acetylation markedly reduces the binding constant of the H4 "tail" to DNA. In *The Journal of biological chemistry* 268 (1), pp. 305–314.

Hu, Jianxia; Wang, Yangang; Gong, Huimin; Yu, Chundong; Guo, Caihong; Wang, Fang et al. (2016): Long term effect and safety of Wharton's jelly-derived mesenchymal stem cells on type 2 diabetes. In *Experimental and therapeutic medicine* 12 (3), pp. 1857–1866. DOI: 10.3892/etm.2016.3544.

Huang, Chen; Walker, Emily M.; Dadi, Prasanna K.; Hu, Ruiying; Xu, Yanwen; Zhang, Wenjian et al. (2018): Synaptotagmin 4 Regulates Pancreatic β Cell Maturation by Modulating the Ca2+ Sensitivity of Insulin Secretion Vesicles. In *Developmental cell* 45 (3), 347-361.e5. DOI: 10.1016/j.devcel.2018.03.013.

Hudson, Michael E.; Pozdnyakova, Irina; Haines, Kenneth; Mor, Gil; Snyder, Michael (2007): Identification of differentially expressed proteins in ovarian cancer using high-density protein microarrays. In *Proceedings of the National Academy of Sciences of the United States of America* 104 (44), pp. 17494–17499. DOI: 10.1073/pnas.0708572104.

Ishihara, H.; Asano, T.; Tsukuda, K.; Katagiri, H.; Inukai, K.; Anai, M. et al. (1993): Pancreatic beta cell line MIN6 exhibits characteristics of glucose metabolism and glucose-stimulated insulin secretion similar to those of normal islets. In *Diabetologia* 36 (11), pp. 1139–1145. DOI: 10.1007/BF00401058.

Ishizuka, Takahiro; Lazar, Mitchell A. (2003): The N-CoR/histone deacetylase 3 complex is required for repression by thyroid hormone receptor. In *Molecular and Cellular Biology* 23 (15), pp. 5122–5131. DOI: 10.1128/MCB.23.15.5122-5131.2003.

Ishizuka, Takahiro; Lazar, Mitchell A. (2005): The nuclear receptor corepressor deacetylase activating domain is essential for repression by thyroid hormone receptor. In *Molecular Endocrinology* 19 (6), pp. 1443–1451. DOI: 10.1210/me.2005-0009.

Itoh, N.; Okamoto, H. (1980): Translational control of proinsulin synthesis by glucose. In *Nature* 283 (5742), pp. 100–102. DOI: 10.1038/283100a0.

Jensen, J.; Heller, R. S.; Funder-Nielsen, T.; Pedersen, E. E.; Lindsell, C.; Weinmaster, G. et al. (2000): Independent development of pancreatic alpha- and beta-cells from neurogenin3-expressing precursors: a role for the notch pathway in repression of premature differentiation. In *Diabetes* 49 (2), pp. 163–176. DOI: 10.2337/diabetes.49.2.163.

Jepsen, K.; Hermanson, O.; Onami, T. M.; Gleiberman, A. S.; Lunyak, V.; McEvilly, R. J. et al. (2000): Combinatorial roles of the nuclear receptor corepressor in transcription and development. In *Cell* 102 (6), pp. 753–763. DOI: 10.1016/s0092-8674(00)00064-7.

Jesus, Daniel S. de; Mak, Tracy C. S.; Wang, Yi-Fang; Ohlen, Yorrick von; Bai, Ying; Kane, Eva et al. (2021): Dysregulation of the Pdx1/Ovol2/Zeb2 axis in dedifferentiated β-cells triggers the induction of genes associated with epithelial-mesenchymal transition in diabetes. In *Molecular Metabolism* 53, p. 101248. DOI: 10.1016/j.molmet.2021.101248.

Jonas, J. C.; Sharma, A.; Hasenkamp, W.; Ilkova, H.; Patanè, G.; Laybutt, R. et al. (1999): Chronic hyperglycemia triggers loss of pancreatic beta cell differentiation in an animal model of diabetes. In *The Journal of biological chemistry* 274 (20), pp. 14112–14121. DOI: 10.1074/jbc.274.20.14112.

Jones, Courtney L.; Bhatla, Teena; Blum, Roy; Wang, Jinhua; Paugh, Steven W.; Wen, Xin et al. (2014): Loss of TBL1XR1 disrupts glucocorticoid receptor recruitment to chromatin and results in glucocorticoid resistance in a B-lymphoblastic leukemia model. In *The Journal of biological chemistry* 289 (30), pp. 20502–20515. DOI: 10.1074/jbc.M114.569889.

Karam, John H.; Grodsky, Gerold M.; Forsham, Peter H.; McWilliams, Nancy B. (1963): Excessive Insulin Response to Glucose in Obese Subjects as Measured by Immunochemical Assay. In *Diabetes* 12 (3), pp. 197–204. DOI: 10.2337/diab.12.3.197.

Kashiwagi, A.; Hueckstead, T. P.; Foley, J. E. (1983): The regulation of glucose transport by cAMP stimulators via three different mechanisms in rat and human adipocytes. In *The Journal of biological chemistry* 258 (22), pp. 13685–13692.

Kataoka, Kohsuke; Han, Song-iee; Shioda, Setsuko; Hirai, Momoki; Nishizawa, Makoto; Handa, Hiroshi (2002): MafA is a glucose-regulated and pancreatic beta-cell-specific transcriptional activator for the insulin gene. In *The Journal of biological chemistry* 277 (51), pp. 49903–49910. DOI: 10.1074/jbc.M206796200.

Katsuta, H.; Akashi, T.; Katsuta, R.; Nagaya, M.; Kim, D.; Arinobu, Y. et al. (2010): Single pancreatic beta cells co-express multiple islet hormone genes in mice. In *Diabetologia* 53 (1), pp. 128–138. DOI: 10.1007/s00125-009-1570-x.

Kawaguchi, Yoshiya; Cooper, Bonnie; Gannon, Maureen; Ray, Michael; MacDonald, Raymond J.; Wright, Christopher V. E. (2002): The role of the transcriptional regulator Ptf1a in converting intestinal to pancreatic progenitors. In *Nature genetics* 32 (1), pp. 128–134. DOI: 10.1038/ng959.

Kelley, D. E.; Mokan, M.; Simoneau, J. A.; Mandarino, L. J. (1993): Interaction between glucose and free fatty acid metabolism in human skeletal muscle. In *The Journal of clinical investigation* 92 (1), pp. 91–98. DOI: 10.1172/JCI116603.

Kieffer, T. J.; Heller, R. S.; Unson, C. G.; Weir, G. C.; Habener, J. F. (1996): Distribution of glucagon receptors on hormone-specific endocrine cells of rat pancreatic islets. In *Endocrinology* 137 (11), pp. 5119–5125. DOI: 10.1210/endo.137.11.8895386.

Kim, Abraham; Miller, Kevin; Jo, Junghyo; Kilimnik, German; Wojcik, Pawel; Hara, Manami (2009): Islet architecture: A comparative study. In *Islets* 1 (2), pp. 129–136. DOI: 10.4161/isl.1.2.9480.

Kim, Chul-Hong; An, Mi-Jin; Kim, Dae-Hyun; Kim, Jung-Woong (2017): Histone deacetylase 1 (HDAC1) regulates retinal development through a PAX6-dependent pathway. In *Biochemical and biophysical research communications* 482 (4), pp. 735–741. DOI: 10.1016/j.bbrc.2016.11.103.

Kim, Hyeonhui; Kim, Minki; Im, Sun-Kyoung; Fang, Sungsoon (2018): Mouse Cre-LoxP system: general principles to determine tissue-specific roles of target genes. In *Laboratory Animal Research* 34 (4), pp. 147–159. DOI: 10.5625/lar.2018.34.4.147.

Kim, Wook; Fiori, Jennifer L.; Shin, Yu-Kyong; Okun, Eitan; Kim, Jung Seok; Rapp, Peter R.; Egan, Josephine M. (2014): Pancreatic polypeptide inhibits somatostatin secretion. In *FEBS letters* 588 (17), pp. 3233–3239. DOI: 10.1016/j.febslet.2014.07.005.

Krapp, A.; Knöfler, M.; Ledermann, B.; Bürki, K.; Berney, C.; Zoerkler, N. et al. (1998): The bHLH protein PTF1-p48 is essential for the formation of the exocrine and the correct spatial organization of the endocrine pancreas. In *Genes & development* 12 (23), pp. 3752–3763. DOI: 10.1101/gad.12.23.3752.

Kulkarni, R. N.; Brüning, J. C.; Winnay, J. N.; Postic, C.; Magnuson, M. A.; Kahn, C. R. (1999): Tissue-specific knockout of the insulin receptor in pancreatic beta cells creates an insulin secretory defect similar to that in type 2 diabetes. In *Cell* 96 (3), pp. 329–339. DOI: 10.1016/s0092-8674(00)80546-2.

Kulozik, Philipp; Jones, Allan; Mattijssen, Frits; Rose, Adam J.; Reimann, Anja; Strzoda, Daniela et al. (2011): Hepatic deficiency in transcriptional cofactor TBL1 promotes liver steatosis and hypertriglyceridemia. In *Cell metabolism* 13 (4), pp. 389–400. DOI: 10.1016/j.cmet.2011.02.011.

Kuroda, Akio; Rauch, Tibor A.; Todorov, Ivan; Ku, Hsun Teresa; Al-Abdullah, Ismail H.; Kandeel, Fouad et al. (2009): Insulin gene expression is regulated by DNA methylation. In *PLOS ONE* 4 (9), e6953. DOI: 10.1371/journal.pone.0006953.

Latos, Paulina A.; Goncalves, Angela; Oxley, David; Mohammed, Hisham; Turro, Ernest; Hemberger, Myriam (2015): Fgf and Esrrb integrate epigenetic and transcriptional networks that regulate self-renewal of trophoblast stem cells. In *Nature communications* 6, p. 7776. DOI: 10.1038/ncomms8776.

Lee, D. Y.; Hayes, J. J.; Pruss, D.; Wolffe, A. P. (1993): A positive role for histone acetylation in transcription factor access to nucleosomal DNA. In *Cell* 72 (1), pp. 73–84. DOI: 10.1016/0092-8674(93)90051-q.

Lemaire, Katleen; Granvik, Mikaela; Schraenen, Anica; Goyvaerts, Lotte; van Lommel, Leentje; Gómez-Ruiz, Ana et al. (2017): How stable is repression of disallowed genes in pancreatic islets in response to metabolic stress? In *PLOS ONE* 12 (8), e0181651. DOI: 10.1371/journal.pone.0181651.

Li, Bing; Cheng, Yu; Yin, Yaqi; Xue, Jing; Yu, Songyan; Gao, Jieqing et al. (2021): Reversion of early- and late-stage β-cell dedifferentiation by human umbilical cord-derived mesenchymal stem cells in type 2 diabetic mice. In *Cytotherapy* 23 (6), pp. 510–520. DOI: 10.1016/j.jcyt.2021.01.005.

Li, Jiong; Wang, Cun-Yu (2008): TBL1-TBLR1 and beta-catenin recruit each other to Wnt target-gene promoter for transcription activation and oncogenesis. In *Nature cell biology* 10 (2), pp. 160–169. DOI: 10.1038/ncb1684.

Li, Xinghua; Liang, Weijiang; Liu, Junling; Lin, Chuyong; Wu, Shu; Song, Libing; Yuan, Zhongyu (2014): Transducin (β)-like 1 X-linked receptor 1 promotes proliferation and tumorigenicity in human breast cancer via activation of beta-catenin signaling. In *Breast cancer research : BCR* 16 (5), p. 465. DOI: 10.1186/s13058-014-0465-z.

Lombardi, A.; Ulianich, L.; Treglia, A. S.; Nigro, C.; Parrillo, L.; Lofrumento, D. D. et al. (2012): Increased hexosamine biosynthetic pathway flux dedifferentiates INS-1E cells and murine islets by an extracellular signal-regulated kinase (ERK)1/2-mediated signal transmission pathway. In *Diabetologia* 55 (1), pp. 141–153. DOI: 10.1007/s00125-011-2315-1.

Long, Amanda N.; Dagogo-Jack, Samuel (2011): Comorbidities of diabetes and hypertension: mechanisms and approach to target organ protection. In *Journal of clinical hypertension (Greenwich, Conn.)* 13 (4), pp. 244–251. DOI: 10.1111/j.1751-7176.2011.00434.x.

Lu, Tess Tsai-Hsiu; Heyne, Steffen; Dror, Erez; Casas, Eduard; Leonhardt, Laura; Boenke, Thorina et al. (2018): The Polycomb-Dependent Epigenome Controls β Cell Dysfunction, Dedifferentiation, and Diabetes. In *Cell metabolism* 27 (6), 1294-1308.e7. DOI: 10.1016/j.cmet.2018.04.013.

Lundh, M.; Christensen, D. P.; Damgaard Nielsen, M.; Richardson, S. J.; Dahllöf, M. S.; Skovgaard, T. et al. (2012): Histone deacetylases 1 and 3 but not 2 mediate cytokine-induced beta cell apoptosis in INS-1 cells and dispersed primary islets from rats and are differentially regulated in the islets of type 1 diabetic children. In *Diabetologia* 55 (9), pp. 2421–2431. DOI: 10.1007/s00125-012-2615-0.

Lundh, M.; Galbo, T.; Poulsen, S. S.; Mandrup-Poulsen, T. (2015): Histone deacetylase 3 inhibition improves glycaemia and insulin secretion in obese diabetic rats. In *Diabetes, obesity & metabolism* 17 (7), pp. 703–707. DOI: 10.1111/dom.12470.

Lyon, James; E Manning Fox, Jocelyn; F Spigelman, Aliya; E Macdonald, Patrick (2018): Thawing Cryopreserved Human Islets v1.

Magnusson, I.; Rothman, D. L.; Katz, L. D.; Shulman, R. G.; Shulman, G. I. (1992): Increased rate of gluconeogenesis in type II diabetes mellitus. A 13C nuclear magnetic resonance study. In *The Journal of clinical investigation* 90 (4), pp. 1323–1327. DOI: 10.1172/JCI115997.

Maluchenko, N. V.; Chang, H. W.; Kozinova, M. T.; Valieva, M. E.; Gerasimova, N. S.; Kitashov, A. V. et al. (2016): Inhibiting the pro-tumor and transcription factor FACT: Mechanisms. In *Mol Biol* 50 (4), pp. 532–541. DOI: 10.1134/S0026893316040087.

Mandarino, L.; Stenner, D.; Blanchard, W.; Nissen, S.; Gerich, J.; Ling, N. et al. (1981): Selective effects of somatostatin-14, -25 and -28 on in vitro insulin and glucagon secretion. In *Nature* 291 (5810), pp. 76–77. DOI: 10.1038/291076a0.

Mastrototaro, Giuseppina; Zaghi, Mattia; Massimino, Luca; Moneta, Matteo; Mohammadi, Neda; Banfi, Federica et al. (2021): TBL1XR1 Ensures Balanced Neural Development Through NCOR Complex-Mediated Regulation of the MAPK Pathway. In *Frontiers in Cell and Developmental Biology* 9, p. 641410. DOI: 10.3389/fcell.2021.641410.

McKenna, Brian; Guo, Min; Reynolds, Albert; Hara, Manami; Stein, Roland (2015): Dynamic recruitment of functionally distinct Swi/Snf chromatin remodeling complexes modulates Pdx1 activity in islet β cells. In *Cell reports* 10 (12), pp. 2032–2042. DOI: 10.1016/j.celrep.2015.02.054.

Meier, Juris J.; Butler, Alexandra E.; Saisho, Yoshifumi; Monchamp, Travis; Galasso, Ryan; Bhushan, Anil et al. (2008): Beta-cell replication is the primary mechanism subserving the postnatal expansion of beta-cell mass in humans. In *Diabetes* 57 (6), pp. 1584–1594. DOI: 10.2337/db07-1369.

Melloul, D.; Ben-Neriah, Y.; Cerasi, E. (1993): Glucose modulates the binding of an islet-specific factor to a conserved sequence within the rat I and the human insulin promoters. In *Proceedings of the National Academy of Sciences of the United States of America* 90 (9), pp. 3865–3869. DOI: 10.1073/pnas.90.9.3865.

Merkle, Florian T.; Ghosh, Sulagna; Genovese, Giulio; Handsaker, Robert E.; Kashin, Seva; Meyer, Daniel et al. (2022): Whole-genome analysis of human embryonic stem cells enables rational line selection based on genetic variation. In *Cell stem cell* 29 (3), 472-486.e7. DOI: 10.1016/j.stem.2022.01.011.

Mezza, Teresa; Muscogiuri, Giovanna; Sorice, Gian Pio; Clemente, Gennaro; Hu, Jiang; Pontecorvi, Alfredo et al. (2014): Insulin resistance alters islet morphology in nondiabetic humans. In *Diabetes* 63 (3), pp. 994–1007. DOI: 10.2337/db13-1013.

Miettinen, P. J.; Huotari, M.; Koivisto, T.; Ustinov, J.; Palgi, J.; Rasilainen, S. et al. (2000): Impaired migration and delayed differentiation of pancreatic islet cells in mice lacking EGF-receptors. In *Development (Cambridge, England)* 127 (12), pp. 2617–2627. DOI: 10.1242/dev.127.12.2617.

Mitchell, Ryan K.; Nguyen-Tu, Marie-Sophie; Chabosseau, Pauline; Callingham, Rebecca M.; Pullen, Timothy J.; Cheung, Rebecca et al. (2017): The transcription factor Pax6 is required for pancreatic β cell identity, glucose-regulated ATP synthesis, and Ca2+ dynamics in adult mice. In *The Journal of biological chemistry* 292 (21), pp. 8892–8906. DOI: 10.1074/jbc.M117.784629.

Møller, Niels; Gormsen, Lars; Fuglsang, Jens; Gjedsted, Jakob (2003): Effects of ageing on insulin secretion and action. In *Hormone research* 60 (Suppl 1), pp. 102–104. DOI: 10.1159/000071233.

Montgomery, Rusty L.; Potthoff, Matthew J.; Haberland, Michael; Qi, Xiaoxia; Matsuzaki, Satoshi; Humphries, Kenneth M. et al. (2008): Maintenance of cardiac energy metabolism by histone deacetylase 3 in mice. In *Journal of Clinical Investigation* 118 (11), pp. 3588–3597. DOI: 10.1172/JCI35847.

Morris, E. Matthew; Meers, Grace M. E.; Booth, Frank W.; Fritsche, Kevin L.; Hardin, Christopher D.; Thyfault, John P.; Ibdah, Jamal A. (2012): PGC-1α overexpression results in increased hepatic fatty acid oxidation with reduced triacylglycerol accumulation and secretion. In *American journal of physiology. Gastrointestinal and liver physiology* 303 (8), G979-92. DOI: 10.1152/ajpgi.00169.2012.

Mosley, Amber L.; Corbett, John A.; Ozcan, Sabire (2004): Glucose regulation of insulin gene expression requires the recruitment of p300 by the beta-cell-specific transcription factor Pdx-1. In *Molecular Endocrinology* 18 (9), pp. 2279–2290. DOI: 10.1210/me.2003-0463.

Mosley, Amber L.; Ozcan, Sabire (2004): The pancreatic duodenal homeobox-1 protein (Pdx-1) interacts with histone deacetylases Hdac-1 and Hdac-2 on low levels of glucose. In *The Journal of biological chemistry* 279 (52), pp. 54241–54247. DOI: 10.1074/jbc.M410379200.

Müller, W. A.; Faloona, G. R.; Aguilar-Parada, E.; Unger, R. H. (1970): Abnormal alpha-cell function in diabetes. Response to carbohydrate and protein ingestion. In *The New England journal of medicine* 283 (3), pp. 109–115. DOI: 10.1056/NEJM197007162830301.

Nair, Gopika; Hebrok, Matthias (2015): Islet formation in mice and men: lessons for the generation of functional insulin-producing β-cells from human pluripotent stem cells. In *Current opinion in genetics & development* 32, pp. 171–180. DOI: 10.1016/j.gde.2015.03.004.

Nath, Dilip S.; Gruessner, Angelika C.; Kandaswamy, Raja; Gruessner, Rainer W.; Sutherland, David E. R.; Humar, Abhinav (2005): Outcomes of pancreas transplants for patients with type 2 diabetes mellitus. In *Clinical transplantation* 19 (6), pp. 792–797. DOI: 10.1111/j.1399-0012.2005.00423.x.

Neelankal John, Abraham; Ram, Ramesh; Jiang, Fang-Xu (2018): RNA-Seq Analysis of Islets to Characterise the Dedifferentiation in Type 2 Diabetes Model Mice db/db. In *Endocrine pathology* 29 (3), pp. 207–221. DOI: 10.1007/s12022-018-9523-x.

Ninkovic, Jovica; Steiner-Mezzadri, Andrea; Jawerka, Melanie; Akinci, Umut; Masserdotti, Giacomo; Petricca, Stefania et al. (2013): The BAF complex interacts with Pax6 in adult neural progenitors to establish a neurogenic cross-regulatory transcriptional network. In *Cell stem cell* 13 (4), pp. 403–418. DOI: 10.1016/j.stem.2013.07.002.

Nishina, S.; Kohsaka, S.; Yamaguchi, Y.; Handa, H.; Kawakami, A.; Fujisawa, H.; Azuma, N. (1999): PAX6 expression in the developing human eye. In *The British journal of ophthalmology* 83 (6), pp. 723–727. DOI: 10.1136/bjo.83.6.723.

Nitzsche, Anja; Paszkowski-Rogacz, Maciej; Matarese, Filomena; Janssen-Megens, Eva M.; Hubner, Nina C.; Schulz, Herbert et al. (2011): RAD21 cooperates with pluripotency transcription factors in the maintenance of embryonic stem cell identity. In *PLOS ONE* 6 (5), e19470. DOI: 10.1371/journal.pone.0019470.

Nordmann, Thierry M.; Dror, Erez; Schulze, Friederike; Traub, Shuyang; Berishvili, Ekaterine; Barbieux, Charlotte et al. (2017): The Role of Inflammation in β-cell Dedifferentiation. In *Scientific reports* 7 (1), p. 6285. DOI: 10.1038/s41598-017-06731-w.

Oberoi, Jasmeen; Fairall, Louise; Watson, Peter J.; Yang, Ji-Chun; Czimmerer, Zsolt; Kampmann, Thorsten et al. (2011): Structural basis for the assembly of the SMRT/NCoR core transcriptional repression machinery. In *Nature structural & molecular biology* 18 (2), pp. 177–184. DOI: 10.1038/nsmb.1983.

Ogawa, Sumito; Lozach, Jean; Jepsen, Kristen; Sawka-Verhelle, Dominique; Perissi, Valentina; Sasik, Roman et al. (2004): A nuclear receptor corepressor transcriptional checkpoint controlling activator protein 1-dependent gene networks required for macrophage activation. In *Proceedings of the National Academy of Sciences of the United States of America* 101 (40), pp. 14461–14466. DOI: 10.1073/pnas.0405786101.

Orphanides, G.; LeRoy, G.; Chang, C. H.; Luse, D. S.; Reinberg, D. (1998): FACT, a factor that facilitates transcript elongation through nucleosomes. In *Cell* 92 (1), pp. 105–116. DOI: 10.1016/s0092-8674(00)80903-4.

Otonkoski, T.; Andersson, S.; Knip, M.; Simell, O. (1988): Maturation of insulin response to glucose during human fetal and neonatal development. Studies with perifusion of pancreatic isletlike cell clusters. In *Diabetes* 37 (3), pp. 286–291. DOI: 10.2337/diab.37.3.286.

Otonkoski, T.; Knip, M.; Wong, I.; Simell, O. (1991): Lack of glucose-induced functional maturation during long-term culture of human fetal islet cells. In *Life sciences* 48 (22), pp. 2157–2163. DOI: 10.1016/0024-3205(91)90149-6.

Park, Soo-Yeon; Na, Younghwa; Lee, Mee-Hee; Seo, Jae-Sung; Lee, Yoo-Hyun; Choi, Kyung-Chul et al. (2016): SUMOylation of TBL1 and TBLR1 promotes androgen-independent prostate cancer cell growth. In *Oncotarget* 7 (27), pp. 41110–41122. DOI: 10.18632/oncotarget.9002.

Pearse, A. G.; Polak, J. M.; Heath, C. M. (1973): Development, differentiation and derivation of the endocrine polypeptide cells of the mouse pancreas. Immunofluorescence, cytochemical and ultrastructural studies. In *Diabetologia* 9 (2), pp. 120–129. DOI: 10.1007/BF01230691.

Perekatt, Ansu O.; Shah, Pooja P.; Cheung, Shannon; Jariwala, Nidhi; Wu, Alex; Gandhi, Vishal et al. (2018): SMAD4 Suppresses WNT-Driven Dedifferentiation and Oncogenesis in the Differentiated Gut Epithelium. In *Cancer research* 78 (17), pp. 4878–4890. DOI: 10.1158/0008-5472.CAN-18-0043.

Perissi, Valentina; Aggarwal, Aneel; Glass, Christopher K.; Rose, David W.; Rosenfeld, Michael G. (2004): A corepressor/coactivator exchange complex required for transcriptional activation by nuclear receptors and other regulated transcription factors. In *Cell* 116 (4), pp. 511–526. DOI: 10.1016/s0092-8674(04)00133-3.

Perissi, Valentina; Jepsen, Kristen; Glass, Christopher K.; Rosenfeld, Michael G. (2010): Deconstructing repression: evolving models of co-repressor action. In *Nature reviews. Genetics* 11 (2), pp. 109–123. DOI: 10.1038/nrg2736.

Perissi, Valentina; Scafoglio, Claudio; Zhang, Jie; Ohgi, Kenneth A.; Rose, David W.; Glass, Christopher K.; Rosenfeld, Michael G. (2008): TBL1 and TBLR1 phosphorylation on regulated gene promoters overcomes dual CtBP and NCoR/SMRT transcriptional repression checkpoints. In *Molecular cell* 29 (6), pp. 755–766. DOI: 10.1016/j.molcel.2008.01.020.

Pictet, R. L.; Clark, W. R.; Williams, R. H.; Rutter, W. J. (1972): An ultrastructural analysis of the developing embryonic pancreas. In *Developmental biology* 29 (4), pp. 436–467. DOI: 10.1016/0012-1606(72)90083-8.

Pöykkö, Seppo M.; Kellokoski, Eija; Hörkkö, Sohvi; Kauma, Heikki; Kesäniemi, Y. Antero; Ukkola, Olavi (2003): Low plasma ghrelin is associated with insulin resistance, hypertension, and the prevalence of type 2 diabetes. In *Diabetes* 52 (10), pp. 2546–2553. DOI: 10.2337/diabetes.52.10.2546.

Pullen, Timothy J.; Khan, Arshad M.; Barton, Geraint; Butcher, Sarah A.; Sun, Gao; Rutter, Guy A. (2010): Identification of genes selectively disallowed in the pancreatic islet. In *Islets* 2 (2), pp. 89–95. DOI: 10.4161/isl.2.2.11025.

Qader, Saleem S.; Håkanson, Rolf; Rehfeld, Jens F.; Lundquist, Ingmar; Salehi, Albert (2008): Proghrelin-derived peptides influence the secretion of insulin, glucagon, pancreatic polypeptide and somatostatin: a study on isolated islets from mouse and rat pancreas. In *Regulatory peptides* 146 (1-3), pp. 230–237. DOI: 10.1016/j.regpep.2007.09.017.

Qiu, Yi; Guo, Min; Huang, Suming; Stein, Roland (2002): Insulin gene transcription is mediated by interactions between the p300 coactivator and PDX-1, BETA2, and E47. In *Molecular and Cellular Biology* 22 (2), pp. 412–420. DOI: 10.1128/MCB.22.2.412-420.2002.

Remsberg, Jarrett R.; Ediger, Benjamin N.; Ho, Wesley Y.; Damle, Manashree; Li, Zhenghui; Teng, Christopher et al. (2017): Deletion of histone deacetylase 3 in adult beta cells improves glucose tolerance via increased insulin secretion. In *Molecular Metabolism* 6 (1), pp. 30–37. DOI: 10.1016/j.molmet.2016.11.007.

Rivero, Sabrina; Gómez-Marín, Elena; Guerrero-Martínez, José A.; García-Martínez, Jorge; Reyes, José C. (2019): TBL1 is required for the mesenchymal phenotype of transformed breast cancer cells. In *Cell death & disease* 10 (2), p. 95. DOI: 10.1038/s41419-019-1310-1.

Rix, Iben; Nexøe-Larsen, Christina; Bergmann, Natasha C.; Lund, Asger; Knop, Filip K. (2000): Endotext. Glucagon Physiology. Available online at https://pubmed.ncbi.nlm.nih.gov/25905350/.

Rochlani, Yogita; Pothineni, Naga Venkata; Kovelamudi, Swathi; Mehta, Jawahar L. (2017): Metabolic syndrome: pathophysiology, management, and modulation by natural compounds. In *Therapeutic Advances in Cardiovascular Disease* 11 (8), pp. 215–225. DOI: 10.1177/1753944717711379.

Roefs, Maaike M.; Carlotti, Françoise; Jones, Katherine; Wills, Hannah; Hamilton, Alexander; Verschoor, Michael et al. (2017): Increased vimentin in human α- and β-cells in type 2 diabetes. In *The Journal of endocrinology* 233 (3), pp. 217–227. DOI: 10.1530/JOE-16-0588.

Rohm, Maria; Sommerfeld, Anke; Strzoda, Daniela; Jones, Allan; Sijmonsma, Tjeerd P.; Rudofsky, Gottfried et al. (2013): Transcriptional cofactor TBLR1 controls lipid mobilization in white adipose tissue. In *Cell metabolism* 17 (4), pp. 575–585. DOI: 10.1016/j.cmet.2013.02.010.

Rorsman, P.; Ashcroft, F. M.; Trube, G. (1988): Single Ca channel currents in mouse pancreatic B-cells. In *Pflugers Archiv : European journal of physiology* 412 (6), pp. 597–603. DOI: 10.1007/BF00583760.

Rorsman, Patrik; Huising, Mark O. (2018): The somatostatin-secreting pancreatic δ-cell in health and disease. In *Nature reviews. Endocrinology* 14 (7), pp. 404–414. DOI: 10.1038/s41574-018-0020-6.

Rosenthal, Nadia; Brown, Steve (2007): The mouse ascending: perspectives for human-disease models. In *Nature cell biology* 9 (9), pp. 993–999. DOI: 10.1038/ncb437.

Sacks, David B.; Arnold, Mark; Bakris, George L.; Bruns, David E.; Horvath, Andrea Rita; Kirkman, M. Sue et al. (2011): Guidelines and recommendations for laboratory analysis in the diagnosis and management of diabetes mellitus. In *Clinical chemistry* 57 (6), e1-e47. DOI: 10.1373/clinchem.2010.161596.

Salinno, Ciro; Büttner, Maren; Cota, Perla; Tritschler, Sophie; Tarquis-Medina, Marta; Bastidas-Ponce, Aimée et al. (2021): CD81 marks immature and dedifferentiated pancreatic β-cells. In *Molecular Metabolism* 49, p. 101188. DOI: 10.1016/j.molmet.2021.101188.

Salmerón, J.; Hu, F. B.; Manson, J. E.; Stampfer, M. J.; Colditz, G. A.; Rimm, E. B.; Willett, W. C. (2001): Dietary fat intake and risk of type 2 diabetes in women. In *The American journal of clinical nutrition* 73 (6), pp. 1019–1026. DOI: 10.1093/ajcn/73.6.1019.

Samudyata; Amaral, Paulo P.; Engström, Pär G.; Robson, Samuel C.; Nielsen, Michael L.; Kouzarides, Tony; Castelo-Branco, Gonçalo (2019): Interaction of Sox2 with RNA binding proteins in mouse embryonic stem cells. In *Experimental cell research* 381 (1), pp. 129–138. DOI: 10.1016/j.yexcr.2019.05.006.

Sander, M.; Neubüser, A.; Kalamaras, J.; Ee, H. C.; Martin, G. R.; German, M. S. (1997): Genetic analysis reveals that PAX6 is required for normal transcription of pancreatic hormone genes and islet development. In *Genes & development* 11 (13), pp. 1662–1673. DOI: 10.1101/gad.11.13.1662.

Sato, Noboru; Meijer, Laurent; Skaltsounis, Leandros; Greengard, Paul; Brivanlou, Ali H. (2004): Maintenance of pluripotency in human and mouse embryonic stem cells through activation of Wnt signaling by a pharmacological GSK-3-specific inhibitor. In *Nat Med* 10 (1), pp. 55–63. DOI: 10.1038/nm979.

Scarpello, John H. B.; Howlett, Harry C. S. (2008): Metformin therapy and clinical uses. In *Diabetes & vascular disease research* 5 (3), pp. 157–167. DOI: 10.3132/dvdr.2008.027.

Schaffer, Ashleigh E.; Freude, Kristine K.; Nelson, Shelley B.; Sander, Maike (2010): Nkx6 transcription factors and Ptf1a function as antagonistic lineage determinants in multipotent pancreatic progenitors. In *Developmental cell* 18 (6), pp. 1022–1029. DOI: 10.1016/j.devcel.2010.05.015.

Schwitalla, Sarah; Fingerle, Alexander A.; Cammareri, Patrizia; Nebelsiek, Tim; Göktuna, Serkan I.; Ziegler, Paul K. et al. (2013): Intestinal tumorigenesis initiated by dedifferentiation and acquisition of stem-cell-like properties. In *Cell* 152 (1-2), pp. 25–38. DOI: 10.1016/j.cell.2012.12.012.

Schwitzgebel, V. M.; Scheel, D. W.; Conners, J. R.; Kalamaras, J.; Lee, J. E.; Anderson, D. J. et al. (2000): Expression of neurogenin3 reveals an islet cell precursor population in the pancreas. In *Development (Cambridge, England)* 127 (16), pp. 3533–3542. DOI: 10.1242/dev.127.16.3533.

Seymour, Philip A.; Freude, Kristine K.; Tran, Man N.; Mayes, Erin E.; Jensen, Jan; Kist, Ralf et al. (2007): SOX9 is required for maintenance of the pancreatic progenitor cell pool. In *Proceedings of the National Academy of Sciences of the United States of America* 104 (6), pp. 1865–1870. DOI: 10.1073/pnas.0609217104.

Shapiro, A. M. James; Ricordi, Camillo; Hering, Bernhard J.; Auchincloss, Hugh; Lindblad, Robert; Robertson, R. Paul et al. (2006): International trial of the Edmonton protocol for islet transplantation. In *The New England journal of medicine* 355 (13), pp. 1318–1330. DOI: 10.1056/NEJMoa061267.

Shapiro, A. M. James; Thompson, David; Donner, Thomas W.; Bellin, Melena D.; Hsueh, Willa; Pettus, Jeremy et al. (2021): Insulin expression and C-peptide in type 1 diabetes subjects implanted with stem cell-derived pancreatic endoderm cells in an encapsulation device. In *Cell reports. Medicine* 2 (12), p. 100466. DOI: 10.1016/j.xcrm.2021.100466.

Sharma, A.; Stein, R. (1994): Glucose-induced transcription of the insulin gene is mediated by factors required for beta-cell-type-specific expression. In *Molecular and Cellular Biology* 14 (2), pp. 871–879. DOI: 10.1128/MCB.14.2.871.

Sharma, Kumar; McCue, Peter; Dunn, Stephen R. (2003): Diabetic kidney disease in the db/db mouse. In *American journal of physiology. Renal physiology* 284 (6), F1138-44. DOI: 10.1152/ajprenal.00315.2002.

Shimabukuro, M.; Zhou, Y. T.; Levi, M.; Unger, R. H. (1998): Fatty acid-induced beta cell apoptosis: a link between obesity and diabetes. In *Proceedings of the National Academy of Sciences of the United States of America* 95 (5), pp. 2498–2502. DOI: 10.1073/pnas.95.5.2498.

Skelin, Masa; Rupnik, Marjan; Cencic, Avrelija (2010): Pancreatic beta cell lines and their applications in diabetes mellitus research. In *ALTEX* 27 (2), pp. 105–113. DOI: 10.14573/altex.2010.2.105.

Soldi, Raffaella; Halder, Tithi Ghosh; Sampson, Samuel; Vankayalapati, Hariprasad; Weston, Alexis; Thode, Trason et al. (2021): The Small Molecule BC-2059 Inhibits Wingless/Integrated (Wnt)-Dependent Gene Transcription in Cancer through Disruption of the Transducin β-Like 1-β-Catenin Protein Complex. In *The Journal of pharmacology and experimental therapeutics* 378 (2), pp. 77–86. DOI: 10.1124/jpet.121.000634.

Sosa-Pineda, Beatriz (2004): The gene Pax4 is an essential regulator of pancreatic beta-cell development. In *Molecules and cells* 18 (3), pp. 289–294.

Spence, Jason R.; Lange, Alex W.; Lin, Suh-Chin J.; Kaestner, Klaus H.; Lowy, Andrew M.; Kim, Injune et al. (2009): Sox17 regulates organ lineage segregation of ventral foregut progenitor cells. In *Developmental cell* 17 (1), pp. 62–74. DOI: 10.1016/j.devcel.2009.05.012.

Stefan, Y.; Orci, L.; Malaisse-Lagae, F.; Perrelet, A.; Patel, Y.; Unger, R. H. (1982): Quantitation of endocrine cell content in the pancreas of nondiabetic and diabetic humans. In *Diabetes* 31 (8 Pt 1), pp. 694–700. DOI: 10.2337/diab.31.8.694.

Stolovich-Rain, Miri; Enk, Jonatan; Vikesa, Jonas; Nielsen, Finn Cilius; Saada, Ann; Glaser, Benjamin; Dor, Yuval (2015): Weaning triggers a maturation step of pancreatic β cells. In *Developmental cell* 32 (5), pp. 535–545. DOI: 10.1016/j.devcel.2015.01.002.

St-Onge, L.; Sosa-Pineda, B.; Chowdhury, K.; Mansouri, A.; Gruss, P. (1997): Pax6 is required for differentiation of glucagon-producing alpha-cells in mouse pancreas. In *Nature* 387 (6631), pp. 406–409. DOI: 10.1038/387406a0.

Stoy, Christian; Sundaram, Aishwarya; Rios Garcia, Marcos; Wang, Xiaoyue; Seibert, Oksana; Zota, Annika et al. (2015): Transcriptional co-factor Transducin beta-like (TBL) 1 acts as a checkpoint in pancreatic cancer malignancy. In *EMBO molecular medicine* 7 (8), pp. 1048–1062. DOI: 10.15252/emmm.201404837.

Sun, Hong; Saeedi, Pouya; Karuranga, Suvi; Pinkepank, Moritz; Ogurtsova, Katherine; Duncan, Bruce B. et al. (2022): IDF Diabetes Atlas: Global, regional and country-level diabetes prevalence estimates

for 2021 and projections for 2045. In *Diabetes research and clinical practice* 183, p. 109119. DOI: 10.1016/j.diabres.2021.109119.

Sussel, L.; Kalamaras, J.; Hartigan-O'Connor, D. J.; Meneses, J. J.; Pedersen, R. A.; Rubenstein, J. L.; German, M. S. (1998): Mice lacking the homeodomain transcription factor Nkx2.2 have diabetes due to arrested differentiation of pancreatic beta cells. In *Development (Cambridge, England)* 125 (12), pp. 2213–2221. DOI: 10.1242/dev.125.12.2213.

Swenne, I. (1983): Effects of aging on the regenerative capacity of the pancreatic B-cell of the rat. In *Diabetes* 32 (1), pp. 14–19. DOI: 10.2337/diab.32.1.14.

Swisa, Avital; Avrahami, Dana; Eden, Noa; Zhang, Jia; Feleke, Eseye; Dahan, Tehila et al. (2017): PAX6 maintains β cell identity by repressing genes of alternative islet cell types. In *The Journal of clinical investigation* 127 (1), pp. 230–243. DOI: 10.1172/JCI88015.

Talchai, Chutima; Xuan, Shouhong; Lin, Hua V.; Sussel, Lori; Accili, Domenico (2012): Pancreatic β cell dedifferentiation as a mechanism of diabetic β cell failure. In *Cell* 150 (6), pp. 1223–1234. DOI: 10.1016/j.cell.2012.07.029.

Taylor, Brandon L.; Liu, Fen-Fen; Sander, Maike (2013): Nkx6.1 is essential for maintaining the functional state of pancreatic beta cells. In *Cell reports* 4 (6), pp. 1262–1275. DOI: 10.1016/j.celrep.2013.08.010.

Thomas, Melissa K.; Nikooienejad, Amir; Bray, Ross; Cui, Xuewei; Wilson, Jonathan; Duffin, Kevin et al. (2021): Dual GIP and GLP-1 Receptor Agonist Tirzepatide Improves Beta-cell Function and Insulin Sensitivity in Type 2 Diabetes. In *The Journal of Clinical Endocrinology and Metabolism* 106 (2), pp. 388–396. DOI: 10.1210/clinem/dgaa863.

Thorens, Bernard; Tarussio, David; Maestro, Miguel Angel; Rovira, Meritxell; Heikkilä, Eija; Ferrer, Jorge (2015): Ins1(Cre) knock-in mice for beta cell-specific gene recombination. In *Diabetologia* 58 (3), pp. 558–565. DOI: 10.1007/s00125-014-3468-5.

Thorrez, Lieven; Laudadio, Ilaria; van Deun, Katrijn; Quintens, Roel; Hendrickx, Nico; Granvik, Mikaela et al. (2011): Tissue-specific disallowance of housekeeping genes: the other face of cell differentiation. In *Genome Res.* 21 (1), pp. 95–105. DOI: 10.1101/gr.109173.110.

Tsonkova, Violeta Georgieva; Sand, Fredrik Wolfhagen; Wolf, Xenia Asbæk; Grunnet, Lars Groth; Kirstine Ringgaard, Anna; Ingvorsen, Camilla et al. (2018): The EndoC-βH1 cell line is a valid model of human beta cells and applicable for screenings to identify novel drug target candidates. In *Molecular Metabolism* 8, pp. 144–157. DOI: 10.1016/j.molmet.2017.12.007.

Unger, R. H. (1991): Diabetic hyperglycemia: link to impaired glucose transport in pancreatic beta cells. In *Science (New York, N.Y.)* 251 (4998), pp. 1200–1205. DOI: 10.1126/science.2006409.

van Arensbergen, Joris; García-Hurtado, Javier; Moran, Ignasi; Maestro, Miguel Angel; Xu, Xiaobo; van de Casteele, Mark et al. (2010): Derepression of Polycomb targets during pancreatic organogenesis allows insulin-producing beta-cells to adopt a neural gene activity program. In *Genome Res.* 20 (6), pp. 722–732. DOI: 10.1101/gr.101709.109.

Vergari, Elisa; Knudsen, Jakob G.; Ramracheya, Reshma; Salehi, Albert; Zhang, Quan; Adam, Julie et al. (2019): Insulin inhibits glucagon release by SGLT2-induced stimulation of somatostatin secretion. In *Nature communications* 10 (1), p. 139. DOI: 10.1038/s41467-018-08193-8.

Walther, C.; Gruss, P. (1991): Pax-6, a murine paired box gene, is expressed in the developing CNS. In *Development (Cambridge, England)* 113 (4), pp. 1435–1449. DOI: 10.1242/dev.113.4.1435.

Walth-Hummel, Alina A.; Herzig, Stephan; Rohm, Maria (2022): Nuclear Receptors in Energy Metabolism. In *Advances in experimental medicine and biology* 1390, pp. 61–82. DOI: 10.1007/978-3-031-11836-4_4.

Wang, H.; Brun, T.; Kataoka, K.; Sharma, A. J.; Wollheim, C. B. (2007): MAFA controls genes implicated in insulin biosynthesis and secretion. In *Diabetologia* 50 (2), pp. 348–358. DOI: 10.1007/s00125-006-0490-2.

Wang, Z.; Wang, R. M.; Owji, A. A.; Smith, D. M.; Ghatei, M. A.; Bloom, S. R. (1995): Glucagon-like peptide-1 is a physiological incretin in rat. In *Journal of Clinical Investigation* 95 (1), pp. 417–421. DOI: 10.1172/JCI117671.

Wang, Zhiyu; York, Nathaniel W.; Nichols, Colin G.; Remedi, Maria S. (2014): Pancreatic β cell dedifferentiation in diabetes and redifferentiation following insulin therapy. In *Cell metabolism* 19 (5), pp. 872–882. DOI: 10.1016/j.cmet.2014.03.010.

Wierup, N.; Svensson, H.; Mulder, H.; Sundler, F. (2002): The ghrelin cell: a novel developmentally regulated islet cell in the human pancreas. In *Regulatory peptides* 107 (1-3), pp. 63–69. DOI: 10.1016/s0167-0115(02)00067-8.

Willi, Carole; Bodenmann, Patrick; Ghali, William A.; Faris, Peter D.; Cornuz, Jacques (2007): Active smoking and the risk of type 2 diabetes: a systematic review and meta-analysis. In *JAMA* 298 (22), pp. 2654–2664. DOI: 10.1001/jama.298.22.2654.

Wren, A. M.; Small, C. J.; Ward, H. L.; Murphy, K. G.; Dakin, C. L.; Taheri, S. et al. (2000): The novel hypothalamic peptide ghrelin stimulates food intake and growth hormone secretion. In *Endocrinology* 141 (11), pp. 4325–4328. DOI: 10.1210/endo.141.11.7873.

Xin, Yurong; Kim, Jinrang; Okamoto, Haruka; Ni, Min; Wei, Yi; Adler, Christina et al. (2016): RNA Sequencing of Single Human Islet Cells Reveals Type 2 Diabetes Genes. In *Cell metabolism* 24 (4), pp. 608–615. DOI: 10.1016/j.cmet.2016.08.018.

Xu, Hongjuan; Yan, Xuejun; Zhu, Hecheng; Kang, Yuanbo; Luo, Weiren; Zhao, Jin et al. (2022): TBL1X and Flot2 form a positive feedback loop to promote metastasis in nasopharyngeal carcinoma. In *International journal of biological sciences* 18 (3), pp. 1134–1149. DOI: 10.7150/ijbs.68091.

Yang, Beatrice T.; Dayeh, Tasnim A.; Volkov, Petr A.; Kirkpatrick, Clare L.; Malmgren, Siri; Jing, Xingjun et al. (2012): Increased DNA methylation and decreased expression of PDX-1 in pancreatic islets from patients with type 2 diabetes. In *Molecular Endocrinology* 26 (7), pp. 1203–1212. DOI: 10.1210/me.2012-1004.

Yang, Jae Jeong; Yu, Danxia; Wen, Wanqing; Saito, Eiko; Rahman, Shafiur; Shu, Xiao-Ou et al. (2019): Association of Diabetes With All-Cause and Cause-Specific Mortality in Asia: A Pooled Analysis of More Than 1 Million Participants. In *JAMA network open* 2 (4), e192696. DOI: 10.1001/jamanetworkopen.2019.2696.

Yang, Yu-Ping; Thorel, Fabrizio; Boyer, Daniel F.; Herrera, Pedro L.; Wright, Christopher V. E. (2011): Context-specific α- to-β-cell reprogramming by forced Pdx1 expression. In *Genes & development* 25 (16), pp. 1680–1685. DOI: 10.1101/gad.16875711.

Yoon, Ho-Geun; Chan, Doug W.; Huang, Zhi-Qing; Li, Jiwen; Fondell, Joseph D.; Qin, Jun; Wong, Jiemin (2003): Purification and functional characterization of the human N-CoR complex: the roles of HDAC3, TBL1 and TBLR1. In *The EMBO journal* 22 (6), pp. 1336–1346. DOI: 10.1093/emboj/cdg120.

Yoon, Ho-Geun; Choi, Youngsok; Cole, Philip A.; Wong, Jiemin (2005): Reading and function of a histone code involved in targeting corepressor complexes for repression. In *Molecular and Cellular Biology* 25 (1), pp. 324–335. DOI: 10.1128/MCB.25.1.324-335.2005.

Yu, Jason S. L.; Cui, Wei (2016): Proliferation, survival and metabolism: the role of PI3K/AKT/mTOR signalling in pluripotency and cell fate determination. In *Development (Cambridge, England)* 143 (17), pp. 3050–3060. DOI: 10.1242/dev.137075.

Zhang, Xin-Min; Chang, Qing; Zeng, Lin; Gu, Judy; Brown, Stuart; Basch, Ross S. (2006): TBLR1 regulates the expression of nuclear hormone receptor co-repressors. In *BMC cell biology* 7, p. 31. DOI: 10.1186/1471-2121-7-31.